Newcastle University

PhD Thesis

A Methodology for Assessing Flood Risk from Multiple Sources

Ben Smith

This thesis is presented for the degree of Doctor of Philosophy

School of Engineering

May 2020
Word Count: 65 000

A Methodology for Assessing Flood Risk from Multiple Sources

Antecedent catchment conditions can affect the severity of flooding, and floods are typically worse when multiple flood sources superimpose. Over one million properties in the UK are at risk of flooding from multiple sources, however, groundwater, fluvial and pluvial flood sources are usually considered separately due to their differing characteristics.

This PhD study was composed of two parts: (1) developing a methodology for assessing the risk of flooding from multiple sources, including the creation of a groundwater-surface water modelling system and (2) conducting a national assessment identifying catchments with potential for flooding from multiple sources.

The modelling system used 1000 years of synthetic weather data to create realistic meteorological inputs for a physically-based, spatially-distributed hydrological catchment model (SHETRAN-GB). The hydrological model then simulated 1/30, 1/100 and 1/1000 year catchment conditions, which were used as inputs for a high resolution hydraulic model (HiPIMS). The hydraulic model then routed rainfall, stream flow and groundwater emergence to generate a detailed and comprehensive assessment of flood risk. Sensitivity tests compared the flood extents and depths from different methods of integrating groundwater and surface water conditions from the hydrological model into the hydraulic model to find the best method for linking the models.

The capability of a national automated hydrological model to simulate groundwater levels was tested at five case study catchments using open source hydrogeological datasets. Automated model configurations were unable to reproduce historical groundwater levels, however simple automated improvements did increase performance. Improved parameterisation of a basic subsurface increased model performance more than the introduction of more complex geology, although the latter was found to be erroneous in places. Correlations between observed and simulated groundwater levels ranged significantly but were as high as 0.9 at some locations. At one case study site, the model domain was given subsurface boundary conditions and increased from its topographic watershed to the estimated groundwater catchment. This dramatically increased the model's performance and its sensitivity to parameters. The automated setups provided a useful modelling base, but local calibration, improved hydrogeological parameters, subsurface boundary conditions and the use of groundwater domains are necessary for producing good simulations in catchments containing groundwater.

New indexes were derived for classifying flow regimes to aid the identification of catchments likely to benefit from the developed methodology, and an initial 29 multisource catchments were identified out of a total of 435 analysed. Multisource catchments are distributed around the UK but are typically confined to areas with permeable bedrock, thus are most commonly found in the South of England.

This research demonstrated that the inclusion of groundwater in the flood risk assessment increased the flood hazard by prolonging the flood duration from hours to days but did not notably increase flood depths. Furthermore, the patterns of flood extent changed depending on the proportion of the flood waters that were derived from the subsurface.

In summary, this study provides a methodology for the better quantification, mapping and understanding of multisource flood risk, and identifies catchments that are likely to benefit from the approach.

Acknowledgements

Thank you to all those who have helped and supported me throughout this PhD and without whom I would be very stuck. To Geoff, Liz and Hayley for their constant interest, guidance and enthusiasm and to Steve Birkinshaw for his willingness to share his SHETRAN expertise. Also to my family and friends for being all round wonderful people and getting me through! Special thanks must go to Fergus for helping with the many coding dilemmas, and for his unwavering support and positivity...

Cast your cares on the Lord and he will sustain you
Psalm 55:22

Contents

List of Figures

List of Tables

1 Introduction

1. Introduction

1.1 What is a Source?

There are four well known sources of flooding: *fluvial flooding, pluvial flooding, groundwater flooding and coastal flooding*. These indicate where the water that is causing the flood originated, i.e. from a river, directly from rainfall, from the ground or from the sea, and each act in different ways, at different locations, and on different time-scales. Coastal flooding is largely independent of the other three and so will not be considered in this study.

1.1.1 Surface Water

Fluvial flooding (i.e. from rivers) refers to flood waters that are derived from the river system when banks are over-topped or when levees fail. Pluvial flooding (i.e. from rainfall) refers to flood waters that have not yet entered a watercourse (Falconer et al., 2009). Pluvial flooding occurs when the ground and drainage network is unable to absorb rainfall, typically due to the intensity of the rainfall or the nature of the surface it falls on, and so causes water to flow along the surface.

Surface water shall be used in this thesis to define water that is derived from fluvial and pluvial inputs, i.e. from rivers and rainfall. This is in line with definitions in the literature (e.g. Falconer et al., 2009). Surface water can quickly cause a flood with issues arising within a number of days or hours following either several days of medium intensity rainfall or, in the case of pluvial flooding, high intensity rainfall over a matter of hours (Falconer et al., 2009). There are a large number of models in existence that simulate surface water flooding and national risk maps are publicly available (e.g. Environment Agency, 2019a). Further information is provided in Section 2.1.

1.1.2 Groundwater

Groundwater flooding occurs when the water table rises above ground level, causing groundwater to emerge from the subsurface (Naughton et al., 2015). This is most likely to occur when high antecedent (i.e. existing) groundwater conditions are combined with increased rainfall (Macdonald et al., 2008), especially if this occurs over an extended duration (Jacobs, 2004). As groundwater flooding requires water to exist in the subsurface, it typically occurs in areas with permeable underlying rocks such as Chalk and limestone (Jacobs, 2007; Cobby et al., 2009; Hughes et al., 2011). For further information on the mechanisms of groundwater flooding see Section 2.2, Zaidman (2014) or Hughes et al. (2011).

Unlike pluvial and fluvial flooding, flooding sourced from groundwater can last for weeks and even months in some instances (Macdonald et al., 2008; Hughes et al., 2011), such as in England during the winter of 2000/2001 (Jacobs, 2004) or in the Somme Basin in April 2001 (Pinault

et al., 2005). This increased duration, relative to fluvial flooding, can increase the economic cost per property (Green et al., 2006; Morris et al., 2007; McKenzie et al., 2010). The BGS groundwater susceptibility map indicates that a little more than 1% of England has the potential to flood from groundwater (Macdonald, 2010). Furthermore, McKenzie and Ward (2015) estimate 122,000 - 290,000 properties in the UK are at risk of groundwater flooding and it is suggested that groundwater flooding alone causes £210 million (ESI, 2015) - £530 million (Karam, 2016) of damage to the UK's economy every year.

Groundwater typically refers to water in a saturated subsurface, however water derived from the unsaturated zone (the region between the ground surface and the water table) may also be of interest to this study. As such, in this study *groundwater* will be taken to include water within the unsaturated zone.

Groundwater susceptibility maps have been produced that can inform users of the likely distribution of potential groundwater flooding in the UK. The BGS created a groundwater susceptibility map in 2009 based on geological and hydrological properties (British Geological Survey, 2013a) while JBA Consulting undertook a modelling based approach using historical groundwater levels and the physical properties of underlying aquifers (JBA Consulting, 2016). ESI (formerly GeoSmart Consulting) created a 5 m resolution groundwater flood risk map (ESI, 2015) that calculates flood risk according to the geologically defined hazard and the likelihood of occurrence, calculated using historical records. Due to the difficulty of discerning groundwater flooding from flooding from pluvial (rainwater) and fluvial (river) sources there is a distinct under reporting of groundwater flooding events and so there is likely to be scope for development in this latter example. More information on groundwater flood mapping can be found in Section 4.3.

1.1.3 'Multiple Sources'

Groundwater conditions can have a significant impact on the behaviour of surface water (An and Yu, 2014; Bennett et al., 2018) and, as such, high groundwater levels can increase the likelihood of flooding events from intense rainfall. In addition to the 122,000 - 290,000 properties at risk of flooding from groundwater, a further 980,000 properties are at risk of flooding from multiple sources (i.e. groundwater combined with fluvial or pluvial floods) (McKenzie and Ward, 2015). Despite this, due to the different time-scales and causes of these sources, they are typically considered separately.

Unlike groundwater or surface water, *flooding from multiple sources* is not yet a phrase that carries a set definition. In some works, such as the Environment Agency's MAST project (Environment Agency, 2011a), *multiple sources* refers to any combination of pluvial, pluvial, groundwater and coastal flooding. In this report it will specifically relate the interplay between surface water and groundwater. Flooding of this type is not thought to require individual sources to have the magnitudes to cause flooding individually. Mechanisms of multisourced flooding can be found in Section 2.3.

Multisourced flooding can occur due to high antecedent groundwater levels and/or conditions that have developed through the duration of a flood event. Multisourced floods refer to floods caused by the interplay of different sources simultaneously or in close temporal succession in a single event. This should not be confused with *areas susceptible to multiple sources of flooding*, which can experience both groundwater floods and surface water floods but may not necessarily experience them at the same time.

Few resources exist for quantifying multisourced risk. Of those in the literature that do, very few of these include groundwater despite the noted importance of antecedent conditions on stream flow (Saksena et al., 2019) and other hydrological processes. An example of this is a multisourced flood risk map proposed by the Environment Agency (Environment Agency, 2011a), which did not include reference to groundwater flooding due to the lack of existing research (Horritt et al.,

2010).

This PhD develops a methodology for classifying the risk of multisourced flooding that will aid future understanding of the relationship between the different sources and their combined hazard.

1.2 Risk, Hazard and Susceptibility

Flood *risk* is the product of the flood hazard and the vulnerability of the area exposed to the hazard (Schanze, 2006). The term *hazard* refers to the event itself, i.e. the extent and depth of a flood, but also takes into account the probability of the event occurring. *Vulnerability* refers to how much harm can be caused by the flood. This is a function of the exposure, susceptibility and resilience of the affected area (Balica and Wright, 2010) and can include factors that are economic (e.g. damage to property), social (e.g. loss of life or mental health impacts) and ecological (e.g. pollution or destruction of habitats). Understanding the overall risk posed by a flood is crucial as a significant hydrological flood does not necessarily mean a significantly damaging flood, or vice versa (Pielke, 1999).

Equation 1.2.1 — Risk. Flood risk takes into account three main factors, the event, its likelihood and the damage done by the event.

$$Risk = Hazard \times Vulnerability$$

$$Hazard = Event \times Probability$$

$$Vulnerability = Exposure + Susceptibility - Resilience$$

I.e. the risk posed by a 1 meter deep flood in an area may be defined as product of the likelihood of the flood's occurrence, the extent of the flood and the damage done to properties within that extent.

Throughout this thesis the term *susceptibility* is also used. Susceptibility differs from *risk* in that it does not take into account likelihood or vulnerability. Instead, it is used to define the potential to be exposed to an event. Examples of this are groundwater susceptibility maps (Sec. 4.3.2), which show areas that are thought to have the potential to flood from groundwater.

1.3 Aims and Objectives

This project develops a methodology for assessing multisource flood risk, considering both surface and subsurface processes as there is no current methodology for doing this in the UK at either a local or national scale. As there are national mechanisms for assessing single source flood risk and the joint risk of flooding from rivers and the sea, the project aims to produce a method that has the potential for national applications. Much of this work will focus on creating a modelling system in which catchment conditions, such as groundwater emergence and stream flow, are simulated in a hydrological model and then fed into hydraulic model for high resolution flow routing across the surface. The combined modelling of groundwater emergence, stream flow and rainfall will facilitate a greater understanding of the interplay between different sources and their combined flood risk. The groundwater levels and stream flows will be modelled using SHETRAN (Ewen et al., 2000), a physically based, spatially distributed hydrological model. HiPIMS (Liang

and Smith, 2015) will be used for the subsequent surface routing. Long duration synthetic weather conditions will be used to drive the modelling system and enable the simulation of extreme events and the attribution of event likelihoods.

The four main research questions for this project are:

1. Which catchments in the UK are most likely to benefit from a multisourced assessment of flood risk? (Chapter III)
2. Can an existing national scale, open source hydrological modelling system with a rapid automated set aid the proposed methodology? (Chapter IV)
3. When creating the multisource modelling system, what is an appropriate method for accounting for the different spatial resolutions of the hydrological and hydraulic models? (Chapter V)
4. How does the risk change when assessing flooding from multiple sources, compared to single sources, and what implications does the multisource assessment have on the way risk is currently considered? (Chapter VI)

1.4 Thesis Structure

Following this introduction, **Chapter II** provides further details on mechanisms of single and multisource flooding as well as details on other modelling strategies and historical floods. This further justifies the project, the choice of methods and models and outlines the research gap in light of the discussed literature.

Chapter III consists of a national scale investigation that identifies catchments most likely to be at risk of multisource flooding. This investigation takes 435 high resolution river flow records and uses them to create groundwater and surface water indexes. These indicate the presence of the respective sources within catchments across the England and Wales.

Setting up hydrological models capable of simulating groundwater levels requires high volumes of input data and is a complex process. Recent developments of the hydrological model *SHETRAN* have created an automated modelling system capable of the rapid set up of hydrological models for catchments across Great Britain. It is hoped that the methodology developed in this work would be simple to implement and, as such, the suitability of this automated national modelling system is assessed for use in this work. SHETRAN-GB can simulate river flows well in many UK catchments, however its ability to simulate groundwater levels is as yet untested (Lewis et al., 2018). **Chapter IV** assesses SHETRAN-GB's ability to accurately simulate groundwater levels by comparing suites of hydrological simulations against observed borehole groundwater levels for five case study catchments. Different setups run at different spatial resolutions and assess the performance of three open source hydrogeological datasets: the British Geological Survey's 1:650 000 scale digital hydrogeology map (British Geological Survey, 2016b), the Environment Agency's Aquifer Property Manual (MacDonald and Allen, 2001) and the British Geological Survey's 3D geology dataset (Mathers et al., 2014; Watson et al., 2015).

Chapter V focusses on creating a modelling system capable of simulating multisource floods. The chapter addresses the method of linking SHETRAN and HiPIMS with the aim of resolving the significant differences in spatial resolutions between the two models. A range of different groundwater redistributions are trialled and compared to each other and against historical groundwater emergence patterns. The village of Kilham in East Yorkshire is used as a case study.

Chapter VI compares single source and multisource flood risk for Kilham village and discusses the implications of such an approach. This implements the modelling system developed in Chapter V within the greater methodology (Fig. 20.1). A weather generator (Kilsby et al., 2007) provides long term synthetic meteorological data that is used in a 1000 year hydrological simulation. This simulation provides hydrological catchment conditions during peak events, that can be fed into the hydraulic model for high resolution mapping of the flood events with estimated likelihoods.

A conclusion in **Chapter VII** steps back and reviews the project and the main findings before discussing limitations and points for further work.

II

Literature Review

2. Sources of Flooding

2.1 Surface Water

Of the three types of flooding that will be looked at in this study, surface water flooding is the most well known and easiest to understand. As discussed in Chapter I, the term *surface water* will be used to refer to pluvial (rainfall) and fluvial (river) flooding (Fig. 2.1). Both of these can occur within a matter of minutes to a number of days following rainfall and have durations of the same range (Falconer et al., 2009). More detail on each of the sources is provided below.

Pluvial Flooding

Pluvial flooding can occur with little warning when the volume of rainfall being converted into runoff exceeds the drainage capacity of an area and ponds on the surface. This typically occurs in intense rainfall events and when high proportions of rainfall are converted into runoff, perhaps due to impermeable surfaces or water logged or frozen ground. Although this is difficult to spatially predict due to a lack of defined floodplain (Houston et al., 2011), pluvial flooding is especially prevalent in urban areas and this is where much of the related research is focussed (e.g. Ashley et al., 2005; ten Veldhuis et al., 2011; Gaitan et al., 2016; Löwe et al., 2017; Sörensen and Mobini, 2017). Cases of pluvial flooding have risen over previous years due to increased development on floodplains, the presence and growth of impermeable surfaces (Ashley et al., 2005; Houston et al., 2011), increasingly dense populations and ageing infrastructure. These factors can increase input to drainage systems during storms and heighten flood risk (ten Veldhuis et al., 2011). Pluvial flooding is thought to be the flood source that will be most affected by climate change, due to an increase in the frequency of intense rainfall events (Houston et al., 2011; Sörensen and Mobini, 2017).

A study by Sörensen and Mobini (2017) found spatial flood patterns to differ according to rainfall intensity. Flooding from short, high intensity storms was found to be more prevalent near to sewers and main drainage systems and flooding from long, less intense rainfall was less topographically controlled. Combined sewer and storm drainage systems were found to cause the majority of flood events in their study area. In these instances, untreated sewage can mix with flood waters to create an even greater hazard (Houston et al., 2011).

A Swedish study ascertained that more intense rainfall led to greater insurance payouts than less intense rainfall but that pluvial flood damages could still be caused by rainfall rates of only 12 mm/day. When looking at aggregated daily rainfall rates they found that 25-40 mm/day was able to cause more damage than rates of 80-100 mm/day (Grahn and Nyberg, 2017).

Fluvial Flooding

Similar to pluvial flood risk, fluvial flood risk[1] is influenced by the runoff rate of precipitation from rural land and the amount of available flow attenuation (Parrott et al., 2009). Runoff rates and flow attenuation are influenced by catchment characteristics such as size, land cover, slope and topography as well as the underlying soils and geology (Kundzewicz et al., 2018). They are also affected by anthropogenic factors such as urbanisation, which typically hastens a river's response to rainfall (Wheater and Evans, 2009).

Urban development on floodplains has created sites prone to fluvial (and groundwater) flooding, as well as creating increased flood risk downstream by reducing flood storage areas (Wheater and Evans, 2009). Urban developments can also reduce flow attenuation, and therefore increase flood risk, via the drainage of wetlands, lakes and ponds. However, where used appropriately, improved drainage can also decrease flood risk by quickly moving water away from vulnerable areas (Kundzewicz et al., 2018). Furthermore, well managed urbanisation coupled with sustainable urban drainage systems (SUDS) can decrease flood risk (Andoh and Iwugo, 2002; Zhou, 2014).

Away from urban areas, the intensification of agriculture may also have increased fluvial flood risk due to the loss of hedgerows, channelisation of rivers and installation of land drains (Wheater and Evans, 2009). The muddy floods of the South Downs are an example of this, where the wartime transition from grazing lands to cereal production led to greatly increased runoff rates (Boardman et al., 2003). The degree to which these factors affect the ratio of runoff to storage can change through time and may be seasonal, for example dry ground in the summer can form a less permeable crust and increase runoff and in winter there may be reduced interception from vegetation.

Reducing fluvial flood hazard typically focusses on decreasing the frequency that the river level reaches a critical depth at which flooding occurs. This can be achieved by altering channel geometry to increase the flow of water through the target area, decreasing the bed level, increasing the bank level, or reducing the peak flow (Lane, 2017). This last point may be achieved via catchment-based flood management (CBFM), a topic that has gained interest over recent years via natural flood management (NFM). CBFM and NFM seek to reduce river discharge during storm events, often via the creation of ponds or dams or by altering land use (Lane, 2017) as this can affect how the catchment responds to rainfall (Kundzewicz et al., 2018). Bare impermeable soils have high runoff coefficients, followed by pasture and agricultural land and then forests, which have low runoff coefficients due to increased interception, infiltration and storage. The addition of forest cover in catchments is broadly supported to decrease flow peaks in smaller events, however much of this evidence is based on models rather than observations (Stratford et al., 2017).

Historical Surface Water Flooding

There have been some significant surface water dominated flood events in the UK in the past few years. Recently, intense rainfall in June 2019 caused flash flooding in Yorkshire leading to the destruction of infrastructure, such as Grinton Moor Bridge, damage to properties and loss of crops and livestock (BBC News, 2019a). At the beginning of August further rainfall caused additional flooding and damage to Toddbrook reservoir (Hannaford et al., 2018), which resulted in the evacuation of 1500 local residents (BBC News, 2019b).

It is also worth mentioning the events of December 2015 in which the UK was hit by three successive storms: *Desmond*, *Eva* and *Frank*. Around 16 000 homes are estimated to have flooded in England as well as additional properties in Scotland. Storm Desmond increased the UK's recorded maximum 24 hr and 48 hr rainfall totals to 341 mm and 405 mm respectively. As these events occurred away from large aquifers they were almost entirely surface water driven, although

[1] See Merz et al. (2010a) for a useful and accessible review of fluvial flood risk management.

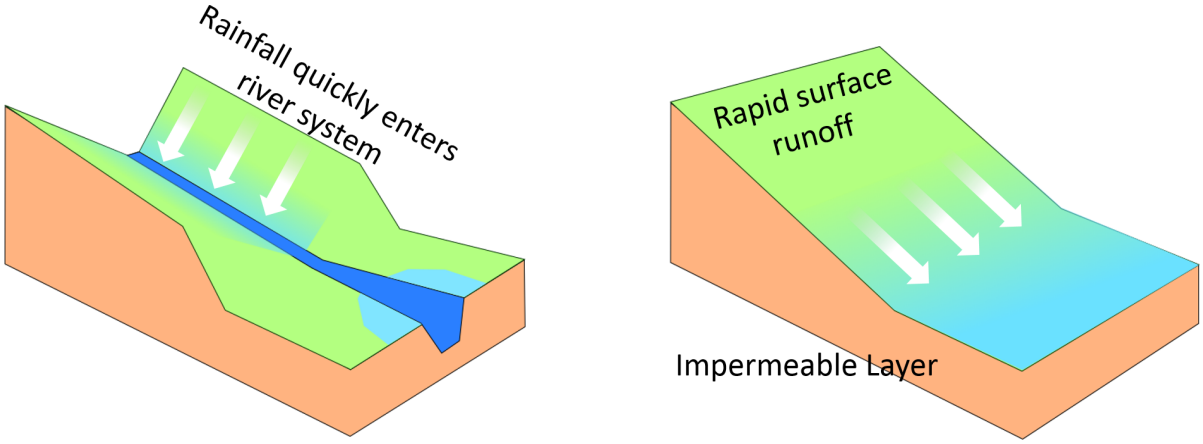

(a) Fluvial Flooding (b) Pluvial Flooding

Figure 2.1: Mechanisms of surface water flooding: Fluvial flooding occurs when water runs off the land and overwhelms the river system, flooding downstream via over topping or bursting banks. Pluvial flooding occurs from rapid surface water runoff prior to it entering the river system.

many soils were already at saturation following November rainfall (Parry et al., 2015). Storm Desmond damaged around 1200 bridges, roads and other infrastructure and led to estimated repair costs of around £120 million in Cumbria alone (ITV News, 2017).

In 2012 there was significant flooding around the country with many of the incidents caused by localised torrential downpours, as opposed to extreme fluvial flooding as was documented in 2007 and winter 2013/14. Around 8000 properties were flooded, but, while more extensive, this was much less damaging than the 2007 floods (Parry et al., 2012).

2.2 Groundwater Flooding

Groundwater flooding occurs when the water table rises above the ground surface (Fig. 2.2a) (Robins and Finch, 2012). This can lead to the flooding of basements and subsurface structures or services as well as the inundation of farmland, properties and infrastructure above ground and the surcharging of sewers and drains (Jacobs, 2007). This can last for weeks or months (e.g. Pinault et al., 2005) and is often regionally extensive (Macdonald et al., 2008) - as such, it can pose a particular risk to transport, disrupting or closing road and rail networks for extended periods (for examples see Hughes et al., 2011).

In addition to the damages normally associated with flooding, high groundwater levels can cause structural damage to subsurface structures due to increased pressure (Kreibich and Thieken, 2008). Furthermore, this additional subsurface pressure can create a buoyancy effect that can further damage buildings, such as in Dresden (Germany) where historical buildings had their basements deliberately flooded to avoid damage of this kind (Kreibich and Thieken, 2008). The diffuse nature of groundwater flooding means that fluvial style flood defences offer little benefit (Cobby et al., 2009).

The main causes for high groundwater levels are:

1. *Autogenic* (or direct) recharge, where high intensity and/or extreme prolonged rainfall occurs over permeable areas.
2. *Allogenic* recharge, where water flows from a watercourse into an underlying aquifer (Jacobs, 2007; Hughes et al., 2011).

Examples of the latter of these can be found in the Upper Rhine (Trémolières et al., 1993) and in the kastic limestones of Ireland (Naughton et al., 2018b). As groundwater can often flow

far through the subsurface, these mechanisms can lead to flooding both within and far from the recharge area.

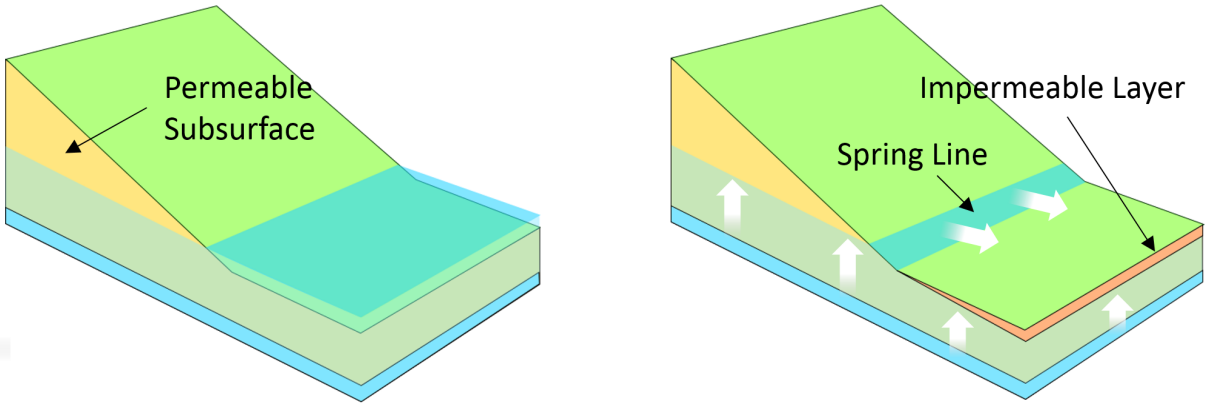

(a) Groundwater flooding (b) Groundwater induced flooding

Figure 2.2: Groundwater flooding occurs as the water table rises above the surface whereas groundwater *induced* flooding occurs from groundwater that has emerged upslope and flowed across the surface, often initiating from springs.

Groundwater Flooding Via Superficial Deposits

Allogenic recharge can pose a particular groundwater flood risk where watercourses are surrounded by permeable superficial deposits. These unconsolidated sediments are often highly permeable but with relatively low storage capacities and have groundwater levels close to the surface for much of the year (Macdonald et al., 2012). Increased river levels during or following storm events can rapidly raise the surrounding groundwater levels (Macdonald et al., 2008), perhaps within a number of hours and may match the levels in the associated watercourse. These groundwater flows can bypass river banks and flood defences (Hughes et al., 2011). As such, groundwater flooding in low lying surrounding areas does not require the river to overtop its banks and may precede the river level peak. Increased river stages caused by fluvial flood defences may increase groundwater flooding by creating enhanced pressure gradients between the river and the subsurface (Jacobs, 2007).

If these unconsolidated materials sit atop of permeable deposits then the antecedent groundwater conditions may influence whether they drain or flood during a storm or river recharge event. Groundwater flooding of this type is unlikely to be as persistent as flooding from consolidated aquifers as levels can drop quickly once river levels decrease (Jacobs, 2007). A well used case study of groundwater flooding via unconsolidated superficial deposits is Oxford, which has flooded in 2000, 2003 and 2007 (Macdonald et al., 2007, 2012).

Groundwater Rebound

One further cause of rising groundwater levels is the cessation of groundwater abstraction, potentially due to a decline in industry, that allows groundwater levels to rebound to their natural levels (Hughes et al., 2011). This may be of particular consequence for previously industrial urban areas or areas where the groundwater levels were previously lowered for mining purposes (Cobby et al., 2009). Such areas include London, Birmingham, Nottingham and Liverpool (Macdonald et al., 2008).

Groundwater Induced Flooding

Springs occur where groundwater emergence is focussed at a point source. These may occur only in periods of high groundwater levels or all year round and may be linked to the presence of a

confining impermeable layer, as is shown in Figure 2.2b. Spring water that has flowed across the surface and caused a flood is termed *groundwater induced* flooding (Robins and Finch, 2012).

Ephemeral Streams

Many rivers that flow over a permeable subsurface are intermittent or ephemeral. This means that they only flow at certain times of the year or following rainfall, when the water table is high. Figure 2.3b shows an example of this where the volume of water emerging into the the stream is enough to cause flooding. Although confining impermeable layers can impede the flow of groundwater to the surface, rivers and other structures can break this boundary and can provide pathways for groundwater flow.

Groundwater flooding of this type lasted several weeks in the Test and Itchen catchments in the winters of 1994-1995, 2000-2001 and 2002-2003. In these instances high winter rainfall caused stream heads to migrate several kilometres upstream (Allen and Crane, 2019).

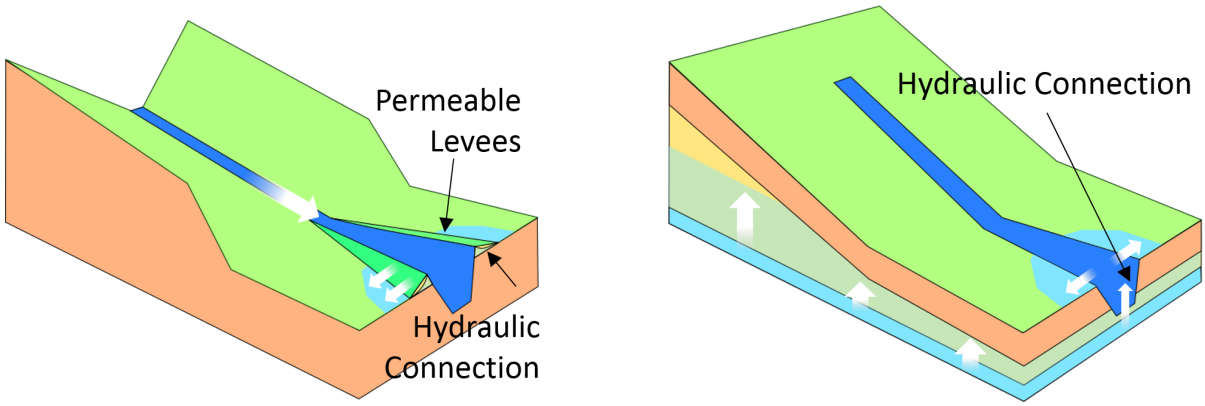

(a) Groundwater flooding via permeable river deposits

(b) Groundwater flooding from gaining stream.

Figure 2.3: Rivers can also play a part in groundwater flooding, either conveying water out of the watercourse through permeable deposits or by providing a pathway for groundwater to reach the surface.

Historical Groundwater Flooding

While groundwater flooding is thought to be under reported (Cobby et al., 2009; Naughton et al., 2018a), there have been numerous notable floods over the past decades. These include localised events in the winters of 1993/1994, 1994/1995, 2002/2003 and larger events in the winter of 2000/2001 in the south east of England (Finch et al., 2007), in the summer of 2007 in England and Wales (Marsh, 2007) and in the winter of 2013/14 in southern and central England (Ascott et al., 2017).

During 2007, extreme rainfall during May, June and July led to above average groundwater recharge in permeable catchments. The high groundwater levels caused increased spring flows and seepages and contributed to the flood peaks and durations in some permeable catchments (Marsh, 2007). These instances, in which groundwater contributed to river flows, demonstrate the potential for interactions between different sources of flooding (e.g. Fig. 2.6) that this project addresses. It was also the summer of 2007 that saw the well known groundwater flooding in Oxford. Here, high river flows caused increased recharge of the superficial sands and gravels surrounding the channel and caused groundwater levels to rise and flood a number of properties (Macdonald et al., 2012).

The winter of 2013/14 was the wettest winter on record with persistent heavy rainfall. At the start of December 2013 groundwater levels were around their usual range, however, by the

end of January, following repeated storms, record levels were measured in many boreholes across the southern Chalk. This led to extensive groundwater flooding during February and continuing localised flooding into early summer. The floods led to several deaths and associated costs estimated up to £1.5 billion (Ascott et al., 2017).

2.2.1 Major Aquifers of the UK

The geology of the UK is diverse, with rocks dating from as far back as the Proterozoic. Although its history has included periods of orogenies, faulting and volcanism, the majority of the UK is now covered in sedimentary rocks, many of which form aquifers. These can be seen in Figure 2.5 (from Rivett et al., 2007). The north of the England contains the oldest of the aquifers, the Carboniferous Limestones; these transition into the Permian limestones, Permo-Triassic sandstones and Jurassic limestones, all running in bands down the country. The youngest aquifers are the Greensands and Chalks that dominate much of the south of the UK. Of these, the Chalk, Permo-Triassic Sandstones, Jurassic Limestones and the Lower Greensands are the most important for water resources (UK Groundwater Forum, 2009), however any that are able to transmit water to the surface have the potential to pose a flood risk.

In Chapter IV several case studies are used to test the groundwater modelling potential of an automated hydrological model - due to the distribution of the previous studies that these are built on, these are all located in England. The brief outline of aquifer systems also focusses on England, however it should be noted that there are also highly productive aquifer systems in Scotland (Ó Dochartaigh et al., 2015b), which can be seen in Figure 2.4 and Ireland. A comprehensive description of the mechanisms of flooding in the karstic limestones of the Republic of Ireland can be found in Naughton et al. (2018b). Much of the following information on the aquifers of England and Wales is summarised from Allen et al. (1997).

Groundwater flooding can occur through superficial deposits (Sec. 2.2), however these are not considered to be major aquifers. Such materials are deposited by fluvio-glacial processes and so are generally restricted to floodplains and river terraces and include sands, gravels, glacial tills and aeolian sands (Jacobs, 2007).

Chalks

Chalk is a soft, white, fine grained ($<$10 μm) limestone. The Chalk aquifer of the UK, and much of north-west Europe, was formed through the Upper Cretaceous period as sea levels rose, covering much of England. The reduced flux of terrestrial material to the marine environment allowed the build up of very pure calcium carbonate from microscopic planktonic algae. The Chalk also contains marl layers. These are cm's thick and can be laterally extensive (Allen et al., 1997). These bands are harder than the Chalk and contain a much higher proportion of clays and silts.

Chalk is the UK's primary aquifer, outcropping over 21 500 km^2 with thicknesses of several hundred meters in parts (Allen et al., 1997) and generating around 80% of the public water supply (Butler et al., 2012). Chalk allows water to flow through both its matrix and its fractures - termed *dual porosity*. This also means that the chalk water table has the potential to respond not only to long term rainfall events but intense storms (Ireson et al., 2009) and can transmit water into the river system very rapidly (Soley et al., 2012).

This dual porosity makes the Chalk difficult to model. Despite its high porosity, the hydraulic conductivity of the chalk matrix is low (e.g. 6.4×10^{-4} m/day), much less so than that of the fractures. These fractures have low permeability, but can transmit water at 100s to 1000s of meters/day. As such, the transmissivity of the Chalk depends of the volume of fractures. This means that there are higher transmissivities closer to the surface and transmissivities are greater in river valleys than in the interfluves (Allen et al., 1997; MacDonald and Allen, 2001), potentially by an order of magnitude. The Chalk aquifer is regionally heterogeneous due to differences in

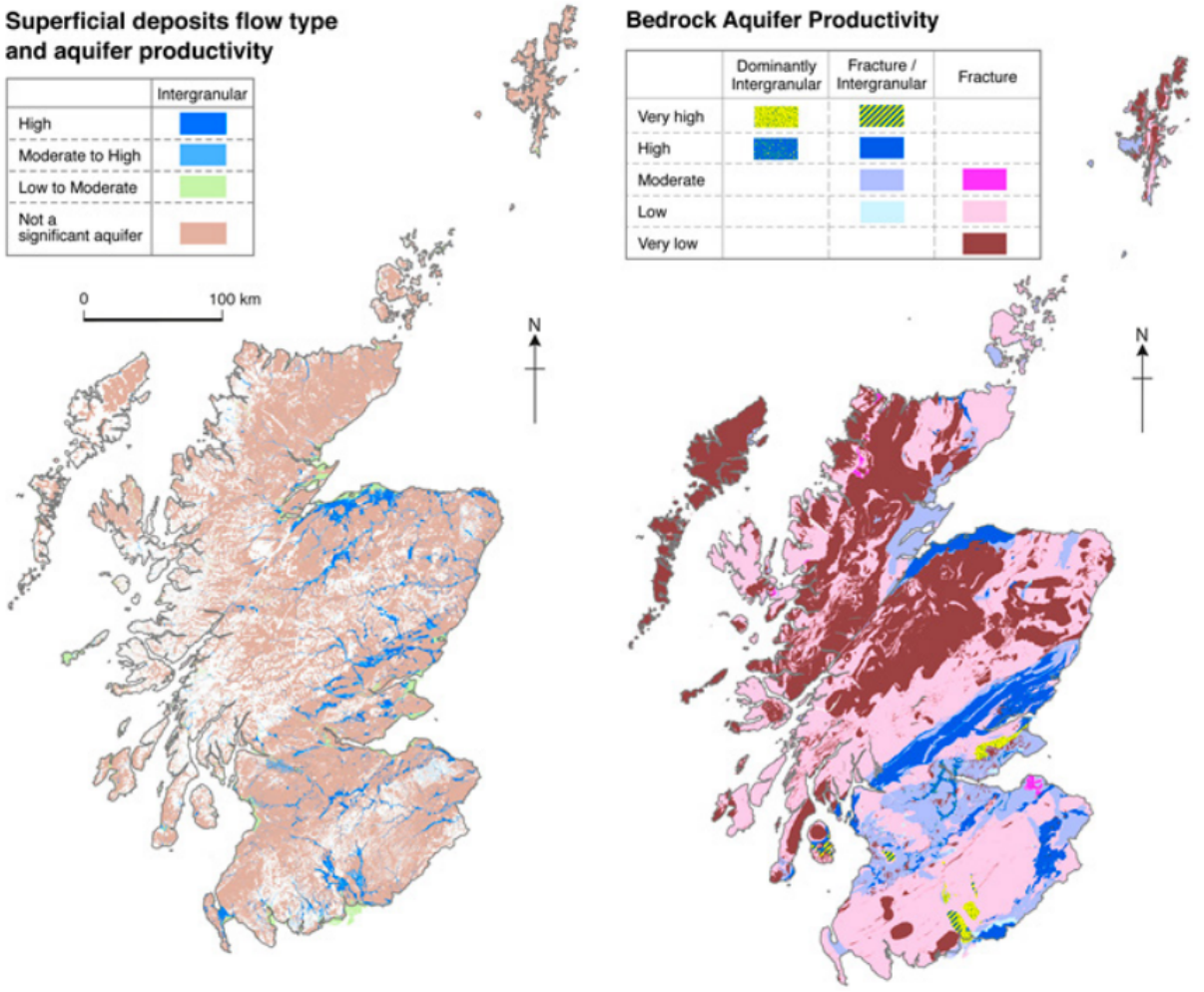

Figure 2.4: Aquifers of Scotland. Taken from Ó Dochartaigh et al. (2015b), original material from Ó Dochartaigh et al. (2015a)

its formation, diagenesis and subsequent tectonic experiences. As such, the Chalk in the north of the UK is generally harder and less porous than that of the south of the UK (Allen et al., 1997). Geological heterogeneity within chalk aquifers mean that they are particularly difficult to model and hard to parametrise. The behaviour of chalk aquifers in extreme conditions is poorly understood and, as such, the ability of traditional approaches to model chalk aquifers has been called into question following recent groundwater flooding and droughts. There is a growing understanding of the dual porosity of chalk and development of coupled matrix-fracture flow models (Butler et al., 2012).

Jacobs (2004) states that there are fewer reports of groundwater flooding in the northern Chalks than in the south and concludes that higher transmissivities and impermeable drift cover may make the northern Chalks slightly less vulnerable to flooding than those of the south. For further details on parametrising the Chalk see MacDonald and Allen (2001) and Sections 13.1.1 & 13.1.5 of this thesis.

Limestones

Many of the limestones in the UK were deposited in the tropical Jurassic period. During this period a variety of sediments were laid down, with limestones forming in shallow marine environments where there was a reduced volume of clastic material from the land. Limestones

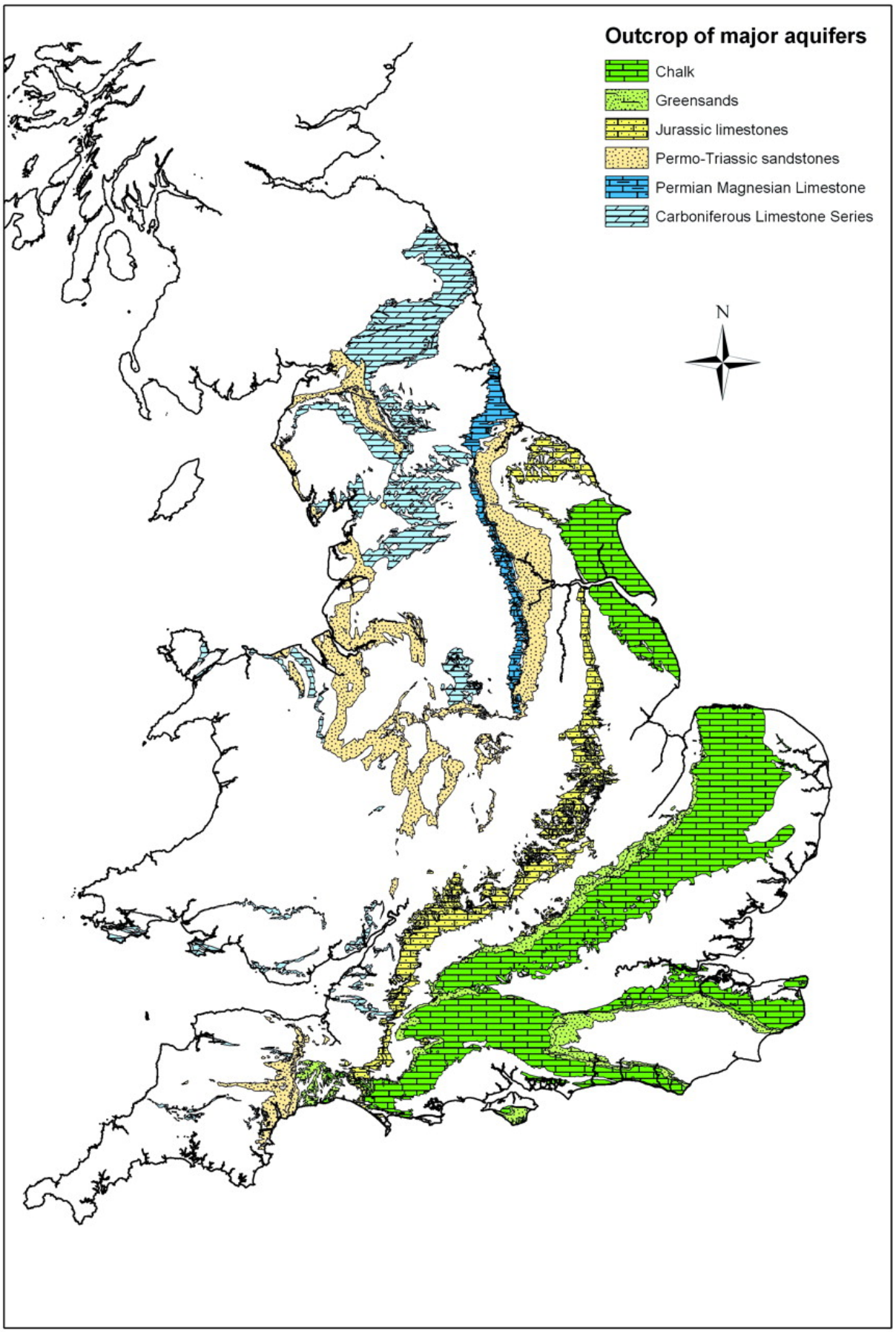

Figure 2.5: Aquifers of England and Wales. Taken from Rivett et al. (2007).

were preferentially laid down in basins with higher, thinner deposits typically eroding. As such, four main basins exist in the UK with different sequences in each, though there is similarity between some. The rise and fall of sea level during this period has interbedded the limestones with shales, clays and sandstones. It is the limestone beds, which are often relatively thin, but extensive, that make up the main Jurassic aquifer. The limestones have high transmissivities but low storage coefficients. This allows limestone outcrops to respond quickly to recharge and to have large seasonal variations in groundwater level. These aquifer beds can be very thin, meaning that in many places they may only form lenses or may be hydraulically isolated by faults (Allen et al., 1997).

As with the Chalk discussed above, intergranular flow is very low and most occurs via fractures. As limestone is soluble in water, many of these fractures are enlarged by groundwater flow and therefore can have considerable yields. As such, the volume of water that can be transmitted through the aquifer varies spatially, depending on the presence of these fractures. The interbedded clay aquitards mean that many of the aquifers are anisotropic, with typically higher conductivities horizontally than vertically (Allen et al., 1997).

The less extensive and slightly older Permian-Magnesian limestones have similar characteristics to those mentioned above, with low matrix hydraulic conductivity and preferential flow in fractures. This is therefore spatially variable, with flow dependent on the presence of fracturing (Allen et al., 1997). As with all of the limestones and Chalks discussed here, the variation between the flow in the matrix and the flow in the fractures makes these units difficult to parametrise and model.

Limestones were also deposited in the earlier Carboniferous period. These outcrop further to the north and west than their Jurassic counterparts and are typically more *karstic*. Karstic limestone refers to instances where high fracture porosity and solubility has led to the formation of enlarged fractures, conduits and caves. Although the limestone matrix has a very low permeability that provides little potential for groundwater flow, instead, the majority of flow occurs via the network of fractures and karst system, which has the potential to transmit water at 100s of meters per hour. This means that groundwater flow can vary spatially dependent on the presence of a fracture system. Such systems can form discrete systems that link recharge areas to certain spring locations (Allen et al., 1997).

Allen et al. (1997) states that the fast response times of unconfined Jurassic aquifers means that the groundwater and surface water processes are closely linked while Jacobs (2008) states that there may be possible groundwater flooding from the Carboniferous limestones as the fracture flow responds rapidly to rainfall. Jacobs (2008) suspected that Jurassic and Magnesian limestones may produce localised flooding. As such, both are potential locations for the multisource investigations of Chapter III. For more information on the Jurassic limestone aquifer see Section 13.1.4.

Sandstones

There are three main sandstone aquifers in the UK. The Cretaceous Upper and Lower Greensands and the Permo-Triassic sandstones. Greensands are a type of sandstone named due to its content of glauconite, a green iron-rich mineral (The Geological Society, 2008).

The Upper Greensand is a poor aquifer with a thickness of up to 60 m that underlies some of the Chalk aquifer, with which it has hydraulic connection. It is lithologically heterogeneous but is typically fine grained and calcareous with flow occurring both through the matrix and through fractures. There is limited recharge to the Upper Greensand from the surface due to a lack of outcropping.

The Lower Greensand is composed of lithologically variable sands and sandstones interbedded with localised clay-rich layers or sandy limestones (Ward, 2014). The Lower Greensand is separated from the Upper Greensand by the Gault (clays). Its shared name with the Upper Greensand is an artefact from earlier times when the two were easily confused. Like the Upper Greensand, it also has a small outcrop area. Although the Group can be found in Norfolk and Lincolnshire,

it is very thin and so is only used as a significant aquifer in its southern extents. The Lower Greensand is not hydraulically connected across its extent and is, in some places separated by clay layers with relatively little mixing of groundwater between the layers (Allen et al., 1997).

The Permo-Triassic sandstones form the largest aquifer system in the UK (Jacobs, 2004). In places the Permian sandstones are separated from the later Triassic sandstones by an aquitard of Permian marls. Unlike the limestones and Chalks, these sands formed in a terrestrial environment from fluvial and aeolian processes. There are multiple fining sequences with a general fining upwards from gravels to sands, silts and muds and these often contain extensive clay layers from flood deposits. Grain size, geometry and cementation are primary controls on hydraulic conductivity. Hydraulic conductivities can range from 10^{-6} m/day to 20 m/day (median of 0.56 m/day) with the finer deposits having lower permeabilities and acting as confining layers. Those sands formed by fluvial processes are anisotropic with layers of differing grain size impeding horizontal flow. Fractures can have significant effects of the parametrisation of the aquifer by offering preferential flow paths along bedding-planes and tectonic and diagenetic joints. While faults can create recharge boundaries some can also impede flow (Allen et al., 1997).

The Upper Greensand poses only a small groundwater flood risk due to its classification as a poor aquifer and small outcrop area. This can also be said for the northern extents of the Lower Greensand due to its thin strata and similar lack of outcrop. Even in the south of the UK, where the Lower Greensands are more extensive, groundwater flooding is unlikely due to due its low permeability (Jacobs, 2004). Furthermore, the Permo-Triassic sandstones, despite their much greater extent, are not thought to pose a significant groundwater flood risk (Finch et al., 2007) and there are very few recorded flooding instances (Jacobs, 2004; Robins and Finch, 2012) even when groundwater levels have been exceptionally high (British Geological Survey, 2014a). Groundwater flood risk from sandstones should not be dismissed however and high groundwater levels may recharge rivers and increase discharge from springs (Finch et al., 2007; GeoSmart Information, 2019b).

2.3 Multisource Flooding

There is relatively little peer reviewed literature on groundwater flooding (Abboud et al., 2018) and this is even more true for multisource (groundwater-surface water) flooding. As such, little documentation on the hazards posed by multisource flooding could be found. The literature that is available on groundwater-surface water interactions focusses on water resources (e.g. Doble et al., 2012), non-flood generating processes (e.g. Fleckenstein et al., 2006; Krause et al., 2007; Parkin et al., 2007; Harish Kumar and Nagaraj, 2018; Li et al., 2019; Salem et al., 2020) and even landslides (e.g Wang et al., 2019). The majority of literature found on river-groundwater interactions addressed groundwater recharge and flooding via superficial deposits, as is discussed in Section 2.2 (e.g. Trémolières et al., 1993; Hoehn and Scholtis, 2011; MacDonald et al., 2014; Macdonald et al., 2018). It has been shown that in some locations intense rainfall can drive groundwater flow in shallow aquifers and that streams can rise due to emergence groundwater before, or more significantly, than from direct runoff from the rainfall event (Guérin et al., 2019).

The interaction of pluvial and fluvial sources during flood events may also be categorised as multisourced flooding, although they are not the focus of this study. These sources frequently coincide creating floods more severe than if they occurred separately (Chen et al., 2010). These are much better studied than their interactions with groundwater flooding (e.g. Patra et al., 2016; Breinl et al., 2017; Rizeei et al., 2019).

Despite the lack of information, it is known that antecedent moisture conditions in soil and the subsurface affect surface water flooding (Vivoni et al., 2007; An and Yu, 2014; Bennett et al., 2018) and it is known that there are many locations around the UK where this is likely to occur (McKenzie and Ward, 2015). Two simple mechanisms for multisourced flooding are proposed

below by which groundwater and surface processes interact to cause enhanced flooding:

1. High groundwater levels, and therefore a saturated subsurface, decrease available storage during rainfall events and thus cause increased runoff and enhanced surface water flooding (Fig. 2.6a. This may be followed or accompanied by a groundwater response either due to *piston flow* or a further increase in groundwater levels. This is proposed to be most likely in areas with highly permeable underlying aquifers that can rapidly respond to rainfall, such as the Chalk.
2. High groundwater levels bolster gaining watercourses and inundated floodplains, decreasing fluvial drainage capacity and increasing the depth and duration of flooding. This can be seen in Figure 2.6b and is said to be one of the greatest groundwater flooding risks (Cobby et al., 2009).

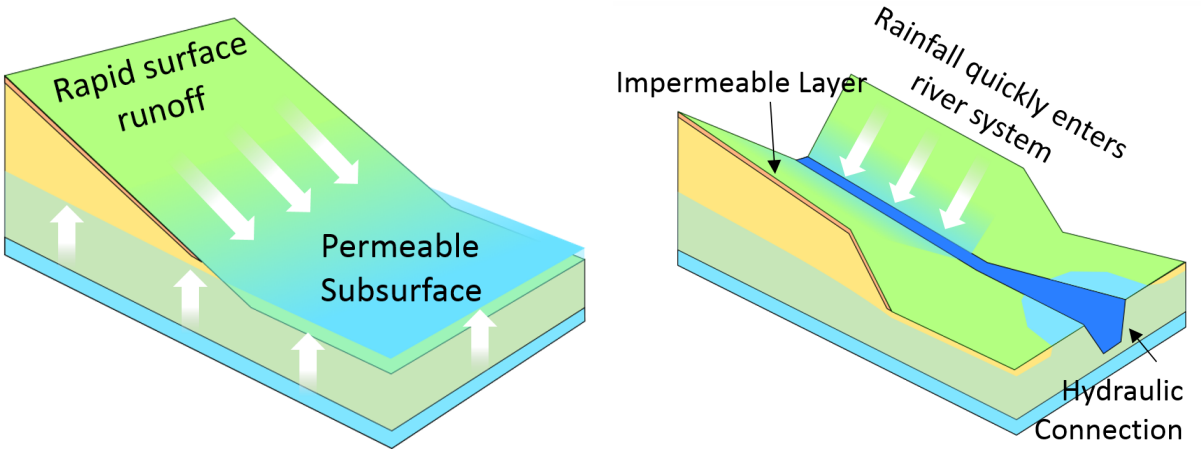

(a) Pluvial and groundwater sources.

(b) Fluvial and groundwater sources.

Figure 2.6: Two proposed mechanisms of multisource flooding.

It is proposed that the magnitude of the surface water and groundwater components in a multisource event are not required to be as large as those in a single source event. For instance, it is unknown what likelihood component sources of a multisource flood event are required to equal that of a comparable single source event - i.e. whether a 1 in 100 year fluvial event can be matched by 1 in 10 year groundwater levels coinciding with 1 in 10 year rainfall. The processes involved between the single source and multisource floods will differ and so direct comparisons may not be appropriate but the temporal interplay of these does warrant further investigation outside of this study (e.g. Lian et al., 2013; Breinl et al., 2017; Rizeei et al., 2019).

Several characteristics are proposed to lead to a catchment being multisource, these can be simplified into characteristics that generate rapid runoff and characteristics that provide a slower subsurface response to rainfall. These relate largely to the geology of the catchment and its land cover however there are a range of contributing factors. These have been split into three groups, described below. Descriptions include example catchments found during initial searches for multisource catchments. These include several tributaries to the Thames around London due to the presence of chalk, low permeability superficial deposits and urbanisation. This pattern reflects well the findings from a regional flood risk appraisal for the South East of England (Halcrow, 2008) that states that the Kent Thames Gateway and the South Hampshire Region have moderate groundwater flood risk with districts such as East Hampshire, Basingstoke and Dean, Winchester, and Chiltern having a high risk of flooding from groundwater and related surface water flooding. The report *"emphasises the importance of assessing flood risk of an area from all sources of flooding, not just fluvial and coastal..."* (Halcrow, 2008, pp.5). Three additional

potential multisource catchments are included in the Appendix (Sec. 27).

2.3.1 Saturated Catchments

It is proposed that the simplest form of multisourced catchment is one that is highly permeable but that can generate surface runoff when fully saturated. The River Ouse catchment near Brighton is an example of this. The catchment is interlaced with permeable Greensands and impermeable clays. After sustained rainfall the sands fill up and the catchment suddenly becomes extremely flashy (pers. com. S. Manning-Jones, Sussex Flow Initiative, 2nd May 2017). There is recorded multisourced flooding in the catchment with several properties flooded by an event in the winter of 2000/2001 (DEFRA, 2015). This area has similar geology to the nearby Wealden geological group (bands of sandstone and clays), which are also known to flood from *'surface water run-off from the South Downs, particularly at times of high groundwater levels'* (Mid Sussex District Council, 2015, pp 57). According the NRFA, the Ouse at Gold Bridge is *"...is subject to flashy flows in summer & more prolonged flooding in winter. Flooding can be extensive with the valleys either side of the river inundated"*.

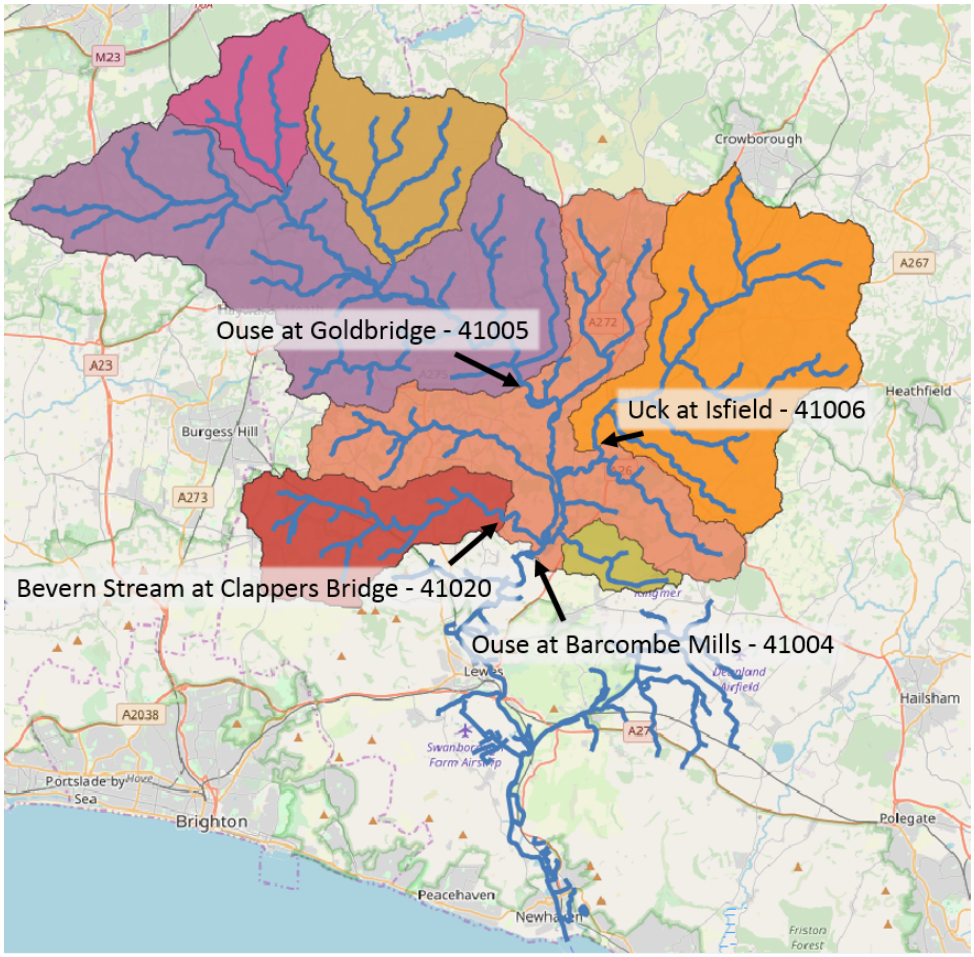

Figure 2.7: The River Ouse and its sub-catchments. ©OpenStreetMap

2.3.2 Mixed Characteristic Catchments

The second group of catchments are proposed to have a mix of characteristics. These require there to be separate characteristics able to generate both groundwater and surface water responses to rainfall. This may be in the form of a highly permeable bedrock layer that responds gradually

to rainfall mixed with a less permeable layer of bedrock or superficial deposit that generates a surface water dominated response. There are a range of possible causes for both of these opposing responses. Surface water, for example, can be generated not only by impermeable geology but also by the presence of urban areas or steep topography.

One example of this is the Pang catchment, a well studied chalk catchment in the south of England. According to the NRFA, the upper catchment has a 97% covering of highly permeable bedrock, decreasing to 83% by the middle of the catchment and to 76% by the lowest gauging station an Pangbourne (NRFA, 2019b). The presence of impermeable tertiary deposits in the lower catchment cause significant surface runoff in contrast to the baseflow dominated upper catchment (Peters and van Lanen, 2005). There have been groundwater floods in the winters of 2001/02 and 2012/13 and groundwater is reported to be a significant contributor to fluvial and pluvial flooding. Groundwater flooding has occurred in multiple locations around the catchment and from groundwater fed water courses such as Sulham Brook. The catchment is also at risk from fluvial and pluvial flooding, with one particularly bad instance of flooding in 2007 following an intense storm after weeks of prolonged rainfall, which had saturated the catchment (West Berkshire Council, 2013).

A similar multisourced response is present in the groundwater dominated Chalk catchment of the River Misbourne, which drains from the Chiltern hills towards London. Although it rests on highly permeable Chalk bedrock it has a 42% covering of low permeability superficial deposits. Here, sharp peaks in river level have been experienced that can be transmitted down the catchment with both upper and lower stage gauges recording rapid peaks (R. Lamb, JBA, pers. com. 12th April 2016). There are multiple Section 19 reports of a good standard for the area (Buckinghamshire County Council, 2017) including reports of flooding due to high groundwater levels and mentions of surface water (Buckinghamshire County Council, 2014). According to Jacobs (2008), both the Misbourne and the neighbouring River Chess have chalk catchments that cause both groundwater and surface water flooding. It is unclear however from the report whether "surface water flooding" is due to runoff in intense rainfall events or poorly maintained, blocked culverts during standard rainfall.

The River Wye is another example flowing from the Chilterns, passing through High Wycombe and into the Thames. According to the NRFA, the Wye, until its confluence with the Thames at Hedsor, is baseflow dominated Chalk catchment with flashy responses. Unlike the two examples above, this is attributed to the presence of urban developments over approximately 20% of the catchment. There are also glacial flints and fine grained glacial clays covering around 40% of the catchment increasing the extent of the low permeability surface further. There is historical groundwater flooding from the River Wye in and around High Wycombe, Hughenden Valley and Radnage in the winter of 2013/2014. High Wycombe is particularly vulnerable to fluvial and pluvial flooding from the Wye and Hughenden due to the steep local topography (an average descent of 90 m/km). Furthermore, there is a known interconnection between surface water and groundwater sources. 17 properties were flooded in the area in the winter of 2000/2001 (Jacobs, 2014). Further information about the south of the catchment can be found in Jacobs (2009).

2.3.3 Split Catchment

One way in which the above conditions could be satisfied is via a split catchment, i.e. a catchment that is composed of sub-catchments with differing characteristics. This is demonstrated by the Kennet catchment (Fig. 2.8), another tributary to the Thames.

The source of the Kennet is near Silbury Hill (Scott Wilson, 2008a), from there it is gauged at Marlborough, Knighton and Newbury before joining the Thames near Reading. The upper reaches are rural with mostly permeable Chalk bedrock and limited impermeable superficial deposits. As such, it is baseflow dominated until its confluence with the Enborne. The Enborne has a

largely impermeable catchment due to the presence of Tertiary clays, which give it a responsive regime. Beyond the confluence, the Enborne adds a flashy, surface water component to the otherwise groundwater dominated River Kennet (NRFA, 2019b). This therefore has the potential for intense rainfall over the Enborne catchment to meet high groundwater flows from long term above average rainfall in Kennet's headwaters, thus creating multisourced events. Figure 2.8 shows the distribution of high permeability and low permeability bedrock in the catchment.

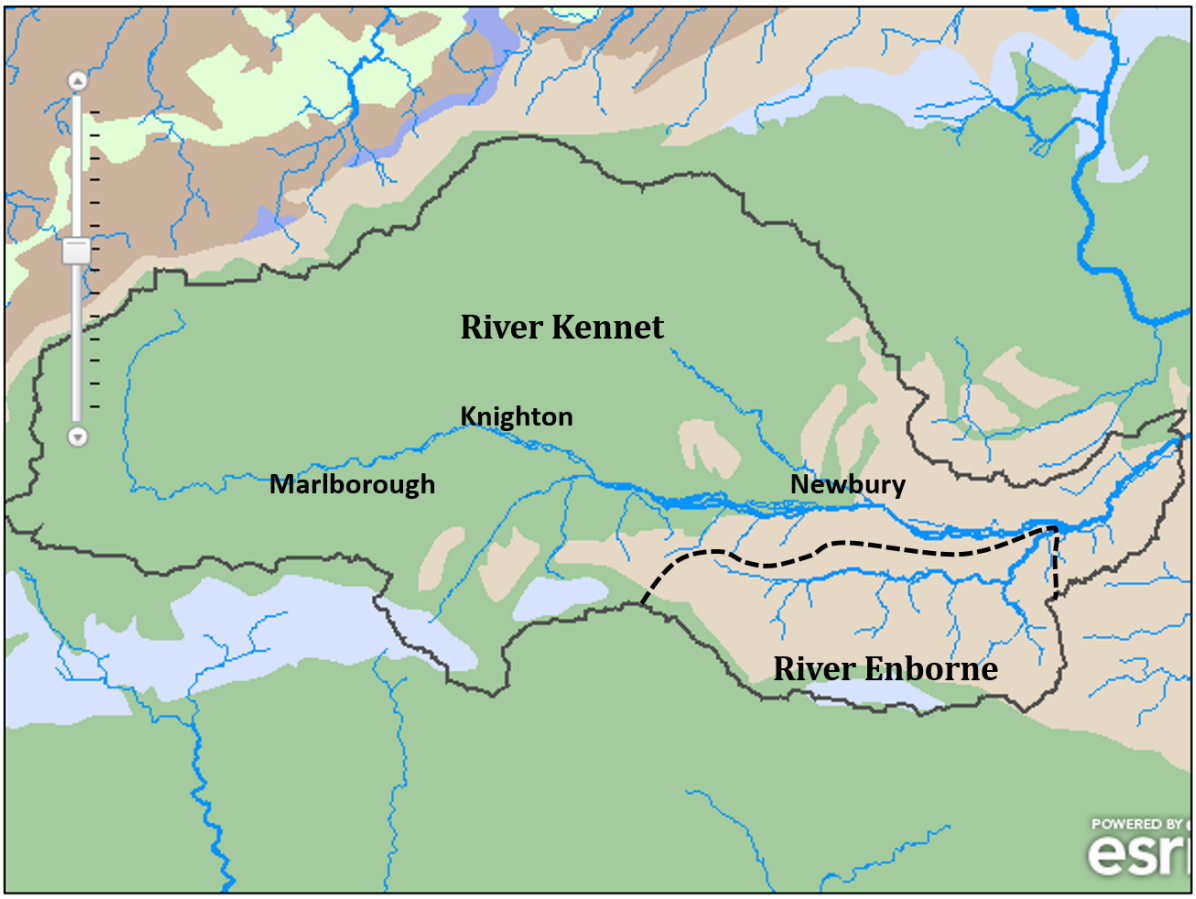

Figure 2.8: The River Kennet catchment, adapted from NRFA (2019b). Green - high permeability geology; brown - low permeability geology. The River Kennet exhibits a multisourced response due to the confluence of the flashy Enborne catchment with its own groundwater regulated regime.

Higher up the catchment, where the chalk aquifer is unconfined, there is potential for groundwater flooding and there are recorded instances in the villages close to the Og tributary (Scott Wilson, 2008a) and the dry valley near Ogbourne Maizey (Scott Wilson, 2008b). In addition, there are reports of combined fluvial and groundwater events in the nearby Avon catchment in 2002 and 2000 in Tidworth and Enford respectively (Scott Wilson, 2008a).

3. Flood Modelling

Computer modelling of hydrological processes can take two main forms. (1) Statistical and empirical modelling, which are based on functions and observations, and (2) physically based modelling, which mathematically describe processes according to their measured properties and established physical laws (Wheater, 2002). Physically based modelling requires detailed knowledge of catchment characteristics (Binley et al., 1991), such as geology and land cover, and attributes these with realistic parameters reflecting hydrological processes, such as how fast surfaces or mediums transmit water or how they interact with meteorological processes.

This section discusses different modelling approaches and some of the models available in the literature[1]. The following terminology is used throughout and is useful to define in advance. Firstly, models can be categorised into either *lumped* or *distributed* models according to how they consider the domain spatially. *Lumped models* treat a domain (i.e. the area being modelled) as a whole with a single output, with parameters representing averages of the whole domain or sections of it. *Distributed models* describe a system by spatially dividing it into multiple units and attributing each with a set of parameters that describe its hydrological processes. These spatial units can be abstract, perhaps representing sub-catchments within a larger system or areas with differing hydrological regimes. They can also be more structured, perhaps dividing a system into a regular grid or TIN (Devia et al., 2015). Outputs can be created for any location within the model. Distributed models are of the most interest to this study and will typically fall into one of two categories: *hydrodynamic* or *hydraulic models* and *hydrological models*. *Hydrodynamic* and *hydraulic models* focus on the mechanics of water movement and solve physically based equations to route water through a domain. *Hydrological models* simulate elements of the wider hydrological system, such as climatic and land surface conditions and can be used to improve the understanding of hydrological processes (Wheater, 2002). These differ in complexity and can be conceptual[2] or physically based (Dechant and Hamid, 2014).

In physically based modelling the number of parameters required for each unit typically depends on the complexity of the model, with complex models often requiring very large or varied data. Parameters may describe runoff speeds or ratios for different vegetation types or slopes, or the permeability and transmissivity of different rock or soil types. It is often very important that the hydrological processes are well parametrised in order to produce accurate simulations. However, these parameters are often adjusted in instances where models are unable to accurately capture hydrological processes or where accurate parametrisation is not possible. This process of manually adjusting parameters to improve model performance is called calibrating; this typically

[1] An accessible review of flood modelling can be found in Wheater (2002).

[2] A conceptual model is a broad term generally referring to simplified description of a system and the relevant processes within it. Examples of conceptual models can include generalised mathematical formulae or diagrams showing the hydrological processes and their relationships.

involves inputting recorded meteorological conditions (i.e. rainfall) into a model and adjusting parameters until outputs (i.e. groundwater levels or river flows) match observations. Calibrating a model may improve its performance but can also decrease how realistically it captures the hydrological processes within the system that it has been built to represent. Furthermore, by adjusting model parameters according to observations the model may no longer be appropriate for use outside of the range of hydrological events that it has been calibrated with.

Spatially distributed, physically based models seek to reduce reliance on calibration by accurately capturing hydrological processes by modelling using accurate parameters. The use of physical parameters enables these types of models to operate outside of their calibration limits (Beven, 2012), a key part of the methodology proposed here and enacted in Chapter VI. It also allows them to be used in ungauged river catchments or areas that do not have observed data to calibrate against. Furthermore, models can be more easily reproduced as they have not undergone manual tuning and are well suited for increasing the understanding of hydrological systems. Two downsides to physically based modelling, however, are the significant demands for data and the high level of complexity required so that models can mathematically capture all necessary hydrological processes (Lewis et al., 2018). In reality, even the most detailed and well parametrised models often require some degree of calibration.

This project will employ a physically based modelling approach as it allows for *fully distributed* simulations in which models are able to describe the hydrological processes at all points within the simulation domain without being constrained to their calibration limits.

As previously discussed, this work will look at surface and subsurface flow modelling and join two models together to make a single multisource modelling system. These surface and subsurface processes differ in both their temporal and spatial scales and typically use different mathematical procedures to compute them. For this reason, surface and subsurface processes are often modelled separately. Calculations for both the surface and the subsurface are constructed around the principal of satisfying two physical laws:

1. The conservation of mass
2. The conservation of momentum.

These laws have been developed differently for surface and subsurface flow calculations. Subsurface flows are typically calculated using Darcy's law, or a simplification thereof. Darcy's law takes into account the hydraulic conductivity of the medium that the water is flowing through, the cross sectional area of the medium and the hydraulic head (i.e. the difference in water level between the source and the destination). Surface flows on the other hand are typically calculated using the Saint-Venant equations, or simplifications thereof, which are commonly referred to as the shallow water equations (Furman, 2008). Both approaches share common roots in the Navier-Stokes equation, which describes the flow of fluids.

3.1 Surface Water Modelling

Surface water modelling focuses on routing water across the ground surface and can be one, two or three dimensional. There are a large number of models in existence, both commercial and open access, and a variety of different methods are used to calculate the flow of water across the model domain (Teng et al., 2017). Empirical models offer a relatively simple, computationally efficient data based approach but are not able to provide the spatially distributed detailed flood extents desired by this project. Instead, physically based hydrodynamic and hydrological models are of interest.

One dimensional models consider flow within a pipe or channel but can extend to floodplains, assuming them to be simple extrapolations of the channel. These typically use the Saint-Venant equations of the conservation of mass and conservation of momentum. These require information on the cross sectional dimensions of the channel or pipe and mathematically calculate the flow

between different cross-sections (Teng et al., 2017). While 1D models are well suited for many purposes they are limited to assume a single direction of a single speed across each cross sectional unit. This makes them unsuited for more complex scenarios where this is unlikely, such as where flow occurs out of bank or across complex topography where flow speeds and directions are likely to vary (Chen et al., 2010). Examples of 1D modelling software include InfoWorks ICM (Innovyze, 2020) and Flood Modeller (Jacobs, 2020).

Two dimensional models combat the limitations of the 1D models when simulating out of channel flows (Hunter et al., 2007). These are the most applicable and widely used surface water models for the mapping and assessing of flood risk. 2D models use spatially distributed (and often high resolution) inputs including topography, precipitation and surface roughness to produce water depths, velocities and inundation times and extents. As with 1D models, 2D models also use the laws of conservation of mass and momentum and typically use the shallow water equations. These are similar to two dimensional Saint-Venant equations and can be obtained from the Navier-Stokes equations. There are different numerical schemes for solving these equations: finite element, finite difference and finite volume. 1D and 2D models do not consider turbulence or differences in flow velocity within the water column, a suitable approximation in many cases. These are accounted for in three dimensional models (Teng et al., 2017).

The rainfall runoff modelling conducted in this work does not have water depths justifying the use of 3D modelling but does require detailed modelling floodplains. As such, a 2D modelling approach has been chosen. As the coupled modelling approach in this study only reconfigures models rather than altering the mathematical processes within them, no further detail on the mechanisms behind the models is given, from which much of the above information is taken. Instead a short review of some well known models is given. These have been selected according to those promoted for use at Newcastle University (CityCAT, HiPIMS), those commonly used in industry (JFLOW+, TUFLOW), and those found to be prominent when conducting this literature review (LISFLOOD-FP). Many of these are also discussed in the EA's 2D hydraulic modelling benchmarking report (Néelz and Pender, 2013) and are therefore thought to be appropriate for consideration. CityCAT, HiPIMS , JFLOW+ and TUFLOW all use the full shallow water equations; this makes them particularly suited to modelling complex 2D flows (i.e. flows involving complex topography or buildings) however does make them computationally demanding (Néelz and Pender, 2013).

CityCAT

The City Catchment Analysis Tool (CityCAT) is a software for two dimensional modelling, analysing and visualising of pluvial and fluvial flood risk. CityCAT was developed at Newcastle University and is a high resolution, shock capturing system focussed on computational efficiency. Unlike HiPIMS and JFLOW, CityCAT runs on CPUs and is deployable on the Cloud for applications requiring high performance computing. CityCAT is set up to use the open source OS MasterMap dat. This is used to mask buildings from the DTM, allowing it to realistically compute urban flow paths. Infiltration is estimated using the Green-Ampt method and roof storage is calculated internally. One further advantage of CityCAT is that it also freely available for researchers (Glenis et al., 2018).

HiPIMS

The High-Performance Integrated Hydrodynamic Modelling System (HiPIMS) is a 2D, shock capturing flood model (Liang and Smith, 2015). HiPIMS is an open source code developed at Newcastle University and has been progressed to run on GPUs (graphics processing units). GPUs have a higher number of processing elements (i.e. cores) than CPUs (central processing units) and so can speed up processing considerably by distributing the repetitive calculations involved with hydraulic modelling across the elements (Smith and Liang, 2013).

HiPIMS uses uniform Cartesian grids to calculate the flow of water from one cell to another based on the water depth within each cell and the cell's elevation. Manning's coefficient is used to specify the surface roughness of each cell, which influences the speed of flow to and from that cell and is typically based on the surface type or land use. HiPIMS can model inputs from point (e.g. stream flow) and diffuse (e.g. rainfall) sources and can return water depths and velocities across the grid (Wang and Yang, 2018).

HiPIMS can be used for a variety of modelling scenarios (Smith et al., 2015) from rainfall runoff events to dam bursts (e.g. Smith and Liang, 2013) at both city (e.g. Liang and Smith, 2015) and catchment scales (e.g. Wang and Yang, 2018).

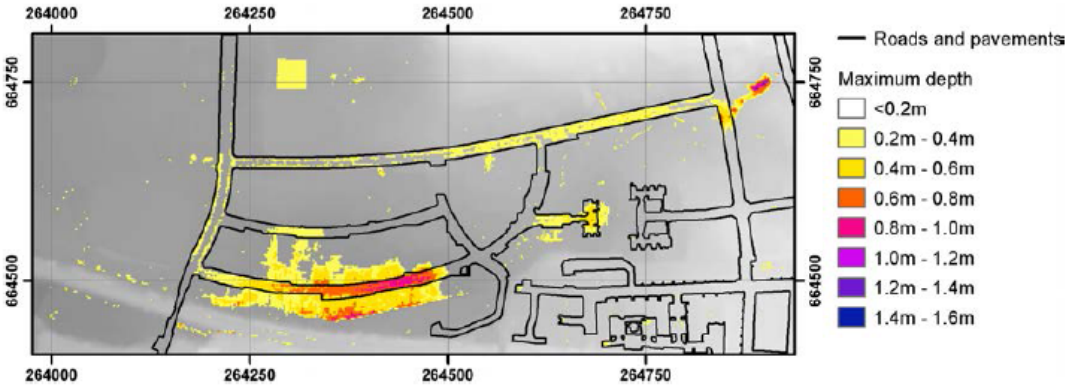

Figure 3.1: Taken from Liang and Smith (2015): outputted flood inundation depths from a uniform precipitation simulation in Glasgow.

JFlow

JFLOW was developed by JBA Consulting in 2002 as a *"reduced complexity 2D flow routing model"* and in 2007 was rewritten to run on GPUs. In 2010 JFlow was developed from using diffusion wave principles into JFlow+, which uses the full shallow water equations (JBA Consulting, 2014b). JFlow+ can run in parallel on multiple GPUs, giving it good computational efficiency (Crossley et al., 2010). Since then it has been further developed to include a GIS user interface and to reduce run times and computational requirements, thus allowing for increased grid sizes (JBA Consulting, 2014b).

It has been used to model large areas, such as a European flood map, and was used to create the EA's Updated Flood Map for Surface Water (Environment Agency, 2013b) and The Comprehensive Flood Map UK for England and Wales (JBA Consulting, 2014b).

TUFLOW

TUFLOW is commercial modelling software that is focussed on providing flexible and robust linking of 1D and 2D flow processes. This allows for modelling complex 1D channel systems and pips within other hydrological systems while still offering a 2D solver similar to those discussed above. The benefit of including 1D solvers within the modelling software is the ability to precisely simulate flows over and through structures such as weirs or bridges that may have significant affects on hydraulics. TUFLOW operates on CPUs but also has the capability to run on GPUs to increase performance (BTM Group Ltd, 2018).

LISFLOOD-FP

LISFLOOD-FP is a two dimensional hydrodynamic model used for simulating floodplain inundation (Coulthard et al., 2013) developed by Bristol University. LISFLOOD-FP was developed from LISFLOOD, one of the oldest surface water models discussed in this section and which formed a platform from which JFlow was developed (Bates, 2017).

As with the four models discussed above LISFLOOD-FP is a 2D hydraulic model that can calculate depths and flows over a 2D raster grid (Neal et al., 2011). However, unlike the previous four models, LISFLOOD-FP uses a simplification of the shallow water equations, not considering the advective acceleration term. This reduces its computational requirements, thus making it well suited for large modelling domains, but makes its use less justified in complex scenarios where flows vary rapidly (Néelz and Pender, 2013). As such, LISFLOOD-FP is not as suitable as the previous models for simulating rapid flooding is urban environments.

3.2 Groundwater Flood Modelling

Groundwater models can be used to generate groundwater levels at a single point or phreatic surfaces across an area. Since the early 1970's, there has been steady development of groundwater modelling in the UK, with a general change from the creation of bespoke models within research institutes to more standardised models that are used by consultants (Shepley et al., 2012).

Models that simulate or predict groundwater levels for a fixed point are typically lumped models. One basic example of this is a system developed by Adams et al. (2010) as an early warning system for groundwater flooding. Adams et al. (2010) first used a linear regression model to mathematically describe the relationship between recharge and the change in groundwater level from annual minima to the subsequent annual maxima. Estimated winter and autumn rainfall could then be entered into the relationship to predict the subsequent groundwater level peak. Data based methods, such as this, rely on precipitation and groundwater level observations and accurate rainfall predictions and is limited to the area where it was developed. Typical of a lumped model, this modelling framework only has a single output: the predicted groundwater level at that observation borehole. While this approach may be suitable for an early warning system, it does not provide the spatial information desired in this project. Furthermore, while Butler et al. (2012) state that simplified or lumped models can provide *'practical tools for flood risk assessment'* due to their relatively low volume of input data, they go on to say that there is a need for new methods for assessing flood risk and that this is occurring through *'a new generation of distributed groundwater models'*.

One bridge between the two methods (distributed and lumped) is described in Upton and Jackson (2011), where lumped model was used to simulate groundwater level hydrographs for 52 boreholes across the Pang and Lambourn catchments. The lumped model took into account 11 catchment characteristics to describe the relationship between precipitation and groundwater level. A piezometric surface was then generated by interpolating between the borehole groundwater levels and river elevations (i.e. GW level was assumed to equal river level). Locations where the water table breached the surface were taken to indicate groundwater emergence. This produced good correlation between modelled and observed emergences in the large 2000/2001 groundwater flood event that hit the South of England. This method does make several assumptions, such as that groundwater is in hydraulic connection with rivers and that the phreatic surface behaves regularly between modelled points.

While some may develop their own models, numerous generalised software are readily available (Brassington, 2017). One of the most widely used groundwater software is MODFLOW, which was developed by the USGS in 1984 (USGS, 2019) and has since become an industry standard (Zhou and Li, 2011). MODFLOW was originally developed for groundwater simulations but has since had further 'modules' developed that allows it to simulate coupled surface water-groundwater processes that account for all major hydrogeological processes. The original groundwater portion of the code, now termed *GWF*, is still a core process within the modelling system. This calculates water movement in three dimensions for different vertical layers within the model according to the hydraulic conductivity of the flow medium and the differences in hydraulic head at each end of the medium (Harbaugh, 2005). It does this for all points within the domain and is able to

construct piezometric surfaces accordingly. MODFLOW is available to download free of charge, as is a base graphical user interface (GUI). Commercial GUIs (e.g. the Groundwater Modelling System) are also available.

Following the exceptional groundwater flooding of the winter of 2015/16 in Ireland Naughton et al. (2018a) created a predictive groundwater flood map for Ireland. This calibrated a lumped hydrological model according to effective rainfall and observed groundwater flood extents - due to a lack of systematic recording of previous groundwater flooding the project established their own monitoring network and extracted data from remote sensing imagery. Once calibrated, the hydrological model was rerun using synthetic weather data that enabled it to capture extreme events and conduct frequency analysis. This approach is very similar to the method used in this project, which generates extreme hydrological data, including groundwater emergence, from synthetic data. This study uses spatially distributed, physically based models as these are less reliant on observed flooding data and enable a greater range of processes to be captured.

3.2.1 Regional Groundwater Models

Towards the end of the 1990's, the Environment Agency began the set up of fully distributed, regional, MODFLOW based groundwater models. Eight regional sub-programmes were constructed for water resource purposed with the aim of using well understood science to aid water resource assessments and abstraction management. The eight regional models cover the South West, Southern, Thames, Anglian, Midlands, Wales, North West and North East EA regions. These are based on MODFLOW code and are cover the major aquifers of the UK (Sec. 2.2.1). Each of these models simulate surface and groundwater flow in large aquifer units and are calibrated using observed hydrometric data predominantly dating from the 1970's. Each model is time variant and has distributed parameter fields (Shepley et al., 2012).

A wrapper for the regional groundwater models has been developed called the National Groundwater Modelling System (NGMS) (Whiteman et al., 2012). This is designed to assist the Environment Agency with the use of the regional groundwater models and to aid the regulation of groundwater systems. The NGMS is hosted on a centralised server and can be accessed by Environment Agency staff for the simulation of 'what-if' scenarios. Scenarios may regard resource management, changes to groundwater abstractions and assessments of climate change impacts.

The NGMS system is progressively updated and, in 2017, covered the majority of the Cretaceous Chalk and Triassic Sandstone principal aquifers in England (Fig. 2.5). The groundwater models typically have horizontal grid resolutions of 200 m and 1-3 time steps per month. While the system was originally designed for regulatory purposes, it has since been developed by fusing the system with recharge models and so enabling the simulation of extreme events such as floods and droughts (Farrell et al., 2017).

3.3 Multisource Modelling

Almost one million properties in the UK may be at risk from multisource flooding in which groundwater plays a role (McKenzie and Ward, 2015) and numerous studies state the importance of accounting for groundwater processes in hydrological studies (e.g. Saksena et al., 2019; Deb et al., 2019). The interactions between surface water and groundwater are not linear and can have significant spatial variation (e.g. Seibert et al., 2003), thus making them hard to predict and understand. Some *integrated* models are able to simulate both surface and groundwater processes but it is also possible to *couple* different model types together to simulate different (i.e. multisource) processes.

There have been advances in multisource modelling over recent years, however these do not typically include groundwater. Of those that do, MIKE SHE and FEFLOW coupled to MIKE

11 are very popular for regional GW-SW modelling; but those focussing on groundwater are typically based around MODFLOW and its associated packages (Barthel and Banzhaf, 2016). This lack of groundwater inclusion may be due to a lack of credible data due to under reporting and source uncertainty, and the difficulties associated with assigning flood probabilities (Cobby et al., 2009). Furthermore, the mathematical processes defining subsurface and surface flows are very different and so calculating the interaction between the two systems is very difficult (Furman, 2008). Barthel and Banzhaf (2016) also say that it is unclear whether well understood point GW-SW interactions can be scaled to regional scale modelling. They go on to suggest that progress in this field is limited by the distributed nature of the subject literature and the difference in approaches, which makes it difficult to compare available models. This later view is also taken by Maxwell et al. (2014).

Coupling groundwater and surface water models together is not a new concept. In 1993 Arnold et al. (1993) linked a groundwater model component to a surface water model called SWRRB (Simulator for Water Resources in Rural Basins) to model surface runoff, percolation, lateral subsurface flow, evapotranspiration, snow melt, transpiration losses, ponds and reservoirs, precipitation, air temperature and groundwater flow. This was at much lower resolution (both spatially and temporally) than is desired in this project, but does show that it has been a point of interest for some time. Whilst coupling groundwater-surface water models together is relatively uncommon however, there are many studies that couple surface water models (e.g. Lerat et al., 2012; Liu et al., 2015; Nguyen et al., 2016; Hdeib et al., 2018; Munar et al., 2018) and there are commercial software that make this common place in industry (e.g. Flood Modeller and TUFLOW).

3.3.1 Integrated Models

Integrated models are able to simulate both surface and subsurface processes within a single modelling system. There are many of these and so only a few of the more popular/prevalent of these shall be detailed below. A very detailed review of a large number of these (FEFLOW, FIPR Hydrologic Model (FHM), IHMS, MODBRANCH, MODCOU, MODHMS, SWAT-MOD / SWAT-MODFLOW, WaSiM, WaSiM-ETH, HEC-HMS, DYNSYSTEM, OpenGeoSys) can be found in Barthel and Banzhaf (2016). Details on other models such as ATS (Advanced Terrestrial Simulator), Cast3M, GEOtop, CATHY (CATchment HYdrology), HGS (HydroGeoSphere) and ParFLOW can be found in Kollet et al. (2017). Details on the latter three of these, along with OGS (OpenGeoSys), PAWS (Process-based Adaptive Watershed Simulator), PIHM (Penn State Integrated Hydrologic Model) and tRIBS+VEGGIE can be found in Maxwell et al. (2014). Four examples of integrated models are discussed below:

GSFLOW

GSFLOW is one of the most widely publicised MODFLOW-based models used for combined groundwater-surface water modelling. It is an integrated hydrological model, built by the USGS. It couples the groundwater/surface water processes from MODFLOW-2005 and MODFLOW-NWT to PRMS (the Precipitation-Runoff Modelling System) (USGS, 2017).

MODFLOW is a popular 3D finite difference modelling software that provides the groundwater component to the model (Brassington, 2017). MODFLOW itself has a modular structure, which allows different modelling capabilities to be added on to increase its capabilities (USGS, 2019). These can include surface water modules (e.g. a streamflow) that allow it to simulate multiple sources.

PRMS is a physically based, spatially distributed model. It simulates hydrologic processes to estimate catchment scale water budgets (U.S. Geological Survey, 2019b). This essentially uses above ground processes such as evapotranspiration, surface runoff, infiltration, etc. to estimate runoff. PRMS then simulates surface flow of this runoff (U.S. Geological Survey,

2019c).

GSFLOW simulations run on a daily time step and so are not of high enough spatial or temporal resolution to meet the objectives of this project. Furthermore, the coupling of groundwater and surface water processes in GSFLOW (or MODFLOW) is the weakest of those discussed. For more information, see Gannett et al. (2017).

HydroGeoSphere

HydroGeoSphere is a fully coupled physically based, spatially distributed modelling software that can simulate stream flow, groundwater flow and surface water flow. One benefit of HydroGeoSphere is that it is able to take into account the dual porosity of the subsurface (Brunner and Simmons, 2012), something potentially useful when modelling Chalk. For a comparison between MODFLOW and HydroGeoSphere see Brunner et al. (2010). Unlike MIKE SHE, SHETRAN and MODFLOW, HydroGeoSphere solves partial differential equations for the surface and sub-surface simultaneously, including the three dimensional form of the Richard's equation (Refsgaard et al., 2010). When discussing the SHE codes below, Refsgaard et al. (2010) stated that HydroGeoSphere was the only code that had the potential to surpass the MIKE SHE.

MIKE SHE

MIKE SHE is a physically based, spatially distributed model that is able to handle large datasets and can compute both surface water and groundwater processes. MIKE SHE has been commercially developed from the Systèm Hydrologique Europeèn (SHE) model and is now several decades old (Abbott et al., 1986). Since the late 1980s SHE was developed into MIKE SHE by the Danish Hydraulic Institute. The SHE model was an integrated model capable of simulating a large number of major hydrological processes: rainfall, interception, evaporation, surface flow on land and in rivers and subsurface flow in both the saturated and unsaturated zones. (Refsgaard et al., 2010).

MIKE SHE uses the same underlying code as in the SHE model, with some modifications and modernisations, and has been developed to include a graphical user interface. It is now used in both research and industry around the world but is not a standard tool for hydrological modellers. The system has also been used to develop a national hydrological model for Denmark for water resource management (Refsgaard et al., 2010).

SHETRAN

SHETRAN has also been developed from the SHE model by Newcastle University and so it too is a spatially distributed, physically based model. 3D surface-subsurface flow processes are fully coupled for simulating water flow and sediment and contaminant transport (Ewen et al., 2000; Lewis et al., 2018) at a catchment scale. SHETRAN has been used for many studies over the past few decades and has been shown to be capable of simulating groundwater and surface water processes well, both in the UK (e.g. Adams and Parkin, 2002; Parkin et al., 2007) and abroad (e.g. Guerreiro et al., 2017b; Op de Hipt et al., 2017). Subsurface flows are modelled using a 3D Richards equation capable of representing saturated and unsaturated mediums. 1D channel flow and 2D overland flow are modelled using the diffusive wave approximation to the Saint-Venant equations. The model domain is divided into a grid with each cell consisting of a column of units representing the layers of the subsurface and soil zone. On the top of these columns the land use can be specified to capture runoff processes at the surface. Rivers are represented by 1D channels, surrounded by a finer grid that enables the model to capture stream-aquifer flows (Parkin et al., 2007). As with other models discussed in this section, meteorological data is fed into the model along with any water exchanges at the edge of the modelling domain (such as groundwater and fluvial flows) and the model simulated hydrological processes to produce, amongst other things, river flows, groundwater levels and groundwater flows.

While SHETRAN is perhaps less well known than MIKE SHE, it has recently undergone development with the creation of the SHETRAN-GB modelling system (Lewis et al., 2018). SHETRAN-GB offers various improvements in the SHETRAN code, but its main purpose is to tackle two of the main limitations of spatially distributed, physically based models: (1) large data requirements and (2) significant setup times. The system provides an online GUI that allows users to freely download ready made hydrological models of UK catchments or, if a shape file is uploaded, an area of the user's choice. The models use national open access soil, geology, land use and climate data. These models are designed to not require calibration, however this may be required. More information on SHETRAN-GB can be found in Chapter IV.

3.3.2 Coupled Models

Coupled models are models that are made up of multiple separate models, this joining can take various forms (e.g. An and Yu, 2014). Furman (2008) states that most coupled models will require a numerical system describing both the surface and subsurface component, external boundary conditions for both elements and internal boundary conditions used for coupling the two together. Furman (2008) goes on to define three levels of coupling: *uncoupled*, *iterative* coupling and *full* coupling.

Uncoupled is the simplest of these and has also been termed *external coupling*: where models are run consecutively. The outputs from one model are used as inputs for a second with no feedback into the original model. This is also termed *weak loose* coupling by Barthel and Banzhaf (2016) and describes well the method of coupling that shall be used in this project. Barthel and Banzhaf (2016) state that models coupled in this way are difficult to review due to their wide variety, and that while many are likely to have been developed (often privately or for single use simulations) they are not all published in peer reviewed literature.

Iterative coupling (or *strong loose coupling*) refers to systems in which the second model provides feedback to the first. *Full coupling* is where both models and the internal boundary conditions are solved simultaneously (Furman, 2008; Barthel and Banzhaf, 2016). Passing information in both directions between the two models allows them to simulate dynamic feedback processes, where outputs from 1 model affect processes in the second model, which then affect processes in the 1st model. Example processes include emergent groundwater that flows up from the subsurface model, is routed through the surface model and then infiltrates back into the subsurface model or where emergent groundwater increases the runoff coefficient in the surface model and therefore affects how much water is passed to the subsurface model. These models are very complex as they have to resolve potentially large differences in the spatial and temporal resolutions of the two models (Camporese et al., 2010). Simulating dynamic processes such as these is important but is beyond the scope of this work. When coupling models, whether loosely of fully, it is important to not account for the same process in both models - a simple example of this would be using rainfall as an input to both the surface and subsurface models, potentially doubling the volume of water in the system). For a detailed review of methods for fully coupling surface and subsurface processes, see Ebel et al. (2009).

Many of the integrated models described in Section 3.3.1 have proven capable of simulating groundwater and surface processes very well. Although many do model multiple sources, they do not do this on the fine spatial and temporal scale that is sought in this project. In order to achieve this increased resolution it is proposed that a high resolution hydrodynamic model be coupled to a hydrological model, such as those above. Below are some studies that do this in some form:

PREVAH & BASEMENT

Felder et al. (2017) conducted coupling of a different kind, they linked a hydrological model to a hydrodynamic model. A semi-distributed hydrological model (PREVAH) simulated rainfall

runoff in sub-catchments and used the resulting hydrographs as boundary conditions (i.e. inputs) in a hydrodynamic model (BASEMENT) of the main catchment (i.e. external coupling).

Calculated Emergence and JFlow

A recently published study by JBA, Jacobs and Buckinghamshire County Council (Morris et al., 2018) conducted a similar project to this work. They estimated the rate of groundwater emergence using Darcy's law and field data from a purposely documented flooding event. They then input the calculated emergence into a 2D hydraulic model (JFlow), which routed the water and provided estimates of the extent and depth of flooding. The purpose of this was to create a groundwater flood risk map more similar to those for other sources of flooding to help mitigate future groundwater flooding events. On page four, they state:

> *"The rate of groundwater emergence could equally be estimated using a detailed hydrogeological model calibrated for high groundwater conditions, although these are rarely coupled to hydraulic surface routing models."*

This is an accurate description of this project - SHETRAN will be used as the detailed hydrogeological model, and HiPIMS will be used as the 2D hydraulic model. They do go on to state however that:

> *"Such models are scarce, expensive and time consuming to develop and require extensive data for calibration."*

It is for this reason that SHETRAN has been chosen, as the developments of SHETRAN-GB are hoped to overcome these difficulties. The more accessible modelling system should enable the process of setting up a representative simulation cheaper and more manageable.

A pan-European flood hazard map

In an effort to create a continental scale flood hazard map, Alfieri et al. (2014) used a hydrodynamic rainfall-runoff model (LISFLOOD) to generate river hydrographs for a 5×5 km resolution grid of Europe. The distributed and physically based LISFLOOD models were calibrated where possible. Meteorological data and extreme value fitting generated hydrographs for each river cell for 1 in 100 year events. These 5 km squares were then downscaled so that each river had a hydrograph for every 100 m stretch of waterway. Each of these 1/100 year hydrographs were used as an input for LISFLOOD-AAC, a 2D hydraulic model. This generated flood extents and depths that could be amalgamated to produce a high resolution hazard map of Europe. While this model did conduct a long term simulation (21 years) and connected hydrological flow outputs into a higher resolution hydraulic model, it did not take groundwater into account.

Grid-to-Grid & JFLOW

In order to increase understanding of surface water flooding Grid-2-Grid was coupled to JFlow and tested on two case studies: Newcastle upon Tyne (28 June 2012) and Canvey Island (20 July 2014). This was used to simulate 1:30, 1:100 and 1:1000 year return period events (Hunter et al., 2016).

Grid-to-Grid is a probabilistic, physically based, distributed hydrological rainfall-runoff model. It is currently used by the Flood Forecasting Center to estimate river flows for producing five day flood forecasts across England and Wales (Centre for Ecology & Hydrology, 2016). Unlike the other models discussed here, it is a physical-conceptual model, taking into account landscape properties, terrain and geology. It is able to simulate river flows and overland flows (Hunter et al., 2016).

JFlow is a 2D hydraulic model produced by JBA. For more information on this see Section 3.1. G2G was used to generate 15 minute, 1×1 km boundary conditions for JFlow in the form of stream flow and overland flow, which JFlow then routed across the surface.

tRIBS-OFM

Kim et al. (2012) present a coupled model consisting of the hydrological model *tRIBS* (TIN-Based Real Time Integrated Basin Simulator) and the hydrodynamic model *OFM* (Overland Flow Model). tRIBS is able to simulate surface and subsurface elements of the hydrological cycle and feed these into OFM via a one way loose coupling. The hydrodynamic model is run at a finer temporal resolution to account for the faster hydraulic processes. Although the subsurface is considered in the hydrological model, there are not many references to groundwater in the paper and there does not seem to be any calibration or testing of the groundwater system, e.g. against borehole levels. The only direct reference to groundwater is a map of emergence in one of the figures.

While this study does have similarities with the work planned in this project, there is no consideration of risk, and there is not the high resolution element that is planned here. Instead, the work focussed on improving the surface runoff element of the hydrological model.

n-TOPMODELs & CARIMA

In 2002 there was a catastrophic flood event in the Gard Region of France. A study by Bonnifait et al. (2009) used n-TOPMODELs and CARIMA to model this event to better understand the catchment processes. The combined modelling approach was taken as it was believed that both subsurface and surface processes were at work in the event.

n-TOPMODELs is a hydrological model that can simulate subsurface flows and any resulting saturated excess overland flow. One difference between TOPMODEL and many of the hydrological models discussed above is that it required far fewer parameters: hydraulic conductivity at the surface, rate of decline in conductivity in the soil with depth and the initial storage deficit in the root zone. The reduced number of parameters helps to constrain uncertainty.

The CARIMA model is a 1D hydraulic model that is used to simulate river flow, presumably taking into account the n-TOPMODELs outputs (overland flow and emergence). This seems to have been used alongside a further 2D model that defines inundated cells, however this is not clear. This paper demonstrates one of the points made in Barthel and Banzhaf (2016): that models are not always well described. The focus of their study, unlike this one, is on understanding a single catchment response, rather than creating a methodology for assessing risk.

One of the limitations of this modelling approach is that the n-TOPMODELs was only calibrated against a single flow record. This means that with the significant geological uncertainty there is little proof that the subsurface is correctly represented. Furthermore, the simplifications in both of the models mean that the n-TOPMODELs parameters lack physical realism, something that is important to this study.

3.4 Summary

Multisource modelling can occur in many forms and there are a wide selection of models that are able to simulate multiple sources. This is done in two ways: (1) integrated modelling that considers both surface and subsurface processes in a single model and (2) coupled modelling, which joins together separate models that consider surface and subsurface processes separately. There are different degrees of coupling, from models that simultaneously feed information between them as they run, to models that run in sequence, using the results of one as the inputs to another.

The integrated models described here do not provide the capability for the high resolution routing desired from this study and so are not appropriate by themselves. Of the coupled models, several are able provide streamflows and surface processes but largely do not consider groundwater processes. Of those that do (e.g. n-TOPMODELs) none have been found that are able to provide the physically based spatially distributed approach that is desired.

None of the models found in this literature suit the full needs of this study and so a modelling system will be created that does. This modelling system will use the integrated, physically based, spatially distributed hydrological model SHETRAN to simulate catchment scale hydrological processes (including groundwater) and the 2D hydraulic model HiPIMS to simulate high resolution surface water routing.

SHETRAN has been selected as it is a spatially distributed, physically based hydrological model that has been proven to be capable of simulating both surface and subsurface flows. Furthermore, it has recently been developed to include an automated setup. This automated setup combats some of the most significant drawbacks of physically based, spatially hydrological models: (1) the significant investment in time and data required when setting up the model and (2) the lack of reproducibility due to different set up methods between different modellers.

HiPIMS was selected as it offers a high resolution 2D environment that is freely available and widely applicable to a range of modelling scenarios, including rainfall runoff modelling. As both of these models have been developed at Newcastle University there is also the further benefit of having in-house expertise that allows for a greater understanding of the models being coupled and the most appropriate methods for doing so.

4. National Assessments of Flooding

The methodology developed in this project relies on the use of case study catchments. However, it is developed to facilitate future applications at a national scale by using automated identification and coupling methods, and by attempting to reduce the need for manual model calibration (see Chapter IV). With this future national application in mind, this section presents a review on some of the existing national scale tools available for assessing flood risk in the UK. While there are well established tools for assessing single source risk, no tools were found that enable a nationally applicable system for assessing flood risk from coupled groundwater-surface water sources. There are no physically based examples of national hydrological modelling in the UK (Lewis et al., 2018), although this has been done in Denmark using MIKE SHE (Refsgaard et al., 2010).

4.1 UK Policy, Responsibility and the Development of the National Assessments

In 2005 Defra (the Department for Environment, Food and Rural Affairs) published the Making Space for Water report. This recognised the importance of developing flood warning tools for mitigating flood risk. It placed the onus for developing flood warning systems on the Environment Agency (Falconer et al., 2009). The 2007 EU flood directive (2007/60/EC) requires member states to map flood hazard and risk in their territories to aid decision making. This led to the production of the surface water maps discussed in Section 4.2. De Moel et al. (2009) provide a review of those maps existing at the time of writing however make no mention of groundwater or multisource flood risk. Following the widespread flooding of 2007, the UK Government commissioned the Pitt Review - an independent investigation into the floods. This recommended that the EA should undertake a national review of both groundwater and surface water flood risk (Falconer et al., 2009). As such, the Environment Agency has a role to provide a strategic overview for all sources of flooding and, in collaboration with the Met Office, to provide flood forecasts and warnings (Local Government Association, 2017). More recently, the Environment Agency has been placed in charge of developing methods for understanding and managing of flooding from all sources, although these do not have to be combined (Flood and Water Management Act, 2010).

Lead Local Flood Authorities, made up of councils and unitary authorities, are responsible for local flood risk from surface water, groundwater and smaller water courses (Fig. 4.1). Amongst many requirements, they must provide strategies for managing these risks and investigate and publish reports on significant local flooding incidents (Local Government Association, 2017).

4.2 Surface Water Flooding

In the UK, there have been several major national scale investigations regarding the flood risk from surface water. These have been conducted by the Environment Agency in partnership with

Flood Source	Environment Agency	Lead Local Flood Authority	District Council	Water company	Highways authority
RIVERS :					
Main river*	✔				
Ordinary watercourse**		✔	✔		
SURFACE RUNOFF:					
Surface water		✔			
Surface water on highway					✔
OTHER:					
Sewer flooding				✔	
The sea	✔				
Groundwater		✔			
Reservoirs	✔				

Figure 4.1: Flooding and the responsible authorities, taken from Dorset County Council (2012)

various other institutions. These focus on two types of hazard – flooding from rivers and the sea and flooding from surface water (here referring specifically to pluvial flooding).

The Risk of Flooding from Rivers and Sea maps (RoFRS) were published in 2013. These were generated from the National Flood Risk Assessment and the National Receptor Dataset by the Environment Agency. Flood extents are available online in the form of interactive maps (e.g. the Long Term Flood Risk Map, Environment Agency, 2019a) but also in large catchment scale reports for different River Basin Districts (e.g. Environment Agency, 2013d). These reports do address to some degree true *risk* by looking at vulnerability. Maps are provided that include information on the risk to people, the economy and the environment. No direct calculation of the risk is made, but the hazard and vulnerability are depicted together.

Prior to the RoFRS map was the Flood Map for Planning (Rivers and Sea) (Environment Agency, 2013a) (previously known as the *Flood Map*). This is still publicly available as it defines risk according to *flood zones* that are still used and are different to the updated risk classifications used in the RoFRS maps (Practical Law, 2013).

In 2008 the EA, in partnership with JBA consulting, produced the first surface water flood map, titled Areas Susceptible to Surface Water Flooding (AStSWF), this was then updated in 2009 with an improved DTM. The AStSWF maps were published to Local Resilience Forums, Local Planning Authorities, the Welsh Local Government Association and the Welsh Planning Inspectorate to help provide the information required to mitigate flood risk. JBA, partnered with Halcrow, further developed this into the Flood Map for Surface Water (FMfSW), which was release to the aforementioned groups in 2010. The FMfSW included high resolution LIDAR, methods for calculating effective rainfall and the influence of buildings. Following the Flood Risk Regulations set by the European Floods Directive in 2009, the map was expanded to a national scale and published openly. In 2016 the FMfSW was renamed as the Risk of Flooding from Surface Water (RoFSW) (Environment Agency, 2013c).

The Risk of Flooding from Surface Water map used JFlow+ to simulate events for 50% of summer rainfall for urban catchments and 75% of winter rainfall for rural catchments for 1 hour,

3 hour and 6 hour storm events. Each was modelled at 1/30, 1/100 and 1/1000 year return intervals and the largest extent of each return interval was taken to indicate the potential for flooding. In urban areas rainfall was reduced by 30% to account for infiltration and 12 mm/hr is removed to account for drainage systems (Environment Agency, 2013c).

As stated above, these maps are available via online portals. The Risk of Flooding from Rivers and Sea and the Risk of Flooding From Surface Water are available using the EA's Long Term Flood Risk Map (Environment Agency, 2019a) and the Flood Map for Planning (Rivers and Sea) is available using the Flood map for planning service (Environment Agency, 2013a). These use different methods to classify the risk. The Flood Map For Planning uses flood zones (1, 2, 3a & 3b) whereas the Long Term Flood Risk Map uses risk categories (very low, low, medium, high). Using categories to communicate risk, rather than return intervals, is likely to be part of a push to remove the dependency on return intervals for conveying flood risk to the public as they are frequently misunderstood (Meyer et al., 2012). That said, both sets of categories are defined in terms of return intervals, although the intervals differ slightly between the systems. These can be seen in Table 23.1. Unlike the Flood Map for Planning, the Long Term Flood Risk Map takes into account flood defences, which reduce the risk level. One benefit of the Long Term Flood Risk Map is that it provides estimated depth and velocity ranges for each of the low, medium and high risk surface water flood extents. Examples of the Long Term Flood Risk map can be seen in Figures 23.1 & 23.2.

Other surface water flood maps exist both nationally and globally. Those of a global scale are too broad to fit with the high resolution scope of this project, however some UK based maps are similar to those of the Environment Agency detailed above. These are typically produced by consultancies (e.g. JBA Consulting, 2014a). One example of this is UK FloodMap^{TM} produced by Ambiental Risk Analytics. The map covers all of the UK and shows fluvial and pluvial risk according to hydrological and hydraulic modelling at a 2 m resolution (Ambiental Risk Analytics, 2019b).

4.3 Groundwater Flood Maps

In 2000/2001, no government agency oversaw groundwater flooding. This changed with Defra's Making Space for Water consultation in 2004 and in early 2006 the Environment Agency took on an overview role in monitoring groundwater flooding (Morris et al., 2007).

There are several open source maps that describe the risk of fluvial, pluvial and tidal flooding to an area but there are a lack of groundwater equivalents. Those maps that do exist typically describe susceptibility, rather than risk, and are of lesser detail. There is a growing interest in the field of groundwater research and some of the recent developments, attempting to categorise the susceptibility and risk of groundwater flooding, are detailed below. One of the issues with these maps is that they describe areas that may have groundwater emergence, but they do not provide any information on the rate of emergence, flood extents or flood depths (Morris et al., 2018).

4.3.1 Defra, Jacobs and GEMs

In a study commissioned by Defra in 2003, Jacobs (2004) attempted to determine the knowledge of and risk of groundwater flooding. They took two approaches:

Firstly, data was collected regarding the occurrence of groundwater flooding during the winters of 1994/1995, 2000/2001 and 2002/2003 in the South East of England, focussing on the Thames Region (Fig. 4.2). Data was mostly collated from reports made by the general public and those held by the Environment Agency.

This approach only represents those flood events that were reported and catalogued. The under reporting of groundwater flooding has been an issue over past decades (Cobby et al., 2009)

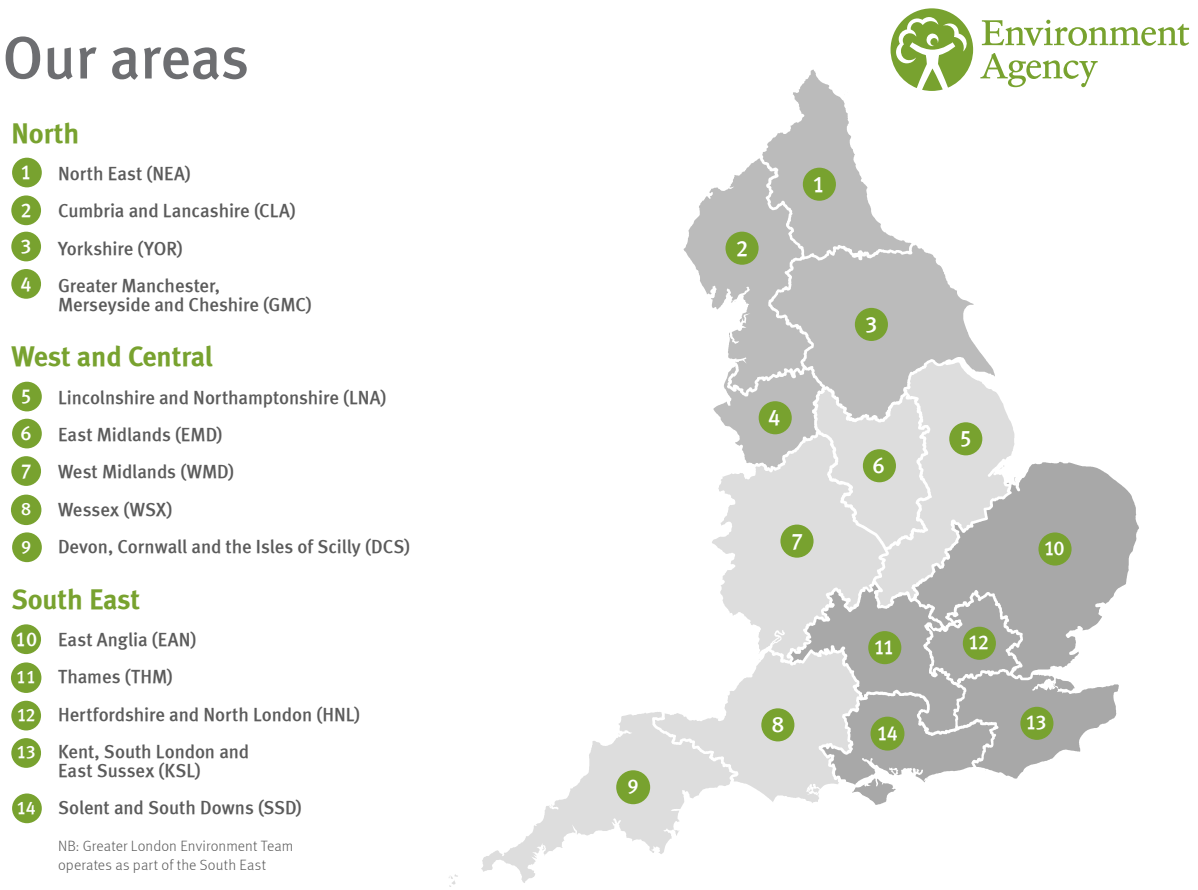

Figure 4.2: Jacobs (2004) focussed on collecting data for the Thames Region to establish the extent of groundwater flooding from past very wet winters. Taken from Environment Agency (2014)

and has stalled research into groundwater flooding. There are multiple reasons for this; including, that there is a nescience regarding groundwater flooding, groundwater processes are typically hidden below ground and so not generally thought about by the public (Kreibich et al., 2009) and also because no official government agency was in charge of dealing with, recording and collating groundwater flood data (Jacobs, 2004). This lack of overarching governing body was partly because controls on groundwater flooding (such as topography, geology and artificial influences) are localised (Cobby et al., 2009).

The second approach produced Groundwater Emergence Maps (GEMs) for all major consolidated aquifers of England. These indicate areas that have underlying consolidated sedimentary rocks in which groundwater levels could be expected to be at or near the surface in the event of a very wet winter. Where data existed, these maps were calibrated against the 2000/2001 event. Where this was not possible, data was extrapolated using aquifer properties (Jacobs, 2004) and existing groundwater contours from the EA and BGS (Morris et al., 2007).

An example of a national GEM can be seen in Figure 4.3 depicting unconfined, consolidated aquifers thought to contain groundwater within 2 m of the surface during wet winters (Morris et al., 2007). While this shows areas thought to be at risk of emergence, actuation of that risk depends on local factors such as geology, topology, drainage and rainfall/aquifer recharge patterns (Morris et al., 2007). Blue areas show where contours matched well to reported groundwater floods - these areas were exclusively over chalk aquifers. However, an MSc thesis by Mills (2004) found additional groundwater events and has suggested that non-chalk aquifers also have reported floods and could also be coloured blue. Red areas represent those areas where emergence was less

certain (due to insufficient flooding data to calibrate the emergences) and so regional groundwater levels were used instead. Orange areas are where flooding was reported, but the data is not of a great enough extent to be fully confident of the calibration.

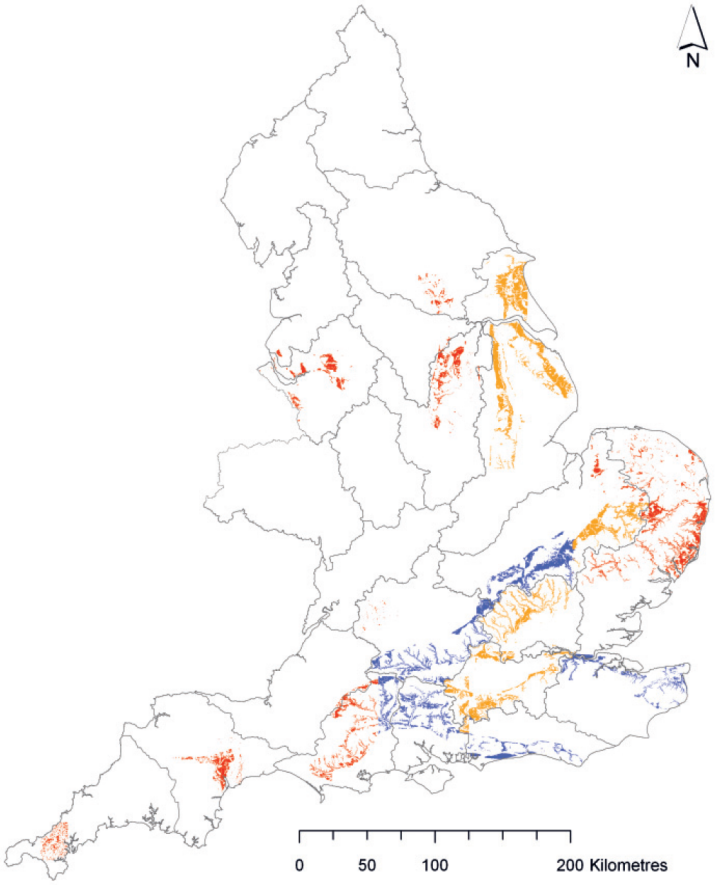

Figure 4.3: A map of national groundwater emergence taken from Morris et al. (2007), original work by Jacobs (2004). Blue - groundwater levels likely to be high during wet winter; red - uncertain calibration; orange - good calibration, but uncertain due to insufficient data. There is also a map in Jacobs (2004) that describes the number of houses at risk within each region.

4.3.2 British Geological Survey

Jacobs (2004) stated the need to produce groundwater flood risk maps, focussing on areas of chalk outcropping, that can be used in planning. While stating that groundwater flooding is largely confined to chalk aquifers, Jacobs (2004) also identify the need to investigate the potential of groundwater flooding from non-chalk aquifers and research further the frequency of groundwater flood events to aid cost-benefit analysis. One of the earliest attempts at this was by the British Geological Survey (BGS).

In 2008, the BGS produced the first national map that identified areas susceptible to groundwater flooding - i.e. where groundwater may rise close to the surface or emerge above it (British Geological Survey, 2019b). This is a GIS rule-based technique based on local geology and hydrology, specifically using permeable superficial deposits flooding and clearwater flooding conceptual models. The map is updated at least bi-annually as more data become available and as methods are improved (British Geological Survey, 2018).

The susceptibility map was produced by using digital geology data to identify areas where

geological conditions allow for potential groundwater flooding. Secondly, groundwater level data was compiled around England and Wales and interpolated to construct groundwater level surfaces. Where data was sparse, water bodies were used as proxies for groundwater level, assuming this to be equal to the elevation of the water body. Seasonal analysis then established the potential range of the groundwater levels and areas where this range came near to the surface were deemed susceptible (McKenzie et al., 2010).

One limitation of this work is that it does not indicate risk, as hazards are not attributed likelihoods (British Geological Survey, 2013b). Unlike the EA flood maps describing fluvial and pluvial flood risk, the resultant susceptibility map is not open source, though it can be accessed via an academic licence. An example of the map can be seen in Figure 23.3. The BGS susceptibility map indicates that just over 1% of England has the potential to flood from groundwater (Macdonald, 2010).

4.3.3 JBA Consulting

A similar, but more modelling based approach has been developed by JBA Consulting to map likely emergences on the unconfined chalks of England. They have produced a national map that highlights areas at risk of groundwater flooding at a 5 m resolution (JBA Consulting, 2016).

Groundwater emergence was modelled using estimated recharge volumes and the aquifer storage and transmissivity and then validated against observed groundwater levels and historical flooding. As such, this produces expected flood zones for 1 in 75, 1 in 100 and 1 in 200 year annual exceedance probability (AEP) flood events. These emergences are then calibrated using historical groundwater flooding events (JBA Consulting, 2014c, 2016).

4.3.4 ESI Consulting

An interesting recent development is that of the national 5 m Groundwater Flood Risk Map (ESI, 2015). This claimed to be the most sophisticated and accurate map on the market. Risk has been defined according to four categories: negligible (which has an annual probability of $<1\%$), and then low, medium and high (all have annual probabilities of $\geq 1\%$) (GeoSmart Information, 2015). From the available information it appears that risk, defined as the product of the hazard and its probability of occurring, has been based on historical recordings of groundwater flooding (Landmark Information Group, 2015). If this is true then there is scope for this to be advanced further by a more detailed investigation into groundwater return intervals. One limitation of this work is that it relies on historical data, a method criticised by Cobby et al. (2009, pp. 115) who state that:

> *"... evidence or lack of evidence of previous flooding is not a sufficient indicator of the likelihood of flooding in the future. A more comprehensive approach is to use our understanding of groundwater flooding mechanisms to produce maps of susceptible areas."*

The map appears to be being developed by GeoSmart Information and distributed via Ambiental Risk Analytics. Ambiental Risk Analytics (2019a) claim that the GeoSmart GW5 groundwater risk map provides the highest resolution groundwater risk data available for the UK and prides itself on describing risk rather than susceptibility. This considers groundwater flooding from the bedrock aquifers (Fig. 2.2a) as well as from rivers and the sea via permeable superficial deposits (Fig. 2.3a). According to the website, risk is calculated using geology data and historic groundwater levels but no longer makes reference to the use of historical groundwater flooding. While it is indicated that groundwater flooding may occur as a result of surface water flooding, the product does not appear to take into account any interdependencies or joint probabilities (Ambiental Risk Analytics, 2019a). Relative to the national availability of detailed hydrogeological

data, a five meter resolution map perhaps stretches the limits of what is an appropriate use of data. This project seeks to route groundwater across the surface, but does not deem it feasible to estimate direct groundwater risk at such high resolutions.

Of further interest is a flood warning system from GeoSmart that generates and distributes daily regional scale indications of potential groundwater flooding according to national weather forecasts. These are based on historical climate data and telemetred borehole levels and can be provided up to 90 days in advance (GeoSmart Information, 2019a). While such approaches can indicate hazards and thus help to reduce the vulnerability of an area they are not able to indicate the overall risk for an area, an important factor when planning longer term mitigation strategies.

4.3.5 The Environment Agency's Areas Susceptible to Groundwater Flooding Map

This map uses the BGS's Groundwater Flooding Susceptibility Map to create a screening tool for Lead Local Flood Authorities. 1 km^2 grid squares are attributed a susceptibility class according to the percentage area that falls within the top two susceptibility bands on the BGS map. This does not take into account any aspect of probability, and therefore risk, and only exists for those areas included in the original map, i.e. consolidated aquifers and superficial deposits. This can be used to establish whether an area marked for future development should have a flood risk assessment. One issue with this approach is that small but highly susceptible areas, such as narrow bournes, can be overlooked if they are averaged in with a low susceptibility surrounding area (Karam, 2016).

4.3.6 Mapping Groundwater and Groundwater Induced Flooding

The newest mapping approach found in this review is that of Morris et al. (2018) who map not only the risk of groundwater flooding, but also that of groundwater induced flooding. The maximum elevation of groundwater emergence from the ground or springs was recorded and overland flows measured. Groundwater levels for the area, taken from boreholes, were then analysed to produce annual exceedance probabilities of 1/30 and 1/100.

A groundwater surface was then created that took into account the shape of the BGS hydrogeology groundwater level maps and the measured emergence elevations. Anywhere where this surface was above ground was assumed to have emergence. This produced a similar shape to the GEMs described above. The emergence zones were then divided to produce many smaller sub-catchments and Darcy's law was used to estimate the flow from each sub-catchment. JFLOW+ was then used to route this water. The overland flow measurements were used to calibrate the set up against simulated overland flows.

Flood extents were found to match well to those from recorded events. This offers a useful tool for local authorities by identifying communities and networks that are likely to be at risk of groundwater and groundwater induced flooding, and helps them decide how to mitigate potential flooding.

One limitation with this approach is that it relies on historical measurements of groundwater emergence locations and flow rates, however future work could use hydrogeological models. It is stated that models are expensive, data intensive, and time consuming to set up. There are efforts to tackle this complex set up and extensive data requirement (e.g. Marker et al., 2015; Lewis et al., 2018). This PhD project aims to progress development of a simple and ergonomic modelling system that will offer an alternative methodology to that of Morris et al. (2018) without the need for groundwater flooding data. This, as stated elsewhere will use a hydrological model to calculate groundwater emergence for subsequent routing. One further advantage of the method being developed here is that it will also use fluvial and pluvial inputs for a more comprehensive understanding of the hazards. Furthermore, Morris et al. (2018) state that using a hydrogeological model would counter many of the necessary assumptions associated with frequency analysis of

borehole levels.

4.4 Multisource Flooding

There is no multisource flood risk map for the UK and although many sources in the literature refer to *multiple sources* (e.g. Keef et al., 2011), no instances could be found where this includes groundwater. In 2010, the Environment Agency set out to produce a prototype tool - *MAST* - that offered an integrated map for England and Wales to aid the assessment of flooding from all sources, not just from rivers and the sea. The purpose of the *Mapping All Sources Tool* was to facilitate the 'practical and flexible' production of susceptibility maps for multiple sources of coastal, river, and surface water flooding. By 2011 probabilistic software had been developed and pilot tested, the results indicating significant potential (Wicks and Lovell, 2011).

The tool was set to map probabilistic flood hazards and to enable them to be combined and a joint probability estimated, along with the potential for indicating the proportion of each source contributing to the total hazard. The document outlined two methods for calculating the joint probability: a *fully integrated* approach and a *map combination* approach. The tool would take this second option, due to its relative simplicity, combining separately calculated flood hazards according to their likelihood. In essence, a 1/30 year fluvial event overlapping with a 1/30 year pluvial event would give that area a 2/30 or 1/15 year chance of flooding for the estimated hazard. As the likelihoods of flooding from different sources is related to one another, it was proposed that the dependency between the different sources also be investigated to improve likelihood estimates. This would not however show any interaction between the sources (Horritt et al., 2010), such as is proposed in this work. This thesis chose the fully integrated method for estimating probabilities, as this was thought to be more realistic and to offer a more comprehensive estimation of the joint hazard.

MAST was aimed at meeting the 'evolving needs of modern flood risk management' (Environment Agency, 2011b) whilst advocating assessing risk from multiple sources and attempting to convey this risk simply. Although the use of the groundwater susceptibility maps is mentioned, it was deemed unfeasible to detail the risk element of groundwater flooding due to lack of existing research (Horritt et al., 2010). Horritt et al. (2010) briefly discuss other relevant projects and reports but make no reference to other projects tackling multiple sources. This helps to demonstrate, at least in 2010, the research gap that this thesis hopes to address. MAST shares objectives with this thesis, which aims to produce a methodology that is capable of meeting these evolving needs by producing a tool that is user friendly and therefore communicable. This work also goes one step further, by including groundwater hazard through hydrological modelling.

Progress with this tool was hard to track and no evidence of it could be found post 2011, however it has developed into a recently released *Risk of Flooding from Multiple Sources (RoFMS)* map (Environment Agency, 2019b). This first version adds together the probability of flooding from the existing flood maps detailing the risk of flooding from surface water and from rivers and sea. It does not include any information on groundwater flooding, nor does it appear to consider joint probabilities as proposed with MAST and does not take into account any interdependencies between sources (Environment Agency, 2017). Instead, it aims to *"give an indication of what areas of land may be at risk of flooding from more than one source"* (Environment Agency, 2019b).

The RoFMS extrapolates the existing flood extent probabilities to give a linear, spatially distributed estimation of risk. The two risks are then added to give a combined risk that is categorised into four risk bands: (1) >3.3%/year, (2) >1%/year, >0.1%/year, <0.1%/year. Each area is given a suitability value that represents what that data can be used for. This ranges from whether it estimates risk at a property level up to whether the data should only be used at a national level. Finally, each location is given a risk contribution score that indicates to what extent the risk is derived from surface water or rivers and sea (Environment Agency, 2017).

5. Data

Many different data types were used in this thesis. These, along with any reformatting, are outlined below.

5.1 River Levels

Chapter III sought to identify locations for potential multisource flooding. This was a national, automated, data based assessment that used 15 minute resolution river flow data. This was initially retrieved in the form of river levels and subsequently converted to flow.

The river level dataset is a national dataset composed of recordings from over 1200 gauging stations situated across England, Wales and Scotland. England and Wales hold the vast majority of the stations, with relatively few (approx. 40), poorly distributed gauges in Scotland. This data was held in the Environment Agency's WISKI hydrometric archive until 2014 when it was compiled and quality controlled by the JBA Trust. This was conducted as part of the SINATRA Project within the Flooding From Intense Rainfall programme (Dance and Cloke, 2013) in an investigation into instances where river levels have risen rapidly. The data was provided for this study by the JBA Trust.

Although many of the river level records are of high resolution, with recordings every 15 minutes, there are instances where this is not the case or where there are gaps in the record. These gaps can vary dramatically in length from a single missing recording to many years of missing data. Of further note, these recordings may not have originated from exact 15 minute intervals but have been rounded to the nearest appropriate 15 minute interval.

Data was quality controlled to some degree during compilation by JBA, however, as this was a mostly automated process, there were still missing dates and errant river levels. These errors may be down to imperfect historical transfers of data between systems or perhaps artefacts from instances when original river levels were steady and so not recorded. This data was quality checked before use, this is detailed in Section 7.

Care was taken during the analysis conducted in Chapter III to identify and deal with the occurrence of missing data.

Elshorbagy et al. (2000) classifies three types of missing data: (1) that which is *trivial*, such as unclustered, non-consecutive missing data points, (2) that which is *significant*, referring to periods of missing data that are important enough to estimate, but not long enough to compromise the legitimacy of the record and (3) that which is *fundamental* i.e. substantial periods of missing data or frequent non-consecutive data. Whilst he states that (3) warrants the cutting short of the record so as to keep only present data, (2) could be in-filled (or patched) if deemed necessary. It is this category that accounted for the majority of errors in the river level data. Trivial missing data, is said to be rectifiable by simple interpolation, and that was the primary approach taken

here.

Trivial Missing Data

Standalone missing data points were linearly interpolated, patching values with the mean of their two neighbours (as in Widaman, 2006). This offered a simple, although perhaps blunt, solution. If the missing data point was neighboured by steep rising and falling limbs (or vice versa), then it may be that this point should represent a river level peak or minimum; by using a simple mean then this outlying level would have been drawn inwards to sit midway between its neighbours, erroneously smoothing the record. However, considering the record lengths under analysis, this decrease in accuracy was not thought to be significant, especially when considering the epistemic uncertainty of base level separation used in the analysis.

Spline interpolation was also considered for patching trivial data. This fits data within the recorded oscillations of the level record. According to the rate of change in level surrounding a missing value, spline interpolation extrapolates fluctuations to predict peaks and minimums. This risks calculating false peaks and minimums and so was not deemed appropriate.

Significant and Fundamental Data

In regard to the longer, *significant* missing data, there are methods in the literature that could allow them to be in-filled (as in Hughes and Smakhtin, 1996; Bennis et al., 1997; Dumedah and Coulibaly, 2011). However, these tend to carry with them a number of caveats and uncertainties and their accurate implementation was considered infeasible in the time frame available. As the majority of the time series are quite long these periods of missing data were cropped and only periods of data over a set length were used in the analysis.

5.2 Groundwater Levels

Chapter IV assesses the performance of an automated hydrological model to simulate groundwater levels. Several options were explored for accessing this data. Initial attempts used an *API* (application program interface) provided by the British Geological Survey. This allowed data to be retrieved directly from the Environment Agency's website via python scripts. Data could be recovered for both telemetered and non-telemetered boreholes with a good coverage around the UK. Data could, however, only be retrieved for the previous two years and so was not suitable for the study.

Instead, groundwater level data had to be requested from the Environment Agency via freedom of information requests. This was not possible at a national scale and so data was requested for a number of case study catchments. The majority of data was provided at a daily time step. The units did vary between records and so all data was reformatted into meters above sea level using approximate heights taken from OS maps. Limited meta data was provided with the records, however this is generally available using the BGS GeoIndex (British Geological Survey, 2015).

5.3 Meteorological Data

Chapter IV used meteorological data to drive hydrological simulations. Details of this can be found in Section 13. Chapter VI used synthetic weather data to drive the multisource modelling system developed in Chapter V. This was produced using the UKCP09 Weather Generator (Kilsby et al., 2007). More details can be found in Section 21.1.

5.4 Topography

Topography data was used throughout Chapters IV, V & VI for both hydrological and hydrodynamic modelling. Two open access digital terrain models (DTMs) were used, both provided

by the Ordnance Survey. DTMs show the ground surface with any additional objects, such as buildings or trees, removed.

High resolution (2 m) LIDAR data was not available to the domain modelled in the hydraulic simulations in Chapters V & VI. The use of high resolution photogrammetry (Nelson et al., 2009) was explored in initial test modelling; this uses a *digital surface model* (rather than a DTM) and was found to merge neighbouring surface objects and so did not reasonably portray streets or gaps between houses etc. Vegetative cover along streams also meant that water courses within the domain were not well portrayed.

OS Terrain 50

The Ordnance Survey's 50 m resolution Terrain 50 dataset provided the topography data for all hydrological modelling. It was also used when setting up the hydraulic model in Chapter V as this provided a useful overview of the landscape and a simple modelling base for testing HiPIMS.

High Resolution OS Terrain 5

The Ordnance Survey's OS Terrain 5 dataset offers an improved horizontal resolution of 5 m. This was used for the hydraulic modelling in Chapters V & VI. The DTM was resampled to a 2m resolution to allow buildings to be more precisely merged with the DTM from the OS MasterMap dataset.

III

Identifying Catchments at Risk of Multisourced Flooding

6. Background

6.1 Aim and Motivation

Alongside developing a methodology for assessing flood risk from multiple sources, this chapter describes a national scale investigation to identify catchments likely to benefit from such an approach. This is done by identifying catchments that have evidence of both groundwater and surface water sources during peak river flow events.

Information related to multisourced flood events is sparse and little to no information exists regarding historical multisourced floods. Even accurate details regarding single source flooding is difficult to collate and especially difficult to assess at a national scale. From initial research in Section 2.3, the main characteristics suspected of generating multisourced responses in catchments are: (1) the presence of permeable subsurface material that can become saturated and create a rapid, flashy response to rainfall (e.g. the River Ouse catchment), (2) subcatchments with opposing hydrological regimes (e.g. the River Kennet and the River Pang), and (3) the presence of mixed catchment characteristics such as impermeable superficial deposits and permeable bedrock (e.g. the River Wye). While catchment descriptors exist to aid the identification of such characteristics, these alone are not notable enough to provide a definitive identification of multisource catchments. Therefore, rather than relying on instances of reported flooding taken from the literature, a data based approach was taken based on river flows. Flows were thought to be a useful proxy for determining different source contributions to the river system and therefore the catchment as a whole. Catchment areas were used in the assessment as these provided a practical and existing method to spatially divide the extensive area under investigation. This data based approach enabled the most robust solution whilst also facilitating a repeatable and expandable national scale assessment. A simple methodology was constructed so that its transparency would minimise the necessity for validation against the lacking historical data. To the author's knowledge, this is the first time that such an approach has been undertaken to identify multisource catchments. It should be noted that while flows were used as an indicator for relative source contributions within the catchments, they were not used to indicate which catchments may be prone to flooding.

Fifteen minute flow data from 435 catchments around England was used to classify hydrograph shape during recorded peak flow events. There are numerous accounts of hydrograph classification in the literature (e.g. Bloomfield et al., 2015; Hannah et al., 2000; Raj, 2004; Ternynck et al., 2016; Upton and Jackson, 2011), but a new method was developed here. Indexes were produced that quantified the degree to which hydrographs were controlled by groundwater or surface water sources. Several hydrograph shapes are thought to be indicative of a multisourced catchment; these are discussed below:

Variable base flow: by definition, and to justify the modelling of antecedent conditions,

groundwater flooding requires the groundwater levels to change. The presence of groundwater and surface water sources is not enough to infer multisource potential. As such, variable groundwater levels are a prerequisite of a multisource catchment and any methodology needs to take this into account. Simply relying on descriptors such as base flow indexes (discussed in Section 8.1) is not enough as this does not necessitate variations in groundwater level.

Asymmetrical hydrographs

An asymmetrical hydrograph refers to a steep rising limb followed by a shallower falling limb. According to Thomas et al. (2015): *"A streamflow hydrograph can be separated into a rising limb reflecting increases in discharge resulting from precipitation events, and recession limbs, which represent streamflow maintained at least in part by discharge from watershed aquifer storage"*. It is therfore hypothesised that catchments with both surface runoff and a groundwater flow would exhibit asymmetrical shape to some degree. The greater the asymmetry, the greater the flashiness or groundwater response is in the catchment.

As well as asymmetry, multisource hydrographs are expected to depict variable base flow following storm events. This would indicate that there is significant groundwater or subsurface flow within the catchment and that it may have the potential for subsequent flooding or difficulties from increased groundwater levels.

Double peak hydrographs

Double peak hydrographs are hypothesised to be the ideal indicator of a multisource catchment. Although poorly understood, they are present in a large number of catchments (Martínez-Carreras et al., 2016) and are, in essence, the extreme of an asymmetrical hydrograph. The slow transit of groundwater into river systems, relative to surface flows, creates hydrographs with a second peak, potentially caused by subsurface flows into the river system. I.e. steep rising and falling hydrograph limbs from surface runoff entering the river, followed by a second, more gradual peak as groundwater reaches the river. Double peaked hydrographs have been witnessed in the UK at sites such as Kilham and Slapton (Birkinshaw, 2008) as well as sites around the world, such as Japan and Luxembourg (Martínez-Carreras et al., 2015, 2016), Williams Creek in Missouri (Yang et al., 2015) and the upper River Saalach in the Austrian Alps (Zillgens et al., 2007). One caveat is that double peak hydrographs can be generated via other mechanisms such as delayed (or accelerated) inflow into rivers from storm drains (Seaburn, 1969), lag whilst flows descend from the upper catchment (Macdonald et al., 2012) and from catchments with split fast and slow surface runoff processes (Yang et al., 2015).

In order to capture some of these hydrograph shapes, groundwater indexes were developed to assess the proportion of base flow (i.e. groundwater source) in peak events, while surface water indexes assessed how suddenly hydrographs responded to rainfall.

Hypotheses for Identifying Multisource Catchments

Using the information above, several hypotheses were made with regard to where multiple source events may be found:

- Geology is the principal location control as groundwater flows require permeable geology. Most multisource catchments will therefore be found around major aquifers (Fig. 2.5).
- For sudden influxes of water into river systems, there must also be appropriate catchment characteristics. These may include low permeability surfaces, steep topography and low interception potential.
- Catchments that exhibit such events may have segregated features. For example, there may be Chalky upper catchments that regulate or sustain groundwater flows into a river that enters a more urbanised, less permeable, and thus flashier, lower catchments. This may also include subcatchments with different flow regimes.

7. Data and Quality Checking

7.1 Introduction

The numerical methodology for identifying multisource catchments allows it to be used nation wide, however this requires good quality data. High resolution, 15 minute, stage data was provided by the JBA Trust, who sourced the data from the Environment Agency and ran various quality checking processing on it. JBA requested that this data was further quality checked (QC) by eye using their graphical summary plots prior to exchange of the full data. An example of one of these plots can be seen in Figure 7.2.

Of the original 1223 stage records, around 800 were removed or had data cropped from them. Of the remaining records, 435 were matched to rating curves and converted to flows and passed further quality checks. The locations of the available stage records and processed flow records can be seen in the Appendix (Sec. 26). Converting levels to flows provided access to higher resolution data than was otherwise available, a key factor when capturing instances of rapid response to rainfall. The use of flows was considered much more reliable than using level (stage) data as hydrograph shapes produced with level data would be affected by the shape of the river channel and so is harder to analyse.

7.2 Identification of Errors

As stated above, prior to being given full access to the data all records were quality checked to ensure that only reliable records, or reliable periods of records, were used. The records were assessed for the following errors.

Missing Data

Missing data was one of the simplest and most common errors to find in the records. It is uncertain why many records are missing data, however it is likely to be a combination of incomplete collation of records and periods of no recording, perhaps during times of flood or drought or when the recording mechanism changed (i.e. structural or a change from analogue recording to digital).

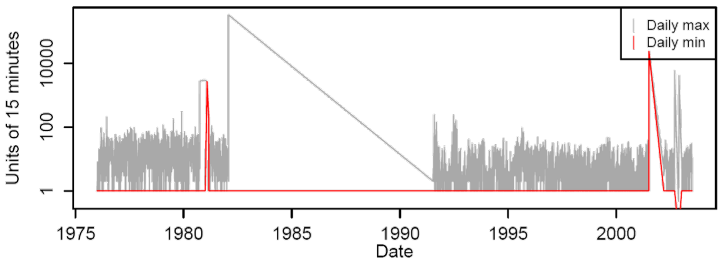

Figure 7.1: The observation interval plot indicates that there was missing data throughout the record, with a hiatus in recordings between 1982 and 1992.

Many of the records contain periods of missing data. Whilst some

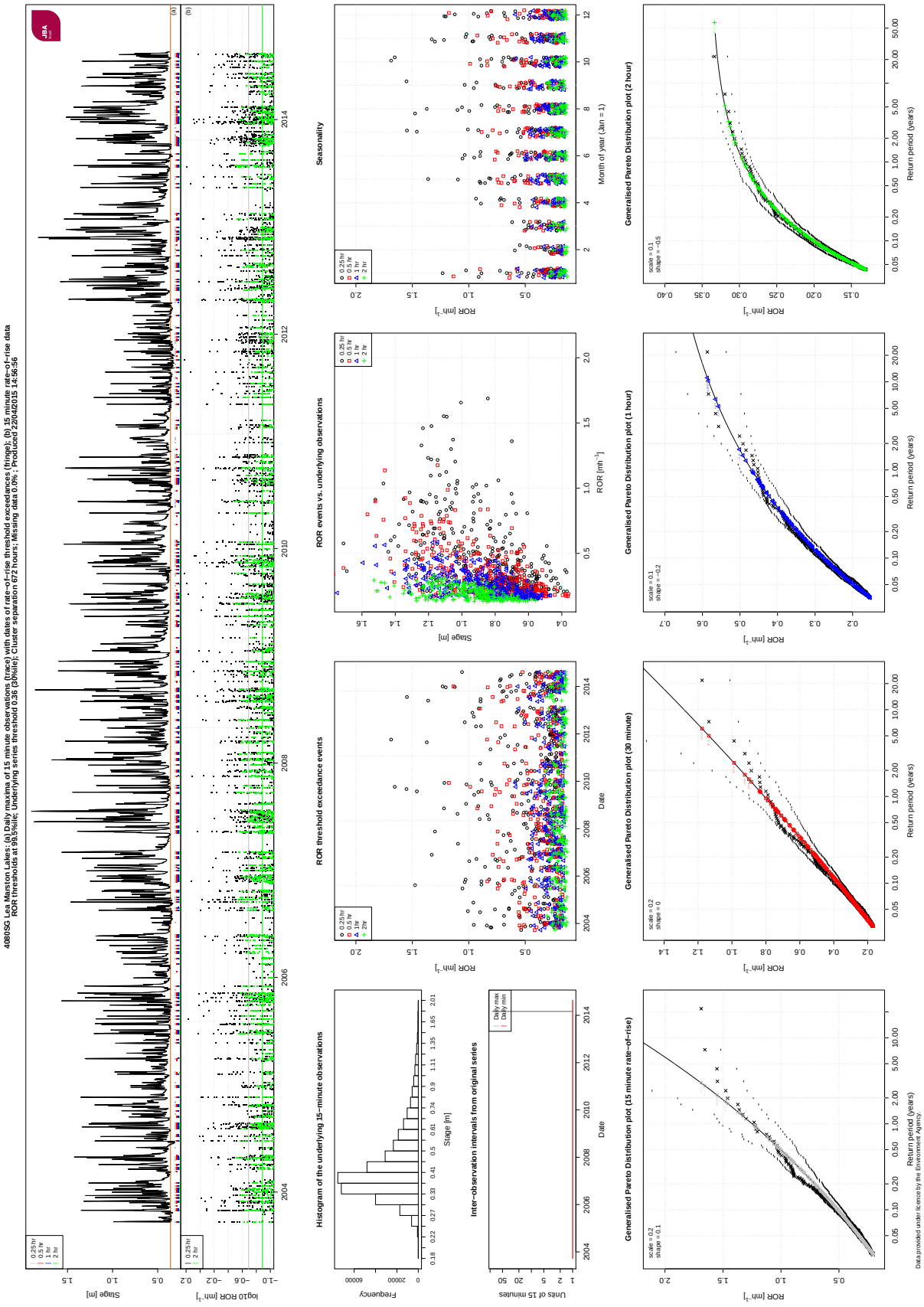

Figure 7.2: An example of one of the JBA summary sheets, here describing high quality data. From top-left to bottom-right, the plot consists of a hydrograph, histogram of stage readings, the amount of missing data over time, three plots that show the relationship between the highest rates of rise events with the variables time, river stage, and season. Finally, there are four Generalised Pareto Distributions indicating return periods. Principal errors to watch for were missing data, anomalous points and step changes in river stage.

of these may only be a single missing reading, some periods can be hours, days or even years. Periods longer than a year were excluded from the analysis. The single missing data points were interpolated and so were of minor concern. Of greater importance were periods of missing data in the order of hours to weeks. These dispersed periods limit the number of extended durations of 'good' data and can mask periods of high rate of rise (RoR), and so influence results. Rate of rise calculated as the increase in river stage or flow divided by the time period over which the increase occurs.

The observation interval plot in Figure 7.1 has two lines; the red line indicates the smallest gap between recordings and the grey line shows the greatest number of 15 minute time steps without recordings per day. Where there were multiple days of missing data this red line shows the number of periods until the next reading. In the example, there are frequent gaps of around one hundred 15 minute periods (approximately one day) throughout most of the record.

Where missing data occurred in clumps, the dates of missing data were recorded so that the period could be excluded. In other records, if there was a significant amount of distributed missing data then the entire record was disqualified.

Quantisation

Quantisation is the approximation of a continuous signal to one whose amplitude is restricted to a prescribed set of values. It occurs when river stages were measured to a subset of values rather than a full range of numbers. This may have taken place when precise stage measurements were not required, when measurements were recorded to too few significant figures, or when stages are typically very low. Quantisation can increase or decrease rise rates if data are severely discretised or rounded.

Quantisation could often be spotted in the set of four graphs shown in Figure 7.3. In this example, it appears that data has been recorded to the nearest 2 mm and so causes the Generalised Pareto Distribution (GPD) plots to fail and become stepped and forms the striped patterns in the rate of rise plots. Here, although this data has been quantised, it was included in analysis as recording to the nearest 2 mm is deemed to be of sufficient precision for this study.

Anomalies and Step Changes in River Stage

Many of the stage time series contained anomalous instances where river stage increases by an implausible height (up to 10's of meters) over a 15 minute period, often for only a single reading. These points are obviously incorrect and will record errantly high rates of rise.

The majority of major river stage errors were simple to spot in the hydrograph. Anomalous outlying data points were also often simple to identify. If there were large numbers of outliers then the data, or periods of it, were disregarded. Normally, major outliers were limited to one or two occurrences and could be easily cropped without losing much data. In subsequent data processing, stages over 10 m were removed to reduce the impact of outliers on analysis. The example in Figure 7.4a shows an anomalous stage at Fiddler's Elbow on the River Taff.

As well as these momentary anomalies, clear step changes also existed in some records where a river adopted a new typical depth for an extended period of time. Step changes occurred multiple times in some records and were likely to be caused by changes in recording mechanism. Step changes were especially likely following periods of missing data, which supports the theory of the implementation of a new recording structure.

Figure 7.4b shows a severe step change in typical river stage at Waddingham. Although it may be possible to correct for such errors, as we know the stages of nearby gauges, no attempt at this is made, mainly for simplicity and the large volume of available data. If the change in stage was significant, a period of consistent river stage was chosen for analysis. Periods were chosen according to the length of the available period, the errors within it, and its age.

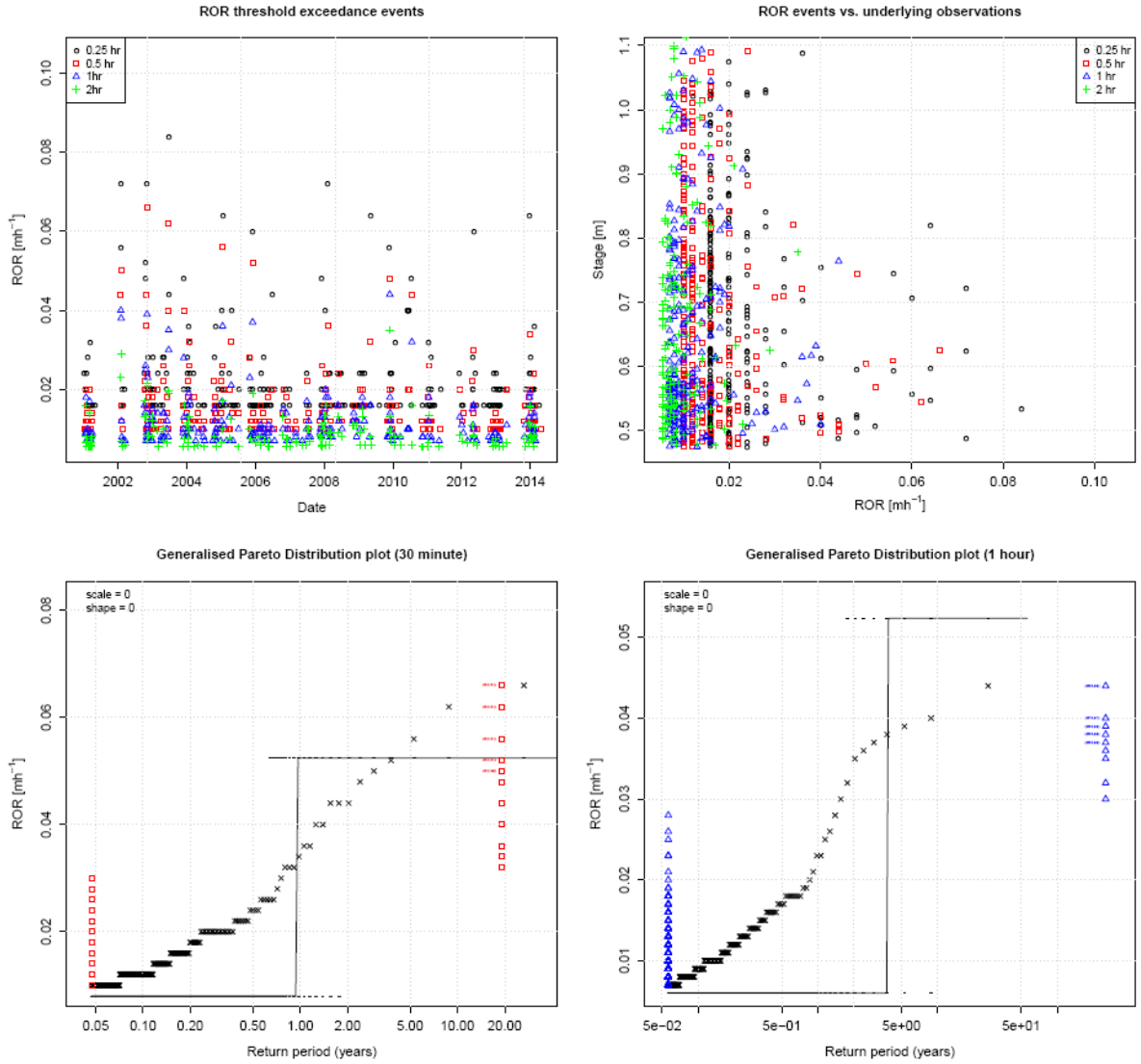

Figure 7.3: Quantised data From Loverley Farm shown in rate of rise (ROR) and Generalised Pareto Distribution plots. RoR is given in m/hour and calculated as the difference in stage divided by the time since the previous observation. This is only calculated for those instances where the river is rising.

In addition to the hydrographs, step changes could also be inferred from the histogram plots. It would be expected that a standard hydrograph would fit a largely Gaussian distribution. In other words, the mid-range river stages would be the most common, with extreme values being less so. The example histogram in Figure 7.4c does not show this however and instead has two peaks reflecting the two typical river stage norms. This can be seen in the accompanying hydrograph, which shows a change in nature midway through the data series with river stages frequently hovering around 0.25 m. In this instance the second half of the data was removed.

Changes in Data Quality Over Time

Many of the records appeared to fluctuate in quality over time. These fluctuations often coincided with other issues, such as changes in typical river stage or changes in the typical rate of river level rise. This indicated that inconsistencies in record quality over time may relate to a change in measurement frequency, recording mechanism, or the re-sampling of analogue records. For

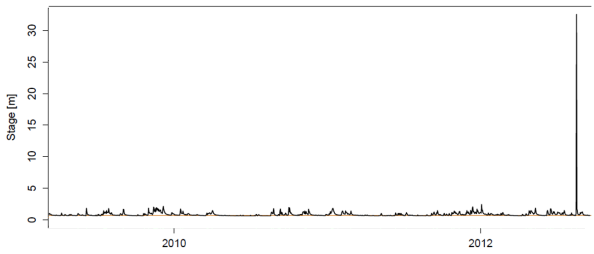

(a) An outlier on the Fiddler's Elbow gauge meant data more recent than 2012 was removed from analysis.

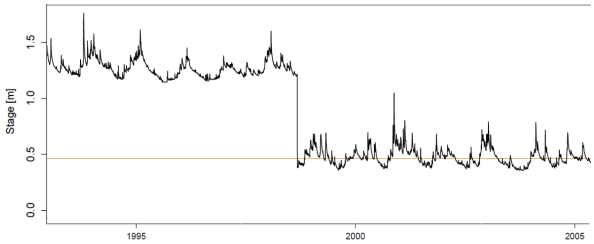

(b) A step change in river stage seen at Waddingham renders the first section of data unusable.

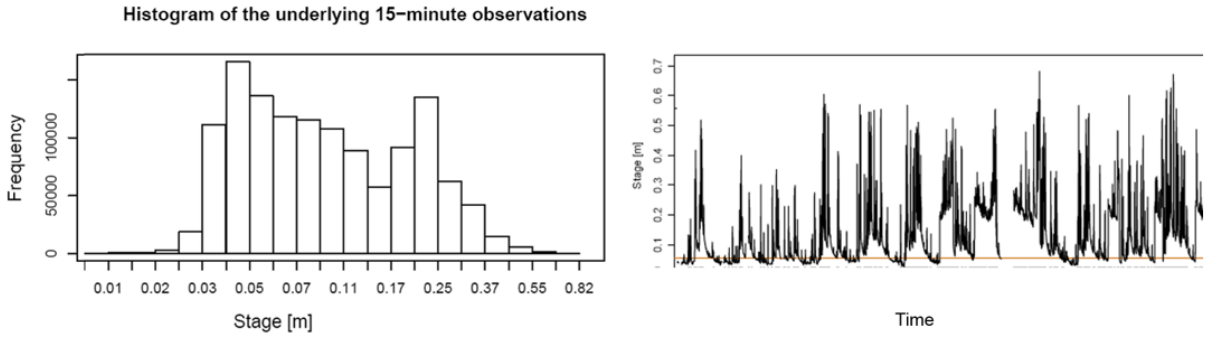

(c) This histogram of river stage frequency at Dewlish Woodsdown shows twin peaks rather than the expected Gaussian distribution. The data for the histogram is shown in the stage hydrograph below.

Figure 7.4: Anomalous data and step changes in stage could be identified from hydrographs and histogram plots.

example: electronic re-sampling of continuous analogue records, termed *digitisation*, was used to convert older paper records into digital formats. This took place in various forms - sometimes data was transferred at a high temporal resolution (e.g. 5 minutes), at others it was a lower resolution, such as hourly, and at others this may have been at a low standard resolution that was increased during 'interesting' periods (R. Lamb - JBA Trust 2017, personal communication, 12th April).

All of the stage data is provided at a 15 minute resolution and, considering the age of some of these records, it is likely that some of these may have been resampled. Interpolated data is unlikely to accurately portray a river's rate of rise.

One of the simplest methods for identifying a change in data quality was through the Rate of Rise Threshold Exceedance Events Over Time plot. Figure 7.5 shows a clear example of interpolation and a change in record quality on the River Nevis at Claggan. We see a sudden change in the nature of the record in 2002. On further inspection, the black circles on the left side of the graph are all contained within the red squares - these represent the rise rates for 15 minute and 30 minute periods respectively. As these are equal for each exceedance event, it is clear that data recorded at 30 minute intervals has been resampled to a higher, 15 minute resolution. In 2003 the rate of recording increases to a 15 minute resolution and so higher rates of rise can be seen in the 15 minute data. All data prior to the 2003 was discarded as it would not accurately portray the rates of river stage rise.

Truncated Measurements

Truncations in river stage were present in some of the records. These can be seen where peaks in stage all reach similar maxima or when troughs only decrease to regular minima. Truncations are likely to be caused by limitations in recording, such as exceeding the range of the recording

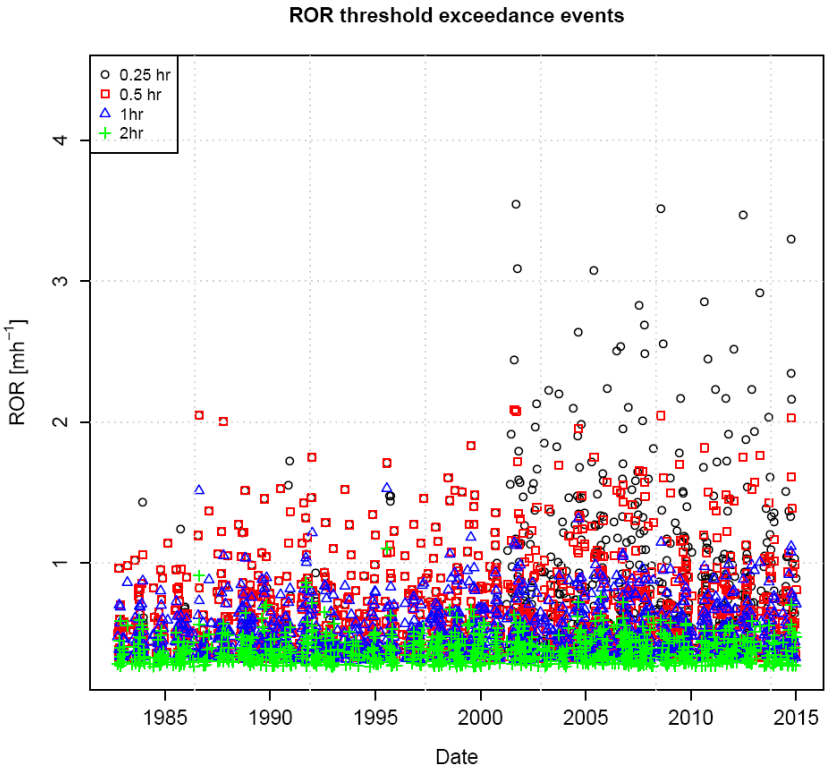

Figure 7.5: Stacking of red and black symbols on the left of the plot imply that 15 minute data has been resampled from 30 minute data to give identical RoR until 2003 when the 15 minute record began.

mechanism during particularly high or low flows. In some instances, truncations appeared at medium stages. The cause of these was unknown, but was still documented as a truncation.

Figure 7.6 shows two hydrographs: at Ugly Dub on the River Tyne and at Ystradffin on the River Towy. Both show truncation and both were removed from analysis. These examples indicate that the flows may be regulated. Ugly Dub, for example, is on the river outlet from Kielder Reservoir and Ystradffin is just downstream of Llyn Brianne Reservoir.

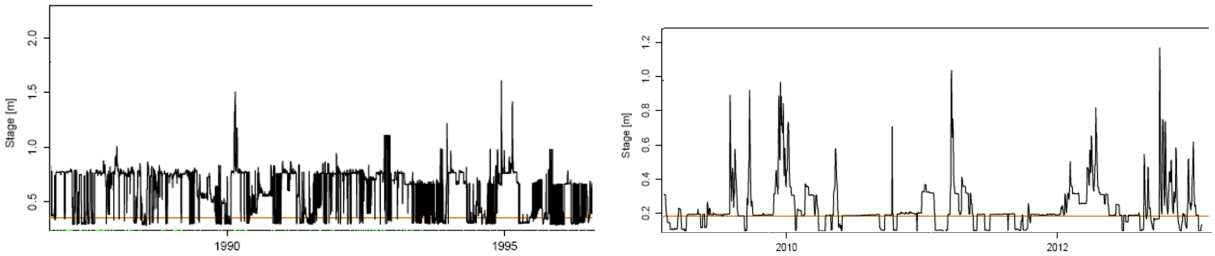

(a) River Tyne at Ugly Dub

(b) River Towy at Ystradffin

Figure 7.6: Two instances of truncated stage records, both were removed from analysis.

Tidal Rivers

These are of no use in the assessment as the rates of rise and base flows are dependent on tides. Tidal influence can be seen by the occurrences of highly regular monthly fluctuations, all rivers suspected of these were removed. Not all rivers close to the sea exhibited these fluctuations.

7.3 Summary

When quality checking the records certain dates yielded higher numbers of errors, with many of the clipping dates in the early 2000's, most notably in 2004. This was due to an apparent lapse in data quality in the early 2000's. One concern was that this was due to a humans' natural tendency to approximate numbers - e.g. rounding numbers to multiple of 5 (Wilby et al., 2017). Clipping dates were checked, and this was not found to be the case but instead showed a good distribution of selected dates. A similar occurrence was observed in 1992 in the Anglian region. This was again due to data quality, but could be linked to low river stages observed over the first few years of the 90's. This apparent drought was not noticed in other regions. There were similarities between the dates used to clip the starts of the North East and North West; although the reason for this is unknown. One of the major observations of note is the lack of data clipping needed in the Scottish records. Almost every Scottish record was immaculate, with no visible evidence of interpolation, missing data or anomalies in over 40 records, each lasting around 40 - 50 years. This is likely to be due to post collection prepossessing of the data by SEPA.

A summary of those gauges found to contain errors can be seen in Table 7.1. When data was converted from stage into flow, only those gauges in England and Wales were matched to rating curves, and so no data from Scotland was used in analysis.

Further, more general observations are that:

- There was an improvement in data quality over time.
- The South East had the largest percentage of records deemed unfit for use - distributed errors meant that there was less potential for clipping out data errors.
- No direct correlation exists between the number of quality flags triggered by a record and its exclusion from analysis.
- Around 50% of the records required clipping to increase data quality.
- The Anglian region had the most frequent occurrence of quantisation, although this largely concluded by the late 1990's. The failure of the GPD plots was largely accountable to the degree of quantisation, not the volume of missing data, as originally instructed by JBA.
- Localised (sub-regional) patterns of errors were frequent, e.g. gauges close to one another having missing data over similar periods or step changes in stage around similar times.

Table 7.1: A summary table of the errors found in each region as percentages and the resulting action (either clipping or removal).

	% Quantised	% with Failed GPD Plots	% with >1% Missing Data	% with Maximum Data Gaps >1 hr	% with Minimum Data Gaps >1 hr	% with Step Changes in Record Quality	% with Anomalies in River Level	% with Step Changes in Typical River Level	% with River Level Truncations	% of Records Removed	% of Records Clipped at Beginning	% of Records Clipped at End	% of Records Clipped at Beginning and End	% of Records Clipped and Removed	Number of records Assessed
Anglia	20	10	90	93	42	11	17	11	7	17	63	4	2	7	209
Midlands	11	3	85	87	48	11	7	15	4	7	68	2	1	2	149
North East	10	4	89	94	49	4	6	6	6	7	54	3	2	3	140
North West	7	2	80	87	55	9	2	8	2	13	62	3	1	4	126
South East	7	4	82	84	18	11	22	16	7	45	34	15	7	11	178
South West	12	3	85	83	40	24	12	10	7	21	50	5	1	7	260
Wales	5	1	42	66	5	0	5	5	7	18	10	2	0	3	119
Scotland	2	0	26	57	2	19	5	7	0	0	36	0	0	0	42
Total	11	4	79	84	36	12	11	10	6	19	49	5	2	6	1223

8. Methodology

The following methodology describes how indexes were calculated to reflect the contribution of groundwater and surface water to the peak river flows. Catchments that scored highly in both of these indexes (i.e. where both surface water and groundwater were present) were then deemed to be multisourced.

As there was no existing method for classifying or identifying catchments at risk of multisource flooding, many methods were trialled before the methodology below was established. These methods included wavelet analysis, hydrograph clustering and principal component analysis, manual identification of double peak hydrographs and correlations between rainfall and river level. These were not used for a variety of reasons, however one of the dominant factors was that the lack of historical data made calibrating and validating the often complex classifications very difficult. The final method is much more transparent to reduce the need for calibration and validation. Several of these unused methods are described in the Appendix in Chapter VIII.

8.1 Identifying Groundwater Catchments

The method for determining whether river water was derived from a groundwater source was relatively simple and rested on the basic assumption that the groundwater contribution to a river is well represented by the river's base flow. Base flow separation was originally developed by what is now the Centre for Ecology and Hydrology (World Meteorological Organization, 2008), although its roots are much older (Brodie and Hostetler, 2005). In theory, base flow (sometimes referred to as groundwater discharge (Thomas et al., 2015)) is derived from stored sources (Gustard et al., 1992; Tallaksen, 1995) and refers to a relatively consistent water volume within the river (Sophocleous, 2002) that is mostly independent of local, short-term rainfall. Although lakes, wetlands, snow melt and glaciers can provide slow release storage (Brodie and Hostetler, 2005), groundwater is the dominant component of base flow (Li et al., 2013; Stewart et al., 2007; Park et al., 2011). Water not classified as base flow is thought to be derived from surface runoff that has entered the stream soon after it was precipitated.

Dudley et al. (2018) tested the correlations between streamflow and baseflow with groundwater records and find that both are strong predictors of groundwater level. Yan et al. (2018) conducted a similar study, also finding streamflow to be correlated with groundwater level (though in this case to a lesser degree than precipitation). These two papers help to support the method proposed here of identifying groundwater regions using stream flows and base flows. One caveat to be aware of is that in cases where the river is regulated or has significant storages or abstractions the base flow separation may not be applicable (Brodie and Hostetler, 2005; World Meteorological Organization, 2008). The aforementioned quality checking process removed several regulated rivers from the analysis.

Nejadhashemi et al. (2009) state that over 40 methods exist to calculate base flow. Numerous works have sought to determine which of these is the most accurate, however, as directly measuring base level is difficult (He et al., 2016), it is hard to determine which of these is most appropriate (Li et al., 2013) and so a 'correct' method of estimation does not exist. There are a range of method types (e.g. graphical, empirical, automated, analytical, geochemical and modelling based (Nejadhashemi et al., 2009)), some of which try and take into account catchment and temporal heterogeneity such as geology, area and evapotranspiration (Brodie and Hostetler, 2005; Tallaksen, 1995; Li et al., 2013).

It was decided that a simple automated method used by the World Meteorological Organisation (WMO) would be adopted. This is detailed in Chapter 5 of their Manual on Low-flow Estimation and Prediction (World Meteorological Organization, 2008). The WMO method is similar in some ways to a moving average. It splits a time series into non-overlapping five day segments and selects the minimum flow of each segments. If any of these minimum points are less than or equal to their adjacent minimum points ÷ 0.9, then they are defined as turning points. This method is then repeated using different 5 day sections until the whole time series has been analysed. These turning points are then connected by straight lines, below which water is attributed to base flow. By taking the base flow as a ratio of the total stream flow, the *base flow index* (BFI) is calculated (Gustard et al., 1992). It is concluded that the BFIs on the NRFA website also use the WMO method or one very similar as these returned a Spearman's rank of 0.99 when BFIs were compared to those calculated here.

8.1.1 Base Flow in Peak Events

Base flow indexes are not suited for describing river processes during peak conditions. As such, base flows were used to create a slightly different *groundwater index* that used only the top ten river flow events from each gauge. Tests did calculate the *groundwater index* for the entire record but this produced high indexes in surface water dominated catchments during periods of sustained low flows that could not be distinguished from catchments with high groundwater contents during high flows. Instead, by analysing only the top ten flow events, the groundwater index focussed on peak conditions, the basis of this study. Those events that fell within a two week period of a larger event were discounted to ensure that the same events were not sampled multiple times. *Events* were defined as the four days preceding and the ten days succeeding the peak. The longer period following the event peak was to allow time for a slow increase in groundwater contribution to the stream or river. The length of the records vary across the dataset from around two years to several decades. As such, the ten events represent a range of return periods.

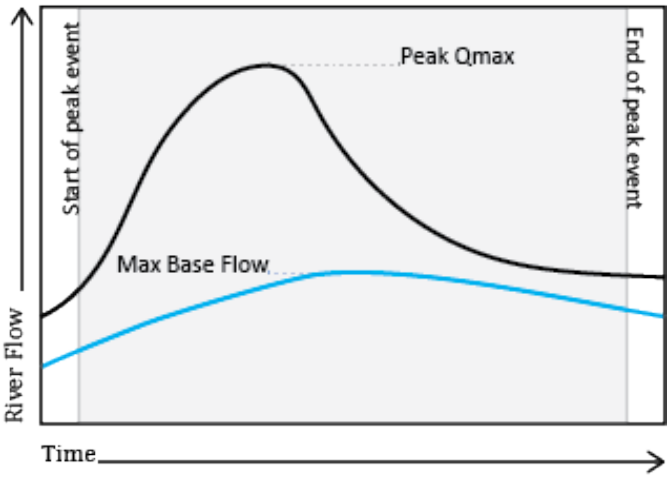

Figure 8.1: To calculate the groundwater indexes for each catchment the ratio of maximum base flow : peak flow was averaged from the top 10 peak flow events.

The WMO base flow separation method was used to estimate groundwater contribution to each event. This was defined as the ratio of the maximum base flow to the maximum stream flow (Equation 8.1.1). This can be seen in Figure 8.1. This method shares some similarity to an

approach in Hannah et al. (2000) in which the ratio of *(peak flow - base flow)/ base flow* is used as a potential proxy for surface runoff.

These ten ratios (one for each event) were then averaged to give a single groundwater index per record. Hydrographs of each of these events were plotted alongside rainfall and a selection of these were examined to qualitatively calibrate the indexes against suspected hydrograph features.

Equation 8.1.1 — Groundwater Index Calculation. The groundwater indexes use the top 10 flow events from each time series. For each event, the maximum base flow is calculated and divided by the maximum steam flow. The 10 event indexes are then averaged into a single index.

$$Groundwater\ \ Index = average\left(\frac{Qbm_{event\_1}}{Qm_{event\_1}}, \frac{Qbm_{event\_2}}{Qm_{event\_2}} \ldots \frac{Qbm_{event\_10}}{Qm_{event\_10}}\right) \tag{8.1}$$

Where Qbm is the maximum base flow in the event; and Qm is the maximum stream flow in the event.

8.1.2 Quantile Based Base Flow Assessment

As a separate line of enquiry, the distribution of base flows throughout each of the records was investigated. It was understood that at low flows the majority of the flow would be categorised as base flow and it was assumed that at high flows only those rivers with significant groundwater contributions would retain a high base flow component.

The base flow separation method above was employed again and each of the river flow readings was attributed with a BFI (i.e. the ratio of base flow : total flow) at that moment. The flows were then grouped into 20% quantiles and the mean base flow index for each of those quantile groups taken. A diagrammatic explanation of this can be seen in Figure 8.2.

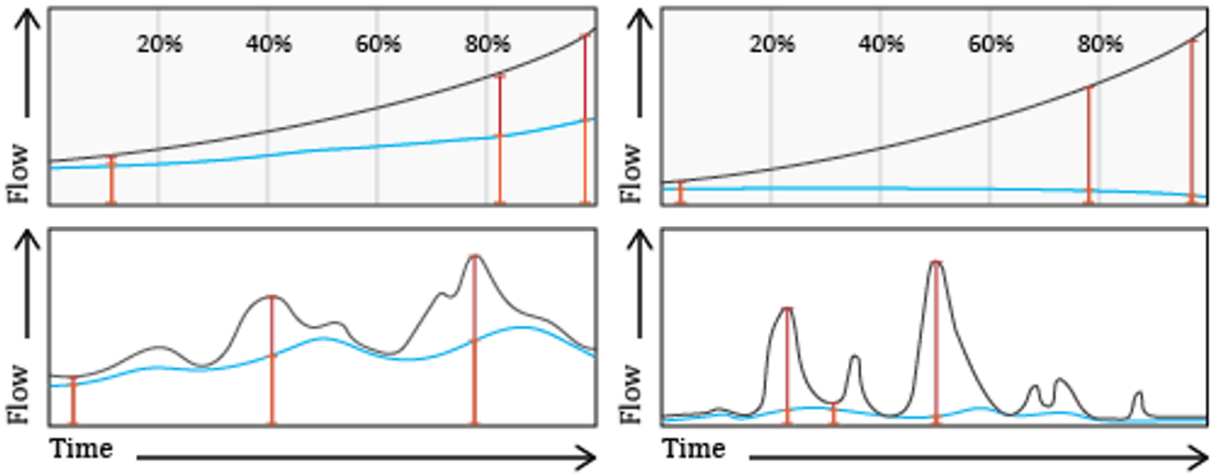

Figure 8.2: The hypothetical groundwater dominated hydrograph on the left maintains base flow when at the higher flow quantiles. The flashier hydrograph on the right does not contain base flows at these high flow events. The blue lines represent base flow; black %s represent quantiles.

No evidence of this method of calculating the BFI distributed according to flow quantile has been found in the literature. It is hoped that this simple method may indicate those rivers which have potential to flood from groundwater, but it will not necessarily show those rivers that have rapid, surface water responses.

8.2 Identifying Surface Water Catchments

The purpose of the surface water indexes was to identify flashy surface water responses during peak flow events, even if they have a large base flow contingent. As with the groundwater indexes, this method used only the top 10 events. For each of these events, the base flow was removed, leaving the water derived from surface runoff. The minimum flow within the preceding 12 hour period was also identified and removed. The hydrograph was then cropped so that it began at the point of this minimum flow. The volume of water between this minimum and the peak (i.e. the area under the curve of the hydrograph) was then calculated and divided by the peak flow (not including the base flow and antecedent river flow) (Eq. 8.2.1). This ratio was calculated for each of the 10 events and the results averaged to generate a single index for each catchment. A diagrammatic outline of this method can be seen in Figure 8.3. Hydrographs of each of these events were plotted alongside rainfall and a selection of these were examined to qualitatively calibrate the indexes against suspected hydrograph features.

Equation 8.2.1 — Surface Water Index Calculation. The surface water indexes use the top 10 flow events from each time series. For each of these 10 events, minimum stream flow prior to the peak is identified, the volume of surface runoff between this minimum and the peak is then calculated and divided by the rise in surface water (see below). Each of the 10 values is then averaged to give the surface water index.

$$\frac{\sum_{n=t_{min}}^{t_{max}} Q_n - Qb_n - (Q_{t\_min} - Qb_{t\_min})}{Q_{t\_max} - Qb_{t\_max} - (Q_{t\_min} - Qb_{t\_min})}$$

Where flow from surface water equals:

$$Q_n - Qb_n$$

and the initial surface water component equals:

$$Q_{t\_min} - Qb_{t\_min}$$

Where Q is the stream flow; Qb is the base flow; t_{max} is the time at peak; t_{min} is the time at the minimum stream flow prior to the peak (i.e. at the start of the calculation period).

The surface water indexes (SWIs) give a statistic similar to rate of river level rise (as used in the JBA quality checking process), except that they account for groundwater flow and antecedent conditions and so are more representative of surface water processes. SWIs are likely to be increased by the presence of impermeable surfaces, low surface storage, steep slopes, and intense pulses of rainfall.

8.3 NFRA Catchment Descriptors

The National River Flow Archive contains a large number of catchment descriptors. These range from indexes describing the steepness or base flow index of the catchment, to its size and altitude. As an additional line of investigation, the relationship between the indexes created above and the NRFA catchment descriptors were tested. The reason for this was twofold:

1. To check whether the indexes from this work appear to be realistic, correlating with simple predictions.
2. To investigate whether there are any catchment features that are indicative of high groundwater or surface water indexes.

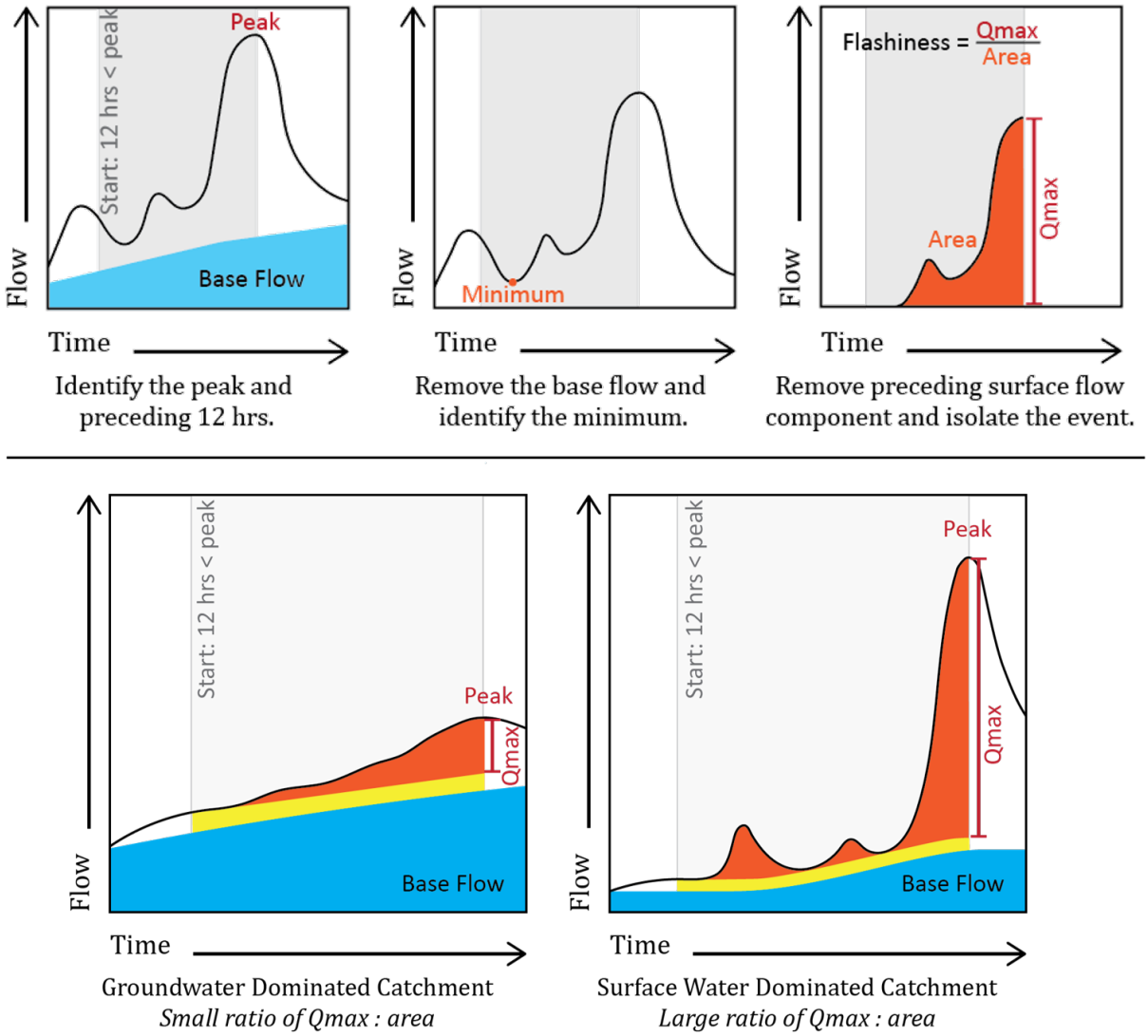

Figure 8.3: The top three diagrams show how the peak integration method works for defining how flashy a record is. The bottom two diagrams demonstrate the differences between a non-flashy and flashy catchment.

The NRFA catchment descriptors were downloaded from the NRFA website and Pearson's correlations were calculated between each of them as well the indexes created in Sections 8.1 and 8.2. Correlation analysis was conducted on the dataset as a whole, and then the highest and lowest thirds of both the surface water and groundwater indexes.

9. Results

9.1 Identifying Groundwater Catchments

We can see from Figure 9.1 that the majority of the groundwater indexes (GWIs) are, numerically, clumped together and are surprisingly low. Only 50/435 are ≥ 0.2, 23 are ≥ 0.3, 15 are ≥ 0.4 and 8 ≥ 0.6.

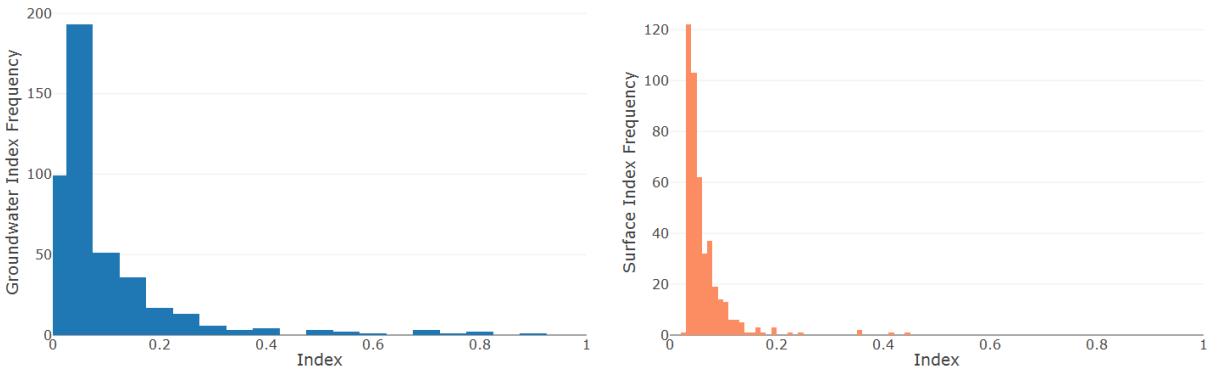

(a) Distribution of groundwater indexes

(b) Distribution of surface water indexes

Figure 9.1: The distribution of the groundwater (blue) and surface water (orange) indexes. While both are heavily clumped around 0.02 and 0.06 respectively, both have several much higher values. It is these higher indexes that are likely to be of the most interest to this study.

Assuming GWIs to be similar to BFI, it had been expected that a GWI of around 0.4 would be a suitable lower bound for defining groundwater presence in a record. However, checking GWIs against event hydrographs showed a lower value of 0.1 to be more appropriate. Hydrographs with GWIs of this value typically exhibited slowly descending limbs and variable and tangible antecedent conditions. A selection of hydrographs can be seen in Figure 9.2 representing a range of GWIs. These show that the method does work as planned with a clear difference in hydrograph shape as the GWI changes. The calculated GWIs are mapped in Figure 9.6a. Coloured points are those that are thought to contain a reasonable proportion of groundwater. The large difference in GWI (which uses only peak events) compared to BFI (which uses the whole record) is due to the exclusion of low flows, which typically have very high BFIs.

Figure 9.3 shows the results of the base flow quantile analysis (Sec. 8.1.2) - the base flow indexes (BFIs) for the top flow quantile are plotted against the middle quantile. As would be expected, the typical BFI for high flows is less that that at mid flows. The colouring of the points in Figure 9.3 show the hydrometric area. Using this plot alongside the map of hydrometric areas

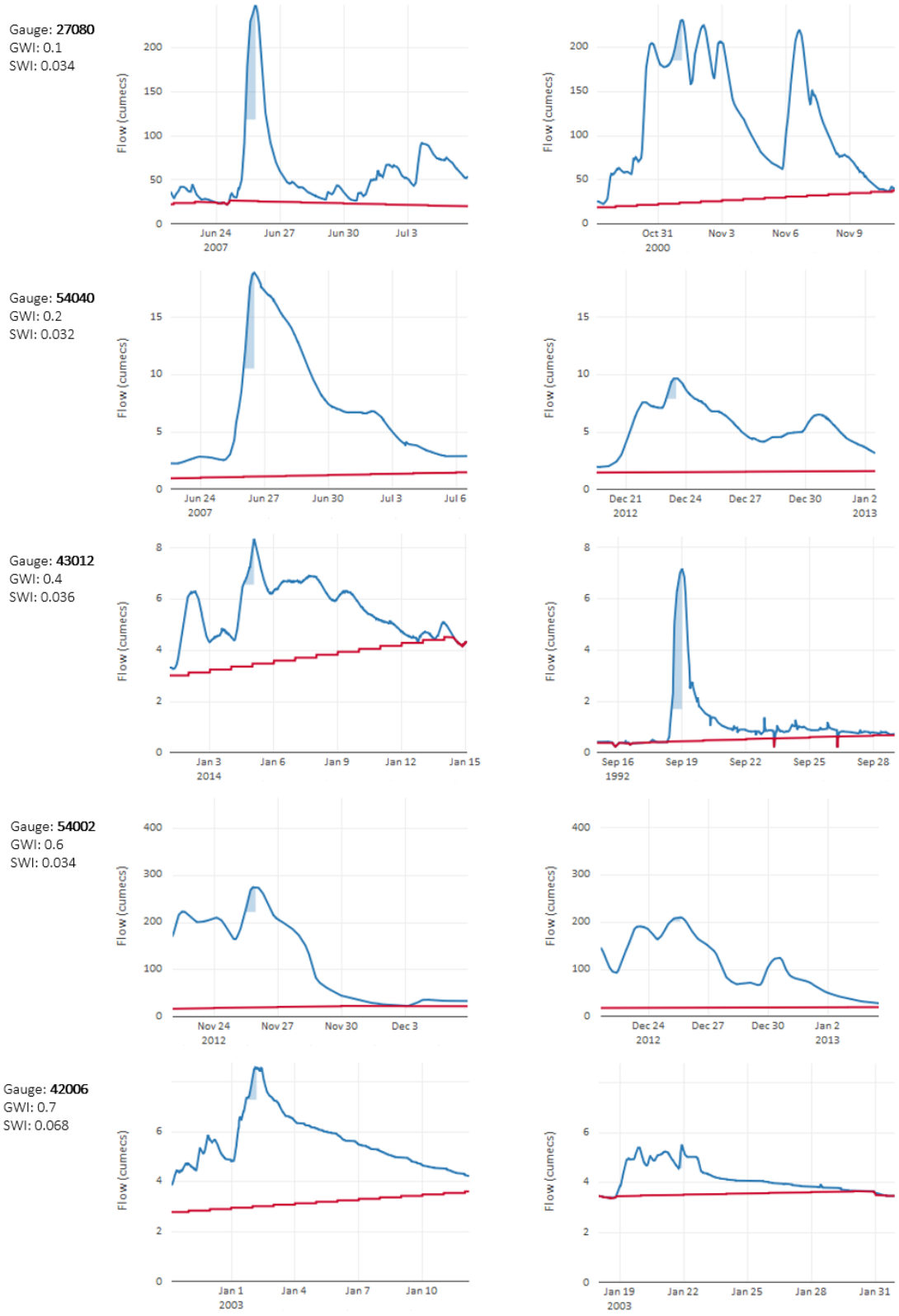

Figure 9.2: **Groundwater Hydrographs -** 6 pairs of hydrographs are shown as examples of a range of GWIs. Examples of GWIs of 0.01 (22001;25012) and 0.02 (30017;74001;25018), can be seen in Figure 9.7. The higher the GWI, the higher the assumed groundwater input to during peak events. Blue lines show river flow; red lines show base flow; shaded areas show the period used for calculating rate of rise.

in Figure 9.4 implies that the majority of records with high BFIs in high flows are located in the south and east of England. A map showing BFI's during the highest flows can be seen in Figure 9.5.

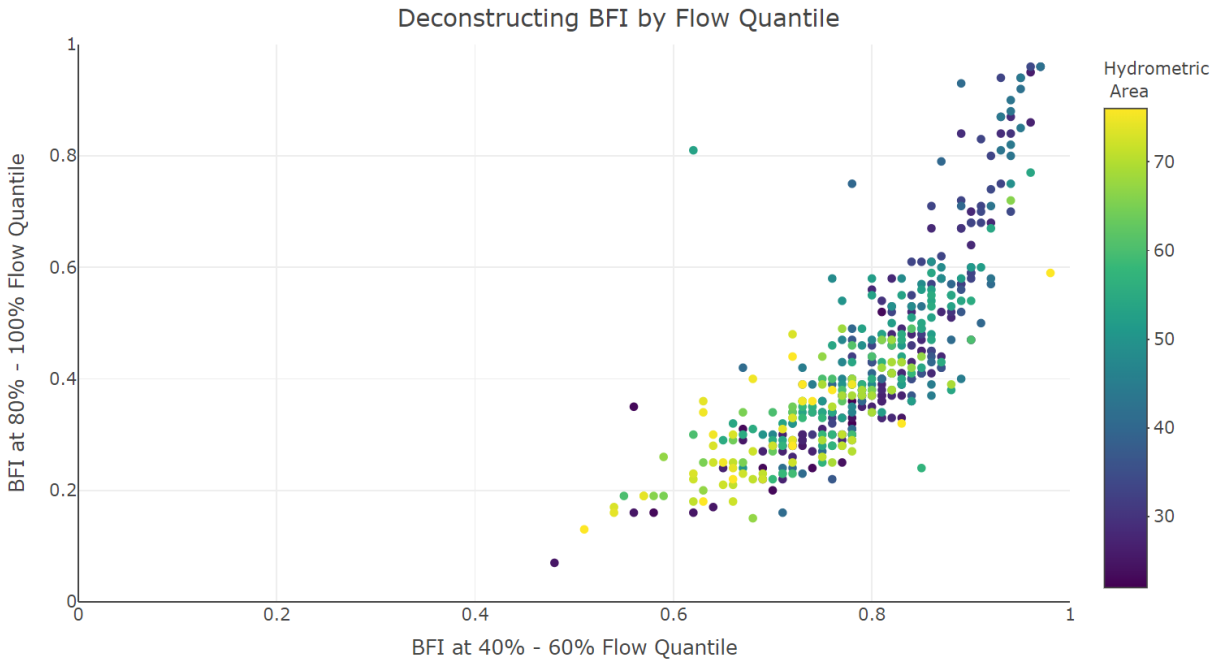

Figure 9.3: The base flow indexes during medium and high flows are plotted against one another. Points are coloured according to the first number of their gauge ID to aid their identification. Regional locations for these can be determined using Figure 9.4.

Those records that show high BFIs at both medium and high flows are likely to be heavily dominated by groundwater. This does not mean that these are necessarily of interest to this study. Instead, it is those that appear to have surface water flashiness imposed upon a reasonable, but not necessarily exceptional, base flow.

9.2 Identifying Surface Water Catchments

Surface water indexes increase relatively linearly from 0.03 to 0.1, however they drop off steeply at this point, with only 46 of the records ≥ 0.1. Like the groundwater indexes, the absolute values of the SWIs are not constrained against any other value and so are only relative, simply to be used in comparisons. The SWIs can be seen mapped in Figure 9.6b.

Figure 9.7 shows a subset of example hydrographs along with their calculated surface water indexes. These example plots have been selected based on their indexes alone to avoid 'cherry picking' of catchments and confirm that flashier catchments produce higher indexes as desired. While the absolute values of the indexes are not important, a threshold value was established above which all catchments could be considered to have a surface water response to rainfall. A visual assessment of a selection of event hydrographs identified a SWI of 0.06 to be an appropriate threshold as all hydrographs with indexes above this displayed steep ascending limbs. This threshold was validated against catchment information taken from the NRFA.

Figure 10.2 shows a plot of GWI against SWI and indicates that high surface water indexes and groundwater indexes are not mutually exclusive. High surface water indexes can be found in the same records as high groundwater indexes. This infers that multisource catchments can indeed be classified using this method.

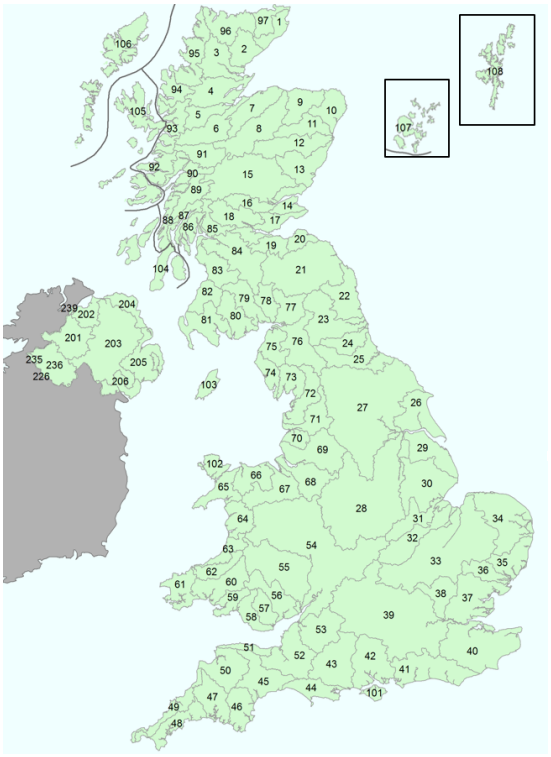

Figure 9.4: The UK's hydrometric areas are labelled clockwise. They make up the first two numbers of the gauging station IDs (National River Flow Archive, 2004).

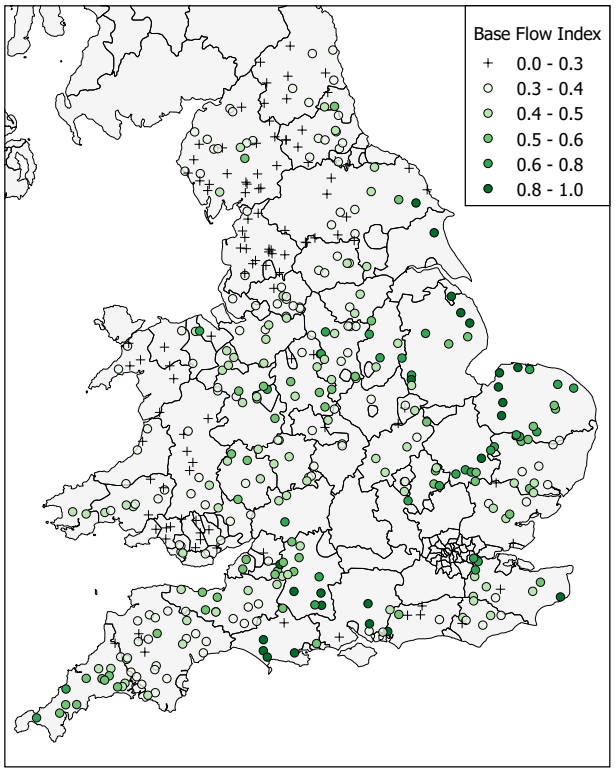

Figure 9.5: The base flow indexes during the highest 20% of flows are displayed. A large scale map can be seen in the Appendix (Sec. 26).

9.3 Correlation Analysis

NRFA catchment descriptors were downloaded for each gauging station and Pearson's correlation analysis performed between each group and the indexes calculated above. All correlation coefficients range from -1 to 1, with 0 indicating no correlation and -1 and 1 indicating strong negative and positive correlation respectively.

NRFA Indexes

We see from Figure 9.8 that several of the NRFA catchment indicators are interlinked. This is unsurprising. Some of the expected correlations are:

- *Catchment area* vs. *flow volume* ($\geq$0.9).
- *BFI* vs. *BFIHOST* (0.81) and *% highly permeable bedrock* (0.55). Interestingly, Jacobs (2004, Map A4.3) did not find BFI HOST to correlate with groundwater flooding events.
- Wetness *(SAAR)* vs. *altitude* (0.34 - 0.78) and *DPSBAR* (steepness) (0.85).

Geology may also have some links to altitude, with high permeability bedrock typically found at lower altitudes and low permeability superficials more often found at higher altitudes. In addition to the correlation between *BFI* and *highly permeable geology*, there is a much smaller (and thus inconclusive) negative correlation with *moderate and low permeability bedrock* and *superficial deposits*. This indicates that while a high permeability bedrock is important for groundwater flooding, other geology is less significant.

Peak Event Indexes

The largest correlations with the surface water indexes are with *station altitude* (0.19), *Minimum altitude* (0.19), *low permeability superficial deposits* (0.2) and *urban extent* (0.19). However, these

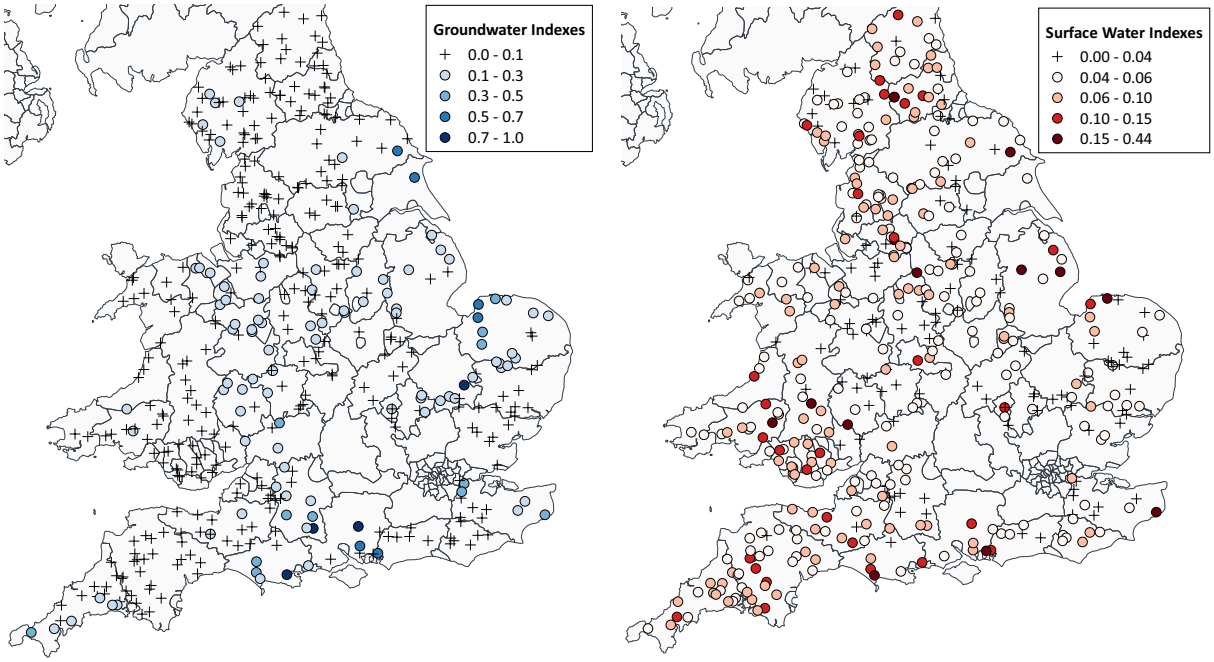

(a) Groundwater indexes

(b) Surface water indexes

Figure 9.6: The two maps show the calculated groundwater and surface water indexes from this chapter. For full page maps, see the Appendix (Sec. 26).

are very low and not significant. SWIs are not correlated with catchment area and therefore are not simply proxies for catchment size or similar, which was a concern with other attempted (and dismissed) methods.

The GWIs do, on the other hand, show a correlation of 0.69 with the *BFI* and *BFIHOST*. This is expected as all three of these are linked. The non-perfect correlation between *BFI* and *GWI* confirms that the proportion of water defined as base flow in low water is not directly proportional to the volume of water classified as baseflow in the peak events. The next greatest correlation with GWI is with *% High Permeability Bedrock (0.55)*.

When splitting the indexes into their top and bottom thirds and repeating correlation analysis slightly different coefficients were calculated. The highest third of the SWIs had a correlation of 0.24 with the *high permeability bedrock* compared to -0.23 for the lower third. There were also differences between the *urban extent* and *arable horticultural* indexes, both increasing for the top third to 0.22 and 0.18 respectively.

When looking at the split GWIs there are also a few noticeable differences. The low GWIs have a negative correlation of -0.32 with the SWIs whereas the high GWIs have a positive correlation of 0.29. This is the opposite of what was expected. The higher GWIs also correlate more with *BFI* and *BFIHOST* (at approx. 0.67) than the lower GWIs do (approx. 0.35). There is also a small change in the correlation with *high permeability bedrock*, increasing to 0.51 for the high GWIs, compared to 0.4 for the lower GWIs but a small decrease in negative correlation with the low permeability deposits. The low GWIs do show a higher correlation with the *low superficial deposit* values at 0.54 compared to 0.24 for the high GWIs.

Base Flow Quantiles

The 0-20, 40-60 and 80-100 quantiles from the quantile based base flow assessments were also included in the correlation testing. There is a significant correlation with the groundwater indexes and NRFA's BFI and BFIHOST. These correlations are expected as they all rely partially, or

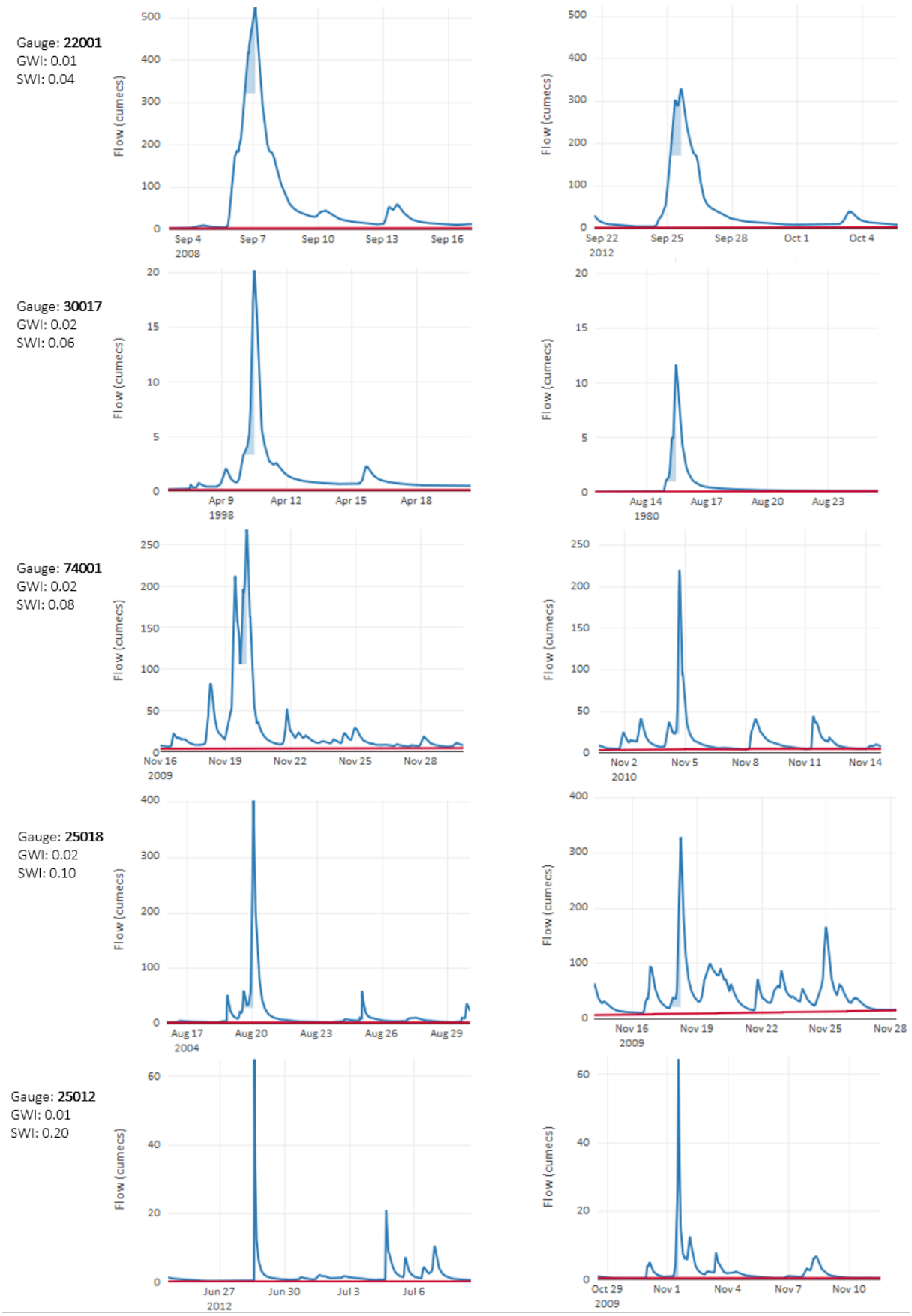

Figure 9.7: **Surface Water Hydrographs -** Here are a selection of hydrographs, chosen to have a range of SWIs and low GWIs. We see an increase in rise rate and 'flashiness' as the SWI increases. Gauges with SWIs above 0.06 are taken to be flashy. Blue lines show river flow; red lines show base flow; shaded areas show the period used for calculating rate of rise

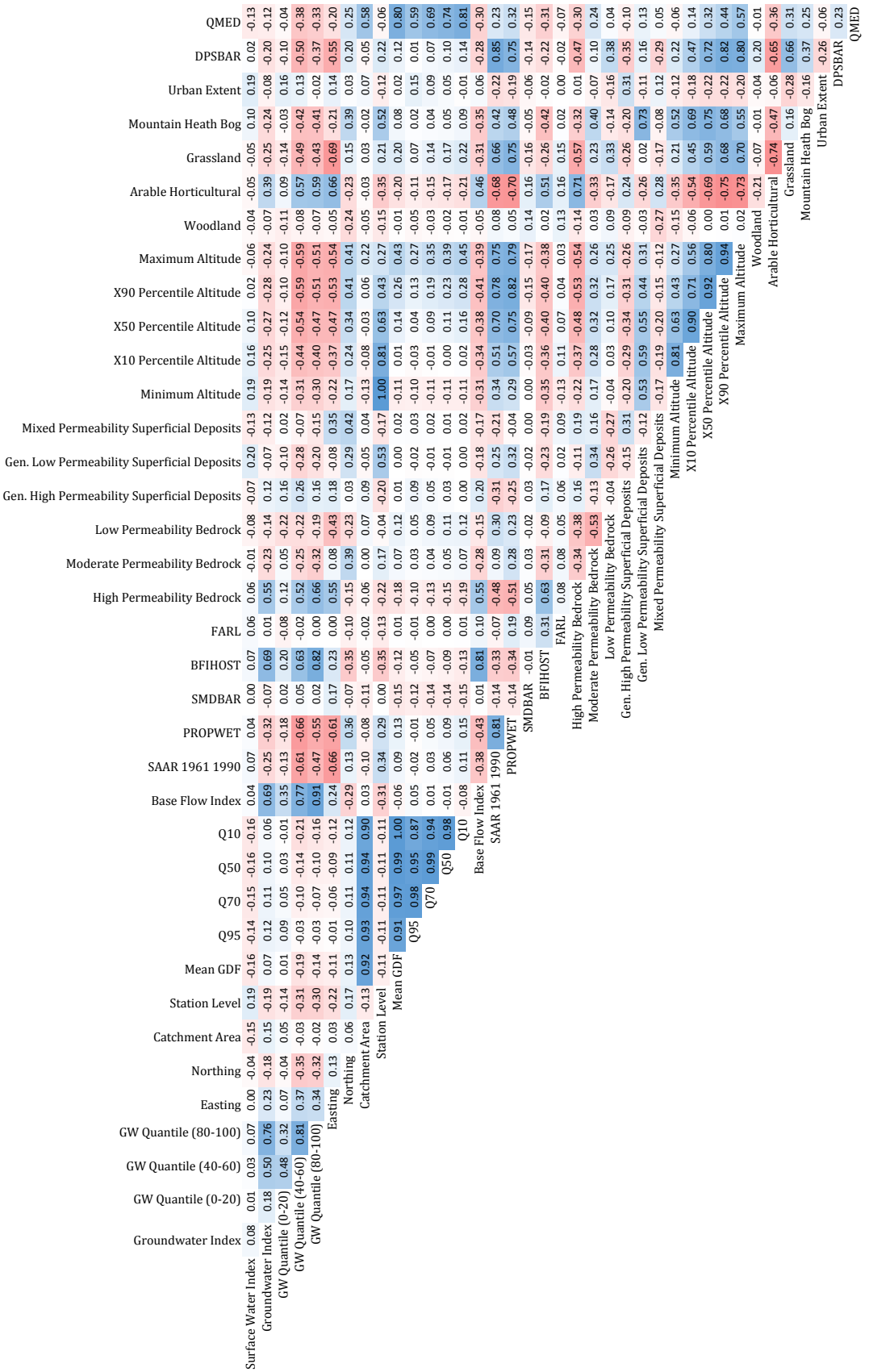

Figure 9.8: A correlation matrix showing how the indexes produced in this study correlate with the NRFA catchment descriptors.

fully on base flow separation. It is interesting that it is the 80-100 BFQ, not the 40-60 BFQ, that correlates most highly with these - it had been assumed that a median quantile would be more representative of the entire record. For both the middle and high BFQs we see an inverse correlation with wetness and altitude.

Summary of Correlation Analysis

Few correlations were strong enough to warrant much more explanation and so this will not be covered in the following Discussion chapter. Although some of the correlations are not what would be expected, these are all relatively small and so of little consequence.

One of the largest correlations, and the main one to note, is the correlation between high GWI and geology, with higher GWIs in regions of permeable bedrock and lower GWIs in regions of low permeability superficial deposits.

10. Discussion

The aim of this section is to identify rivers that have both significant groundwater inputs along with potential for flashy responses during peak flows. Analysis of the top ten flow events from each of the 435 flow records provided two indexes for each record: (1) A groundwater index (GWI), describing the groundwater response to the rainfall event, and (2) a surface water index (SWI), which indicates the flashiness of the catchment's response to rainfall. Both of these indexes are between 0 and 1.

Record lengths can be seen in Figure 10.1. 95% of the records are longer than 10 years, meaning that the vast majority of sampled events have return periods greater than of an annual event. The largest return period event sampled was a 1 in 63 year event.

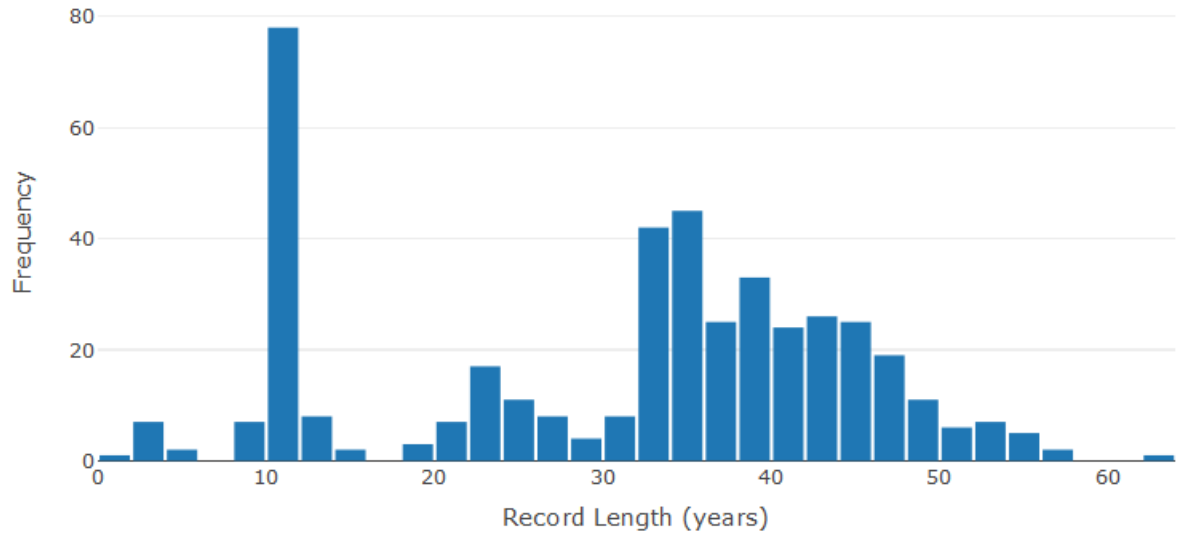

Figure 10.1: Record lengths for the flow time series used in the analysis.

From studying these indexes alongside hydrographs of peak flows, records with groundwater and surface water indexes above 0.1 and 0.06 respectively are thought to be significant. As such, catchments with both GWIs and SWIs above these thresholds are proposed likely to be multisourced. These indexes are plotted against one another in Figure 10.2 along with a full list of indexes that class as multisource in Table 10.1. Of the 435 records assessed, 29 fall above this multisource threshold. These 29 records vary considerably with some having very high groundwater contents and minimal flashiness, and vice versa. The shape of the plot in Figure 10.2 shows that high GWI and high SWI are relatively exclusive of one another in most instances.

Catchments with high groundwater indexes justify the use of a hydrological model when

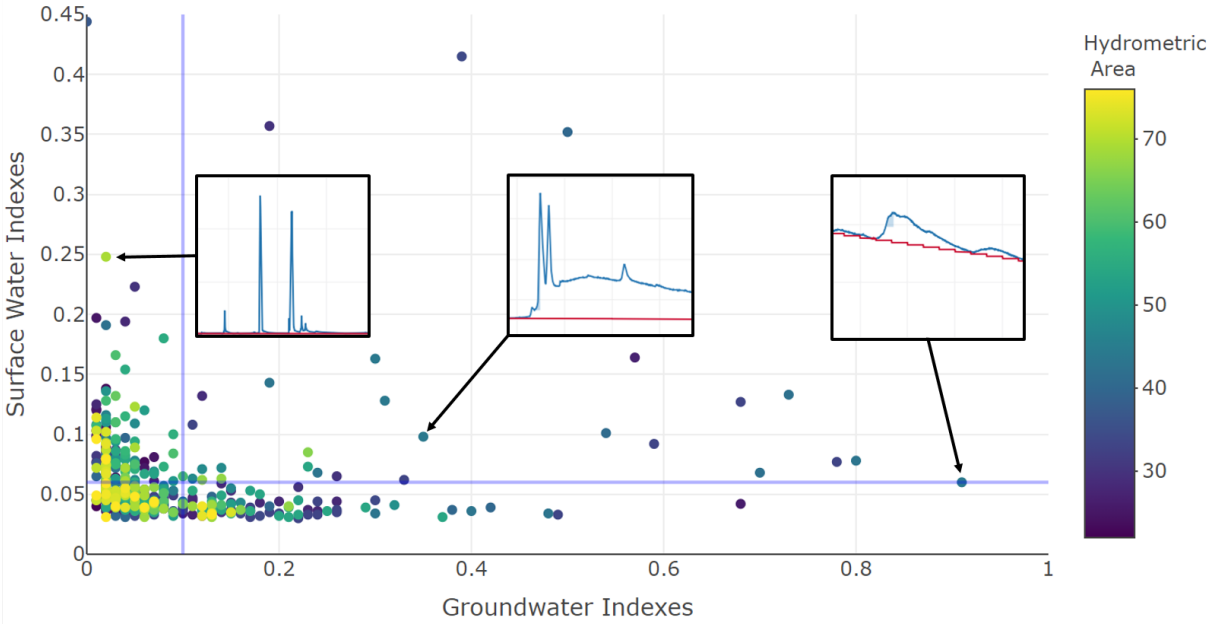

Figure 10.2: GWIs plotted against SWIs. Blue lines show the estimated thresholds for multisource catchments. Gauges with indexes above these are listed in Table 10.1. Inserted hydrographs show the typical discharge patterns of rivers of that index - blues line show stream flow and red lines show calculated base flow.

assessing flood risk as these require groundwater processes to be accounted for. Figure 9.6a shows that groundwater catchments are present across much of the UK, and demonstrates the importance of developing the national hydrological model discussed in Chapter IV (Lewis et al., 2018). Conversely, catchments with high surface water indexes and low groundwater indexes are unlikely to require complex hydrological simulations, but instead may be modelled using higher resolution hydraulic models. Those catchments with simultaneously high GWIs and SWIs, or those thought likely to exhibit groundwater induced flooding, justify the use of the multisource modelling system developed in subsequent chapters that combines both modelling approaches.

10.1 Do Indexes Match Expectations?

As discussed at the beginning of this chapter, it is very difficult to validate this work against historical flooding due to a lack of recording of multisourced floods in the literature. As such, indexes for the records shown in Figure 10.3 were validated against catchment characteristics and hydrology. This information has largely been sourced from the NRFA (2019b).

The River Heacham - Station No. 33032

GWI: 0.68 | SWI 0.13 | Expecting: variable base flow & rapid rises.

The River Heacham in Norfolk is identified as having significant groundwater and surface water inputs. It exhibits a variable baseflow and, as such, modelling a surface water response to a rainfall event would necessitate taking into account the antecedent conditions. The catchment is made of 100% high permeability bedrock, predominantly Chalk (CAPITA SYMONDS, 2012, Map A.14), but has 40% coverage of mixed permeability superficial deposits. This clearly allows for groundwater dominance. However a report in 2009 stated that there had not been any recorded instances of groundwater floods (Entec, 2009). Even if there are not groundwater floods recorded in an area, groundwater, as a source, may still be an important factor by affecting antecedent conditions. According to CAPITA SYMONDS (2012, Fig. 4.0), there is a moderate to very high

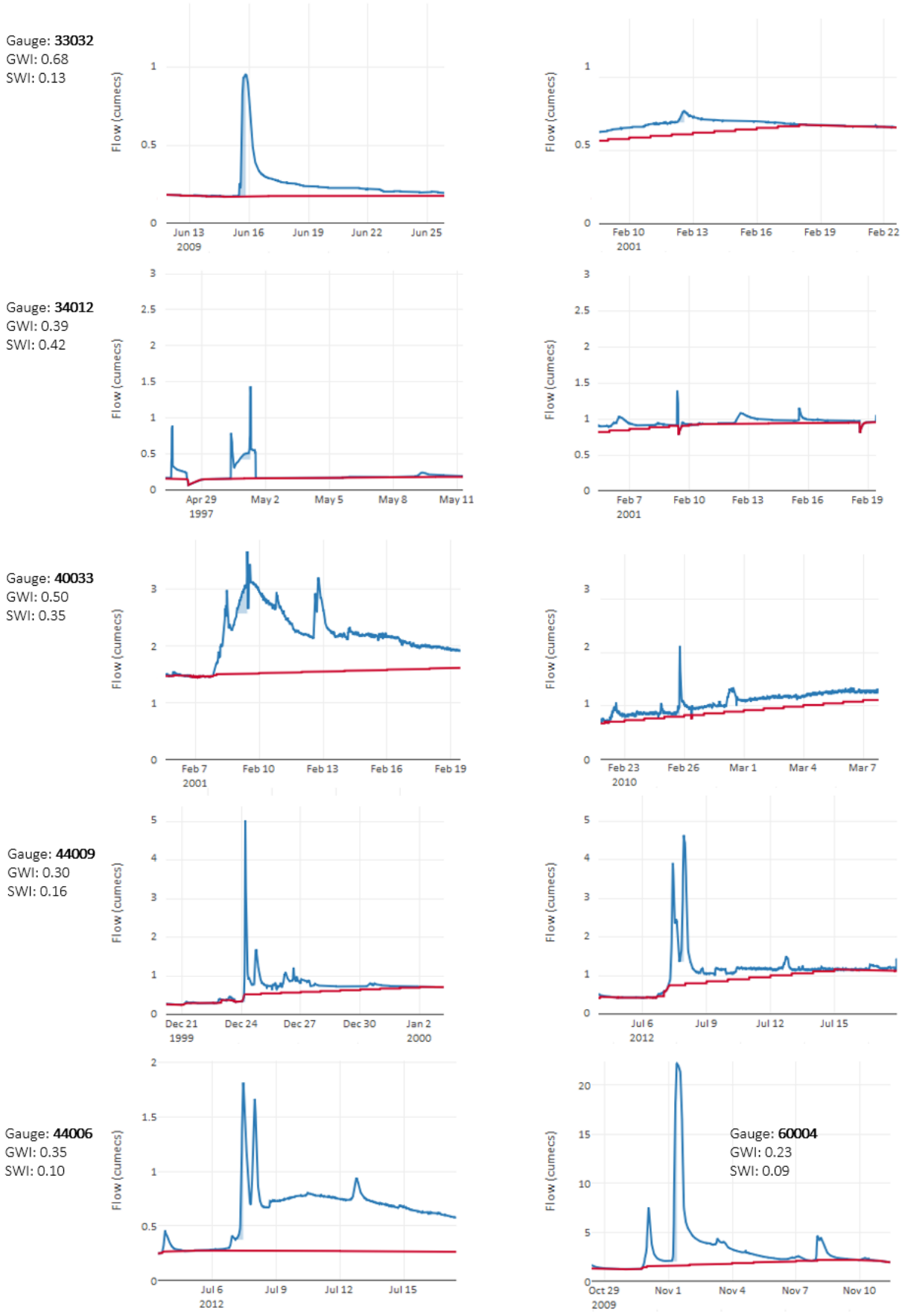

Figure 10.3: **Multisource Hydrographs -** Above is a selection of peak events from records that have both high SWIs and high GWIs. These show seasonal base flow (33032 & 34012), asymmetrical limbs (60004), rising base flow following events (40033 & 44009), and a double peak (44006).

Table 10.1: Gauges with indexes above the thresholds thought to indicate significant surface water or groundwater input are listed in the table below. The gauge locations for these catchments can be seen in Figure 26.5 in the Appendix.

Station Number	River	Location	Surface Water Index	Groundwater Index
27073	Brompton Beck	Snainton Ings	0.164	0.57
29003	Lud	Louth	0.132	0.12
30013	East Glen	Irnham	0.357	0.19
30015	Cringle Brook	Stoke Rochford	0.065	0.26
33007	Nar	Marham	0.062	0.33
33015	Ouzel	Willen	0.108	0.11
33032	Heacham	Heacham	0.127	0.68
33052	Swaffham Lode	Swaffham Bulbeck	0.077	0.78
33054	Babingley	Castle Rising	0.092	0.59
34012	Burn	Burnham Overy	0.415	0.39
40033	Dour	Crabble Mill	0.352	0.50
41015	Ems	Westbourne	0.101	0.54
42006	Meon	Mislingford	0.068	0.70
42008	Cheriton Stream	Sewards Bridge	0.133	0.73
43004	Bourne	Laverstock	0.078	0.80
43006	Nadder	Wilton	0.068	0.24
43007	Stour	Throop	0.143	0.19
44002	Piddle	Baggs Mill	0.060	0.91
44006	Sydling Water	Sydling St Nicholas	0.098	0.35
44008	South Winterbourne	Winterbourne Steepleton	0.128	0.31
44009	Wey	Broadwey	0.163	0.30
48007	Kennal	Ponsanooth	0.072	0.14
48009	St Neot	Craigshill Wood	0.063	0.11
48010	Seaton	Trebrownbridge	0.071	0.12
54027	Frome	Ebley Mill	0.073	0.23
60004	Dewi Fawr	Glasfryn Ford	0.065	0.10
66004	Wheeler	Bodfari	0.085	0.23
67005	Ceiriog	Brynkinalt Weir	0.063	0.14
67008	Alyn	Pont-y-Capel	0.062	0.12

risk of groundwater flooding along the River Heacham and in the town of Heacham itself.

The river is deemed a source of potential fluvial flooding (Entec, 2009). The superficial deposits and largely arable and grassland land cover may account for the rapid runoff. Although the February flow peak of gauge 33032 (Fig. 10.3) does not show an intense rainfall event or sudden rise, there is evidence of this in its other hydrographs.

River Burn - Station No. 34012

GWI: 0.39 | SWI: 0.42 | Expecting: variable base flow & rapid rises.

According to its SWI, the River Burn in Norfolk has the second flashiest catchment in the analysis and, as above, clearly shows variable base flow. The NRFA (2019b) state that the catchment is composed of 100% highly permeable bedrock and around 60% mixed permeability superficial deposits, including boulder clay. The presence of boulder clay and 95% coverage of arable and grassland supports this high SWI. There are only minor artificial influences in the catchment.

River Dour - Station No. 40033

GWI: 0.50 | SWI: 0.35 | Expecting: Groundwater dominated & highly flashy.

The River Dour in Kent flows to the Chalk cliffs of Dover and thus is groundwater dominated, fed by Chalk springs. This supports the very high GWI. There is also responsive urban runoff in large storms due to the urban developments. It also has around 50% low permeability superficial deposits and 9% mixed permeability superficial deposits. This aligns with the expected characteristics of a multisource river. The Dour's hydrographs in Figure 10.3 are asymmetrical with variable base flow, a shape previously associated with multisource catchments in Section 6.1.

River Wey - Station No. 44009

GWI: 0.35 | SWI: 0.06 | Expecting: Variable base flow & presence of some flashiness.

The River Wey in Dorset has the minimum SWI to be classified as flashy. Again this is a groundwater stream, this time flowing through limestone, justifying the GWI. It does however have steep slopes (with a DPSBAR of 118) and mixed geology, including sandstones and mudstones (BGS 1:10 000 Scale Geology Data). These characteristics are in line with fast surface run off. As with the River Dour, the Wey exhibits asymmetrical hydrographs with variable base flow, an expected indicator of a multisource catchment.

Sydling Water - Station No. 44006

GWI: 0.3 | SWI: 0.1 | Expecting: Strong groundwater contribution, sharp rises.

In the South West, Sydling Water has 100% high permeability Chalk bedrock. Atop this, in the higher regions of the relatively small catchment are superficial deposits formed of clays, silts, sands and gravels (BGS 1:10 000 Scale Geology Data). The NRFA state that 50% of the catchment is covered in low permeability superficial deposits. These are likely to increase the runoff and account for the higher SWI. This catchment is also relatively steep with a DPSBAR of 129.

Sydling Water is perhaps the most interesting of the catchments described here as it exhibits a double peak hydrograph in Figure 10.3. The double peaks are consistent across many of the peak events and are thus not thought to be a consequence of multiple rainfall pulses. Sydling Water appears to indicate a prime example of a multisource catchment. In the winter of 2000 and 2001, Sydling St. Nicholas, the main village of the catchment, was flooded from all sources following heavy rain (Halcrow Group Limited, 2010) and has since had further flooding in July 2007 (Dorset County Council and Environment Agency, 2012). Contact was made with the local flood warden with regards to past flood events, however this proved unfruitful.

Investigations also drew attention to the nearby South Winterbourne catchment, which also exhibits double peak hydrographs. It has a GWI of 0.3 and a SWI of 0.13, classifying it too as multisourced. These catchments are relatively similar, sharing the pattern of impermeable superficials in the headwaters and Chalks in the lower catchment and valley bottoms. Both catchments are small, with sizes of 12 km^2 and 20 km^2 respectively.

Dewi Fawr - Station No. 60004

GWI: 0.1 | SWI: 0.07 | Expecting: Small groundwater presence, some sudden events.

It was not expected that a Welsh river, the Dewi Fawr, would be classified as multisourced; although both indexes are at or near the minimum thresholds to classify it as such. Figure 10.3 shows Dewi Fawr with an asymmetrical hydrograph with rising base flows following several of the events, however its hydrographs also show frequent rises in flow, presumably from repeated rainfall. It is possible that this is the cause of the base flow increases rather than a notable groundwater presence. Another possibility is that the asymmetrical hydrograph is caused by the elongated catchment, which may dissipate the flood peak and sustain the falling limb of the hydrograph. The geology is 100% impermeable with over 80% grassland cover and a DPSBAR of

123, though it should be noted that there was no correlation between SWI and DPSBAR in the correlation analysis (Fig. 9.8). This is indicative of a surface water catchment and does not fit the multisource categorisation.

Summary

The catchment descriptors support the indexes calculated in this work and provide a useful method for sorting catchments. Other factors can influence the indexes, such as the possible repeated rainfall events of the Dewi Fawr and complications involving catchment shape. Indexes should therefore be used as an indicative tool for sorting catchments but should be verified against catchment hydrology in instances where they are thought unlikely.

10.2 Geographical Distributions of GWIs and SWIs

The majority of larger GWIs (>0.5) are distributed in the south of England and the East of Wales (Fig. 9.6a). The very largest GWIs (>0.7) are located in the south east of England, with the exception of Station 49002 in the south west and the two stations in East Yorkshire (26003 & 27003). As would be expected, those catchments that score highly in the quantile based groundwater assessment share a similar spatial distribution. These are mapped in Figure 9.5.

Figure 10.4a shows the distribution of permeable rocks through the UK along with GWIs. All stations with GWIs greater than 0.3 are situated upon, or very close to, highly permeable or moderately permeable aquifers. This confirms what was seen in Section 9.3: that high GWIs correlate well with highly permeable bedrock, with higher indexes being more constrained than lower ones.

There are instances where catchments with GWIs between 0.3 and 0.5 sit upon bedrock said to contain no groundwater. These are still all relatively close to boundaries with a higher permeability bedrock, three examples of which can be seen in Figure 10.5. On the far left of the figure is station 27073 at Snainton Ings, just south west of Scarborough. Although this is situated on rock with essentially no groundwater, its catchment is split across this rock and a moderately permeable aquifer to the north. The stations in Norfolk and the South Coast (in the middle and right of the figure) have high GWIs but are also located on rocks with essentially no groundwater; again, the majority of their catchments fall on the highly permeable strata to their east and north respectively. It should also be noted that groundwater catchments are not necessarily the same as the surface water catchments, which are defined topographically. Groundwater recharge may occur within neighbouring catchments and enter the catchment via the subsurface. This is discussed further in Chapter IV.

The spatial distribution of stations with lower GWIs (0.1-0.3) is less controlled by underlying geology. While many of these also have catchments dominated by highly or moderately permeable geologies, a large proportion have mixed permeabilities or are located on low productivity aquifers (such as those in Wales and the South West). Some of the gauges are situated almost entirely on bedrock with essentially no groundwater and yet are above the benchmark thought to indicate a presence of groundwater. Many of these are located below lakes. This will regulate flow and raise the base flow index (Brodie and Hostetler, 2005). Of the four stations showing GWIs over 0.1 in the Lake District, one has a FARL value of 0.85 and the other three have FARL values below 0.8, the threshold below which reservoirs or lakes are said to have substantial influences on flood response (NRFA, 2019a). The six stations in Cornwall in the south west of England are situated on low permeability bedrock and have GWIs of 0.11 to 0.16. The two most westerly of these also sit within a groundwater emergence zone in the assessment by Jacobs (2004) (Fig. 4.3). The other Cornwall sites were not in an area assessed by the GEMs project (due to lack of data). As these are not particularly high the stipulated presence of groundwater does not conflict with expectations. Similarly, those stations located on low permeability aquifers in Wales have

GWIs below 0.2 in all but one instance (River Lugg at Butts Bridge). According to the NRFA (2019b) this baseflow component is likely to be caused by gravels that are present around the river system and in the lower catchment.

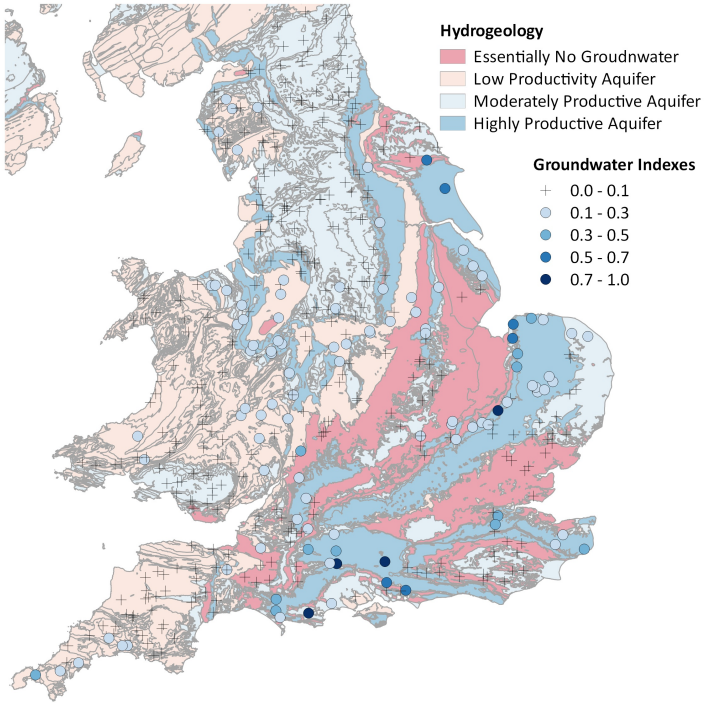

(a) Groundwater indexes shown on the BGS 1:650 000 scale digital hydrogeology map (British Geological Survey, 2016b). A large scale map can be seen in the Appendix (Sec. 26).

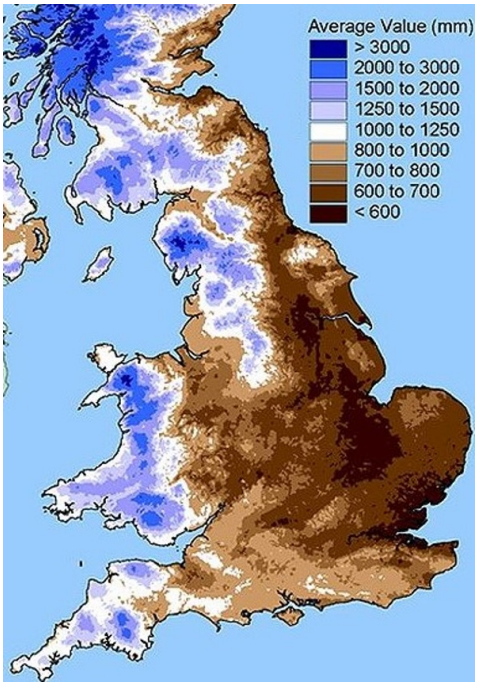

(b) UK average annual rainfall 1981-2010 (Met Office, 2017).

Figure 10.4: Differing controls on indexes - we see that geology exerts a dominant control on the groundwater of a catchment. Rainfall pattern has less of a control on SWI than was originally expected. Instead it seems that SWI is based on a combination of those factors typically assumed to influence flashiness such as land cover and altitude.

Catchments that are estimated to have very little groundwater in peak flow events (<0.1) are typically in regions with poor aquifers. Interestingly, there are numerous stations that are estimated to have no base flow in peak flow events that are situated on moderate or high productivity aquifers. The most obvious examples of this are the stations situated on moderate productivity aquifers in the north of England. This implies that geology alone is not enough to cause high base flows in peak events and that simple indexes such as BFI are perhaps not fully appropriate for identifying catchments that may do so.

A different distribution is clear from the SWIs, which are more typically located in the west of the country (Fig. 9.6b). Rainfall patterns were therefore considered as a possible explanation as on average the west of the country receives more intense rainfall than the east of the country. Figure 10.4b shows the average annual rainfall of the UK; while there is some correlation between the rainfall patterns and SWI, rainfall does not appear to be the dominant control. There is also no correlation between the SWIs and the NRFA PROPWET or SAAR catchment descriptors, which respectively describe the proportion of the time the soils are wet and the average annual rainfall. Instead, with aid from the correlation analysis (Fig. 9.8) it seems that SWI has no strong single control but is instead based upon a combination of minor factors such as land cover, altitude and superficial deposits.

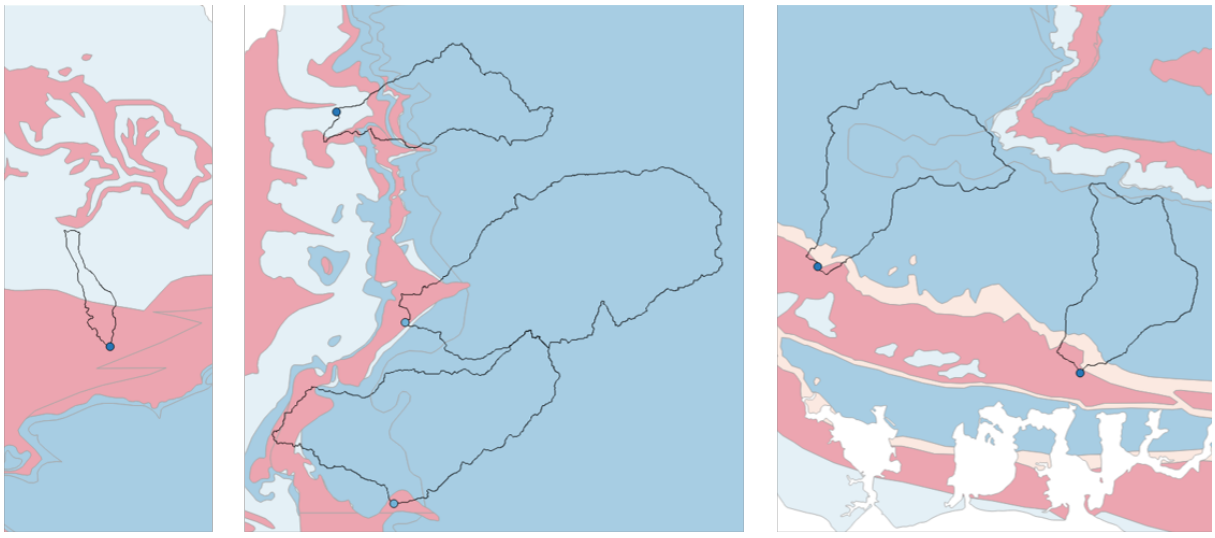

Figure 10.5: Some stations with high GWIs are located on rocks with essentially no groundwater (Fig. 10.4a), however all of these have catchments that are situated largely on more permeable strata. Catchments shown from left to right are of indexes in Yorkshire, Norfolk and the South Coast. Catchment details are given from top left to bottom right. BGS 1:650 000 scale digital hydrogeology map (British Geological Survey, 2016b)

11. Conclusion

A methodology for identifying multisource rivers has been developed and an initial 435 flow gauges assessed around England and Wales. Each dataset underwent a quality control process and was then used to calculate two indexes that are averaged from the top ten flow events of each record:

- **The groundwater index (GWI)** is the ratio of the maximum base flow to the maximum stream flow. High indexes indicate significant groundwater contribution to river flow during peak events.
- **The surface water index (SWI)** uses the surface water competent of flow and is a ratio of the peak flow to the volume of water leading up to the peak. High indexes indicate significant surface water contributions to river flow during peak events.

The indexes were manually benchmarked against hydrographs to determine appropriate thresholds for indicating significant source contribution. 29 locations had both indexes above these thresholds and were thus identified as having both constituent sources (groundwater & surface water) during peak events. This assessment only used approximately a third of the available data due to data quality issues and the availability of rating curves for the conversion of stage to flow. As such, many more multisource catchments are likely to exist, especially in the south of England where many datasets were unavailable or dismissed.

Six of the 29 locations identified as 'multisource' were then investigated on a case by case basis and found to show promising results. There was one known instance of incorrect identification (Dewi Fawr) where it is stipulated that repeated rainfall events or the elongated catchment artificially increased the perceived base flow. A list of catchments classified as multisource can be seen in Table 10.1.

Correlation analysis was also undertaken between both a suite of NRFA catchment descriptors and the indexes created in this study. This did not show anything particularly unexpected, however bolstered hypotheses: such as the importance of high permeability bedrock for the presence of groundwater in peak flow events. Notable correlations included the positive relationship between the groundwater indexes, BFI and highly permeable geology. A sensible requirement for the identification of multisource catchments is the presence of permeable bedrock in the catchment. This would remove erroneous catchments that score highly in the index analysis, such as the Dewi Fawr. However, several highly permeable catchments had very low GWIs, showing that the presence of highly permeable bedrock does not necessitate groundwater contributions to peak flow events. In at least one instance this observation is thought to be due to extensive low permeability superficial deposits. Furthermore, it is advised that the NRFA FARL catchment descriptor (Flood Attenuation from Reservoirs and Lakes) be used alongside the GWIs to insure that high GWIs are not a product of large surface storages in the catchment, as was found to some degree in the Lake District. It had been hoped that correlation analysis would identify key

catchment characteristics that would enable automated identification of ungauged multisource catchments. However, with only a few notable correlations, this is not possible. Those indicative characteristics may still be useful for initial catchment screenings prior to manual research into their multisource potential.

Of those suspected multisource catchments found through non-data based investigations in the Literature Review (Sec. 2.3), a high proportion are situated around London, the Thames and the south of England. This may be due to increased reporting on catchments in these areas but is likely to also be linked to the presence of extensive underlying Chalk geology, allowing groundwater regimes, and the presence of clays and urbanised areas, providing the necessary surface water component.

Further work should involve the application of this method to those catchments not included in this assessment to identify other likely multisource catchments. Further work may also be able to include data on maximum gauging flow or bankfull stage to indicate whether flooding is likely in the catchments or to better constrain which peak events resulted in flooding, rather than simply analysing the top 10 events from each record.

In conclusion, the peak event indexes created here proved a useful automated tool for identifying potential multisource events. They should however be treated with some caution and investigated further on a case by case basis if their hydrology does not match their classification or if there is the presence of man-made flow regulations. Multisource rivers are heavily constrained by underlying geology, with the locations of groundwater dominated rivers correlating with highly permeable geology. Thus, multisourced rivers are typically, but not categorically, situated in the south of England. Surface water catchments were found to have no strong correlations with catchment characteristics, such as rainfall, and so no pattern or rule could be applied to describe their distribution. Distribution was taken to be in general agreement with previous assumptions of controls on runoff.

IV

The Automated Setup of Hydrological Models

12. Background

The methodology developed in this thesis relies on the use of physically based, spatially distributed hydrological modelling for generating catchment conditions that feed into a high resolution hydraulic model. Setting up hydrological models can be prohibitively time and data intensive (Beven, 2012) and so the hydrological model SHETRAN (Sec. 3.3.1) was chosen due to the reduced set up times following the recent development of SHETRAN-GB by Lewis et al. (2018). SHETRAN-GB enables the near instant set up of a working SHETRAN model for almost any catchment in Great Britain via an online downloader with a graphical user interface. Importantly, the automated setup standardises simulations by reducing human interaction with the model prior to use, therefore facilitate sharing and critiquing of research. This chapter assesses the performance of SHETRAN-GB for simulating groundwater levels as these are vital for this study and have yet to be tested.

Where the necessary data is available, physically based, spatially distributed models offer a globally applicable modelling system and can, in theory, simulate catchment processes without the need for calibration. These models are ideal for this study as they offer the necessary spatially distributed information for multiple realistic catchment processes both within and beyond the limits of their calibration (Beven, 2012). SHETRAN-GB has been shown to perform well when simulating river flows, especially in non-permeable catchments (Lewis et al., 2018).

Calibrated SHETRAN models have already been successfully used to model groundwater in a variety of studies (e.g. Adams and Parkin, 2002; Parkin et al., 2007). The aim of this chapter is instead to assess SHETRAN-GB's ability to simulate groundwater levels without calibration. This used the same open source, national scale hydrogeological datasets used by Lewis et al. (2018) to establish which offer the most ergonomic potential for use in the multisource modelling system in Chapter V. This was done at five catchments across the UK: the River Allen, River Creedy, River Frome, Sydling Water and Foston Beck. These were chosen to represent catchments distributed across England with a variety of catchment characteristics such as catchment size, topography and geology. These can be seen in Figure 13.1.

12.1 Automated Model Setups

As a physically based, spatially distributed model, SHETRAN divides an area into a grid. Each grid cell is given a specified time series of meteorological conditions. The subsurface of each cell is described by a vertical column consisting of layers of soil and rock, with each layer given appropriate hydraulic properties. The surface of each cell is also given hydraulic properties that relate to its land use (Parkin et al., 2007). Data used by the default SHETRAN-GB system are referenced in Table 12.1 and details can be found in Lewis et al. (2018). Aquifer properties, which are dependent on the setup type are detailed in the subsections below.

Table 12.1: SHETRAN-GB uses the following datasets in its default setup. Geology and climate data differed in the 3D geology and Sydling water simulations respectively (see sections below). Daily PET was calculated using the Penman-Monteith method using daily minimum and maximum temperature and monthly relative humidity, wind speed and sunshine hours. Table adapted from Lewis et al. (2018).

Data (resolution)	Dataset - Source Institution	Reference
Elevation (50 m)	OS Land-form PANORAMA DEM - Ordnance Survey	Ordnance Survey (2013a)
Lakes	OS Meridian 2 Lake layer - Ordnance Survey	Ordnance Survey (2013b)
Soil (1 km)	Created from the European Soil Database layers - European Commission and Joint Research Centre	Liedekerke et al. (2006)
Land use (1 km)	CEH LCM 2007 - Centre for Ecology and Hydrology	Morton et al. (2011)
Geology	1:650 000 BGS Hydrogeology map - British Geological Survey	British Geological Survey (2014b)
Catchment boundaries	NRFA catchment boundaries - National River Flow Archive	Morris et al. (1990)
Daily rainfall and PET (5 km)	UKCP09 climate data - UK Met. Office	Perry et al. (2009) Perry and Hollis (2005)

Three different automated SHETRAN model types are available for use in this study and are detailed below. Each setup differs in how it represent the subsurface columns. All simulations used open source data.

12.1.1 Standard Setup

In the Standard setup, the subsurface is represented by a single, 20 m thick bedrock layer. Hydraulic properties are split into four categories according to the BGS 1:650 000 scale digital hydrogeology map (British Geological Survey, 2016b): *high productivity aquifer*, *moderate productivity aquifer*, *low productivity aquifer*, and *rocks with essentially no groundwater*. The properties of each class are based on the developer's previous modelling experience (Lewis, 2015) and can be found in Table 12.2. The Standard model does not include geological features and complexities such as lenses or faults and does not include superficial deposits.

This setup was tested at three different resolutions (1000 m, 500 m & 100 m) to explore the model's sensitivity to cell size and input resolution. As can be seen in Table 12.1, the spatial resolution of the soil, land use and climate data are limited and so their resolutions are not increased in these higher resolution runs. SHETRAN has an imposed limitation on the number of horizontal cells per simulation due to large computational requirements of large grids. For this reason the very high resolution 100 m simulations for the Rivers Allen, Frome and Creedy are not available as their catchments are too large.

12.1.2 Aquifer Properties Manual (APM)

This suite of simulations used an identical model structure to the Standard model but used the aquifer properties manual (MacDonald and Allen, 2001) to parametrise the *highly productive bedrock* units.

SHETRAN calculates the rate of flow through the subsurface using a parameter called *saturated conductivity* - this setup used increased saturated conductivities, which can be seen in Table 12.3. These apply to all of the case study catchments apart from the Creedy, which does not have any highly productive bedrock. For this reason no results are given for the Creedy catchment in runs using APM values. The aquifer property manual does not always provide

Table 12.2: Subsurface parameters for the Standard SHETRAN-GB setup. These were also used in the 3D geology simulations. All soils, bar peat, had two sets of parameters that varied spatially within the models or between different soil layers. *Medium grained soil* encompassed two different grain size combinations. All subsurface types had a specific storativity of 0.001.

Subsurface Type - Composition	**Saturated Conductivity (m/day)**	**Saturated Water Content**	**Residual Water Content**	**Van Genuchten n**	**Van Genuchten α**
Coarse Soil:	60	0.403	0.025	1.3774	0.0383
- 18% clay, 65% sand	70	0.366	0.025	1.5206	0.0430
Medium Soil:					
- 18-35% clay, 15% sand	10.755	0.329	0.01	1.1689	0.0249
- 18% clay, 15-65% sand	12.061	0.439	0.01	1.1804	0.0314
Medium Fine Soil:	2.272	0.430	0.01	1.2539	0.0083
- 35% clay, 15% sand	4	0.412	0.01	1.2179	0.0082
Fine Soil:	24.8	0.520	0.01	1.1012	0.0367
- 35-60% clay	8.5	0.481	0.01	1.0861	0.0198
Very Fine Soil:	15	0.614	0.01	1.1033	0.0265
- clay 60%	8.235	0.538	0.01	1.0730	0.0168
Peat	8	0.766	0.01	1.2039	0.0130
Highly Productive Aquifer	0.1	0.3	0.2	5.0	0.01
Moderately Productive Aquifer	0.01	0.3	0.2	5.0	0.01
Low Productivity Aquifer	0.001	0.3	0.2	5.0	0.01
No Groundwater	0.0001	0.3	0.2	5.0	0.01

saturated conductivities directly, and so many were calculated from transmissivity values. This is done by dividing the transmissivity by the thickness of the medium, in this case 20 m.

Along with the increased saturated conductivities (and therefore transmissivities) the model's van Genuchten parameters were also altered. These can also be found in Table 12.3. All other parameters remained the same as in the Standard simulations.

12.1.3 3D Geology

The most significant limitation of the Standard setup is the use of a single 20 m thick unit to represent underlying geology. This is a relic of the model's original set up, which was designed for producing river flows rather than groundwater levels. In this setup the BGS 3D geology model (Mathers et al., 2014; Watson et al., 2015) is used to create a more realistic, and significantly more complex, portrayal of the subsurface.

The 3D model is constructed from an interpolated fence diagram based on cross sections, borehole data and the BGS 2D geological map. As with a lot of geological data, this dataset is based on the interpretation of point information by geologists and so does not fully capture the complexities of the subsurface. Furthermore, data density changes across the country and so some areas are less constrained than others. The 3D model does not include superficial deposits.

Hydraulic properties of the subsurface geology in this setup are consistent with the Standard

Table 12.3: Properties for major aquifers: the *highly productive aquifer* was used in the Standard and 3D geology simulations, while the increased saturated conductivities were used in those runs that took values from the aquifer properties manual (MacDonald and Allen, 2001). The Creedy catchment does not contain a highly productive aquifer.

Catchment	**Rock**	**Saturated Conductivity (m/day)**	**Transmissivity (m^2/day)**	**Van Genuchten n**	**Van Genuchten α**
Allen, Foston Beck, Frome, Sydling Water	Highly Productive Aquifer	0.1	2	5	0.010
Frome	Limestone	40	800	6	0.001
Allen, Sydling Water	Chalk	49.25	985	6	0.001
Foston Beck	Chalk	62.5	1250	6	0.001

setup and can be found in Table 12.2. A second suite of runs were conducted that incorporated the 3D geology with the increased transmissivities in the highly productive aquifers taken from the aquifer properties manual (Tab. 12.3). These simulations aimed to combine the most appropriate parameters with the most realistic description of the subsurface.

12.2 Previous River Flow Testing

Lewis (2015) tested the above setups nationally against river flows along with setups that contained superficial deposits and transmissivities taken from the Environment Agency's regional MODFLOW groundwater models (Shepley et al., 2012).

The setups were found to perform relatively well, though struggled in more permeable catchments due to the additional complexities of characterising the subsurface. The inclusion of 3D geology improved the Nash-Sutcliffe efficiency coefficient (NSE, Eq. 13.2.3) for flows. This is supported by a recent study by Saksena et al. (2019), who found that the representation of surface-groundwater interactions can reduce the need for extensive model calibration. Improvements in Nash-Sutcliffe efficiency occurred mainly in Chalk catchments, however sometimes decreased model performance in other permeable catchments. The inclusion of superficial deposit data was found to have potential for further work, but was not extensive or detailed enough to be fully appropriate for use in its current state, hence it is not tested in this thesis. Altering the hydraulic properties of the subsurface by using the APM also proved to be largely effective in improving NSE for the Chalkier areas, but still allowed for significant improvement through further parametrization.

In these simulations the river channels were enlarged to ensure that flow was not lost out of channel in flood events. These wide channels are also present in the simulations conducted in this chapter, but are not anticipated to affect the groundwater levels.

13. Methodology

The current online model downloader for SHETRAN-GB is able to deliver models with the Standard set up at three different horizontal spatial resolutions - 1000 m, 500 m and 100 m. The two other setups, which use transmissivities from the aquifer properties manual and BGS 3D geology data, are available directly through the developer (Lewis, 2015) at a 1000 m resolution. The methodology first ran the simpler Standard simulations and then increased in complexity with each suite of simulations building in APM values and detailed geology. Following the testing of the automated setups, the Allen catchment was selected for further development to address issues with the automated setups and to identify points for future development of SHETRAN-GB that would be of use for the multisource modelling system.

The developed Allen simulations used a horizontal resolution of 1 km and an extended catchment size so as to simulate the processes occurring across the groundwater catchment, rather than just the surface water catchment that was used with the automated setups. The development of the Allen catchment model took three steps, these are:

1. The Standard set up (single 20 m thick subsurface unit).
2. The Standard set up with a single 40 m thick subsurface unit and enhanced Chalk aquifer properties (detailed below).
3. Addition of a detailed subsurface taken from the BGS 3D geology data and enhanced Chalk aquifer properties (as previous).

The enhanced aquifer properties were taken from the aquifer properties manual (Allen et al., 1997) and a hydrological map of the area (Institute of Geological Sciences & Wessex Water Authority, 1979). This increased the saturated conductivity of the Chalk from 0.1 m/day (in the Standard simulations) to 100 m/day and increased the Chalk's residual water content and thus decresed the specific yield to 0.2 (from 0.1 in the Standard simulations). Although increasing these parameters meant that the aquifer properties were more in line with those in the literature, it decreased model stability and caused some simulations to crash. To increase stability, SHETRAN's van Genuchten α and n parameters were decreased and increased respectively. these did not have notable effect on the groundwater levels, only model stability. The extended Allen catchment can be seen in Figure 13.1.

Simulations were run for the five catchments described below and compared against observed groundwater levels and streamflows. Observed groundwater levels were taken from boreholes within each catchment. All groundwater level data was provided by the Environment Agency through freedom of information requests. The available data, time periods and resolutions can be seen in Table 28.2 in the Appendix. It was not possible to assess the performance of SHETRAN-GB's groundwater simulations at a national scale, as was done for flow testing by Lewis et al. (2018). This was due to the difficulty in obtaining groundwater level data. Limited information is available on what data exists, and this showed little correlation with what data was

actually supplied. The selection of catchments was limited by the accessibility and availability of groundwater level data.

Models for four of the catchments used meteorological data from the UKCP09 5 km daily gridded dataset and simulated a period from 1990 - 2002. Groundwater level data for the Sydling Water catchment could only be found from 2006 onwards and so did not coincide with the UKCP09 data, which is only available up to 2006. Instead, the Sydling Water simulations used the 1 km CEH-GEAR dataset (Gridded Estimates of Areal Rainfall) (Centre for Ecology and Hydrology (NERC), 2015) and ran from 2006 - 2016.

13.1 Case study Catchments

Following on from Chapter III, which indicates that most multisource catchments are in areas with a permeable subsurface, the five test catchments were selected to represent a variety of groundwater catchment types. All catchments have base flow indexes between 0.46 and 0.96 and thus all exhibit significant subsurface processes. The five study catchments are described below. Catchment locations can be seen in Figure 13.1 and, in more detail, in the appendix.

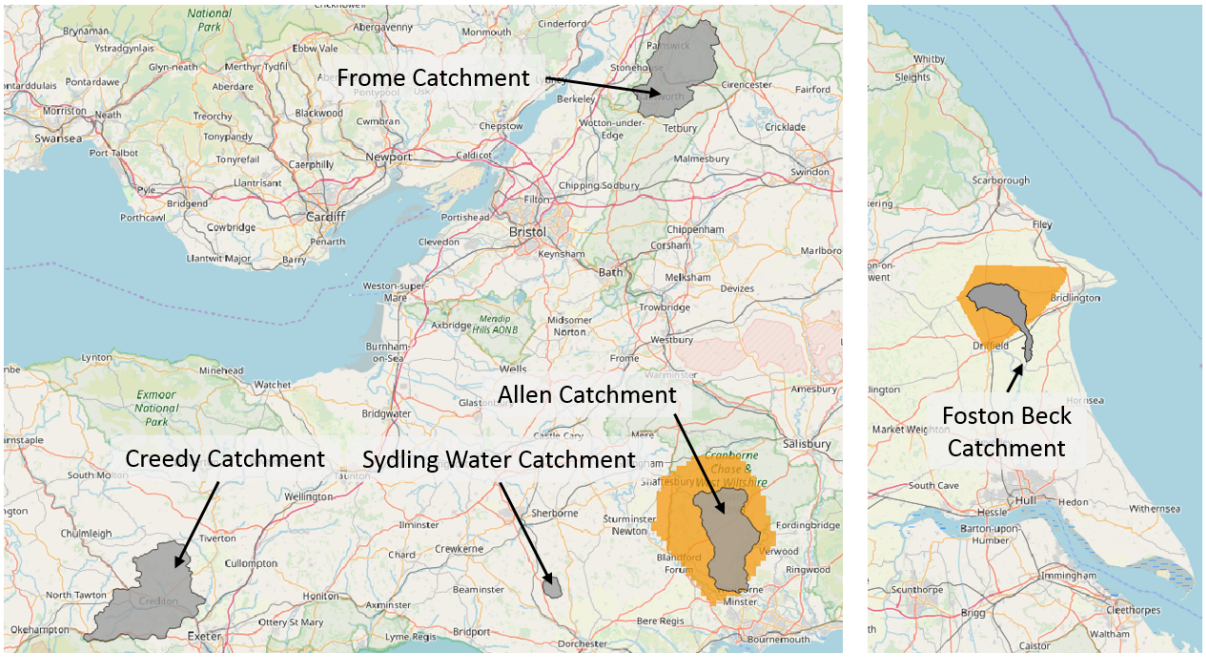

Figure 13.1: The five case study catchments are shown. Simulations were run for Foston Beck and the Allen using both surface water and groundwater catchments. The groundwater catchments had respective areas of 205 km^2 and 505 km^2 and are shown in orange. ©OpenStreetMap

Table 13.1: Catchment descriptors for the five case study catchments used for testing SHETRAN-GB. Surface water and groundwater indexes from Chapter III are also included and show that both the Frome and Sydling Water have been identified as being multisource catchments.

Catchment	Area	BFI	DPSBAR	QMED	Permeable Bedrock	SWI	GWI
Allen	177 km^2	0.91	52 m/km	1.26 m^3/s	94%	-	-
Creedy	262 km^2	0.46	111 m/km	76.62 m^3/s	29%	0.06	0.03
Frome	198 km^2	0.87	124 m/km	11.36 m^3/s	88%	0.07	0.23
Foston Beck	57 km^2	0.96	48 m/km	1.70 m^3/s	100%	0.04	0.68
Sydling Water	12 km^2	0.88	129 m/km	0.90 m^3/s	100%	0.10	0.35

13.1.1 River Allen

River Allen (gauged at Walford Mill) is a largely rural catchment on the south coast of England. The Allen flows south through Devon, meeting the River Stour at Wimborne Minster. The catchment is largely permeable with the bedrock dominated by unconfined Upper, Middle and Lower Chalks. Only in the south east corner of the catchment are these confined by a relatively impermeable Palaeogene mudstone. The Upper Chalk is the most extensively outcropping Chalk in the catchment with the older Lower and Middle Chalks only exhibiting narrow outcrops in the north west of the catchment. Figure 13.2 shows a cross section of these units dipping towards the sea to the south east, the direction of the groundwater flow. The Allen shares many characteristics with the Sydling Water catchment as they both sit on the Chalk of the Wessex Basin. More information on the aquifer properties can be found in Section 13.1.5. Transmisivities for the Chalk in these areas range from around 500 m^2/day to 1000 m^2/day, but are typically above 800 m^2/day. Some estimates are as low as 0.04 m^2/day. Storage coefficients have been estimated at 5×10^{-4} to 3.5 $\times10^{-2}$ (Allen et al., 1997).

In the headwaters of the catchment some of the streams are intermittent and so do not flow all year round. The majority of the Allen catchment has a highly permeable Chalk surface that allows flow through fractures and along discontinuities. Moving from the north west of the catchment to the south east, one descends through the Seaford Chalk Formation, the Newhaven Chalk Formation, the Tarrant Chalk Member, the Portsdown Chalk Formation, and the Spetisbury Chalk Member, all reclassified subdivisions of the Upper Chalk. These Chalks are overlaid by Pleistocene clays, silts sands and gravels. The southern tip of the catchment has a covering of sands, gravels and clays. These can be hydraulically connected to the Chalk and allow low yields through significant intergranular flow. Below the Chalk is a thick layer of impermeable mudstones - this can be seen in Figure 13.2. Further information of the Chalk of this area can be found in Allen and Crane (2019).

The Allen has been selected for use as it showed a significant increase in performance in the work of Lewis (2015). Lewis (2015) found that adding the transmissivities from the aquifer properties manual significantly improved the simulated flows in comparison to the Standard runs.

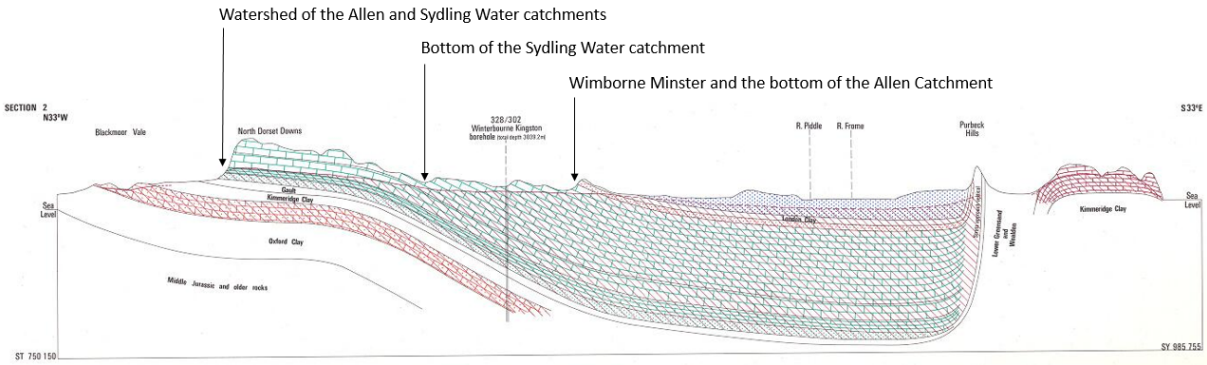

Figure 13.2: A geological cross section of the Allen and Sydling Water catchments shows the Chalk aquifer outcropping over the majority of the catchment, making way for Greensands at the northerly extent. Taken from the Institute of Geological Sciences & Wessex Water Authority (1979).

13.1.2 River Creedy

The River Creedy in Devon feeds into the River Exe north west of Exeter. The catchment is forked, with moderate to high relief in the two grassy headwaters converging into arable and horticultural land to the south east (Fig. 13.3a).

Hydrogeologically, the Creedy is the least permeable of the catchments under investigation.

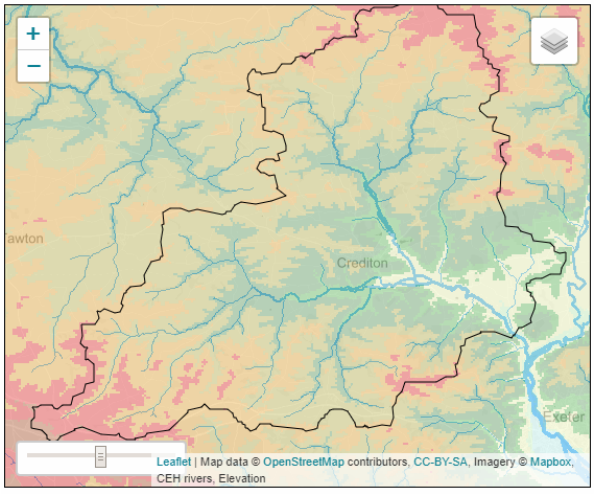

(a) Topography of the Creedy catchment. Headwaters have elevations of over 200 m, decreasing to around 30 m at the catchment outlet.

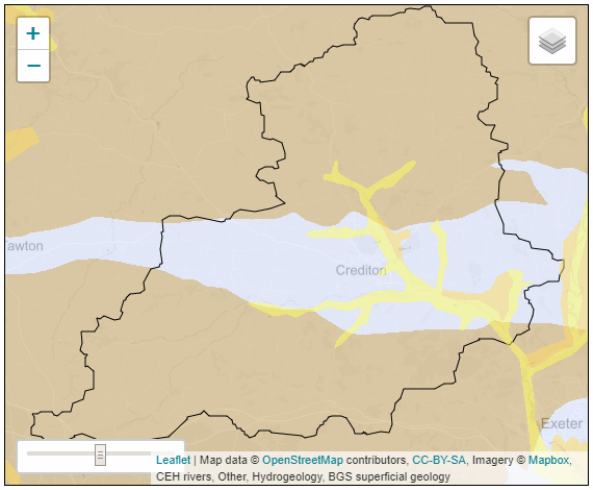

(b) BGS Hydrogeology Map: brown represents bedrock of very low permeability, blue represents bedrock with moderate permeability through intergranular flow, yellow and orange represent superficials sands and gravels.

Figure 13.3: The topography and basic hydrogeology of the Creedy catchment in Devon. Maps taken from the NRFA (2019b).

Much of the catchment consists of interbedded Carboniferous mudstones, siltstones and sandstones called the Culm Measures. These allow for minor groundwater flows with the largest flows occurring in the lower, more fissured beds (Institute of Geological Sciences, 1982).

Running west to east through the centre of the catchment is a fault bounded trough with an estimated depth of up to 900 m. This trough is filled with a sequence of spatially variable Permian breccio-conglomerates, sandstones and mudstones that form a layered aquifer system. This can be seen in Figure 13.3b. Coarser grained sandstones outcrop, within the trough, higher in the catchment (Institute of Geological Sciences, 1982).

Groundwater flow occurs mostly within this trough of higher permeability material. The older materials in the higher reaches of the catchment exhibit flow mainly through poorly developed fracture systems, while younger material lower in the catchment is less cemented and allows for a higher proportion of intergranular flow. Transmissivities are estimated to be from 10 m^2/day in the poorly fractured older material to 10-50 m^2/day in the sandier and more fractured materials and can be as high as 100-300 m^2/day in the less cemented, younger sandstones. Transmissivities can increase during periods of recharge from rivers. Fluctuations in groundwater level in the base of the catchment are greater than in the headwaters of the catchment by approximately 3 m due to the reduced porosity. Groundwater flows from the headwaters of the western fork of the catchment towards the east, dropping by over 50 m (Institute of Geological Sciences, 1982).

The River Creedy catchment was chosen for testing due to its lower proportion of highly permeable bedrock and thus its supposed reduced sensitivity to the different model setups. Even so, the reasonably high BFI shows that there is still a groundwater component. This is evidenced by the groundwater abstraction in the catchment (NRFA, 2019b).

13.1.3 Foston Beck

Foston Beck is an arable catchment in East Yorkshire. It has a relatively rounded upper catchment that narrows significantly in its lower reaches. The catchment is composed of a highly productive Cretaceous Chalk bedrock that creates a groundwater dominated catchment with a very high base

flow index of 0.96 (Tab. 13.1) and seasonal changes in groundwater level. The lower catchment is largely confined by superficial drift deposits (Fig. 13.4; NRFA, 2019b). These Boulder Clay, alluvium, sand and gravel deposits give river flows a flashier response in the lower catchment.

Across the Chalk there is very little surface drainage due to its high permeability and the correspondingly low water table. Springs that appear at the edge of the drift create streams flowing towards the River Hull.

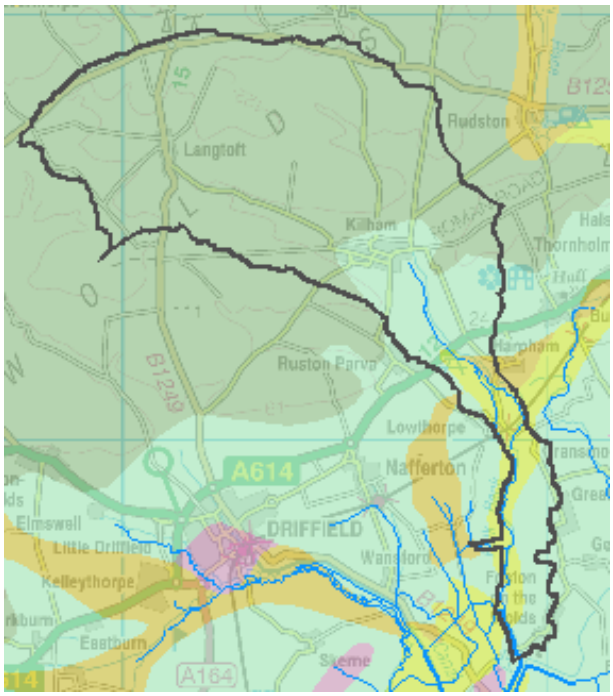

Figure 13.4: Dark green shows the highly productive aquifer outcropping in the north of the catchment. This is then over topped by glacial till and boulder clay (light green) and alluvium deposits in the river valley in the south (yellow). Taken from the NRFA (2019b)

Floods are understood to occur in periods of high groundwater level (Gale and Rutter, 2006) although surface water flooding is noted as a potential issue for future developments in the Local Flood Risk Management Strategy (East Riding of Yorkshire Council, 2015b).

Significant flooding occurred in the East Yorkshire area in June 2007 due to heavy and prolonged rainfall (East Riding of Yorkshire Council, 2015b). More recently, during the exceptionally wet winter of 2012-13 groundwater flooding affected the village of Kilham in the north of the catchment (East Riding of Yorkshire Council, 2015a). This resulted from high groundwater levels following a prolonged wet period during the summer and autumn of 2012. The high groundwater levels in the lower catchment slowed drainage to the river system, increasing river flows and triggering springs in and around the village. These occur due to the outcropping of the Chalk aquifer upstream of the village, this can be seen in Figure 13.5. The drainage systems within the village were overwhelmed and problems with flooding and sewer systems lasted for several weeks (East Riding of Yorkshire Council, 2013). Flooding in Kilham also occurred in the winter of 2001-02 from high groundwater levels, however this was relatively short-lived (Farrell, 2001).

The Foston Beck catchment is the only catchment here that has been fully calibrated as it has been used in other work at Newcastle University, simulating groundwater flooding in the village of Kilham. The results from the already calibrated model have been included here (Tab. 28.3 & 28.4 in the Appendix) as a benchmark, indicating the calibre of model that can be created with the additional time and resources. Its strong performance further demonstrates that SHETRAN is an appropriate model for simulating groundwater levels.

The calibrated catchment is significantly more detailed than those set up via the automated method and is able to capture both river flow and groundwater levels well. The catchment size was increased from 57 km^2 to 205 km^2, extending north, east and west, covering the northern half of Foston Beck and the surrounding area (Fig. 13.1). The catchment is enlarged to capture the groundwater catchment rather than just the surface water catchments used in the automated setups. The calibrated model also operates at a higher spatial resolution with 200 m cells and uses hourly meteorological inputs. The geology for the simulation is based on the same geology as is used here but with additional detail provided by the BGS.

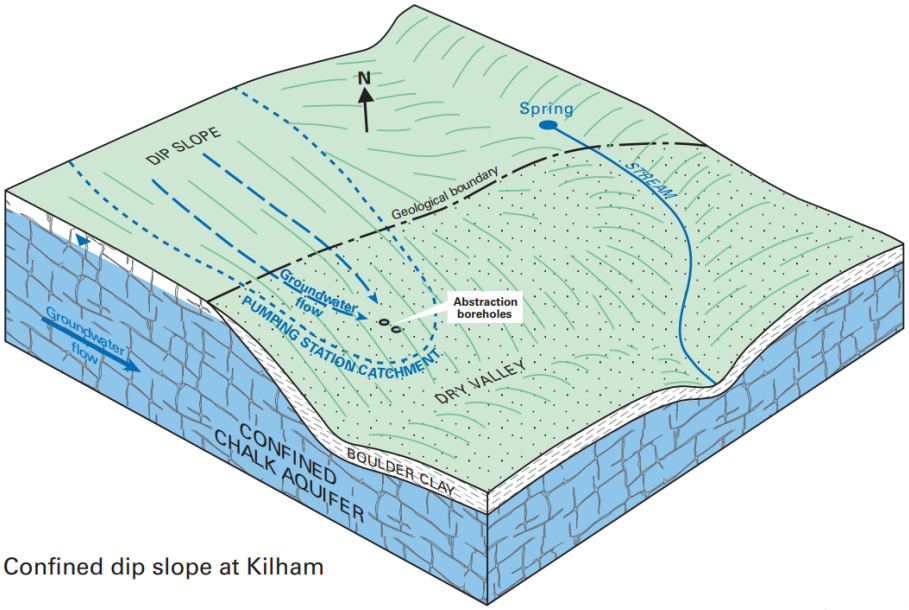

Figure 13.5: Foston Beck - as the impermeable boulder clay thins out, springs occur in and around Kilham village due to the outcropping of the confined Chalk aquifer. Taken from Gale and Rutter (2006)

13.1.4 River Frome

The River Frome in South Gloucester flows west to join the River Severn shortly before it opens up into the Severn Estuary. The Frome is gauged a few miles east of this confluence at Ebley Mill in Stroud. The northern headwaters of the catchment are steep and grassy with its the highest elevations in the northern reaches of the catchment (Fig. 13.6a).

The catchment is permeable, largely dominated by the Upper Lias Sands (sandstones) and the Great Oolite Group (mostly limestones) of the Jurassic. Figure 13.6b shows the distribution of these bedrocks and Table 13.2 shows their approximate thicknesses. The highest regions of the catchment have outcrops of the Forest Marble Formation succeeded by the Great Oolite Group, which covers much of the middle catchment, followed by the older Inferior Oolite Group in the lower catchment (British Geological Survey, 2007). The Frome river valley cuts through these three units to expose the Uppper Lias Sands in the valley bottoms.

Within the Great Oolite Group is a group called the Fuller's Earth formation. Within which is the Fuller's Earth Rock Formation: a silicate-mudstone, grading towards limestones and bedded with sandy limestones. This is bounded by Upper and Lower Fuller's Earth Formations, which consist of mudstones (British Geological Survey, 2008). The thickness of the Fuller's Earth affects the hydraulic connectivity between the Great and Inferior Oolite aquifers, with a reduced connection in the west where the Fuller's Earth is thicker. The presence of faulting also allows for hydraulic connection horizontally between the two aquifers (Allen et al., 1997); the only major faulting in the catchment is in the east along Holy Brook (British Geological Survey, 2019a).

Streams in the catchment that flow over the outcropping Great Oolite Group are typically in hydraulic connection with the aquifer and springs often occur where the Upper Fuller's Earth - Great Oolite Formation boundary outcrops (Allen et al., 1997).

Storage coefficients for the Inferior Oolite Group range from 7×10^{-5} and 1×10^{-4} (confined) to 8×10^{-2} (unconfined). Transmisivities vary largely from 3 m^2/day to 11 000 m^2/day and have a geometric mean of 139 m^2/day. In this area, these are typically between 200 m^2/day - 700 m^2/day (Allen et al., 1997).

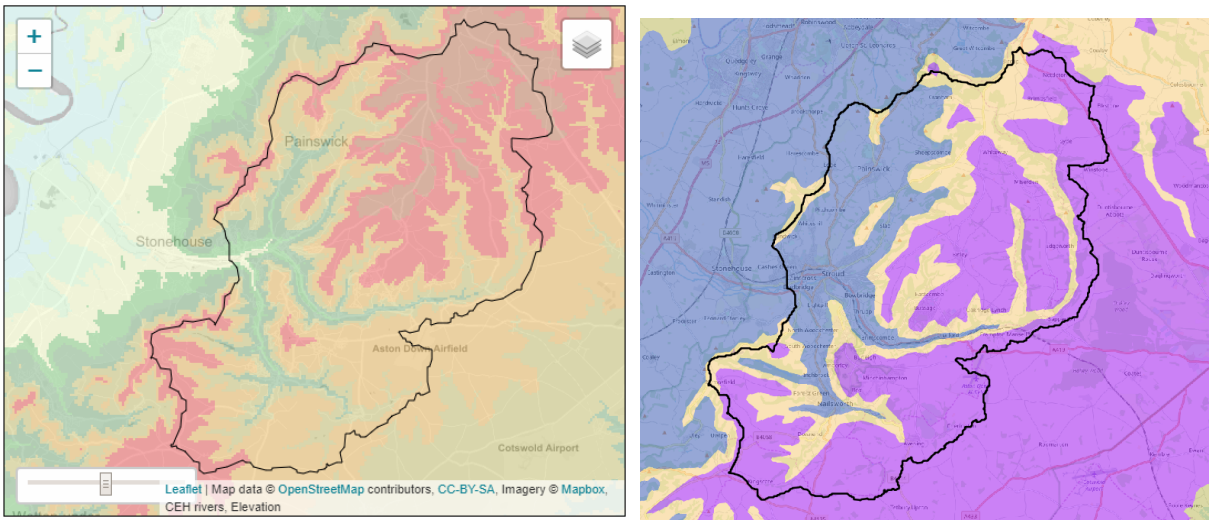

(a) Topography of the catchment - elevations range from 296 m in the northern headwaters of the catchment down to 36 m at the river gauge at Ebley Mill. Map taken from the NRFA (2019b).

(b) BGS 1:650 000 geology map: purple indicates the Great Oolite Group, beige indicates the Inferior Oolite Group and blue indicates the Lias Sands Group.

Figure 13.6: The topography and basic geology of the Frome catchment in South Gloucestershire.

Table 13.2: Stratigraphy of the Jurassic Aquifer of the Cotswolds and the Frome catchment. Capitals denote the main aquifers and italics denote minor aquifers. The highest regions of the catchment have outcrops of the forest marble formation. Adapted from Allen et al. (1997).

Group	**Unit**	**Thickness and Lithology**
GREAT OOLITE GROUP 50 - 100 m Oolitic Limestone	*Cornbrash Formation*	up to 10 m shelly limestone
	FOREST MARBLE FORMATION	up to 35 m
	GREAT OOLITE FORMATION	20–30 m
	Upper Fuller's Earth Formation	up to 28 m
	Fuller's Earth Rock Formation	up to 5 m
	Lower Fuller's Earth Formation	10–15 m
INFERIOR OOLITE GROUP		10–110 m of oolitic limestones
Upper Lias	COTTESWOLD/MIDFORD SANDS	up to 75 m
	Mudstones	up to 80 m
	Junction Bed	0.5 m
Middle Lias	*Marlstone Rock Formation*	up to 7 m
	Dyrham Siltstone Formation	up to 50 m
Lower Lias	Mudstone	200 m
	Mudstone with limestone bands	up to 100 m

In the Great Oolite Group hydraulic conductivities have an average of 9.8 $\times 10^{-5}$ m/day and an interquartile range of 2.54×10^{-4} m/day - 2.97×10^{-3} m/day. A specific yield of 1.4% has been estimated for the Group. Transmissivities in the oolite aquifers are known to vary with depth, with the higher oolites having higher productivity higher up (Allen et al., 1997).

The BGS 1:650 000 superficial geology map shows a 40% covering of mixed permeability quaternary superficial deposits in the lower areas of the catchment and the valley bottoms. The 1:50 000 superficial map shows further Holocene alluvium (clay, silt, sand and gravel) in the river valleys.

13.1.5 Sydling Water

Sydling Water is a very small (12 km^2) catchment in the south west of England. In Chapter III Sydling Water was classified as multisourced with indexes well above the necessary thresholds (Tab. 13.1) and, as such, it is an ideal candidate for a case study. With such a small area, it was also included to test whether increasing the spatial resolution of the simulations is important at smaller scales.

Figure 13.2 shows that Sydling Water is situated on the northern edge of the Chalk aquifer, with the groundwater flowing south, becoming closer to the surface, until the confluence with the river Frome (different to above), at which point it flows more eastward. The bedrock of the Sydling Water catchment is dominated by the Lower Chalk, with some Middle and Upper Chalk in the headwaters (NRFA, 2019b). These are the same units found in the Allen catchment. Grey Chalk (the uppermost layer of the lower Chalk) is hard and marly, with bands of softer marls and is on the order of 20-30 metres thick (British Geological Survey, 2016a). Below the Chalk is a thicker band of mudstones, sandstones and limestones making up the Gault and Upper Greensand Formations. Upstream of the main village of Sydling St. Nicholas the river cuts through the Chalk and exposes the Upper Greensand outcrops in the river valley 2 km.

The Chalk that makes up the catchment has a matrix with a generally low hydraulic conductivity but can allow much faster flows through fissures, which are more common in the harder, more brittle horizons. As the fissuring is controlled by the structural geology of the area, fissures develop more in the valleys than under the headwaters (Institute of Geological Sciences & Wessex Water Authority, 1979) and so transmissivities may vary within the catchment. Furthermore, transmissivity typically decreases from the Upper to Lower Chalk due to a decrease in permeability, and so may be greater in the headwaters of the catchment than in the valley. This decreased permeability can reduce the hydraulic connection between the Middle and Upper Chalk and the Upper Green Sands (Institute of Geological Sciences & Wessex Water Authority, 1979). South Dorset is the most structurally deformed region of the Chalk Aquifer of the south of England; some areas are tectonically hardened, decreasing the matrix hydraulic conductivity and storage coefficient, but potentially locally increasing transmissivity in highly fissured areas (Allen et al., 1997). As the aquifer is largely unconfined, much of the rainfall (minus evapotranspiration) recharges the aquifer due to minimal surface runoff (Institute of Geological Sciences & Wessex Water Authority, 1979).

Superficial deposits of clays, silts sands and gravels top the headlands and line much of the river valley (British Geological Survey). Directly upstream of Sydling St. Nicholas the superficial river valley deposits are dominated by sands and gravels rather than clays and silts (British Geological Survey, 2019a).

Transmissivities for the Chalks in the catchment can be seen in Section 13.1.1. Beneath the Chalks, the Upper Greensand have much lower transmissivities, estimated at 2 m^2/day - 25 m^2/day, typically being below 10 m^2/day (Allen et al., 1997).

The National River Flow Archive does not mention abstractions in the catchment.

13.2 Quantifying Model Performance

Groundwater level records for each of the catchments were compared to simulated groundwater levels using Pearson's correlation and root mean squared error. Stream flows were compared to measured flows using the Nash-Sutcliffe efficiency coefficient, as is common practice in hydrology. These three performance measures are detailed in the sections below. The first two years of the SHETRAN simulations were discounted from analysis as these years are spin up periods and likely to be inaccurate.

13.2.1 Pearson's Correlation Coefficient (PCC)

Pearson's correlation coefficient (PCC) is a measure of correlation between linear variables. It was used to quantify how well SHETRAN-GB captured the fluctuations in observed groundwater level. PCCs range from -1 (a strong inverse correlation) and 1 (a strong direct correlation). The equation for calculating PCC can be seen in Equation 13.2.1.

Pearson's correlation analysis assumes that data fits a normal distribution. Samples of observed and simulated groundwater level distributions were checked and found to be approximately normal. Spearman's rank is an alternate correlation test that can be used on non-normal (i.e. asymmetrical) distributions - this was trialled on a selection of the results and found to show very similar or identical patterns to Pearson's correlation.

Equation 13.2.1 — Pearson's Correlation Coefficient. Pearson's Correlation Coefficient (PCC) is defined as the covariance of x and y divided by the product of the standard deviations of x and y. Where x and y represent the modelled and observed data. The formula for calculating Pearson's Correlation Coefficient is as follows:

$$r = \frac{\sum \Big((m_i - \bar{m})(o_i - \bar{o}) \Big)}{\sqrt{\frac{\sum_{i=1}^{N} (m_i - \bar{m})^2)}{N-1}} \sqrt{\frac{\sum_{i=1}^{N} (o_i - \bar{o})^2)}{N-1}}}$$

Where N is the number of values; m_i and o_i are the modelled and the observed values at instance i; $\bar{m}$ and $\bar{o}$ are the mean modelled and mean observed values.

13.2.2 Root Mean Squared Error (RMSE)

Root Mean Squared Error (RMSE) was used to quantify the vertical difference between the simulated and observed groundwater level (Eq. 13.2.2). RMSE is the square root of the variance of the residuals, residuals referring to the difference between the observed and modelled GW level. As groundwater levels are measured in metres above sea level this returns an absolute value of in metres, and is an important descriptor of how close the model is to the observed data (Theanalysisfactor, 2008). The lower the calculated value, the closer the modelled levels are to the observed.

RMSE is a relatively common statistic in groundwater comparisons - for example by Sreekanth et al. (2011) who created two statistical models for predicting groundwater levels. The goodness of their models were measured using error variation, root mean square error (RMSE) and the regression coefficient R^2. Further examples of its application to groundwater modelling can be found in Zhou and Li (2011) and Tian et al. (2016).

Equation 13.2.2 — Root Mean Squared Error. RMSE can be calculated using the following

equation (Tian et al., 2016):

$$RMSE = \sqrt{\frac{1}{N}\sum_{i=1}^{N}(m_i - o_i)^2}$$

Where N is the number of values; m_i and o_i are the modelled and observed values at instance i.

13.2.3 Nash-Sutcliffe efficiency (NSE)

Nash-Sutcliffe efficiency is a common measure of the goodness of fit of a modelled flow to an observed flow. For the two time series, a single value is calculated that ranges from -∞ (very bad) to 1 (a perfect match). A calculated NSE of 0 indicates that the model is performing as well as taking a simple mean of the observations. Less than this indicates that the model performs worse at simulating the river flows than taking a mean of observations.

There are some examples in the literature of NSE being used as a performance indicator for groundwater levels. One such example use is in a paper by Dudley et al. (2018) to test the correlations between groundwater levels and streamflow and baseflow. There is also evidence of its use comparing modelled and recorded groundwater levels in a paper by Tian et al. (2016). Tian et al. (2016) first normalised the groundwater levels to *"avoid disturbance of dimensions"* but, like other papers reviewed on the subject, did not justify their choice of statistics. Other than these instances, NSE is not a common metric found in the literature for testing the relationships between groundwater levels. Hence, in this thesis, the use of NSE is confined to flow analysis.

Equation 13.2.3 — Nash-Sutcliffe efficiency. Nash-Sutcliffe efficiency is defined by the following equation (Tian et al., 2016):

$$NSE = 1 - \frac{\sum_{i=1}^{N}(m_i - o_i)^2}{\sum_{i=1}^{N}(o_i - \bar{o_i})^2}$$

Where N is the number of values; m_i and o_i are the modelled and observed values at instance i; $\bar{o_i}$ is the mean observed value.

14. Results

14.1 The Automated Setups

The Pearson's correlation coefficient (PCC) and root mean squared error (RMSE) have been calculated for six different automated SHETRAN setups of five case study catchments. Resultant statistics can be seen in Table 14.1. The majority of models appear to hold some degree of truth, with an average PCC around 0.5.

The use of transmissivity data from the aquifer properties manual (MacDonald and Allen, 2001) typically improves PCC, increasing them from an overall average of 0.51 to 0.61. The increased transmissivity values cause the simulated groundwater levels to drop at many of the borehole locations. As the APM simulations use a single 20 m thick layer to represent the subsurface geology, this decrease in level often goes beyond the depth of the cell and cells become unsaturated, resulting in 20 m deep static groundwater levels in several locations. These constant, bottomed-out groundwater levels meant that correlation analysis was not possible for some of the borehole records. Those locations where the groundwater levels did not bottom out typically showed increased PCCs, often significantly so.

None of the automated setups caused unanimous improvement in PCCs or RMSEs. Nor is there a simple correlation of improving accuracy with increased model resolution. A breakdown of all of the Pearson's correlations and RMSEs can be seen in Tables 28.3 and 28.4 in the Appendix.

Hydrographs of groundwater levels can be seen in Figures 14.1, 14.2, 14.3, 14.5 & 14.7. All plots also include the elevations of the SHETRAN cells from which *groundwater depth below cell* has been converted to metres above sea level. Approximate borehole elevations are also plotted, however these are estimated from Ordinance Survey maps and were not typically required for calculating groundwater level as these were normally provided with the datasets in metres above ordnance datum (i.e. sea level).

Many of the groundwater hydrographs show an upper bound on groundwater level, where water levels plateau in periods of high groundwater. This plateau occurs when the water level reaches the surface of the SHETRAN cell, with the groundwater level being simulated at or just below ground surface. SHETRAN can simulate perched groundwater systems close to the surface with a deeper band of unsaturated cells and then a deeper true groundwater level. This, however, was not found to be the cause of those groundwater levels simulated to be consistently close to the surface. This errant tendency to fully saturate the subsurface causes a loss of information regarding the fluctuations in groundwater level and greatly reduces the usefulness of such models in producing accurate groundwater emergence maps. As such, it is clear that none of the automated setups are appropriate for simulating groundwater levels in their fully automated state. Most simulations do show definite potential and all depict the seasonal increase and decrease in groundwater level to some degree. Each of the catchments are discussed below in

Table 14.1: Average catchment RMSE and PCC. *s denote statistics calculated on a reduced numbers of records due to static water level the in APM simulations. The number of unusable locations are as follows: Allen 5/10; Frome 4/5; Foston Beck 5/10; Sydling Water 2/3. See full breakdown in Table 28.3.

Root Mean Squared Error	**R. Allen**	**R. Creedy**	**Foston Beck**	**R. Frome**	**Sydling Water**
Standard 100 m	-	-	29.09 m	-	47.21 m
Standard 500 m	22.72 m	24.67 m	33.98 m	43.29 m	56.37 m
Standard 1000 m	22.27 m	14.77 m	48.39 m	40.31 m	54.53 m
APM	9.29 m*	-	34.14 m*	38.85 m*	40.92 m*
3D Geology	31.81 m	11.31 m	47.70 m	41.28 m	54.59 m
3D Geology & APM	16.92 m	-	34.63 m	40.97 m	18.63 m
Calibrated	-	-	2.19 m	-	-
Pearson's Correlation	**R. Allen**	**R. Creedy**	**Foston Beck**	**R. Frome**	**Sydling Water**
Standard 100 m	-	-	0.34	-	0.32
Standard 500 m	0.67	0.63	0.51	0.39	0.61
Standard 1000 m	0.65	0.49	0.44	0.44	0.45
APM	0.85*	-	0.54*	0.58*	0.64*
3D Geology	0.69	0.26	0.45	0.36	0.48
3D Geology & APM	0.52	-	0.22	0.43	0.11
Calibrated	-	-	0.78	-	-

Table 14.2: The Nash Sutcliffe efficiencies for the different simulations. These are calculated from daily flows. Hourly flows for the calibrated Foston Beck catchment yield a NSE of 0.64. This was calibrated focussing on groundwater levels and could most likely be improved if desired.

Nash Sutcliffe Efficiency	**R. Allen**	**R. Creedy**	**Foston Beck**	**R. Frome**	**Sydling Water**
Standard 100 m	-	-	-0.17	-	-1.58
Standard 500 m	-0.59	0.55	-0.60	0.68	-2.24
Standard 1000 m	-1.89	0.51	-1.80	0.64	-7.45
APM	0.55	-	0.42	0.74	-0.14
3D Geology	-1.38	0.48	-0.71	0.62	-6.66
3D Geology & APM	-0.10	-	-0.03	0.62	-0.06

turn with regard to the different setups and how they perform.

Table 14.2 shows the Nash Sutcliffe efficiencies for the simulated flows. These confirm the statement in the introduction: that SHETRAN-GB simulates flows much better in less permeable catchments, such as the Frome and the Creedy. Even without calibration a reasonable correlation is found between the observed and simulated flows in these catchments.

In the more permeable catchments the NSEs are much lower, with the APM generating the 'best' setup with an average NSE of 0.39, and 0.11 when combined with the 3D geology. This indicates that these updated parameters are more appropriate for the simulations. Overall, the use of detailed geology slightly improves the NSEs relative to the 1000 m Standard simulations (from -2.5 -1.5) however the 3D geology still performs very poorly in the Chalk catchments of the River Allen, Foston Beck and Sydling Water.

In all of the catchments, increasing the resolution improves the NSEs. This is expected and is most evident in the smallest catchment, Sydling Water, demonstrating the need for models of a sufficiently high resolution.

14.1.1 The Creedy Catchment

The simulations of the Creedy catchment are the only ones that show no improvement in model performance when the 3D geology data and parameters from the aquifer property manual are

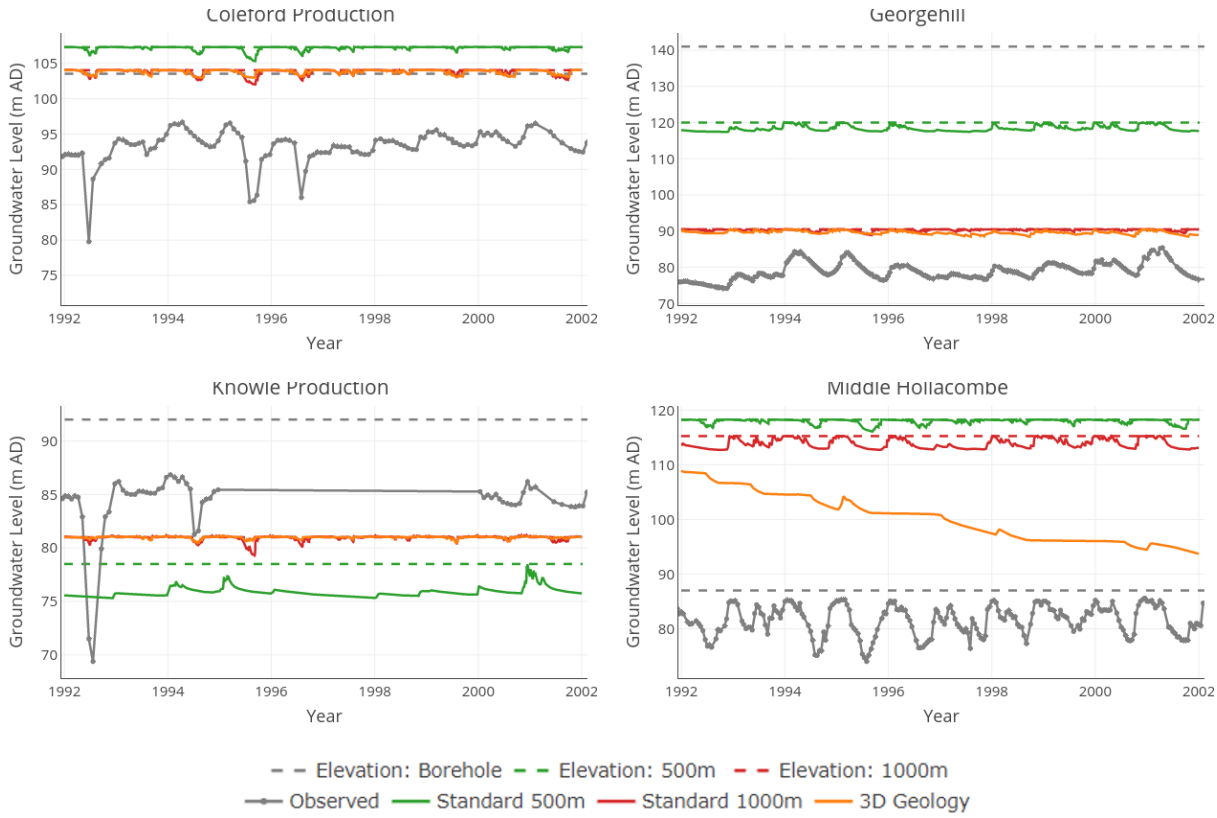

Figure 14.1: Groundwater hydrographs for the Creedy catchment.

included. The 'best' simulation is the higher resolution, 500 m Standard run, which has a PCC of 0.63 and a RMSE of 24.67 m.

For the 1000 m resolution simulations, the simulated groundwater level in three of the four boreholes fluctuates within only the topmost 2 metres of the subsurface column, with only groundwater levels at Middle Hollacombe dropping below this in the simulations involving detailed geology (Fig. 14.1). The reason for this dropping off is unknown, however it is speculated that it may be due to the significant change in topography within and around the Middle Hollacombe borehole cell.

The groundwater levels are similar across the different setups, as the changes in parameters are relatively limited, with only the structure of the models altering between the setups. Although the detailed subsurface geology does increase the depth, and in some places the extent, of the permeable bedrock that transects the centre of the catchment by 180 m, it does not change its properties. Furthermore, the 3D geology data only contains information regarding the central, more permeable trough of the catchment and had no additional regarding the structure of the mudstones in the north and south of the catchment.

None of the simulations perform well or are able to capture any more than a basic seasonal pattern, and even this is heavily muted.

14.1.2 The Allen Catchment

The majority of the groundwater levels in the Allen simulations fluctuate within the top few metres of the subsurface column. This is typical for many of the simulations across all of the catchments.

In the standard simulation almost the whole catchment, apart from the very south east corner,

is classified as a highly productive aquifer. In the 3D geology simulation the muds of the south east are extended northwards and cover much of the southern half of the catchment and the Chalk of the north catchment is interbedded with bands of mudstone. Despite this, the use of the detailed 3D geology has minimal effect on the simulated groundwater levels (Fig. 14.2).

The use of the aquifer properties manual parameters generates a much greater change in simulated groundwater level, with decreases in water level and increases in the amplitude of fluctuation. In four of the five instances where the APM groundwater levels bottom out, the observed groundwater levels are deeper than 20 m below the surface. This suggests that the APM parameters are shifting groundwater levels towards the observed level. This is supported by the decrease in the catchment RMSE from 22.72 m to 9.29 m. The increase in fluctuation also appears to be effective, with an increase in average PCC from 0.65 to 0.85.

When the aquifer properties manual parameters are combined with the detailed geology there is a decrease in the average PPC to 0.52, from 0.65 in the Standard run. This is likely due to the smoothing affect that this has had on the groundwater levels, decreasing the frequency and amplitude of fluctuations. Examples of this smoothing can be seen at Barnsley Farm, Crichel Chitterwood, High Hall, Hogstock Cottages and West Acre. Unlike in the APM simulation, none of this smoothness is due to bottoming out as all cells are 200 m deep. Instead, the smoothing occurs in instances where the Chalk layer is confined below a mud layer. At all borehole locations the modelled Chalk-mudstone boundary is close to the simulated groundwater level. At the Woodyates Telemetry borehole in the north, where there is Chalk above the mudstone, there is an increase in the fluctuation of groundwater level. At Dean Farm, Nine Yews and Squirrels Corner the inclusion of the 3D geology makes little difference to the simulation again, these are confined by an impermeable mudstone for 56 m, 70 m and 81 m below the surface respectively.

14.1.3 The Foston Beck Catchment

As in the other catchments, Foston Beck simulated bottomed out groundwater levels in the APM simulation when the observed groundwater levels are more than 20 m deep (Fig. 14.5). When this is not the case the groundwater levels are typically more variable than in the Standard 1000 m simulation and show greater promise for the necessary future calibrations. When the detailed geology data is added to the APM simulation there are mixed responses with some locations having only small changes relative to the Standard 1000 m simulation (e.g. Bartondale & Henpit Hole), while other show greatly decreased groundwater levels (e.g. Honey Hill & Octon Crossroads). Much of the central catchment is reclassified from highly productive Chalk aquifer to much less permeable sand stones and mudstones with a saturated conductivity of 0.01 m/day. This is not in agreement with the BGS 1:50 000 bedrock geology map, which shows the whole area to be underlain by Chalk.

Foston Beck is one of the few catchments small enough to allow for modelling at a 100 m resolution. Although all of the Standard simulations have the same properties, changing the resolution of the simulations alters the simulated groundwater levels. Statistically, the 500 m model performs best, with a PPC of 0.51 compared to 0.34 and 0.44 for the 100 m and 1000 m simulations (Tab. 14.1). It is the 100 m simulation however that has the lowest RMSE, something also seen in the Sydling Water catchment. This is to be expected as the higher the resolution, the more specific the simulated levels are for the area surrounding the borehole. It is not a unanimous improvement in RMSE across the other catchments however as the 1000 m simulations more frequently have lower RMSEs than the 500 m simulations. Increasing the resolution can also have different affects on different cells. The simulated groundwater levels at the Kilham PS borehole shows the 500 m simulation to produce a variable groundwater level, while the 100 m simulation produces a comparatively smooth profile. This pattern is then reversed at the Tancred Pit Hole borehole. It is difficult to find the definitive reason for this, however, the different

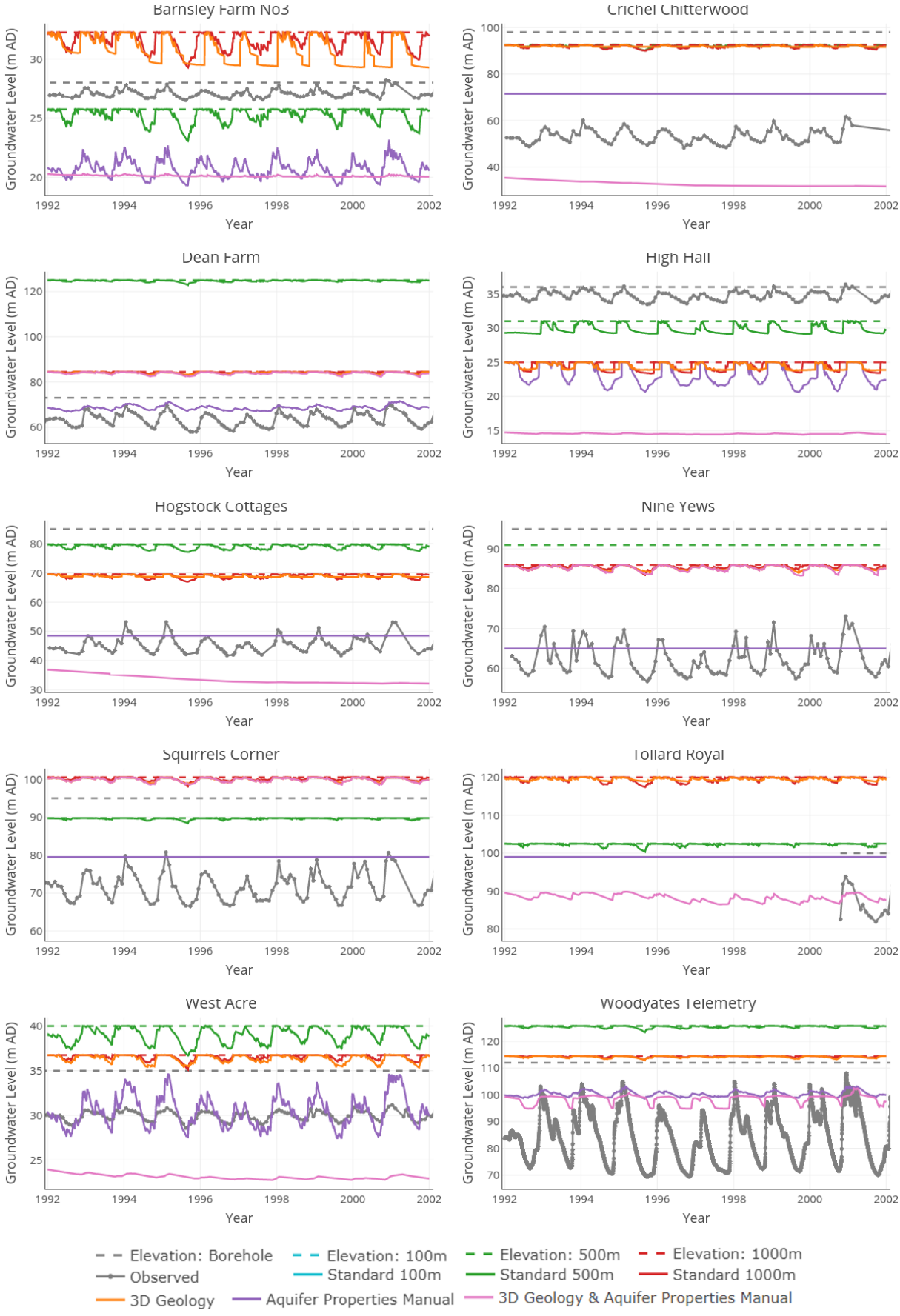

Figure 14.2: Groundwater hydrographs from ten boreholes in the Allen catchment.

resolution topographies may be responsible - the 100 m model has relatively gradual changes in elevation between adjacent cells whereas Tancred Pit Hole borehole in the 500 m simulation is in a depression of over 10 metres and so may well have its groundwater levels dragged closer to the surface to be more in line with those of the higher adjacent cells.

14.1.4 The Frome Catchment

Figure 14.3 shows the groundwater level hydrographs for the Frome catchment. Due to the large range in simulated and observed groundwater levels, the five monitoring sites are shown at an increased vertical resolution on the right hand side of the figure.

It is clear to see from the left hand side of Figure 14.3 that, as with the other catchments, groundwater levels are simulated too close to the ground surface. This is especially true at the Edgeworth and Minchinhampton Golf Club boreholes where the observed levels are around 100 and 90 metres below ground respectively. This leads to an average RMSE of around 40 m for the catchment.

As with other catchments the APM simulation yields the lowest RMSE. However, only at Longridge does the groundwater level not bottom out during the APM simulation. Here, even though the subsurface is composed of highly productive bedrock with increased hydraulic conductivity, the groundwater level stays near to the surface. This is likely to be because the cell is in a depression, surrounded by cells of higher elevations (7 m - 120 m), however this is also the only borehole to be in an area of bedrock containing *no groundwater*. All others are in regions of *highly productive bedrock*.

One other conspicuous detail of the hydrographs is the decreasing groundwater level at Kingscote in the 500 m Standard simulation. The reason for this is unknown as Kingscote does not have any unusual features in its parameters or DEM. This is known to happen in some of the models, however when looking at a map of simulated groundwater level across the catchment this does not appear to be particularly anomalous.

The introduction of the 3D geology data alters the catchment structure considerably. The subsurface layout used in the Standard model can be seen in Figure 14.4. This shows a mixture of highly productive and moderately productive bedrock and a band of bedrock classed as containing virtually no groundwater. In the 3D geology model this is reclassified almost entirely as an extensive, catchment wide layer of sandstone, limestone and argillaceous (i.e. containing clays) material tens of metres thick, underlain by a layer of inter-bedded mudstones and limestones down to the base of the 200 m deep cells. These have respective saturated conductivities of 0.01 m/day and 0.0001 m/day. As such, the use of 3D geology and parameters from the aquifer properties manual have minimal influence on the simulation.

14.1.5 The Sydling Water Catchment

Sydling Water is the smallest catchment being modelled in this study and has a highly productive bedrock. As such, with only 13 cells in the 1000 m simulation, it was expected to be one of those that benefited most from the increased resolution simulations. Figure 14.6 shows the simulated depth to groundwater in the 100 m and 1000 m Standard simulations. It demonstrates the difference that the resolution makes to the spatial distribution of areas of high and low groundwater. The increased resolution has differing affects at the different borehole locations. Despite this, the average PCC from the 100 m simulation is lower than that of the 1000 m simulations. This is due in part to the poor results around Folly Hill (Tab. 28.3), however even if this statistic is excluded, no statements can be made relating increased resolution to increased accuracy. Qualitatively however, the higher resolution simulations show more promise than the 1000 m simulation as they exhibit a greater range of groundwater levels, more in line with those observed, and do not hug the ground surface as consistently as the 1000 m simulation.

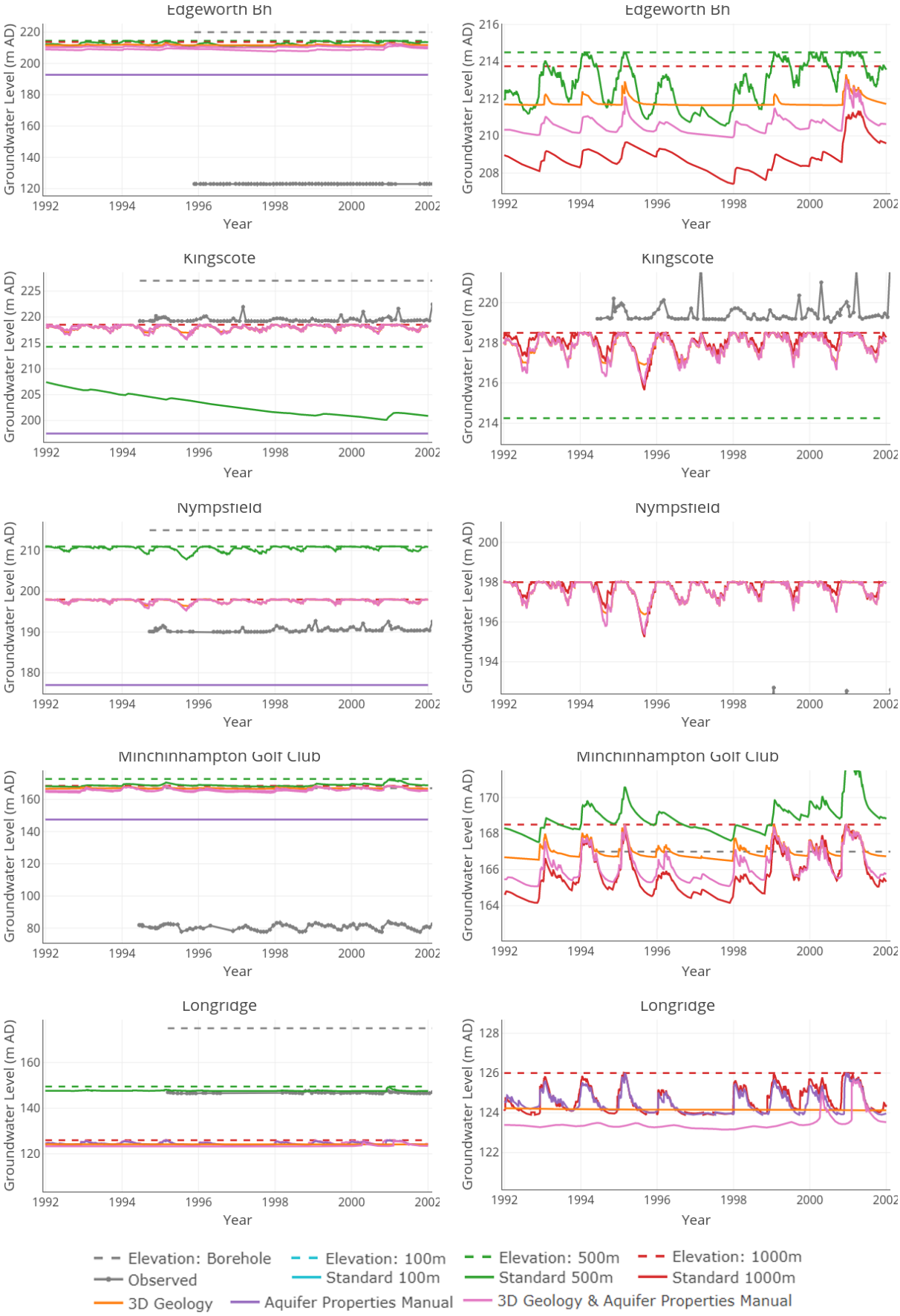

Figure 14.3: Groundwater hydrographs for five boreholes in the Frome catchment - hydrographs on the right hand side of the figure show extracts of the hydrographs at a higher resolution.

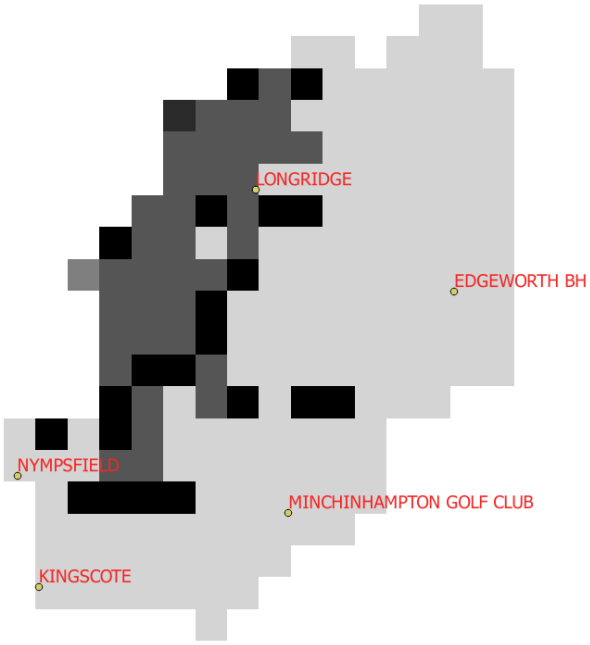

Figure 14.4: The bedrock from the Standard and APM simulations in the Frome catchment: light grey shows highly productive bedrock, dark grey shows moderately productive bedrock and black shows bedrock with virtually no groundwater. Labels show borehole locations.

The inclusion of the 3D geology data smooths the plotted groundwater levels at both Dickley Down and Folly Hill, bringing them closer to the surface. The subsurface for the Sydling Water catchment was complicated by the inclusion of 3D geology. In place of the original high productivity bedrock layer of there are three bedrock layers: a permeable layer of Chalk of variable thickness, a very low permeability layer of mudstone and, finally, a layer of rock of intermediate permeability. Much of the upper catchment is dominated by a thick mud layer, beneath a layer of Chalk a few metres thick. This may be a reasonable representation of the geology in the headwaters but the low resolution of the model relative to the catchment size means that there are very few cells able to transmit groundwater, which is not a fair representation of the catchment. In the centre of the catchment the Chalk layers are significantly thicker than they are in the Standard model.

Adding the higher saturated conductivities of the APM drops the groundwater level at all borehole locations, bringing the simulated groundwater level closer to the observed level. This indicates that the higher conductivity is a more appropriate value than that in the standard simulation. The bottoming out of the groundwater in the APM simulations shows that the cells are again not deep enough. The smoothing of the groundwater level in the combined 3D geology and APM simulation may indicate further issues with the resolution of the 1000 m simulation - the groundwater levels in several of the model cells are equal, showing a flat groundwater profile. This is despite differing layer depths in their subsurfaces and different cell elevations.

14.2 The Developed Allen Catchment

The different national scale datasets discussed above were each found to have some effect on the simulations, however none can be deemed fit for use without further calibration. As such, to identify points for future work on the SHETRAN-GB modelling system, further development took place for the Allen catchment. The Allen was selected as it showed the most promise with the inclusion of the various datasets, showing improvements statistically (Tab. 14.1) and visually

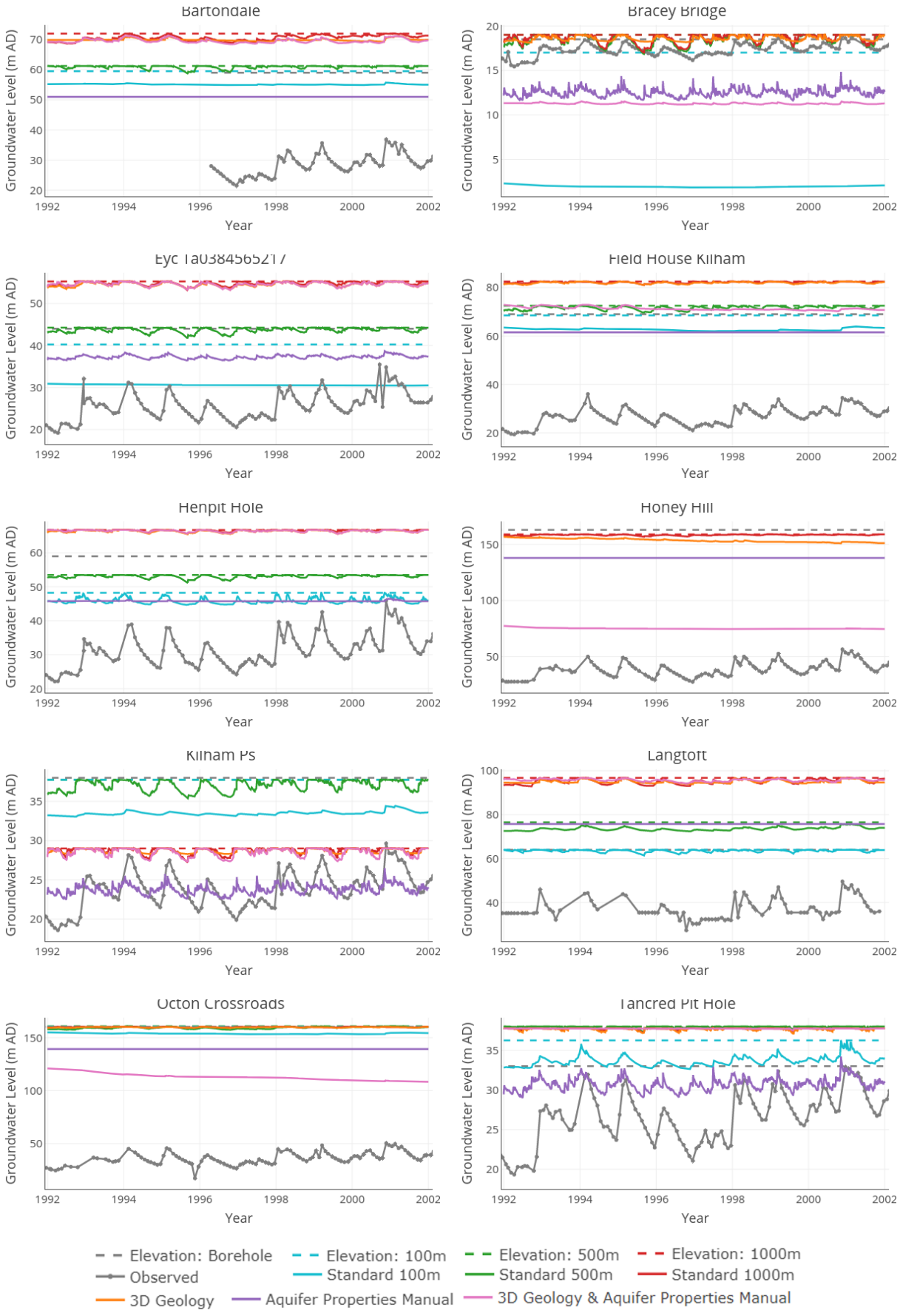

Figure 14.5: Groundwater hydrographs for ten boreholes in the Foston Beck catchment.

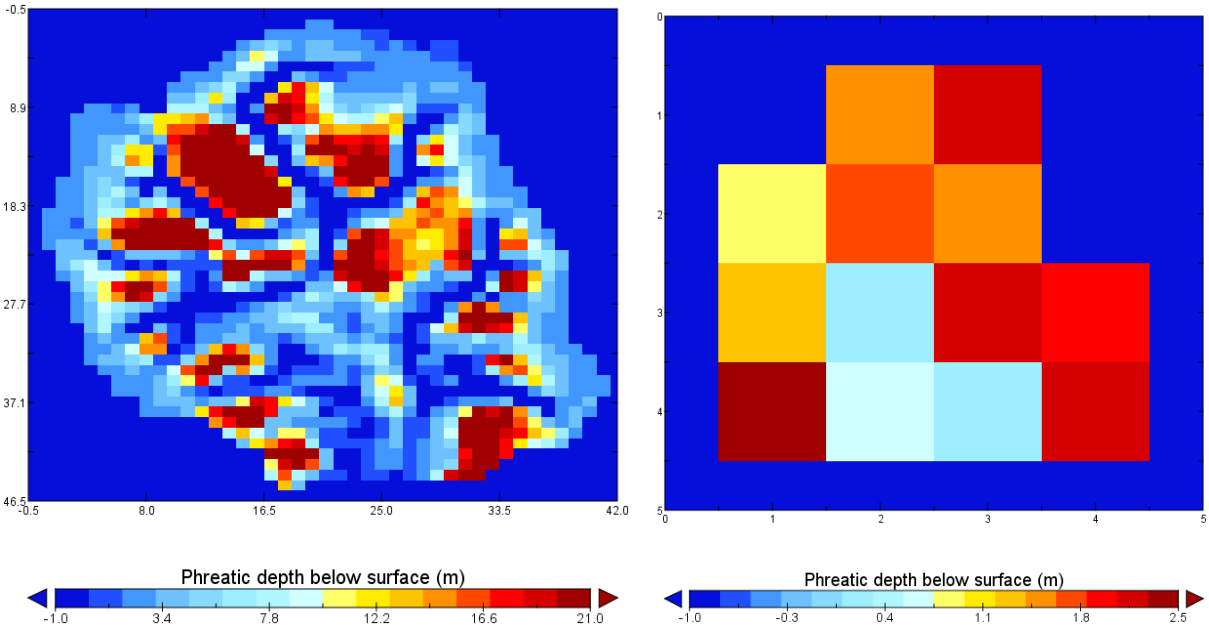

(a) 100 m Standard Simulation

(b) 1000 m Standard Simulation

Figure 14.6: The depth to groundwater in the Sydling Water simulations as two different horizontal resolutions: 100 m and 1000 m.

in the hydrographs (Fig. 14.2). One of the chief differences between the automated setups and the actual hydrogeology of the Allen was the catchment shape. The topographic restrains on catchment shape were removed and the catchment area was increased northwards to reflect a more realistic groundwater catchment (Institute of Geological Sciences & Wessex Water Authority, 1979). This was found to improve the quality of the simulation, decreasing the instances of anomalous groundwater levels and also increased the amplitude of level changes in the south of the catchment (e.g. Barnsley Farm). This did not solve instances where the groundwater level was simulated too close to the surface.

Following the success of the increased saturated conductivities in the automated APM set up, saturated conductivities were increased to 100 m/day. This was double the saturated conductivities used in the original AMP simulations as these were still deemed too low. Increasing the saturated conductivity of the Chalk greatly improved the simulations, dropping the groundwater levels away from the surface at the upper end of the catchment. This simulation resulted in PCCs of 0.69-0.93 with a mean of 0.86 and a RMSE of 8.97 m. Following the bottoming out of groundwater levels along the cell bases in previous runs, the subsurface had been deepened to 40 m. As a result of the deeper subsurface and extended catchment, only Tollard Royal bottomed out. These simulations show seasonal fluctuations in level as well as higher resolution, sub-monthly variations.

The introduction of the BGS 3D geology along with the improved catchment size and aquifer properties was expected to further increase model performance. This was not found however, with PCCs dropping back down to an average of 0.5 and the RMSE increasing to 16.38 m. Hydrographs show that the five boreholes in the south of the catchment show very subdued groundwater profiles while those in the north have risen back to the surface. This is due to the extensive mudstone layer introduced by 3D geology (discussed in 14.1.2). Only at Woodyates Telemetry, the northern most borehole, is the groundwater profile still able to oscillate unhindered by its proximity to the surface.

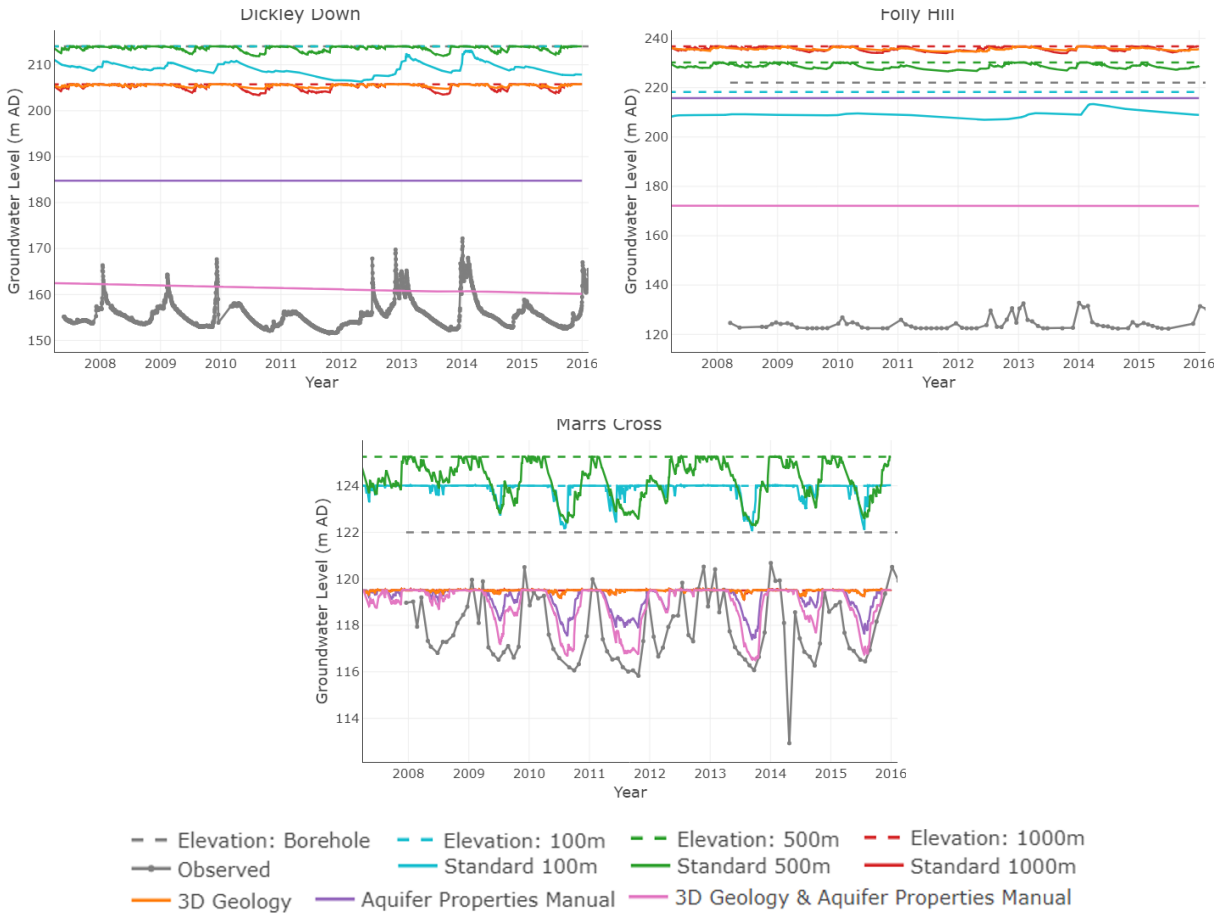

Figure 14.7: Groundwater hydrographs for the Sydling Water catchment.

Table 14.3: Statistical results from the developed Allen catchment. Simulation numbering refers to that in Section 13. *Combined* refers to the work of Bence (2019) detailed in Section 15.3.

Simulation	Subsurface	Saturated Conductivity	Specific Yield	PCC	RMSE	NSE
1	Single unit - 20 m	0.1 m^2/day	0.10	0.64	22.26	-9.13
2	Single unit - 40 m	100 m^2/day	0.02	0.86	8.97 m	-3.99
3	3D Geology - 200 m	100 m^2/day	0.02	0.50	16.38 m	-3.35
Bence (2019)	Combined	100 m^2/day	0.05	0.30	16.22 m	-1.05

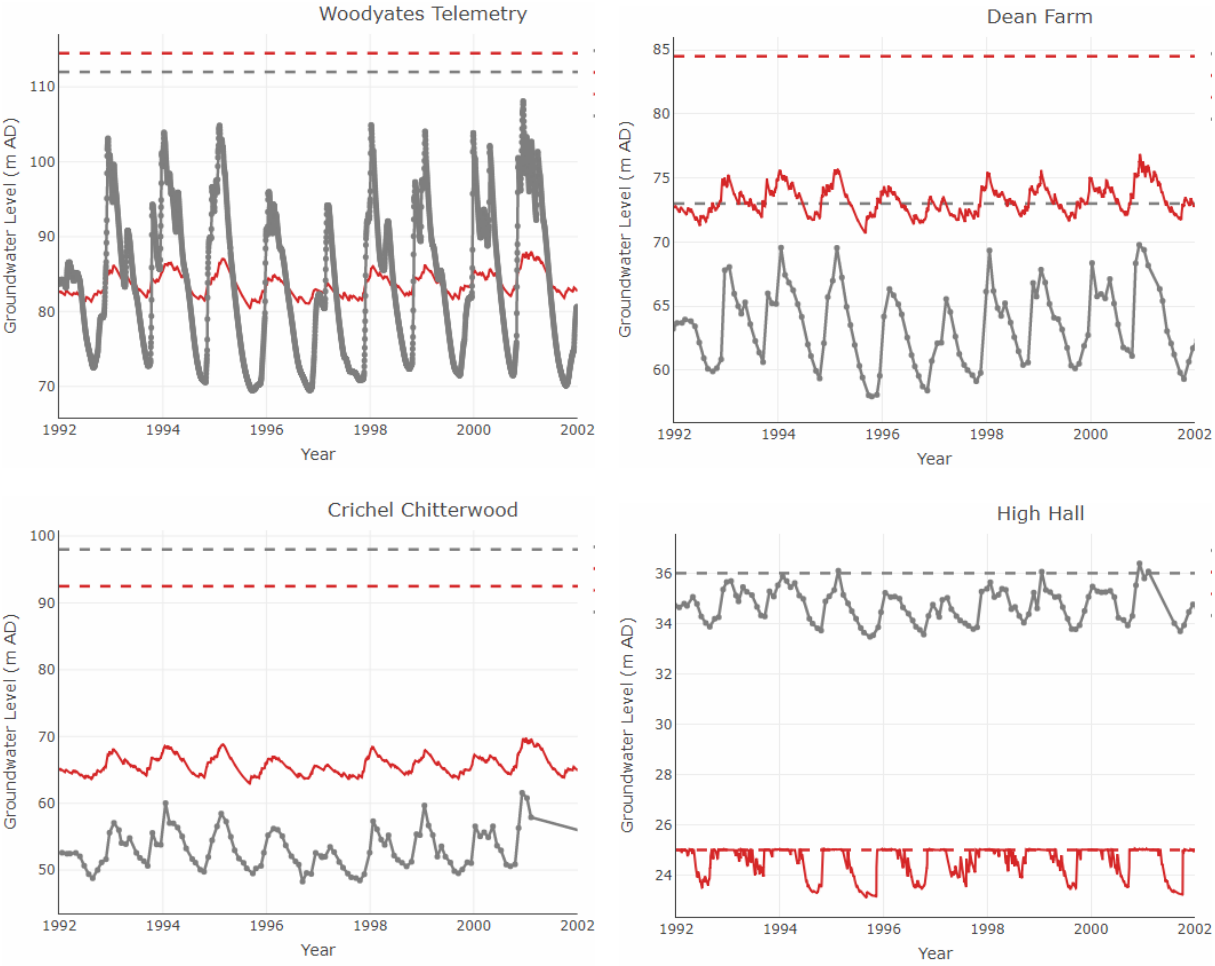

Figure 14.8: Four hydrographs progressing from the top to the bottom of the Allen catchment are shown from the developed model. These are from setup 2, with an extended catchment size and increased saturated conductivity. Red shows the simulated groundwater level in the cell containing the borehole, grey shows observed data. Red and grey dashed lined indicate the height of the SHETRAN cell and the estimated height of the borehole respectively.

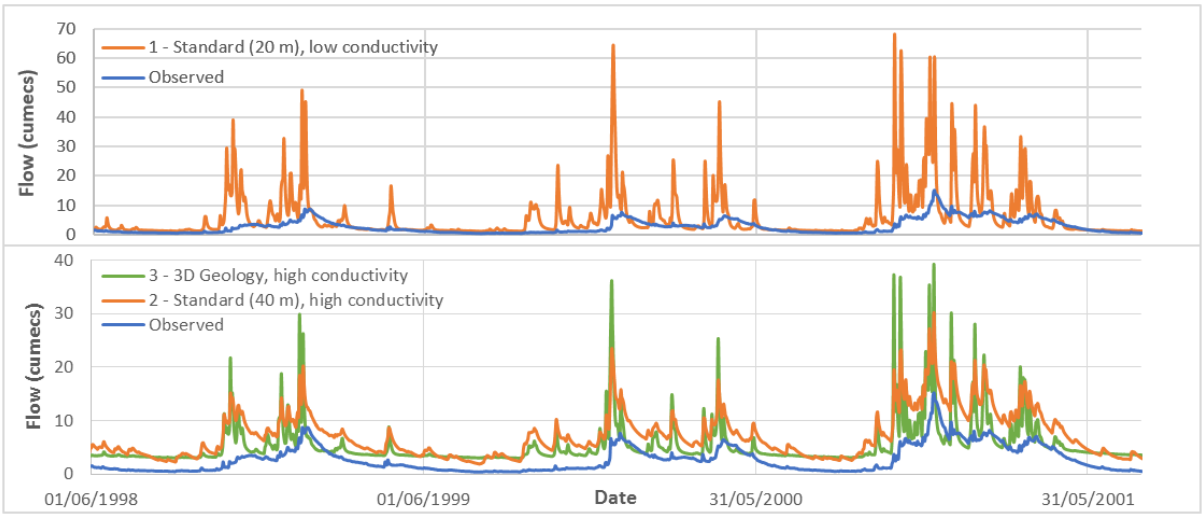

Figure 14.9: River flows from the developed Allen catchment.

15. Discussion and Conclusion

15.1 The National Datasets

Each of the different automated simulation setups detailed previously employed different national datasets. The purpose of these suites of simulations was to explore the potential for a national physically based modelling system capable of simulating groundwater processes. Previous work by Lewis (2015) demonstrated the potential for their use in a national river flow modelling system. This was shown to be capable of producing good results in less permeable catchments but struggled in areas with more permeable bedrocks, especially Chalks. One of the unknowns in that work was the role of groundwater in the models and how realistically groundwater processes were being portrayed. In this study groundwater levels were extracted for five case study sites and compared to observed groundwater levels. The performance of each of the national datasets within the modelling system is discussed below.

15.1.1 Standard

The Standard model runs describe the subsurface as a 20 m thick bedrock layer with properties taken from the BGS hydrogeology map. These simulations capture some of the seasonal fluctuations in groundwater level however many are confined to near the surface and only show groundwater levels changing within the top few metres of the subsurface column, often restricted to the soil layer. This thin upper layer was a simple starting point from which to base the stepwise sensitivity test conducted in this chapter and was anticipated to be an over simplification, hence the inclusion of the 3D geology to increase realism and depths of the simulations (200 m in these examples). Despite the simplicity of these simulations, there are promising NSEs in the two less permeable catchments of the Frome and Creedy of 0.64 and 0.51.

15.1.2 The Aquifer Properties Manual

Increasing the transmissivities of the high productive bedrock causes results largely in line with what would be expected. The Chalk and limestone catchments of the Allen, Foston Beck, Frome and Sydling Water all became more responsive and the majority of groundwater levels decreased. This decrease in level was especially prevalent in the upper catchment.

In the majority of the simulations the use of the APM parameters significantly reduces the groundwater levels to be more in line with the observed level. While this could be considered an improvement, this was frequently limited by the depth of the cells - when the groundwater level dropped to more than 20 m deep the groundwater level became constant at the cell base and so lost usefulness for simulating the water level. In those instances where the groundwater level did not 'bottom out' the use of APM parameters typically improved PPCs. Using the APM parameters also shows significant improvements in flow correlation in four of the five catchments.

Furthermore, model mass balances improve slightly with the use of APM values due to a slight reduction in the volume of water stored in the subsurface.

15.1.3 3D Geology

To increase the realism of the models, and to address the issues associated with bottoming out of the groundwater levels, detailed subsurface geology was added to the simulations, replacing the previous simple 20 m thick subsurface layer. This had a range of effects on the models but did not offer great improvements in the RMSE or PPCs. Changes in PCC were generally improvements in the more permeable catchments and but hindered performance in the less permeable Frome and Creedy.

This addition did not have the desired effect of drawing groundwater levels away from the surface however, indicating that the depth of the geology is less of a control on the simulations than the use of the aquifer properties manual parameters. In the Allen and Foston Beck simulations, this was likely to be due to the errant addition of low permeability geology into highly permeable catchments, confining the more productive layers below or interbedding them with aquicludes.

15.1.4 3D Geology and Aquifer Properties Manual

The combination of detailed geology and the use of the aquifer properties manual was thought to offer the greatest potential for setting up realistic and accurate uncalibrated catchments. Statistically, this does appear more promising than using the detailed geology with the Standard parameters (Tab. 14.2), however many of the PCCs are lower in this suite of simulations than when the APM parameters are used with the Standard geology. This combination does solve many of the instances of bottoming out, a significant drawback of the APM simulations.

There are still instances where the subsurface is fully saturated, however, and the groundwater levels fluctuate at or very near the surface. This indicates that further work should include sensitivity testing using hydraulic properties for bedrocks and soils other than those deemed highly productive.

Comparing these runs to the APM suite of simulations also indicates those instances where there may be errors in the 3D geology model - i.e. locations that are unsaturated in the APM simulations but fully saturated when 3D geology is added. Examples include Henpit Hole, Kilham PS, Langtoft and Tancred Pit Hole from the Foston Beck catchment (Fig. 14.5), all of which had highly productive bedrock incorrectly replaced by a low productivity layer.

15.2 Model Resolution

It may be assumed that increasing the resolution of the simulation would increase the accuracy of groundwater level estimations, however this could not be concluded here. Earlier studies have also found that SHETRAN performance is not necessarily proportional to the model resolution (Zhang, 2012). While the RMSEs of both of the 100 m resolution simulations were decreased relative to the 1000 m simulations, they performed poorly in terms of PCCs. Modelling at such high resolutions can be justified where the catchment area allows as it offers significant improvements in NSE, with the higher resolution models unanimously outperforming the lower resolution models. Furthermore, it is difficult to justify modelling catchments as small as Sydling Water at the 1000 m scale, as demonstrated both statistically in Tables 28.3 & 28.4 and objectively in Figure 14.6. The increased resolution also avoided instances where steep topographic gradients between neighbouring cells caused the groundwater level to be dragged up or down to match its neighbours.

Although not considered here, Lewis et al. (2018) report that Zhang (2012) found that increasing the temporal resolution of rainfall data, and, to a lesser extent, the other drivers, has

the potential to improve model performance. This enables the simulation of intense storm events in the simulations, which are averaged into steady drizzle in the daily rainfall simulations. This transition into higher resolution driving data is now possible with the recent publication of a gridded hourly dataset for the UK (Blenkinsop et al., 2016).

15.3 The Developed Allen Catchment - Implications for Future Work

Until the simulations developing the Allen catchment took place, the majority of the automated simulations were unable to provide suitable estimates of groundwater level and few of the alterations in either model parameters or in the subsurface structure were able to offer improvement. The subsequent runs of the Allen model used a greatly enlarged catchment so as to capture the groundwater catchment, rather than just the surface water catchment as had been the case with the national scale tests. Enlarging the catchment had a profound effect on the sensitivity of the model to parameter changes and greatly improved the representation of groundwater processes and levels. Once the catchment was extended, increasing the saturated conductivities had the expected effect of dropping the groundwater levels in the upper regions and increasing the responsiveness of the aquifer system. It is suggested therefore that the relatively simple inclusion of groundwater catchments into SHETRAN-GB can yield significant improvements in the performance of the model's groundwater simulation. Increasing the size of the catchment did increase the computational requirements, however the 20 year simulation at a 1 km resolution with daily meteorological inputs only took around 30 minutes on a standard PC, and so is still relatively quick.

However, one issue with increasing the catchment size was that, although the PCCs and RMSE of the groundwater levels were improved, the NSE of the river flows decreased. Simply increasing the catchment size, while still using the single unit, 20 m thick subsurface from the Standard simulations, decreased the NSE from -1.89 to -9.13. Increasing the saturated conductivity did improve the NSE somewhat, but only to -3.49, considerably lower than in the roughly equivalent APM run, which scored an NSE of 0.55.

This decrease in flow simulation accuracy is likely to be due to differences in the representation of rivers between the different sized models. SHETRAN-GB creates its own river network based on the input DEM and a minimum elevation DEM, which states the minimum elevation within each cell. The river network created for the simulations can be seen in Figure 15.1a. Both the surface water and groundwater catchments have more channels in them than are present in reality, however there are an even higher volume in the larger model. The figure shows a reasonable representation of the River Frome in the west of the groundwater catchment, but also two rivers that are less reasonable. The first wrapping around the north of the catchment and joining the Allen in the east, and the second running along the south east of the catchment perpendicular to the actual river flows of that area. This is because the default for the automated set up is to force rivers into a single outlet, however this can be manually altered in order to direct the anomalous rivers onto a more appropriate courses, or to remove them altogether. The deliberately dense channel network in the groundwater catchment is to increase the stability of the simulation. This desire for stability was to counteract the increase in saturated conductivity, which typically decreases model stability and can causes simulation crashes. It is clear that using the groundwater catchment is key to producing realistic groundwater levels but it indicates that there needs to be further developments within SHETRAN-GB in designing appropriate river networks. It is also possible to improve stability through other means (such as altering model time steps), which would be a useful focus for future work.

Figure 15.1b shows groundwater contours for the Allen catchment. Blue contours are based on observations (taken from Institute of Geological Sciences & Wessex Water Authority (1979)) and brown contours show simulated groundwater levels for an autumn period considered representative

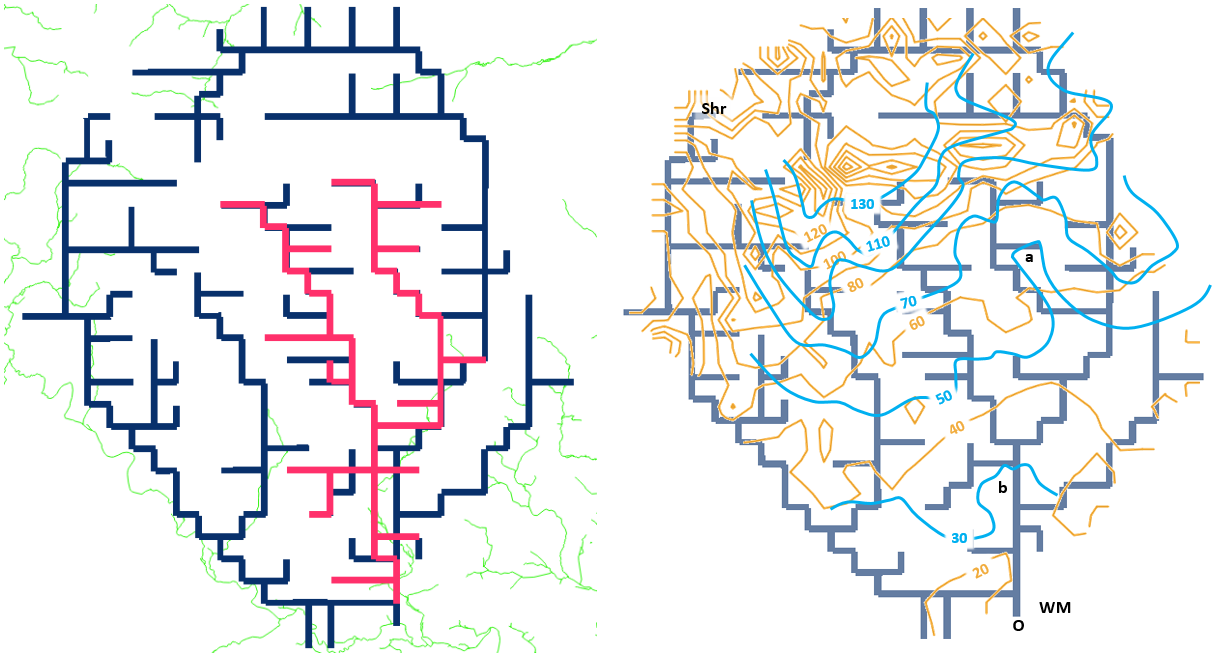

(a) The river system as modelled by SHETRAN. The larger simulations that use the groundwater catchment is in dark blue, the original simulations that use the surface water catchment are overlaid in red.

(b) Recorded (blue) and simulated (brown) groundwater contours showing the depth the groundwater level in the aquifer. Observed levels are taken from Institute of Geological Sciences & Wessex Water Authority (1979).

Figure 15.1: Structure and groundwater contours of the developed Allen catchment. **O** indicates the locations of the river outflow from the catchment; **WM** indicates the location of Wimborne Minster.

of the simulation. The observed groundwater contours show the groundwater levels dipping south east, towards the sea, generally following the dip of the Chalk aquifer. At points **a** and **b** on the map the contours bow to the north as they are transacted by the River Allen. This also happens to a lesser degree for smaller streams around the catchment. The curved contours show that at both **a** and **b** the Allen is a *gaining* river, gaining water from the subsurface. This is not captured in the SHETRAN simulations, or at least not to the same degree, as the simulated contours run largely parallel to the regional groundwater profile. This may indicate that the model does not capture the connection between the groundwater and the river system at these points. This may be due to the groundwater levels being too low to affect the streams, something that may improve with calibration following the initial automated set up.

A recent MSc project at Newcastle University by Bence (2019) constructed a SHETRAN model for the Allen using detailed 3D geology. This was manually constructed from 189 borehole records using the BGS Groundhog software and then converted into a SHETRAN model using a python script. This used the surface water catchment boundary used in original setups here. The model was then calibrated and validated against groundwater and flow data to produce a mean PCC and RMSE of 0.71 and 14.70 m and an NSE of around 0.74.

The addition of the detailed geology did not simulate groundwater levels as well as the simple, extended automated setup discussed here, but it did greatly improve the simulation of river flows. The model by Bence (2019) outperformed all of the initial automated setups that used the surface water catchment. This demonstrates the potential performance benefits of integrating the 3D geology data into the automated setup.

Further testing was done in which the model of Bence (2019) was combined within the extended Allen model developed here, essentially wrapping the detailed geology of Bence (2019)

with a simple, 40 m deep subsurface. This used parameters largely consistent with those of this work. The model produced muted groundwater levels that did not fluctuate to the same amplitude as found with the extended, simple model used here. RMSE and PCCs were also not as good (Tab. 14.3), however the NSE was increased to -1.05. This indicates that geological structure is important across the whole model domain, not just the regions containing calibration data.

15.4 Boundary Conditions

At many of the borehole sites used in the case study simulations, the groundwater levels are found to be too high, staying within the top one or two metres of the subsurface. One of the main causes of this is the lack of boundary conditions in the automated setups. With no boundary conditions at the edges or base of the models, water is only able to leave the catchments via the single river outlets. In the Developed Allen example above, the Chalk at the southern edge of the domain fills until it is in hydraulic connection with the river. This is likely to be the cause of the very high water levels shown at High Hall, the borehole nearest the outlet (Fig. 14.8). As SHETRAN-GB is being tested to see whether it is appropriate for use with the multisource modelling system, this does pose a limitation in that it is over predicting emergence at the ground surface.

Additional simulations were conducted using the initial river Allen models (1000 m grid size with the surface water catchment) to demonstrate the effects of including subsurface boundary conditions. This subsurface boundary condition was estimated using a simple water balance. Monthly estimates of the catchment's water loss via subsurface flows loss were calculated by deducting catchment water losses via river flows from water input via effective rainfall. The *base flow boundary* allowed water to flow from the base of permeable columns out of the model at the specified monthly rate. Initial simulation groundwater levels were also decreased to 10 m below the surface.

The results of these simulations can be seen in Figure 15.2. Dotted lines show decreased groundwater levels for the Standard and APM simulations that are no longer constrained by a fully saturated subsurface. While this improves the Standard simulations by allowing the groundwater levels to drop away from the surface, deeper cells were required in many locations to facilitate its use with the APM parameters. Combining subsurface boundary conditions with the detailed BGS geology dataset did not show improvements due to its misrepresentation of the subsurface.

The process of generating basic subsurface boundary conditions via construction of a water balance is simple and could easily be automated for gauged catchments within the SHETRAN-GB system. Spatially varying the base flow conditions according to the permeability of the columns, as was done here, could also be easily added to the system. Performance may be further increased through the introduction of lateral flow boundaries (allowing water to be added or removed from the model edge) or by increasing simulation spinup times to increase the realism of initial groundwater levels. One limitation with the basic water balance approach taken here is that no groundwater is added to the system from potential groundwater inflows. This could be achieved, at least to some degree, by modelling the extended groundwater catchment and therefore including subsurface inputs directly from their point of recharge.

15.5 Groundwater Level Data

If the models set up here were to be developed further, one limitation would be the availability of high-resolution groundwater level data. Of the 33 boreholes used in this study, only two contain data at a resolution higher than monthly. While it has been possible to show that

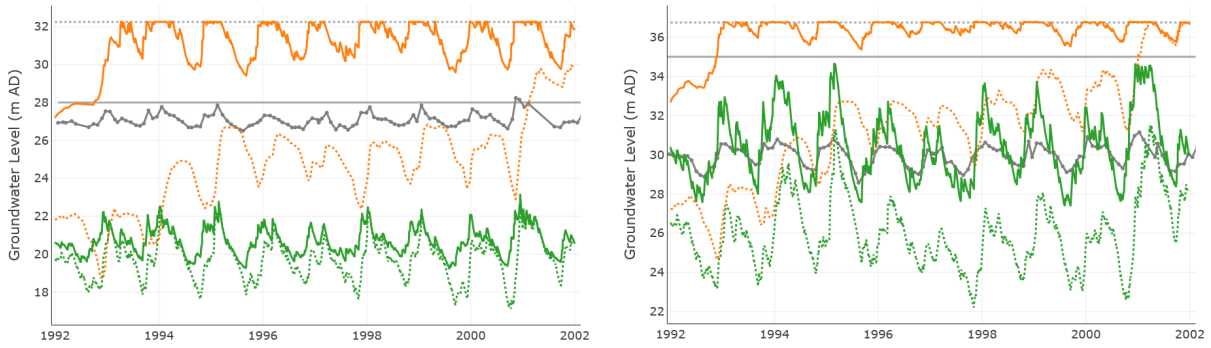

(a) Barnsley Farm No. 3 (b) West Acre

Figure 15.2: A comparison of groundwater levels for the Allen catchment with and without subsurface boundary conditions. Grey solid lines show the observed groundwater level at the two boreholes and the land surface elevation; the grey dashed line shows the SHETRAN cell elevation; orange and green lines show levels from the Standard and APM simulations respectively, with dotted lines indicating simulations with base flow boundary conditions. All four simulations initiated with groundwater levels set at 10 m below the surface.

SHETRAN is able to capture the monthly flow patterns, in the developed Allen catchment at least, it is not possible to investigate the sub-monthly patterns, i.e. to determine whether the flashy groundwater levels simulated are realistic or overly responsive, something very important if looking at groundwater emergence with regard to the multisource modelling system. A further point of note is that the automated simulations do at times produce statistically high results where they are not deserved, as, on closer inspection, they perform poorly. Many of these instances are due to the low resolution of the available groundwater data. As such, it is appropriate to ensure that any future testing does not rely solely on statistical methods, or that there is an awareness of the limitations of data resolution.

It should also be noted that the range of values found for parametrizing the Chalk in the Allen catchment were very large. As such, it is not plausible to attribute specific values to each of the geological units across the catchment, let alone on a national scale. Instead, it would be more appropriate to give more general values, perhaps at a regional level, that provide a stable modelling platform for subsequent manual calibration. Improved parameterization of aquifers in the future may allow for this and maximise the potential usefulness of physically based models for capturing hydrological processes.

There are many instances in this study of SHETRAN simulating piezometric heads within mudstones and layers that are largely impermeable and which have minimal subsurface flows. This highlights one limitation of assessing and calibrating the groundwater component of SHETRAN-GB using automated methods: that the groundwater level simulated using SHETRAN may not be directly comparable to observation datasets. This is because boreholes sample different strata depending on their intended use. Most are likely to sample aquifers and may be screened above or below the aquifer so that water enters the borehole only from the desired strata. If the aquifer is confined, this will mean that the groundwater level measured via the borehole will report the piezometric head rather than the depth to groundwater, as is calculated by SHETRAN. In the catchments here none of the aquifers are confined, but this could be a problem in other catchments around the country. Details on borehole construction and screens can be found online using the BGS's GeoIndex site, however such data is not available for all boreholes, and compiling this data for a national assessment would be too time consuming for this study.

Finally, the majority of data in the literature regarding parameterizing the Chalk discuss transmissivity (m^2/day) rather than saturated conductivity (m/day). For models such as

SHETRAN this poses an issue, as the majority of transmissivity values are not given alongside the necessary aquifer thickness to allow their conversion to saturated conductivity. While it is possible to estimate likely thicknesses, or a range of potential thicknesses, this introduces further uncertainty in parameter estimation.

15.6 Conclusion

Accurately simulating groundwater levels is typically more complex than simulating river flows and, while it is possible to simulate flows reasonably well with the uncalibrated national model, it is not possible to accurately simulate groundwater levels using the existing system. The four automated national setups tested in this chapter all show promise, however, and provide a strong and advanced point for manual calibration. Offering more promise are the simulations of the Allen catchment that use an extended catchment of similar extent to the groundwater catchment. This greatly improved the simulation results and showed marked improvements when the parameters, namely saturated conductivity and specific yield, were brought in line with those found in the literature. Furthermore, the simple addition of basic subsurface flow boundaries was able to decrease groundwater levels in the overly saturated cells - this allowed for increased fluctuation in groundwater level and greatly decreased instances of falsely simulated groundwater emergence.

The ability to set up hydrological models with detailed 3D subsurface geology in a matter of minutes offers a fantastic resource and greatly simplifies the process of developing the model. However, setups using this 3D data were unable to outperform the most basic models. This is likely to be due to the necessity for groundwater catchments, as described above, but is also due to errors in the model structure - such as were found in the Allen catchment, where much of the outcropping Chalk aquifer was erroneously confined by a thick mudstone and in the Foston Beck catchment where a band of impermeable material wrongly cut across the centre of the catchment. It was unclear whether these errors were introduced directly from the 3D geology data or from the setup method as the latter capture the BGS data well when interrogated. If the 3D geology layer is to be used with SHETRAN-GB then more testing is needed to ensure its appropriateness for the task of modelling. The work of Bence (2019) demonstrates the potential of detailed subsurface geology for improving performance when simulating groundwater and surface water flows.

Using properties from the aquifer properties manual (Allen et al., 1997) for highly productive aquifers improved the majority of the simulations. Further modelling in the Allen showed that even higher saturated conductivities improved model performance. These increased values are still in line with estimates from the literature and demonstrate the wide range of values that can be gleaned from existing studies due to both the natural range in geological properties and also the lack, in some instances, of information allowing the widely reported transmissivity values to be converted to the less common, but necessary, saturated conductivity values. Although many localities will have existing hydrogeological parameters available in the literature, collating these at a scale appropriate for a national scale model, such as SHETRAN-GB, would be a large task. Furthermore, this increased range of values may cause instabilities in the model. This study finds that greater performance yields could be gained from developing other factors, such as accessibility to groundwater data and the development of a database of groundwater catchments from which good, stable models can be automatically set up and then manually calibrated.

Increasing the spatial resolution of the models from 1000 m to 500 m or 100 m was found to be an effective method for increasing the performance of the flow simulation. In terms of groundwater however, increasing the spatial resolution from 1000 m to 500 m had mixed success, both increasing and decreasing RMSE for different borehole locations. Increasing resolution to 100 m was, however, found to decrease the majority of RMSE, especially in areas with steep topography. Increasing resolution was not found improve correlation with observed groundwater levels however, and in some cases (such as at Foston Beck and Sydling Water) increasing the

resolution decreased correlations with groundwater levels. The reason for this is unknown, however, as the resolution testing was done using the Standard simulations (single subsurface unit, 20 m thick) it may be that these simulations were running at a resolution for which they were under parametrized.

One other take away from this chapter is the difficulty of obtaining the groundwater level data used in quantifying model performance. Little information was available on what data exists and getting hold of that data was impossible at a large scale. Furthermore, the data that was provided requires further meta data if it is to be used to its full advantage. Such information includes the elevation of the borehole, its depth and the depth of the screen so that it can be determined which hydrological unit is being measured. It was assumed here that the boreholes are all open along their whole length however it may be that they sample a confined aquifer with a piezometric head in the non-permeable layer above it. This would falsely imply that the non-permeable layer has a fluctuating groundwater level. The statistics performed in this study are done on a pairwise comparison method. These pairs can at times be far apart as much of the data was of low resolution. It would therefore be ideal if resolution of such datasets are improved or standardised.

The work detailed in this chapter shows that while SHETRAN-GB is able to provide rapid automated set ups of surface water catchments it is not yet able to realistically simulate subsurface processes in its uncalibrated form. Further modelling work in the Allen catchment showed that adding subsurface flow boundary conditions and increasing the catchment size to reflect that of the subsurface, groundwater catchment dramatically increased performance and the sensitivity of the model to parameter improvements. As such, if developed to include the option for automatic generation of groundwater catchments, SHETRAN-GB offers a useful tool in the development of a multisource modelling system. Further improvements in national saturated conductivity data and improved and extended coverage of subsurface geology could enable a modelling system for Great Britain that is simple to set up and use and requires minimal calibration. It provides a strong modelling platform from which hydrological models can be set up in a matter of minutes and then calibrated ready for the modelling system developed in Chapter V.

V

Creating a Multisource Modelling System

16. Background

The aim of this chapter is to develop a modelling system capable of simulating multisource flood events by capturing both surface and subsurface hydrological processes. This chapter describes the process and practicalities of developing the modelling system and explores its associated sensitivities.

Some hydrological models are already capable of describing both surface and subsurface processes. SHETRAN has been chosen as the hydrological model for providing catchment conditions for the modelling system as it offers the potential for rapid, automated set up (using the SHETRAN-GB system) and has been proved capable of providing accurate catchment scale simulations, including groundwater flows. Chapter IV found that SHETRAN-GB may provide a useful tool for the modelling system in the future, but is not appropriate for use in its current form. As such, an existing, fully calibrated SHETRAN model is used in this chapter.

Any modelling system designed to capture multisource events must therefore be able to operate at high spatial resolutions so as to capture high intensity storms in both urban and rural environments. This is because urban surface water floods often have complex overland flow processes - flowing along different drainage pathways and interacting with buildings, obstructions and drainage systems (Mignot et al., 2019). As such, precise surface water flooding assessments require horizontal resolution of a model's input DEM to be high enough to capture these high-resolution topographic details as well as gullies and passageways. Failure to represent building layouts and micro-topography while modelling surface water may cause the over or under estimation of flood depths (Fewtrell et al., 2008). Furthermore, research has shown that increasing the horizontal resolution of DEMs from 1 m to 10 cm can notably alter the flow depths and velocities and that capturing micro-topography (e.g. curbs) and micro-channels (e.g. those caused by road cambers) can control hydraulic connectivity across a model domain and thus affect drainage speeds (Ozdemir et al., 2013; de Almeida et al., 2018). Low resolution DEMs can degrade finer-scale terrain features by averaging elevations across the cell area and further affect flow conveyance and available storages, the former of which can open or close different flow pathways (de Almeida et al., 2018). Accurate topography is especially important in slow moving flows, as may be experienced with groundwater and groundwater induced flooding.

While SHETRAN is an appropriate tool for simulating catchment scale processes in the multisource modelling system, it was designed for use in rural environments and cannot provide the level of precision necessary for flood risk assessments in urban environments. Such environments require accurate estimations of flood depths, flow speeds and flow paths in order to make good decisions regarding flood management and mitigation. Furthermore, hydrological models are typically unsuited for simulating important physical processes such as backwater effects and transcritical flows, which are often present in high intensity rainfall runoff events (Xia et al., 2018). A higher resolution hydraulic model is therefore required when modelling urban areas. Hydraulic

models can operate at spatial resolutions of under a metre and are able to route water through areas with complex topography, running water through gullies and between buildings. This enables more precise assessments of flood hazard, indicating those buildings and infrastructures that may be at particular risk, or those streets likely to become unusable. As yet, the inclusion of groundwater into such models is typically unheard of, partly due to the general lack of research into groundwater flooding, but also partly because the two sources operate at two very different temporal and spatial scales. This chapter addresses this research gap by linking SHETRAN, a catchment scale, physically based hydrological model, to HiPIMS, a high-resolution, event scale hydraulic model. A recent version of HiPIMS (called cuflood[1]) was used as it includes improved shallow water equations that increase model stability when simulating very shallow water depths (Xia et al., 2017). This makes it especially appropriate for use with rainfall runoff simulations and routing of groundwater emergence. More detail of HiPIMS can be found in Section 3.1. Where appropriate, it can be beneficial to include subsurface drainage systems in within hydraulics (Guerreiro et al., 2017a), however this was seen to be beyond the scope of this work.

Both SHETRAN and HiPIMS have been shown to be capable models and are suited for use in this study:

HiPIMS: Liang and Smith (2015) tested HiPIMS against the Environment Agency's 2D hydraulic model benchmarking reports (Néelz and Pender, 2010, 2013). Simulations of a complex test case in Glasgow performed well and estimated time series of flood depths and extents were consistent with those from comparable software. More recently, HiPIMS was used to recreate flooding in the Eden catchment from Storm Desmond in 2015. In this instance, HiPIMS was applied over a 2500 m^2 catchment with a horizontal resolutions of 20 m (Xia et al., 2018) and 5 m (Xia et al., 2019) and again performed well. Simulated inundation extents and gauged water levels compared well to field observations without the need for intensive calibration.

SHETRAN: Calibrated SHETRAN models have already been successfully used to model both groundwater (e.g. Adams and Parkin, 2002; Parkin et al., 2007) and discharge (Op de Hipt et al., 2017, Tab. 2). The specific SHETRAN model used in this case study, as well as in Chapters IV & VI has been manually calibrated prior to this work and as such performs well. A full breakdown of groundwater level statistics can be found in Tables 28.3 & 28.4, however these have an average Pearson's correlation coefficient of 0.81 and an average RMSE of 2.79 m. Statistics for the groundwater level in the borehole on the edge of Kilham village were 0.78 and 2.62 m. Hourly discharge from the model outlet yields an NSE of 0.64 when compared to the Foston Beck flow gauge, approximately five miles downstream.

For the multisource modelling system, SHETRAN will simulate catchment hydrology over long time-scales and at periods of interest (such as known or simulated floods) simulated groundwater emergence, fluvial flows and rainfall will be exported from SHETRAN and input into HiPIMS. HiPIMS will then route water across the surface at a much higher resolution for days or weeks until the flood event subsides. A workflow of this can be seen in Figure 16.1 and a diagram of model processes can be seen in Figure 16.2. This approach enables a comprehensive, physically based assessment of the flood hazard at that time. While these two models have been selected for the modelling system, this is for developing the methodology and any equivalent models could be used in future work. Information on the models and their performance can be found in the Chapter II.

One of the challenges of this task is resolving the differences in spatial resolution between the hydrological model (SHETRAN) and the hydraulic model (HiPIMS). Both of the models are spatially distributed, splitting the catchment into a series of regularly sized cells. As the

[1]cuflood was provided by Xilin Xia, Newcastle University

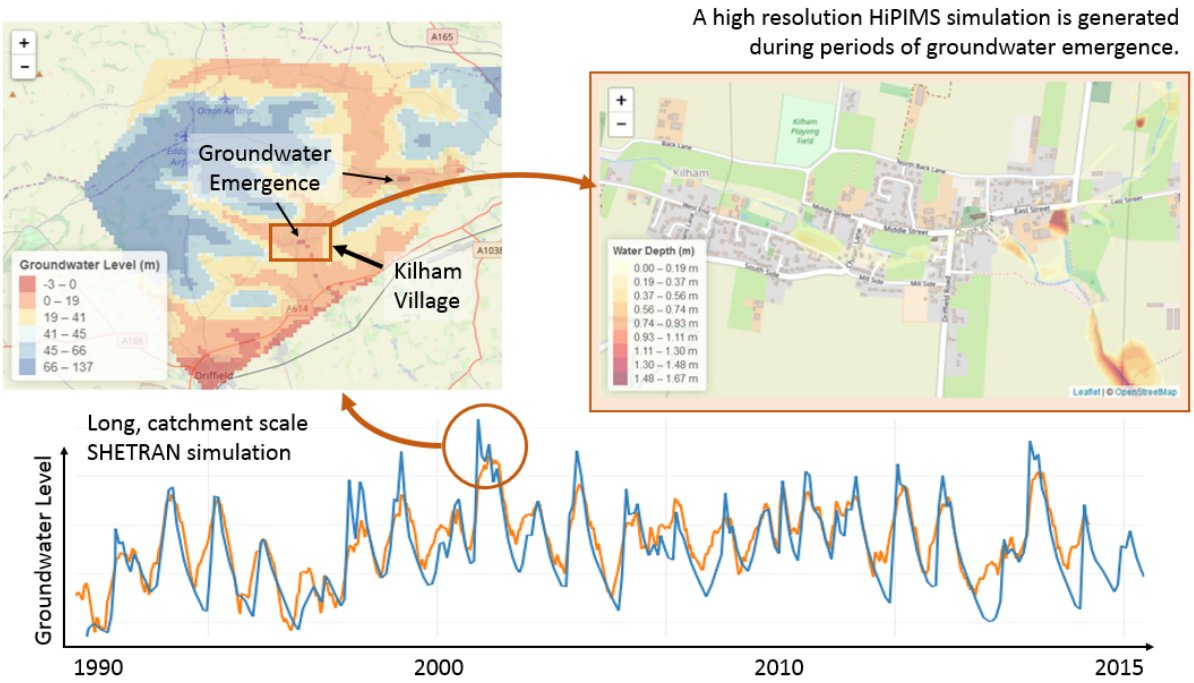

Figure 16.1: This figure shows the concept of the modelling system developed in this chapter. A long hydrological simulation is sampled for peak events that are then used to generate a hydraulic model for high-resolution routing of rainfall and groundwater emergence. ©OpenStreetMap contributors.

hydrological model represents an entire catchment its cells are relatively large in comparison to the hydraulic model, which, representing a much smaller area of interest, has much smaller cells. In this case, SHETRAN's cells are 200 metres across, whereas HiPIMS has cells only 2 metres across. This means that a single 200×200 metre groundwater emergence value from SHETRAN would cover 10 000 2×2 metre HiPIMS cells. Those 10 000 cells have a range of heights, land covers, both permeable and impermeable, and variably permeable underlying geology. As such, the distribution of any emergent groundwater is unlikely to be uniformly distributed over this area. Emergence would instead be likely to occur at lower elevations, where the piezometric surface breaches the surface, preferentially seeping upwards through permeable superficial deposits and surfaces. All of these factors add complexity and uncertainty to the coupling process.

Similar problems also exist with other processes, such as overland flow and channel flow. The channels in SHETRAN are a fixed width for the catchment and are potentially larger than in reality and than in the hydraulic model, which can be as low as 2 m wide (the size of one grid cell). Furthermore, as SHETRAN routes rivers between its regularly spaced grid cells the river in the hydrological model may be several 10's or 100's of metres from its actual location or from where it is represented in the hydraulic model. This issue is addressed in Section 17.1.2.

The coarse, blocky emergence patterns of SHETRAN, caused by the lower resolution grid size (relative to HiPIMS) are unrealistic when moving to a higher resolution investigation. This is because groundwater emergence is likely to vary spatially over much smaller distances than the 200 m SHETRAN cells. As such, it may be appropriate or necessary to redistribute the SHETRAN outputs into the HiPIMS domain to account for variation in topography. This chapter will therefore address research question 3:

> *When creating the multisource modelling system, what is an appropriate method for accounting for the different spatial resolutions of the hydrological and hydraulic models?*

The village of Kilham in East Yorkshire will be used as a case study for the development of the

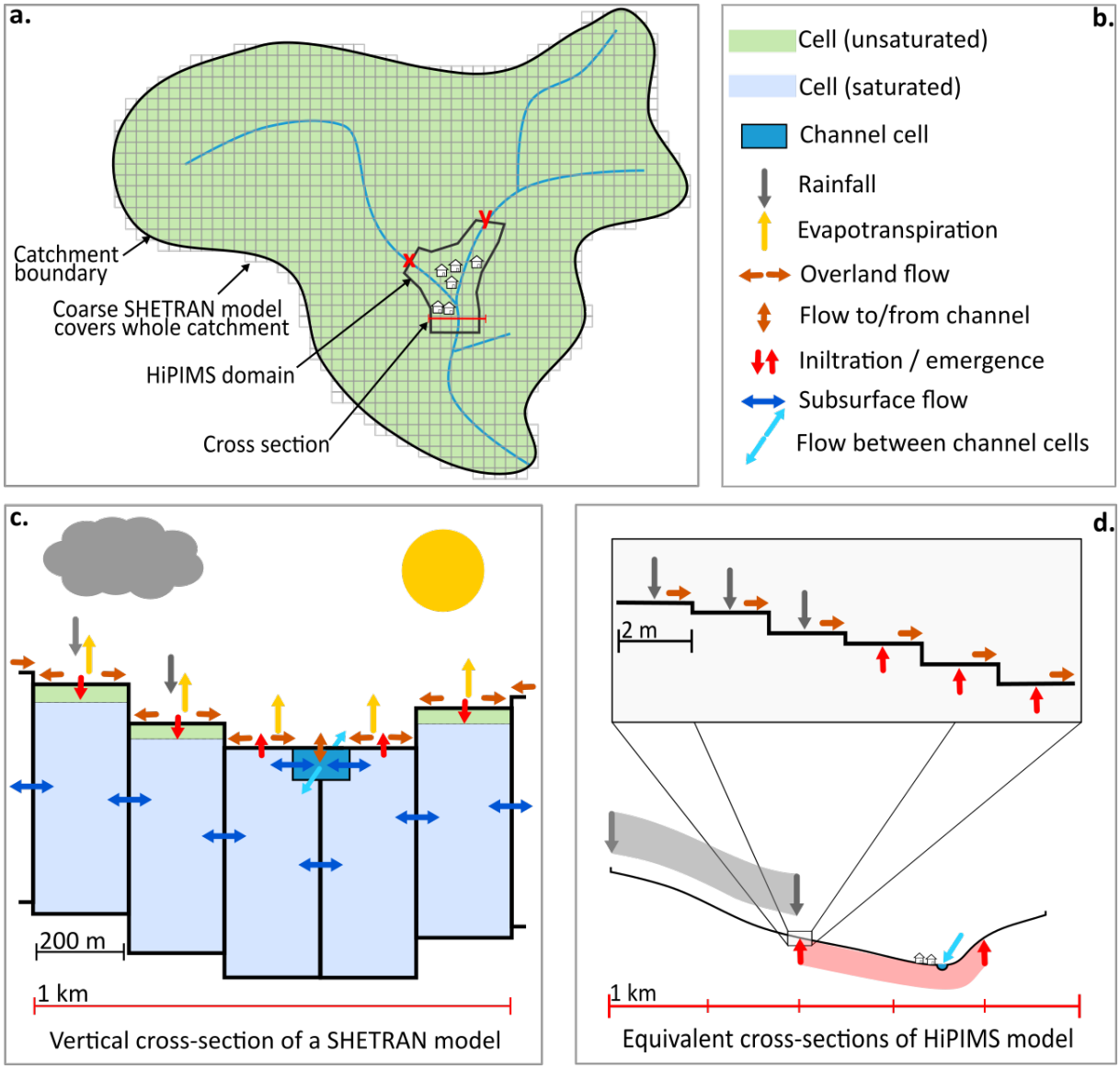

Figure 16.2: Overview of model processes: **a.** The hydrological model (SHETRAN) simulates catchment scale processes; the hydraulic model (HiPIMS) simulates surface processes for the area where multisource flood risk is being assessed (i.e. a town or village). **b.** A key for subsequent diagrams. **c.** A cross section though the SHETRAN model showing inputs and model processes. For each time step, rainfall is input into the model and evapotranspiration is used to calculate effective rainfall. This is then either routed across the surface as overland flow or infiltrated into the subsurface. Below the surface, water flows between cells can re-emerge at the surface if the groundwater level is calculated to be higher than the cell elevation. River channels allow flow along the river (in the 3^{rd} dimension, i.e. into and out of the page) and allow for flow in and out of the subsurface (assuming hydraulic connection). Overland flow can also flow into/out of the channel cells according to water level. **d.** A cross section of the HiPIMS model over the same area as **c.**. HiPIMS uses the same rainfall input as the SHETRAN and also takes the emergence calculated by SHETRAN as a further input. Points **x.** and **y.** use river flows calculated by SHETRAN as further inputs. HiPIMS deals only with surface processes, routing rainfall, river flow and rainfall across a high resolution impermeable surface. Unlike in SHETRAN, river flows are treated as the same way as overland flows, with no specific channel cells. However, cells where the channel runs were burned into the DEM (i.e. lowered) to ensure than the channel was represented topographically.

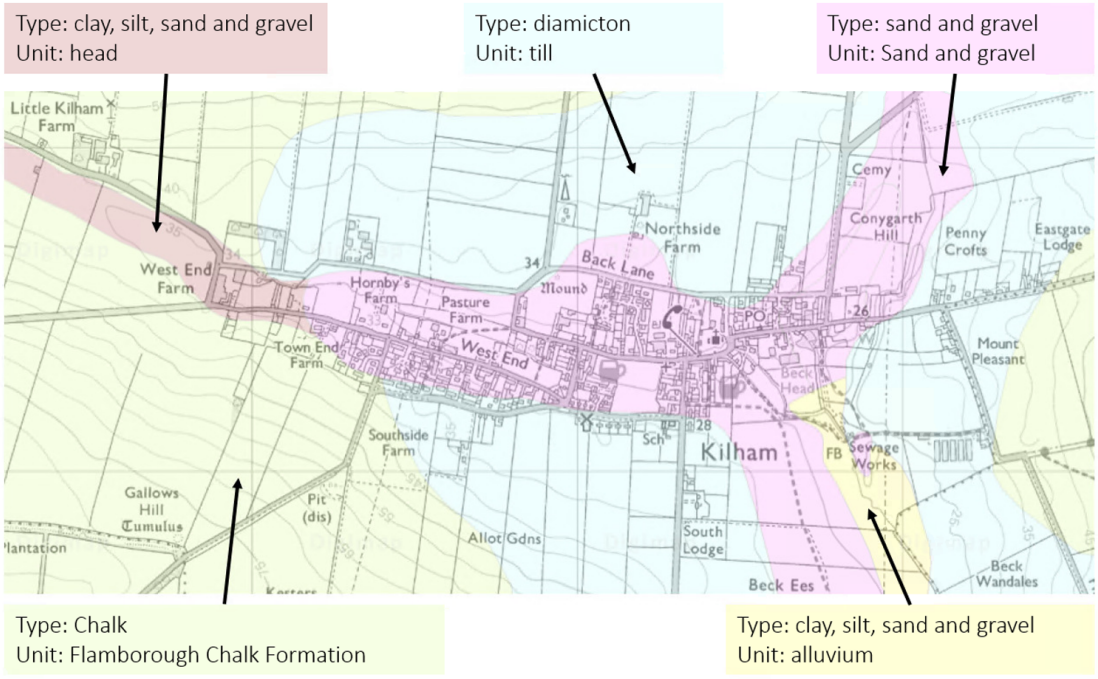

Figure 16.3: The village of Kilham sits on top of permeable superficial deposits of sand and gravels, underlaid by less permeable superficial till and alluvium deposits. The whole village is then underlain by a permeable Chalk bedrock. BGS 1:50 000 Bedrock and Superficial Geology (British Geological Survey, 2019a).

modelling system. Kilham is a small village that sits within the Chalk and clay catchment of Foston Beck (Fig. 16.3) and has evidence of multisource flooding (see Section 13.1.3). Furthermore, past hydrological simulations with SHETRAN have shown double peak hydrographs due to split surface and subsurface pathways (S. Birkinshaw, Newcastle University, Pers. Com. 25^{th} September 2019), an indicator of multisource flood potential. The Kilham catchment has had significant work invested in it already at Newcastle University and so has a comprehensive integrated groundwater-surface water model that provides an ideal basis for the work in this study. HiPIMS will be tested in instances where SHETRAN simulates flooding or groundwater emergence in the village.

The SHETRAN model of the catchment is discussed in Chapter IV (the calibrated Foston Beck catchment) and catchment details can be found throughout. The model uses daily meteorological inputs and has detailed geology with calibrated parameters.

Kilham has suffered multiple flood events, the most recent of which occurred in the winter of 2012/13 (East Riding of Yorkshire Council, 2013). This flooding was due to a combination of high groundwater levels and winter rainfall. Flooding occurred mainly on the east end of West End, across Chapel Lane, Middle Street (between High Farm and Chantry Meadows) and also on the corner of Church Street (where it meets Bakehouse Lane) and East Street, just east of the post office. This can be seen in Figure 16.4.

16.1 Double Counting of Inputs

A further complication to the joint modelling system is the issue of *double counting*. Double counting refers to the act of inputting the same source into the hydraulic model multiple times. The purpose of joining the two models is to take antecedent conditions from the hydrological

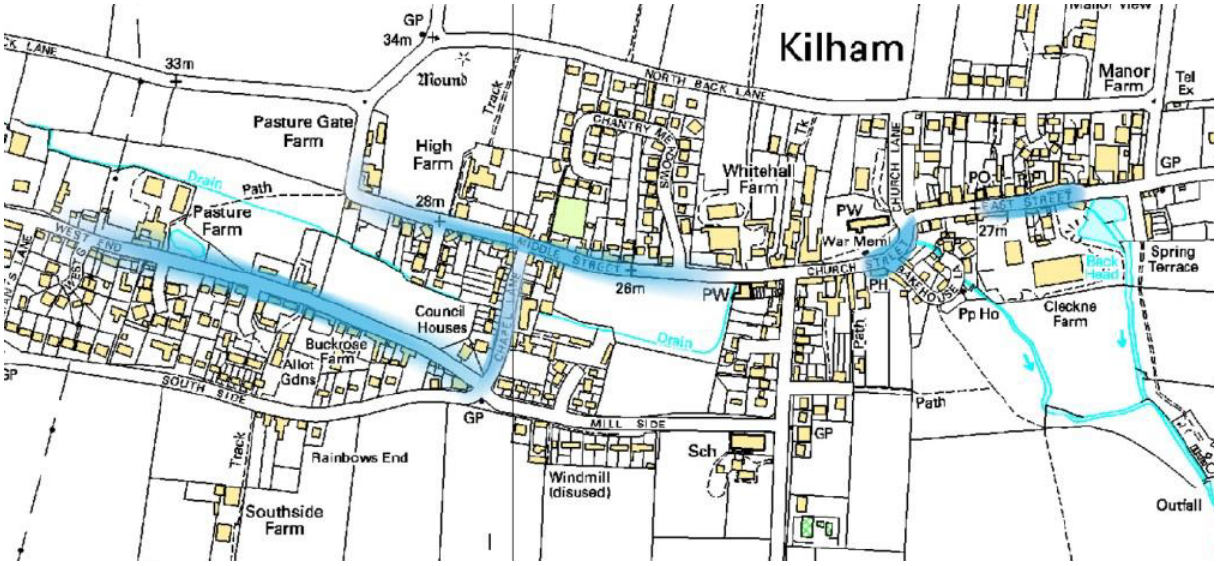

Figure 16.4: Taken from East Riding of Yorkshire Council (2013). Blue shaded areas represent areas flooded during the 2012-2013 winter flooding.

model and add them to the hydraulic model, which will then route rainfall at a high resolution. In this instance, the groundwater emergence rate (vertical flow speed) exported from SHETRAN and added to HiPIMS already takes into account rainfall. Thus, if rainfall is then added separately to HiPIMS it is erroneously accounted for both in the groundwater flows and the direct rainfall.

In this instance it was believed that the vertical groundwater flows and the rainfall operate on different timescales and so the double counting issue would not be significant. This hypothesis was tested using the SHETRAN model used in this chapter - the model was run and stream flows were extracted for Kilham and peak flow events identified. For each of these peak flow events the original model inputs were altered to remove all rainfall over the village from one day before to seven days after the event. This volume of rainfall was then added back into the simulation from 8-15 days following the peak. The total vertical flow over the event was then calculated for each of the 16 days and compared to the original simulation. The removal of rainfall over the village around the peak decreased the vertical groundwater flows on the order of 10^{-3} mm/hr. As this is a minor difference the double counting of rainfall in vertical groundwater flow was ignored, however, in future modelling work the effect of double counting should be checked to ensure that errors do not arise. In instances where this error proves to be significant, the following approach is suggested:

Firstly, a hydrological simulation should be run and used to identify periods that will undergo further simulation in the hydraulic model, such as peak flows or known flood events.

Secondly, the hydrological model could be rerun over the desired time periods but with rainfall inputs removed. The vertical groundwater flows taken from these reruns would no longer double count the rainfall, which can then be included directly into the hydraulic model. If higher resolution vertical groundwater flow inputs are desired then the hydrological model can be rerun multiple times with the removal of rainfall delayed by 24 hours between each step, thus progressively generating a vertical flow time series. This could also be done for the other processes, such as river flow or overland flow. Accounting for double counting in this way clearly adds additional computational resources. This method was tested and achieved relatively simply through the use of a version of SHETRAN that is able to *hotstart* from monthly points throughout the simulation. This reduced the simulated length of the reruns to only 1 or two months, a relatively small and simple to automate process.

17. Methodology

This methodology describes how the models, and their associated hydrological processes, are coupled and then outlines the simulations used to assess the system's sensitivity to different methods for coupling groundwater processes.

17.1 Model Coupling

A simple conceptual diagram of the coupling can be seen in Figure 17.1.

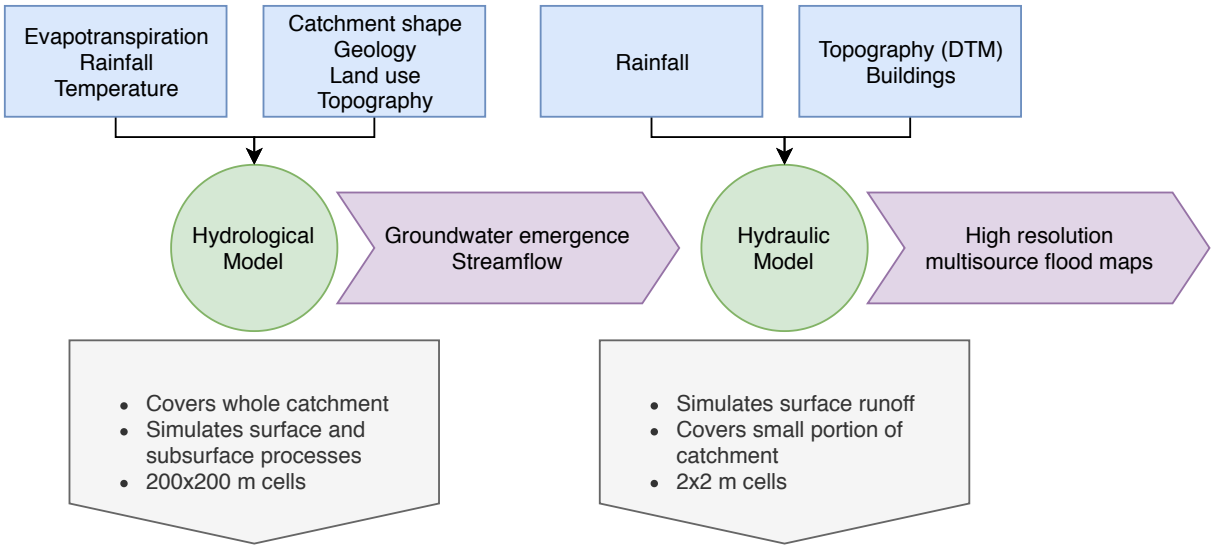

Figure 17.1: A conceptual overview of the multisource modelling system.

17.1.1 Basic HiPIMS Set Up

The HiPIMS model covered the village of Kilham using a rectangular domain of around 2.8 km × 1.2 km, with around 798 600 active cells. Each of these cells was attributed a Manning's number of 0.03 to represent the surface roughness. All simulations had an initial time step of 0.001 second and a CFL number of 0.5. All edge boundaries were open to allow for flow out of the domain.

HiPIMS takes inputs in two forms: point data and inflow data. Point data can be mapped to cells within the domain, with each cell having an associated time series of inputs. Inflow data is mapped to the domain edges and again has associated time series. Point data was used for inputting groundwater emergence and rainfall into the model and inflow data was used to input streamflows. More detail on these inputs can be found in the following sections.

As a high-resolution hydraulic model, HiPIMS requires an accurate digital elevation model (DEM) and so the Ordnance Survey's 5 m OS Terrain 5 digital terrain model (DTM) was used. Although Environment Agency LiDAR data would have provided the highest resolution elevation data, it was unavailable for the Kilham area. 2 m photogrammetry digital surface model (DSM) (downloaded from `www.blueskymapshop.com`) was also tested but this was found to poorly represent buildings. The DTM was given the following three edits:

1. The DTM was resampled from a horizontal resolution of 5 m to 2 m. High resolution, 2 m grid cells were important as these allowed water to be routed between buildings and for streams and buildings to be represented at an appropriate resolution (in accordance with advice in Käser et al., 2014).
2. The stream channels were burned into the DTM as these were not captured in the original data. The channels were given continuous downstream slopes (in accordance with advice in Käser et al., 2014), widths of 2 m (i.e. one HiPIMS grid cell) and depths of 0.4 m as this was estimated to give a similar cross-sectional area to the actual channel. As Lowthorpe Beck (Sec. 17.1.2) flows through the village it passes through culverts beneath Chapel Lane and Driffield Road. These were not captured by the model.
3. Buildings were added to the finer resolution DTM with a standard height of 3 m. Building data was taken from the OS MasterMap database.

17.1.2 Coupling River Flow Processes

When linking the hydrological processes between the two models it is important to consider river flows and, if these are present, to input them correctly from the hydrological model to the hydraulic model. One thing to bear in mind is that the periods of interest, which will be exported from the hydrological model, may be times of flood and the river may have overspilled its banks. This could mean that some of the water is lost if only considering the flow within the channel. The channel cells in the hydrological simulation were enlarged, so as to avoid any issues of overspilling. If there is a risk that flows may have over-topped the channel then overland flows around the channel input should also be exported into the hydraulic model.

Each SHETRAN river channel cell has four boundaries, one at each edge. Each of these boundaries has an associated flow. When coupling the models, the downstream flow from SHETRAN boundary that was adjacent to the edge of the HiPIMS domain was used as the input for HiPIMS. If the SHETRAN grid was cut by the HiPIMS domain, the flows were weighted according to the ratio of water flowing in and out of the SHETRAN cell and the proportion of the cell that is within the HiPIMS domain. This is explained in Figure 17.2.

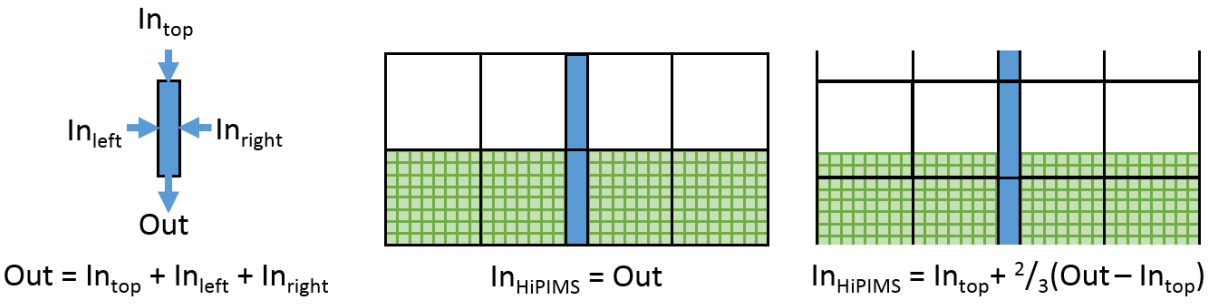

Figure 17.2: Where the edge of the hydraulic domain matches the edge of a hydrological river cell, the output from that cell at the boundary was taken. Where there is no approximate match, the flow from the cell was estimated according to the proportion of it within the hydraulic domain. Black squares represent the hydrological cells and green squares represent the hydraulic cells; blue represents the hydrological river cells.

SHETRAN writes simulation details and results to a H5 file containing all outputs along with a map of cell indexes. An R script was written that extracts cell indexes and writes them to an ASSCI file that is viewable in a GIS. The resultant file can be seen showing the location of the rivers within the hydrological model in Figure 17.4. This script allowed the SHETRAN channel cells to be easily identified and for appropriate cells to be chosen to provide flow inputs for the hydraulic domain. Furthermore, by layering this GIS output onto the hydraulic model's DEM it was simple to select appropriate cells in the hydraulic model for the desired channel input.

A subsequent script was written that extracted simulated flows from the selected SHETRAN channel cells and reformatted them into the structure desired by HiPIMS. This involved generating a text file containing a time series of flows for the desired period, naming this file with an index and then mapping that index onto the HiPIMS domain mask at the specified coordinates. This can be done for as many streams as required. All flows must be input at the edges of the HiPIMS domain. Any hydrological channels that initiate within the HiPIMS domain (e.g. springs) need to be input at point source inputs, which have a different file format. In HiPIMS, point source inputs refer to inputs that are linked via an index to a specific cell/cells within the domain. The groundwater and rainfall processes are also transferred from SHETRAN to HiPIMS as point source inputs and so, if the stream flow is also to be added as a point source, it may have to be added to a groundwater or rainfall time series that shares the same cell. A graphic describing the HiPIMS inputs can be seen in Figure 17.3.

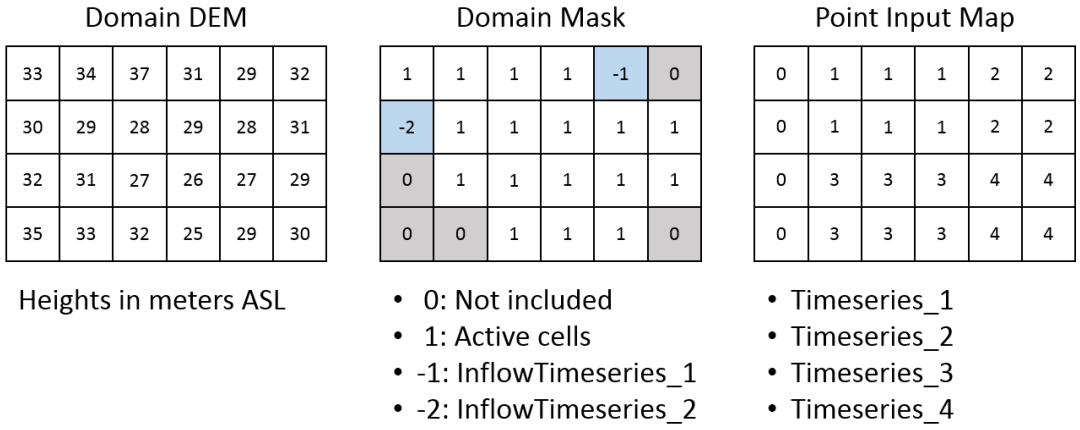

Figure 17.3: This figure shows the basic file components of a HiPIMS simulation. An ASSCI file contains a spatially referenced DEM describing the heights of each cell, some of which represent buildings. A mask file describes those cells that are to be included in the simulation and also contains the locations of any cells that will be used as inflow points - in this case there are two inflows, each with a corresponding file containing flow data. Finally a point source ASSCI file maps inputs to cells - here there are four distinct input time series, which are used to describe groundwater and rainfall inputs as well as any flows that initiate within the domain.

Each stream flow input was mapped into the hydraulic domain across 4 cells (8 metres) to ensure that model calculations remained stable. When fewer cells than this were used the model sometimes became unstable, causing extreme water depths. A set of tests were performed with different length inflow boundaries and it was found that even when inflows were spread across multiple cells they quickly rejoined the channel system and did not further affect the simulation. As such, if the model is unstable the boundary length should be increased, but not unrealistically, and not beyond its watershed.

Two streams enter the village and were inputted into HiPIMS. The larger of these, Old Gypsey, enters the east of the village from the north, meeting Lowthorpe Beck, which flows eastwards through the village from a spring in the west. Flow from Old Gypsey was input on the northern

boundary of the HiPIMS domain at the stream clearly visible in Figure 17.4. The SHETRAN simulation classifies Lowthorpe Beck as an overland channel flowing from Lancroft in the west. As such, although this actually initialize as a spring in the west of the village, Lowthorpe Beck was input at the western boundary of the hydraulic domain. The exact locations for inputting SHETRAN flows were selected to match the river's location and topographic lows rather than the locations in the SHETRAN model, which are rounded to the nearest cell boundary.

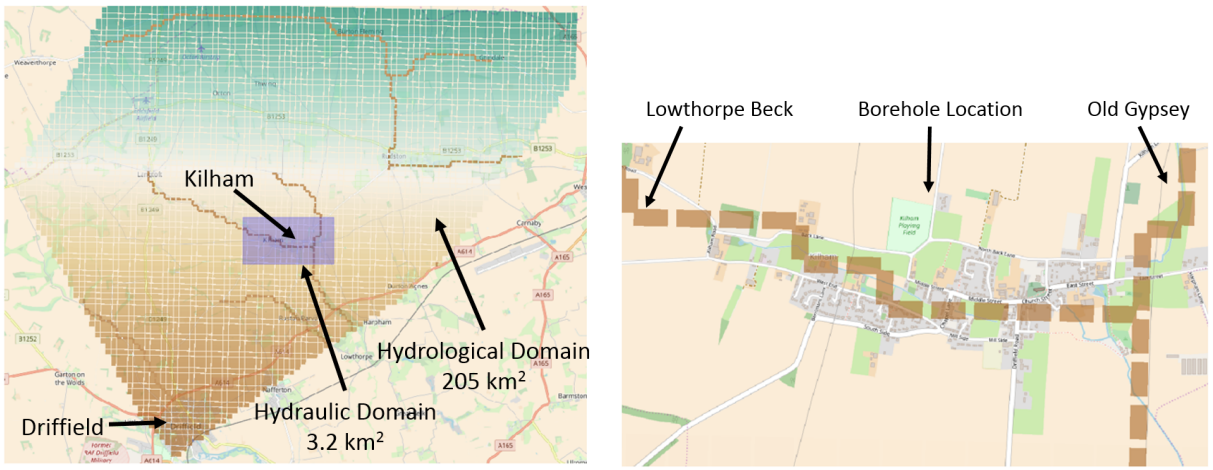

(a) The extent of the Kilham SHETRAN model.

(b) The extent of the HiPIMS model domain, with the location of SHETRAN's river cells (brown).

Figure 17.4: The hydrological and hydraulic domains of the case study models. These maps are the outputs of the river identification script used to choose appropriate cells for matching the stream flows between the two models. ©OpenStreetMap contributors.

Another mechanism for achieving the above was demonstrated in a study by Komi et al. (2017), who linked the distributed hydrological model LISFLOOD to the hydraulic inundation model LISFLOOD-FP to simulate flood extents in a catchment in Africa. Although LISFLOOD is capable of simulating groundwater and surface water processes, the groundwater processes were not used, and the paper makes no mention of calibrating against groundwater levels. However, the study only intended to link river flows, for which it gets high correlations with observations. Unlike the approach taken here, Komi et al. (2017) take the river flow at the base of the hydrological domain (which was also the base of the hydraulic domain) and use it as the inflow for the top of the hydraulic domain. This means that all of the surface and subsurface processes are accounted for by the hydrological model, but without the need to link overland flows, rainfall or groundwater emergences. While this is a simple approach, it does risk altering the distribution of flood waters as processes from the bottom of the catchment are amalgamated with those higher up the catchment. As such, it is deemed that such an approach is not applicable to this study, especially as such limitations are likely to significantly hinder the ability of the modelling system to capture groundwater induced flooding. Furthermore, Saksena et al. (2019), and references therein, state that such an approach can lead to uncertainties in the modelling.

17.1.3 Coupling Groundwater Processes

SHETRAN outputs information regarding groundwater processes for every cell in the domain. This can be done in three ways: (1) the phreatic depth of the groundwater above or below the surface, (2) the vertical flow speed of groundwater within the component layers of the subsurface and (3) the subsurface moisture content.

Vertical flow speed (ms^{-1}) was deemed to be the most appropriate for use. This provided the cleanest exchange between the two models as it did not impose controls on surface water depths -

the hydraulic modelling of which is the purpose of this coupling. There were also concerns that using phreatic depth in instances where the water table rose above the surface may have led to unrealistic surface water depth boundary conditions that may have compromised the mass balance of the simulations. The soil moisture content could not be used for coupling the models, as it does not provide information regarding water movement, however was used in Chapter IV for establishing whether cells were fully saturated or whether they had perched water tables.

An R Shiny app was written that extracted vertical groundwater flows from the SHETRAN simulation and allowed them to be visualized interactively. The app allowed fluctuations in groundwater to be mapped and viewed, and spatial and temporal fluctuations to be investigated. The app also allowed the interactive plotting of simulated and recorded groundwater levels. This aided understanding of the simulated groundwater processes within the catchment.

In order to input the groundwater into HiPIMS, an R script was written that extracted simulation data from the SHETRAN output file for given dates, converted it to the correct format desired by HiPIMS and then rewrote it as a series of time series files (one file per SHETRAN cell) and an accompanying ASCII grid mapping the time series files to the appropriate HiPIMS cells (Fig. 17.3). The script also allowed for additional rainfall inputs and domain wide inputs to be added.

As previously discussed, the hydrological and hydraulic models operate on very different spatial resolutions. To explore whether the difference in spatial resolution between the hydrological and hydraulic models pose an issue to the coupling process (research question 3, Sec. 1.3) the following experiments were conducted to explore the sensitivities associated with this issue. The above script enabled different redistributions of groundwater be generated in a fully automated way setting up models in a matter of seconds rather than hours or days when done manually. Sensitivity testing of river connections was carried out more concisely as these are less spatially distributed than groundwater emergence and therefore simpler.

17.2 Sensitivity Testing

Earlier in this chapter it is stated that groundwater emergence in the hydrological model may require redistributing when it is entered into the hydraulic model to account for preferential emergence in lower elevations. To assess the sensitivity of the hydraulic model to the spatial distribution of groundwater inputs, five different redistribution setups were designed. Each of these distributed either synthetic inputs or **re**distributing simulated groundwater emergence from a small number of cells. All distributions and redistributions are applied as they would be in the finished modelling system in Chapter VI, downscaling from single 200×200 m cells to 100×100 2×2 m cells. The different distribution/redistribution patterns are listed below. The first three setups are based on topography as this is one of the most dominant controls on emergence (Desbarats et al., 2002; Rinderer et al., 2014). The five setups are:

- **Lowest** - Inputs are distributed in the lowest 25% of the area and quadrupled to maintain mass.
- **Highest** - Inputs are distributed in the highest 25% of the area and quadrupled to maintain mass.
- **Height Weighted** - The most complex distribution, this splits the area into topographic bands and distributes inputs across these bands, with greater inputs in the lower regions than the higher regions.
- **Uniform** - Inputs are distributed equally across the area. When using groundwater emergence as an input, the input pattern is identical to that depicted by SHETRAN.
- **Random** - This was an additional distribution used only in the domain scale simulations - inputs were averaged, randomised by +/- 10% and distributed randomly across the domain.

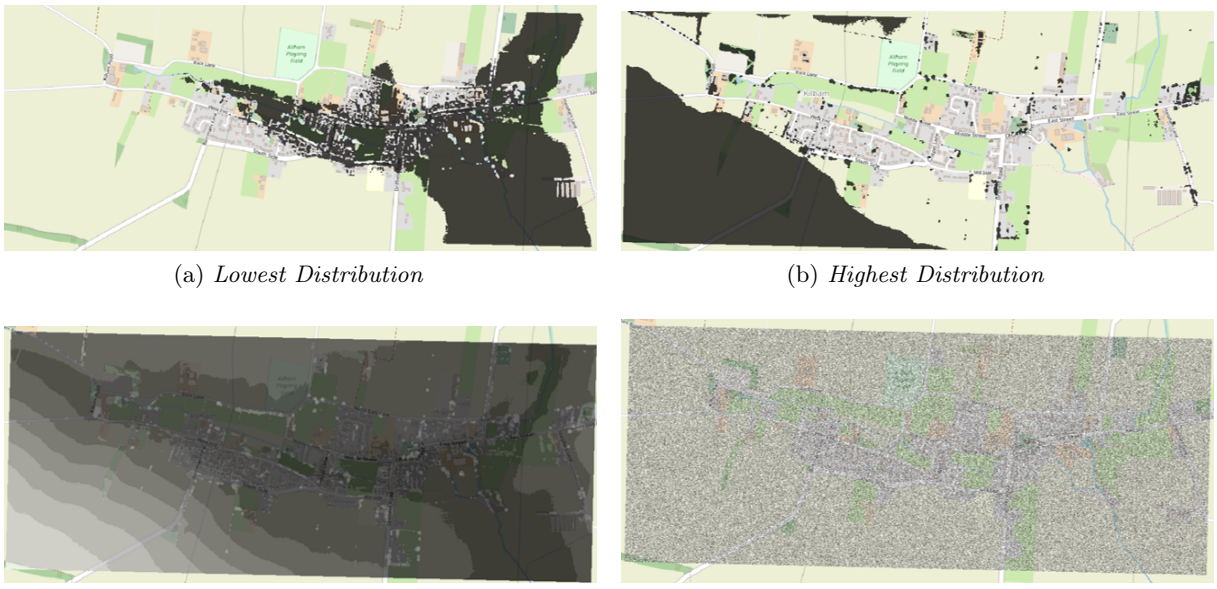

(a) *Lowest Distribution*

(b) *Highest Distribution*

(c) *Height Weighted Distribution*

(d) *Random Distribution*

Figure 17.5: The domain scale distribution patterns. Water was input into the domain at a domain averaged rate of 20 mm/hr. Buildings create height anomalies in the distributions but these are not considered significant. ©OpenStreetMap contributors.

The **Uniform** distribution pattern is the simplest and introduces the least uncertainty into the coupling as it takes inputs directly from the hydrological model. Its main limitation is that it does not account for the preferential emergence of groundwater at lower topographies. The **Lowest** distribution is a simplistic attempt at accounting for this preference, with the **Highest** distribution included for contrast to show the sensitivity of distributing emergence according to cell elevations. This latter distribution is not realistic and would not be used in the modelling system. The **Height Weighted** distribution is the most realistic, distributing emergence rates across the range of elevations rather than simply confined to the lowest of highest quartile. The **Random** distribution is again unrealistic, but included as a contrast to the **Uniform** distribution.

Three suites of simulations were run, each applying the aforementioned distributions and progressively building understanding and becoming increasingly realistic. These are described in detail in the three subsections below and in Table 17.1. The first suite of simulations distributed synthetic inputs across the whole domain, the second distributed synthetic inputs within the cells and the third, also at a cell scale, redistributed simulated groundwater emergence from a hydrological simulation. Flood extents and depths from different simulations were then compared against one another and against the historical flooding in Figure 16.4. For simplicity, these simulations did not involve any fluvial flows.

17.2.1 Domain Scale Distribution of a Synthetic Input

A synthetic input was simulated across the entire HiPIMS domain. This oversimplified scenario aimed to certify that the spatial pattern of model inputs was indeed a control on the model outputs.

Water was input into the domain at three paired intensities and durations: 40 mm/hr for 1 hr, 20 mm/hr for 2 hrs and 10 mm/hr for 4 hrs. All simulations ran for 24 hrs and had inputs at the very start. Distribution patterns for these simulations can be seen in Figure 17.5. The only pattern not shown is the *uniform* distribution as inputs are equal across the whole of the HiPIMS model.

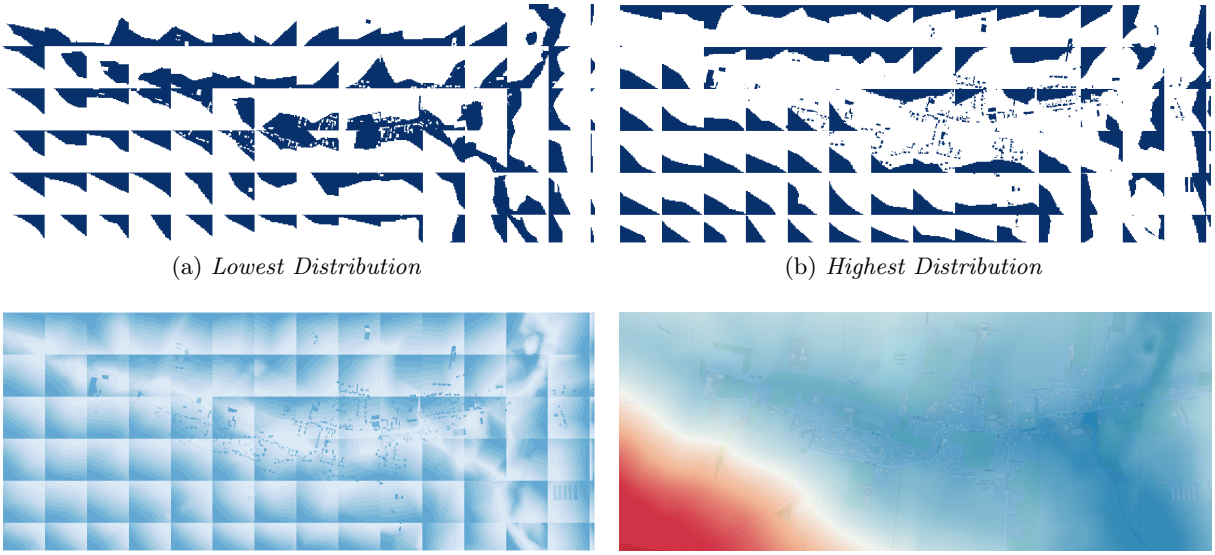

(a) *Lowest Distribution* (b) *Highest Distribution*

(c) *Height Weighted Distribution* (d) Domain DEM

Figure 17.6: The distributions of the cell scale synthetic storm event.

17.2.2 Cell Scale Distribution of a Synthetic Input

In this suite of runs the distributions took place on a cell by cell basis. I.e. from each 200 m × 200 m input grid to the corresponding 10 000 2 m × 2 m HiPIMS cells. Three of the four distributions can be seen in Figure 17.6 along with the DEM used in the hydraulic model. The blocky 14×6 grid extracted from the SHETRAN simulation can be clearly seen as can the patterns of distribution within each cell. Again, the uniform distribution is not included as this is relatively unambiguous. The uniform simulation performed here is identical to a domain scale simulation. As in the simulations above, inputs are at 40 mm/hr for 1 hr, 20 mm/hr for 2 hrs and 10 mm/hr for 4 hrs for the initial hours of the simulations.

In the *height weighted* distribution pattern (Fig. 17.5c), inputs are distributed linearly across the 10 bands with the lowest elevation band having 10× the input rate of the highest.

17.2.3 Groundwater Emergence Event

This suite of model runs uses simulated SHETRAN groundwater emergence (i.e. vertical flow rates) from the 9^{th}-11^{th} November 2001. The purpose of these simulations, as in the two previous suites, is to see what effect the different emergent patterns have on the simulation results and to see whether the effects are different when spatially variable inputs are used that only affect a subset of cell in the domain. According to Morris et al. (2007), modelled flooding should be similar to historical flooding and so these simulations should also indicate whether the joint modelling system is capable of recreating past flood events.

The simulated emergences range spatially and temporally from 2.8 mm/hr to 12.6 mm/hr and can be seen in Figure 17.7. As expected, emergence is topographically confined to the valley that runs through the village (Fig. 17.6d). This emergence pattern is redistributed in the *highest*, *lowest*, and *height weighted* simulations and untouched in the uniform simulation.

Figure 17.7: The blue cells show a snapshot of the hydrologically simulated groundwater emergence pattern prior to any redistributions. On this day there is a range of emergences from 1.7 mm/hr to 12.6 mm/hr. The topographically controlled emergence is focussed in the shallow valley through the village. Monitoring locations for the simulation can also be seen labelled as red circles, these correspond to sites with recorded flooding in Figure 16.4. OS VectorMap^{TM} (Ordnance Survey (GB), 2019).

Table 17.1: The following runs were performed to establish sensitivity to different input patterns. The uniform runs with *s are identical.

(Re)distribution Scale	**Input Rate**	**Input Period**	**(Re)distribution Pattern**
Domain (synthetic inputs)	40 mm/hr	1 hr	Uniform* Lowest Highest Random Height Weighted
Domain (synthetic inputs)	20 mm/hr	2 hrs	Uniform** Lowest Highest Random Height Weighted
Domain (synthetic inputs)	10 mm/hr	4 hrs	Uniform*** Lowest Highest Random Height Weighted
Cell (synthetic inputs)	40 mm/hr	1 hr	Uniform* Lowest Highest Random Height Weighted
Cell (synthetic inputs)	20 mm/hr	2 hrs	Uniform** Lowest Highest Random DEM150
Cell (synthetic inputs)	10 mm/hr	4 hrs	Uniform*** Lowest Highest Random Height Weighted
12 Cells (48 hr simulated groundwater inputs)	Average of: 5.8 mm/hr 5.2 mm/hr 4.7 mm/hr	Of duration: 12 hrs 24 hrs 12 hrs	Uniform Lowest Highest Height Weighted

18. Results

For each of the simulations, hydrographs of water depth have been extracted at key points around the village known to have flooded in the 2012/13 event, this follows examples in the literature (e.g. Hunter et al., 2008). These locations can be seen in Figure 17.7. The hydrographs are used to determine whether different redistributions affected the onset, duration and severity of any simulated flooding. A subset of these hydrographs are shown in this chapter and additional hydrographs (including those from the 20 mm/hr simulations) can be found in the Appendix.

The pond in the east of the village is approximately 1 m deep and, once full, does not drain below this. The storage capacity of the pond at the start of the simulation is inconsequential as it is downstream of the village and has a very small volume relative to the total volume of inputs.

18.1 The Synthetic Event - Domain Scale Distributions

Hydrographs from the suite of simulations that distributed inputs at the domain scale (Sec. 17.2.1) can be seen in Figures 18.1 & 18.2. In the 20 mm/hr simulation (Fig. 28.12) the *uniform* simulation is almost identical to the *random* simulation. The variation in the different hydrograph traces show that there can be significant differences in the flood depth depending on the location of the inputs relative to the whole domain. Flood depths are largely proportional to the volume of water distributed upstream. This is clear in the *lowest* distribution, where much of the water is input below the monitoring sites. There are also differences in the time to peak depth of up to half an hour. In the *lowest* simulation the reduced time-to-peak depth is caused by the proximity of the lower monitoring sites to the input cells.

There are clear patterns visible in the hydrographs in terms of the depths and time-to-peak of inundations from the different distributions. These are consistent across all three input intensities. All show that the *random* distribution is similar to the *height weighted* distribution but with a slightly greater depth. This is likely to be because they both distribute water across the domain, rather than just in sections of it. The *highest* and *lowest* are largely opposites, with the inundation from the *highest* decreasing relative to the *lowest* distribution with distance downstream. The flood depths are typically proportional to the intensity of the events. These may be slightly deeper than is realistic as the model does not consider man made drains or infiltration.

The inundation areas from the domain scale simulations can be seen in Figures 18.3 & 18.4. Depths below 5 mm were removed for clarity; when these shallow depths are included the inundation patterns are less distinct. Inundation maps from the 40 mm/hr and 10 mm/hr simulation suites show approximately the same patterns, although differences may be more obvious between the different distribution pattern in the less intense 10 mm/hr event.

The inundation maps show that the *highest* simulation has the greatest volume of upstream storage relative to other simulations. Distributing water higher up the domain also causes a

greatly reduced volume of water to be input upstream of the Old Gypsey channel to the north east relative to the other simulations, especially the *lowest*. Distributing the water on different drainage paths caused differences in available storage between the simulations - thus much of the water in the *highest* distribution bypassed the pond. The DEM simulation is an average of the *lowest* and *highest* - it distributes water in the Old Gypsey to the east, thus covering multiple drainage paths, while also distributing water in the higher reaches of the catchment. The *uniform* and *DEM* simulations distribute the waters most evenly across the domain.

18.2 The Synthetic Event - Cell Scale Distributions

Hydrographs from the monitoring locations for the three suites of cell scale distributions can be seen in Figures 18.5 & 18.6. With the obvious exception of the pond, all show peak inundations in the region of a few millimetres to tens of centimetres. The hydrograph peaks all occur at approximately the same time, thus changing the distributions has not altered the response time of the storm. Looking closely, we see that the *lowest* redistribution causes peaks to occur marginally faster and with slightly greater depths in all localities bar East Street. East Street behaves in this way because the closest upstream inputs are in the *highest* redistribution simulation. The descending limbs of the hydrographs are also all very similar, again having waters from the *lowest* redistribution simulation lagging slightly behind. As in the domain scale simulations, the intensity of the event does not affect the distribution.

18.3 Groundwater Emergence Event

The flood extents and depths can be seen in Figure 18.7. The extents are shown 10 hours into the simulation when many of the hydrographs show inundations depths to be peaking. The flood extents are very similar, only the extent from the *lowest* redistribution has a notability different pattern with a more condensed outline. In the *lowest* simulation the water emerging in the north east of the domain flows down the stream however in the other simulations it takes additional paths either side of the channel and also causes some inundation near the buildings in the far east of the domain.

Although not all of the localities recorded the expected inundation, those that do, show depths similar to those in photographs of historical flooding (East Riding of Yorkshire Council, 2013). In addition to the stream and pond, flooding is simulated in Chapel Lane, Church Street and in the central field.

The blocky pattern of the inputs is still seen in the results from the *uniform*, *highest* and *height weighted* simulations. This is unsurprising as emergence is still entering the model at the end of the simulation. All simulations show the most significant flood occurring in the same areas, capturing the locations of recorded flooding in the south of Chapel lane and West End but not matching the recorded flooding in Middle Street or East Street. Simulations also showed surface water in the field in the centre of the village that was not recorded in 2013. It is unknown whether this is because it did not flood, or because it was not deemed important to record.

The hydrographs from the monitoring sites (Fig. 18.8) show that the different redistributions follow the same onset pattern at each locality, with the *lowest* distribution causing the greatest depth and fastest onset, followed by the *uniform* and *highest* redistributions and then the height weighted *DEM* distribution. However, the degree to which the redistributions affect the hydrographs does change between the different localities. At Chapel Lane the DEM redistribution has around half the depth of the simulated flooding as the other distributions, whereas in the central field all simulations are approximately the same. While the hydrographs in this suite of simulations show greater variability to the synthetic cell scale simulations, the depths in the groundwater event are relatively small and so the differences are minor.

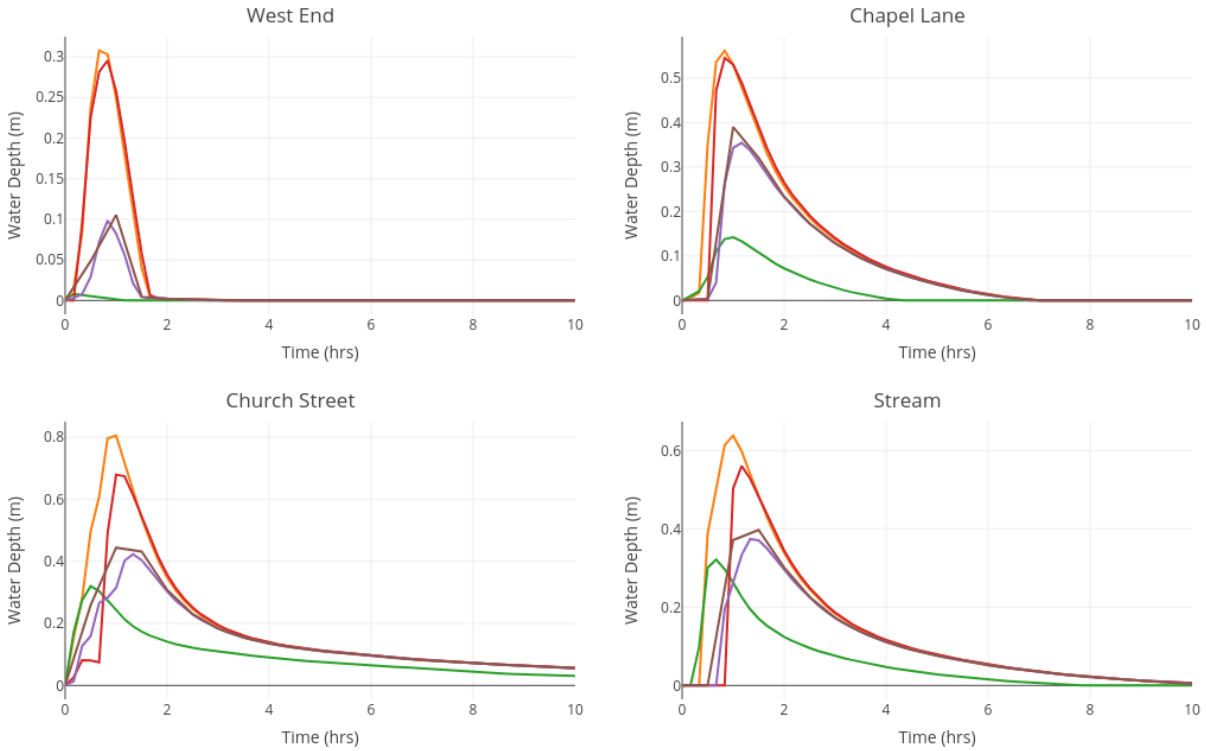

Figure 18.1: Hydrographs of domain scale distributions with synthetic rainfall inputs of 40 mm/hr for 1 hr.
Orange - uniform, green - lowest, red - highest, purple - height weighted, brown - random.

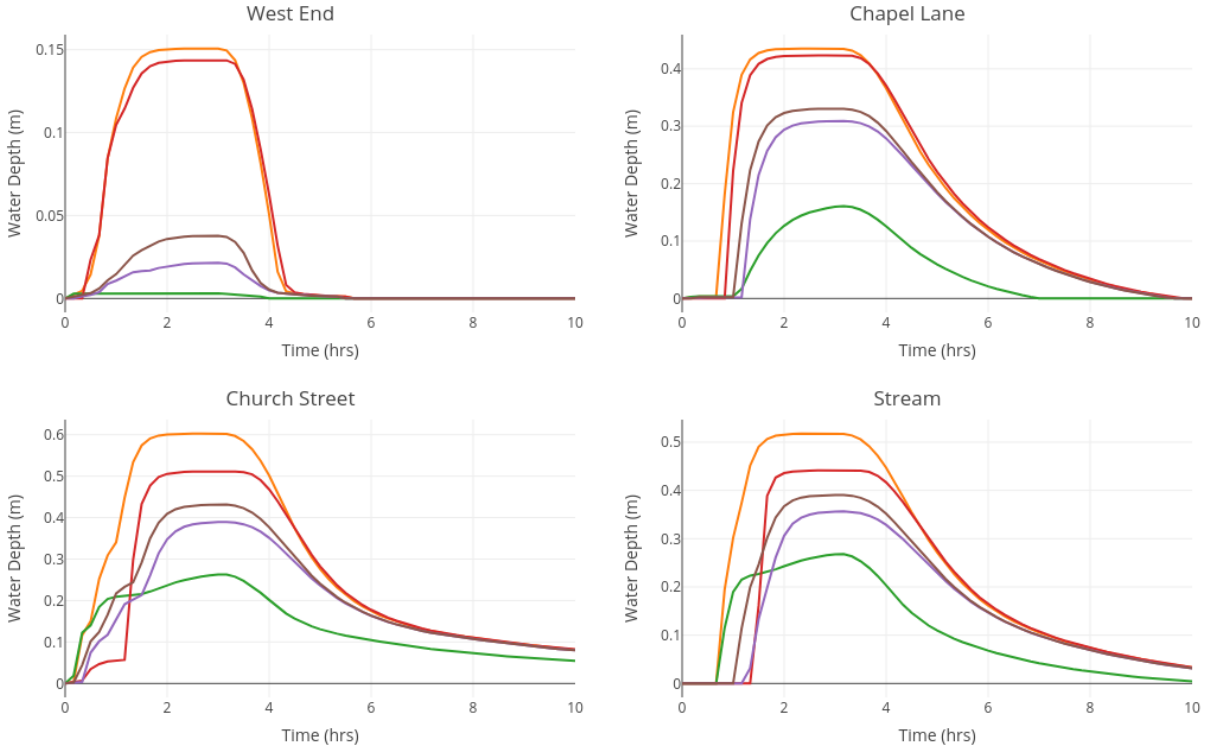

Figure 18.2: Hydrographs of domain scale distributions with synthetic rainfall inputs of 10 mm/hr for 4 hrs.
Orange - uniform, green - lowest, red - highest, purple - height weighted, brown - random.

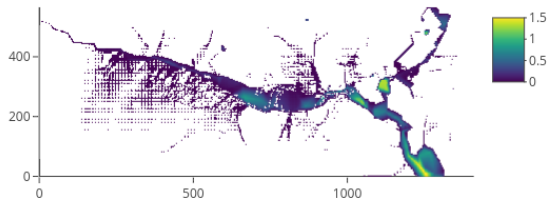

(a) *Uniform Distribution*

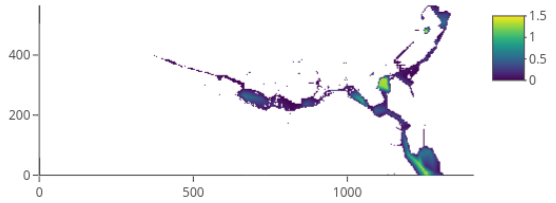

(b) *Lowest Distribution*

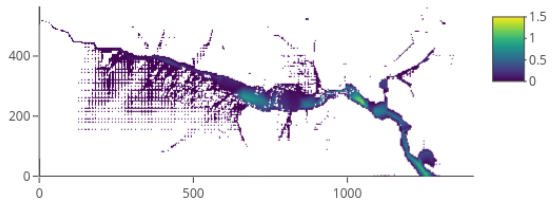

(c) *Highest Distribution*

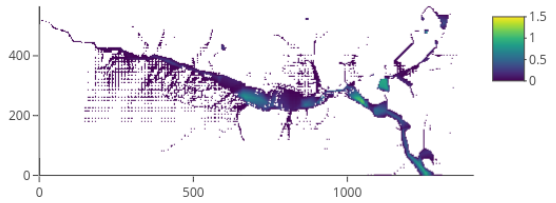

(d) *Height Weighted Distribution*

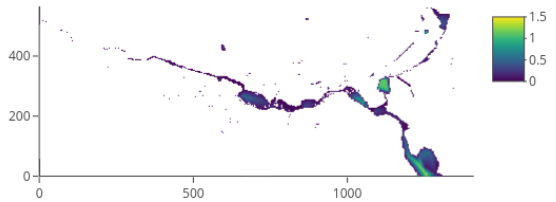

(e) *Random Distribution*

Figure 18.3: Surface water depths 2.5 hours into the simulation for the domain scale distributions of the synthetic 40 mm/hr storm events. Units are metres. Depths less than 5 mm are excluded for clarity.

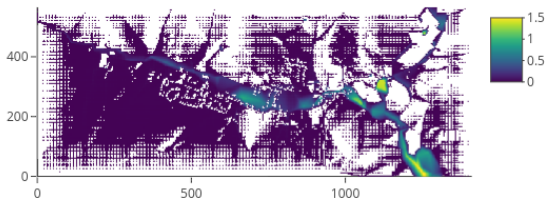

(a) *Uniform Distribution*

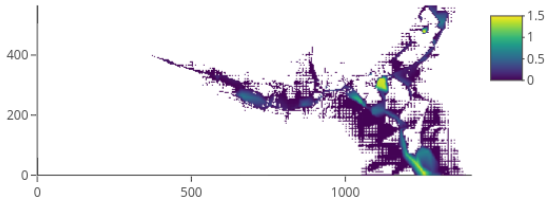

(b) *Lowest Distribution*

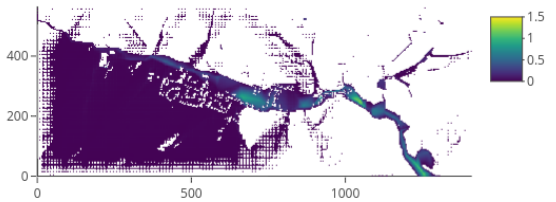

(c) *Highest Distribution*

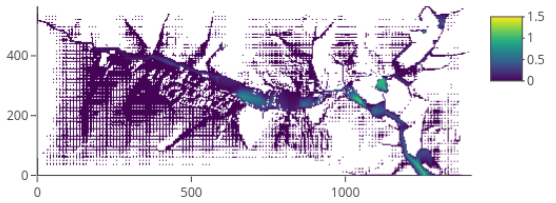

(d) *Height Weighted Distribution*

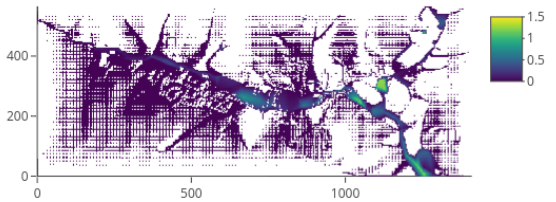

(e) *Random Distribution*

Figure 18.4: Surface water depths 2.5 hours into the simulation for the domain scale distributions of the synthetic 10 mm/hr storm events. Units are metres. Depths less than 5 mm are excluded for clarity.

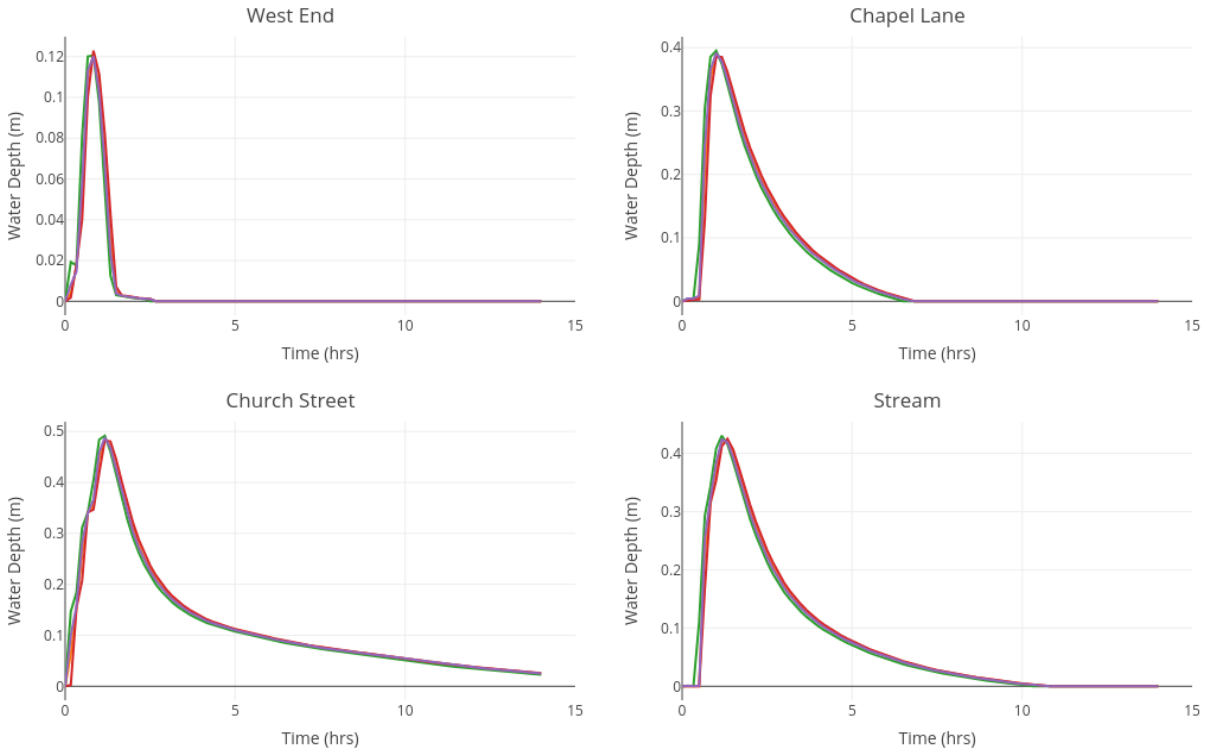

Figure 18.5: Hydrographs of cell scale distributions with synthetic rainfall inputs of 40 mm/hr for 1 hrs. Orange - uniform, green - lowest, red - highest, purple - height weighted.

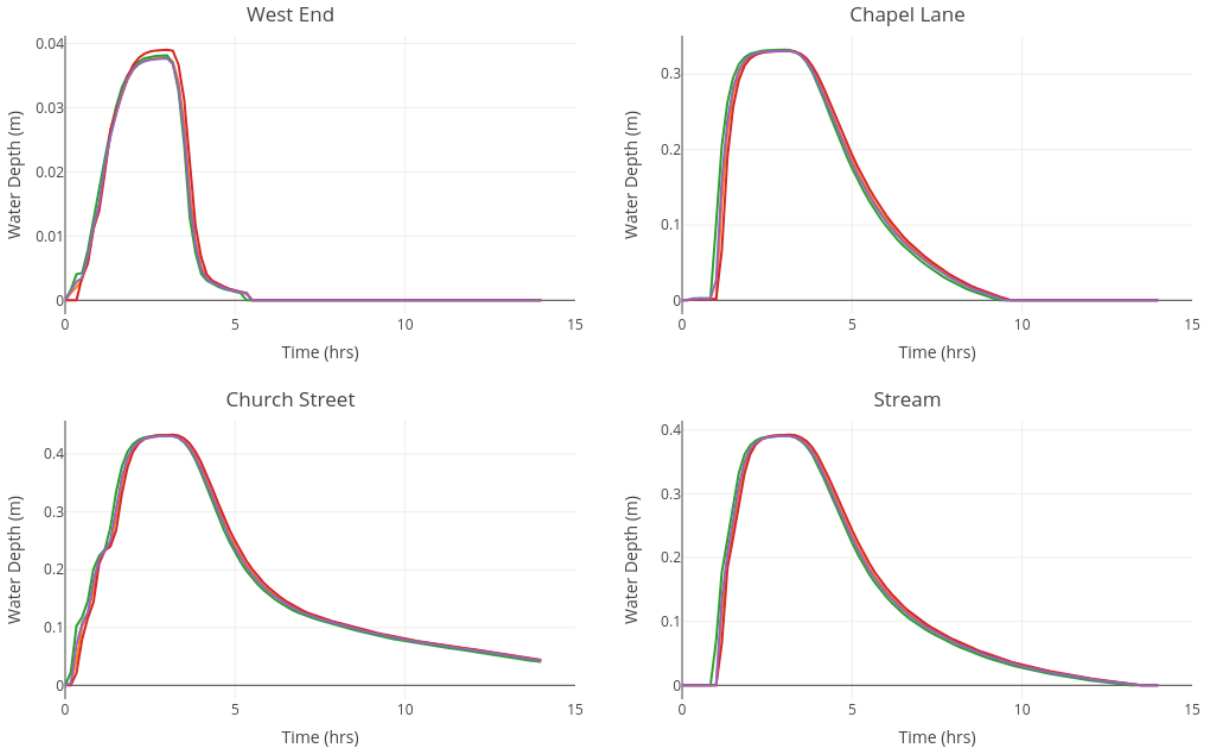

Figure 18.6: Hydrographs of cell scale distributions with synthetic rainfall inputs of 10 mm/hr for 4 hrs. Orange - uniform, green - lowest, red - highest, purple - height weighted.

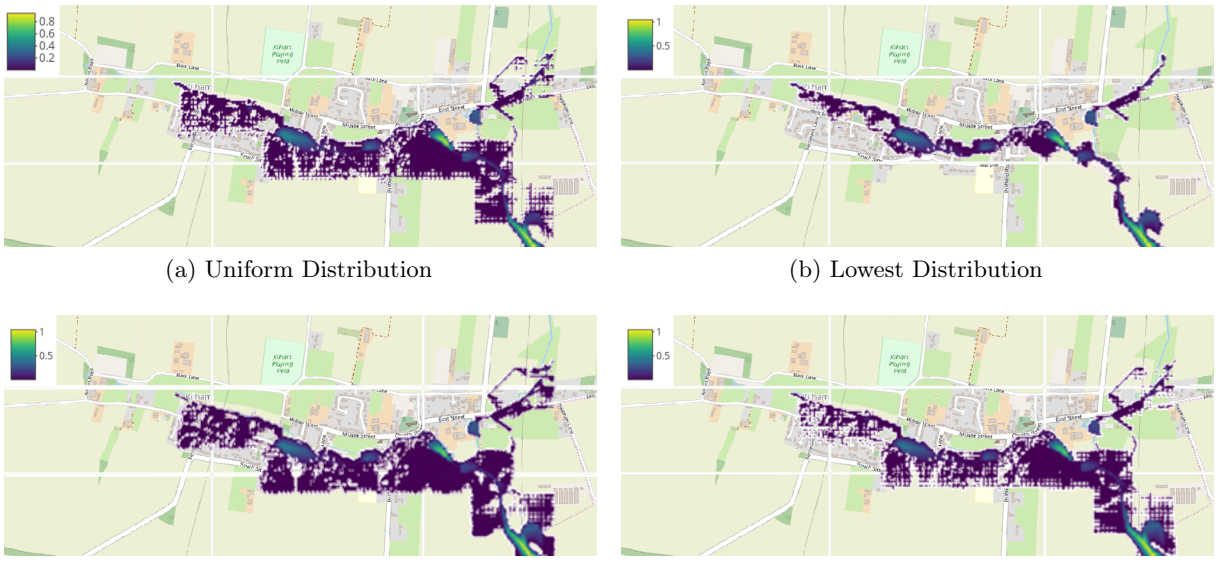

(a) Uniform Distribution

(b) Lowest Distribution

(c) Highest Distribution

(d) Height Weighted Distribution

Figure 18.7: Surface water depths (m) 10 hours into the suite of groundwater emergence simulations (Sec. 17.2.3). Flood depths are typically at their peak. Depths less than 5 mm are not shown for clarity though inundation patterns are similar when these shallower depths are included - with the exception of the *lowest* simulation, all have shallow water over the lower 3/4 of their input cells. ©OpenStreetMap

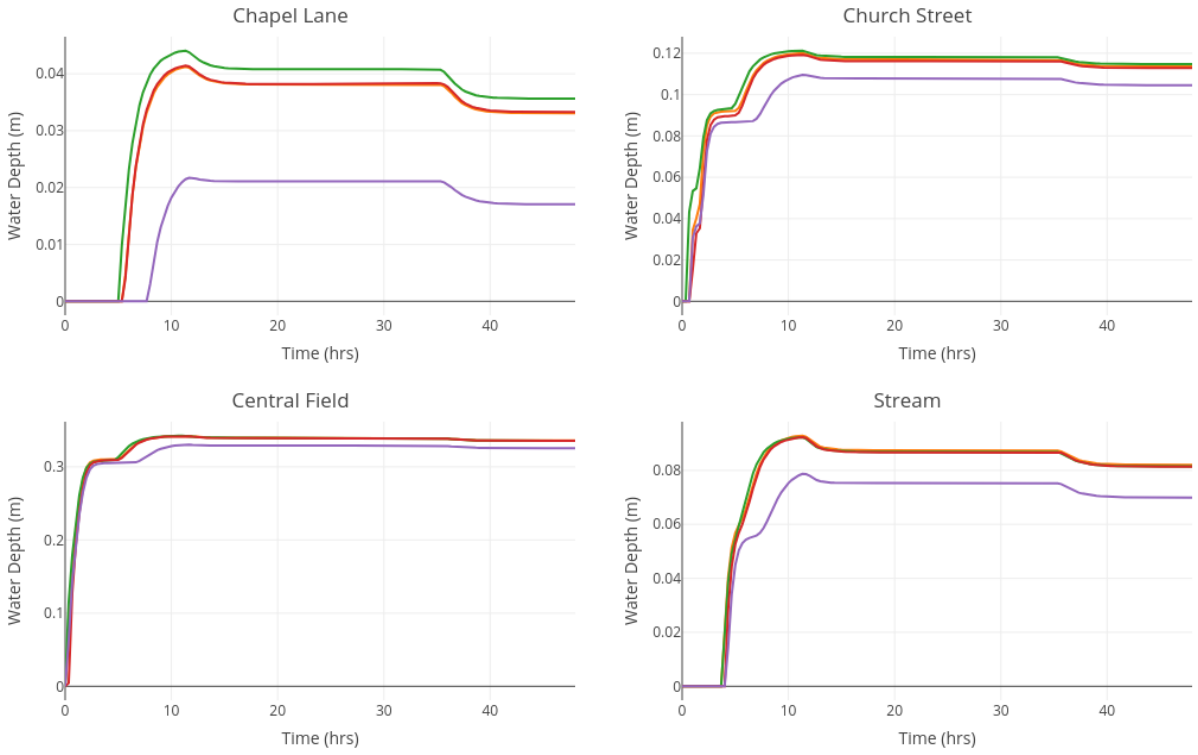

Figure 18.8: Hydrographs that took modelled groundwater emergence as an input. Unlike those seen the synthetic simulations, only four of the measurement points had recorded flooding. Orange - uniform, green - lowest, red - highest, purple - height weighted.

19. Discussion and Conclusions

19.1 Distributing Groundwater Emergence

It was expected that the method by which groundwater emergence was input into the hydraulic model would be a significant challenge and control on the hydraulic model. The domain scale distributions (e.g. Fig. 18.2) clearly show that the distribution pattern can influence the simulation, and therefore justified further investigation. However, the modelling system is not sensitive to the method of (re)distribution when done at a cell scale. There were minor and typically insignificant differences between the simulations' time to peak depths and inundation depths. (Re)distributing inputs to the higher regions of the domain/cells was an unrealistic scenario included to provide contrast to the redistribution that focussed emergence in the lower regions. This high redistribution was always going to be discredited but it demonstrated the insensitivity of the modelling system between the two contrasting end-member redistributions.

One of the greatest influences on the simulations was the effect of altering the drainage paths utilised by the inputs. This altered the volume of storage available and so affected how much water flowed downstream. Also, distributing water in the higher reaches of the domain increased the potential storage area, but, as stated above, this was not significant in the cell scale (re)distributions. When choosing a redistribution method in future modelling, it should be considered whether this opens up any large or unrealistic storage locations. Interpolation of the hydrological grid to a slightly higher resolution may resolve this by smoothing the blocky emergence patterns.

Two methods were used for producing the *height weighted* redistributions. The first, used in the simulation with synthetic inputs, split each 200 m $\times$ 200 m area into 10 bands according to topography and linearly distributed inputs across them, with the lowest elevation band having 10$\times$ the input of the highest elevation band. The second method was used in the groundwater emergence simulations. Here, the elevations were weighted from a given value. By altering this value the difference between the input bands could be controlled; a value was used that generated less extreme differences than in the first method. Both methods produced similar results and are thought to be more realistic than the other (re)distribution patterns. This complexity is unwarranted considering that cell scale (re)distribution patterns proved not to be an important control on the simulation. Height weighted approaches may be more warranted for hydrological simulations with greater topographic variation or lower resolution.

19.2 Historical Flooding

In the suite of groundwater emergence simulations it was expected that the routed emergence would cause flooding at the sites recorded during the groundwater flooding of the winter of 2012/2013 (Fig. 16.4). Notable flooding was simulated at Chapel Lane and Church Street,

matching the historical extents. However, West End only showed patches of surface water and East Street only showed surface water to the east of the historical extent (Fig. 18.7). Middle Street was not simulated to experience any flooding. This shows that the models are able to capture the approximate flood extents but that there are instances where this is not the case. Simulated river flows during this period were minimal and so excluding them from the simulations is not thought to be the cause of reduced flooding. Instead, this is attributed to the following three factors:

1. The flood extents recorded in Figure 16.4 are approximate. Photos of the event show that the flooding was not uniform across the recorded extents and that the micro-topography of curbs and verges affected the distribution of flood water (East Riding of Yorkshire Council, 2013). This may account for the irregular flood pattern in West Street.
2. Emergence is likely to have been less during the simulated November 2001 event than in the winter of 2012/13 during which the flood outline was recorded. Borehole data from just north of Kilham (Fig. 17.4b - Kilham P.S. OH_TA06KPS0CC) recorded a groundwater level of around 29 m AOD over the winter of 2012/13, 5 m higher than in November 2001.
3. The SHETRAN model grid is offset to the south of the village valley. Thus, it would be expected that the true emergence patterns in Figure 17.7 would be around 100 m to the north of its simulated position to match the topographic low and stream location. If this was the case then .
4. The relatively low resolution of the SHETRAN grid means that the village's valley, to which the groundwater emergence is topographically confined, is represented approximately 100 m south of its true position (Fig. 17.7). If this offset was accounted for then emergence would be present at almost all of the expected sites.

To address point 3 above, the hydrological grid could be pre-aligned with the topographic lows though to be of the greatest interest with regard to groundwater emergence. This is impractical however and difficult to do prior to conducting the hydrological modelling. Instead, it may be possible to increasing the spatial resolution of the hydrological model as this should improve the likelihood of correct placement of emergence patterns. There are examples in the literature where SHETRAN has been successfully run at a 20 m horizontal resolution (Elliott et al., 2012) however, as stated in Chapter IV, this makes the simulation more computationally intensive. It may be possible to reduce the computational requirements through the use of nested grids in which a simulation of a higher resolution is 'nested' within the standard resolution simulation by using outputs from the original simulation as boundary conditions. It may also be possible to use variable cell shapes, rather than the regular square grid used by SHETRAN. This could be achieved through the use of MODFLOW 6, which has the capacity to use unstructured grids (U.S. Geological Survey, 2019a).

An approach that would reduce, though not eliminate, the consequences of the offset hydrological grid is the spatial interpretation of vertical flows to a higher resolution, such as in Desbarats et al. (2002). Interpolation is a simple and automated process and may also help to breakdown the unrealistic gridded pattern of the SHETRAN outputs.

19.3 The Hydraulic Connection of Rivers

In the joint model the rivers are input into the hydraulic model at the domain boundaries using flows from the hydrological model. One limitation of this is that gaining rivers are not well represented by the hydraulic model. In SHETRAN-GB rivers are generated to have widths of 10% of grid resolution. The issues outlined above regarding the offset of emergence and the blocky nature of the emergence patterns means that it is unlikely that the hydrological models will be used at resolutions much lower than they are used here. As such, the river cells have a relatively small width in comparison to the width of the interfluves. Groundwater emergence into the rivers

is not therefore thought to pose significant issue. In the following chapter, this is investigated further and river emergences were found to be trivial in the hydraulic domain relative to the other inputs, which were orders of magnitude larger.

If the hydraulic connectivity of the river cells is thought to exercise a notable control on the river flow then it would be possible to couple them into the hydraulic model. This would however have two main complexities:

1. The river would need routing through the hydraulic model.
2. There is further potential for double counting of groundwater inputs via streamflows.

Routing rivers through the hydraulic domain requires remapping the hydrological vertical flow speeds to the channel in the hydraulic domain. The sensitivity tests in this chapter demonstrate that spatially approximate input of the channel emergence into the hydraulic domain is appropriate and that it is not vital to input this into a specific hydraulic channel. Efforts should be made however to limit the input of hydrological channel emergence far from the topographic lows of the hydraulic model. This could be achieved by creating a raster of the channel path in a GIS and mapping the hydrological inputs to the hydraulic domain. As the channel will be longer in the hydraulic model than in the hydrological model the vertical flows may need to be normalised to the extended length. Hydrological cells could be mapped in sections, or between nodes, such as domain boundaries or confluences (Fig. 19.1).

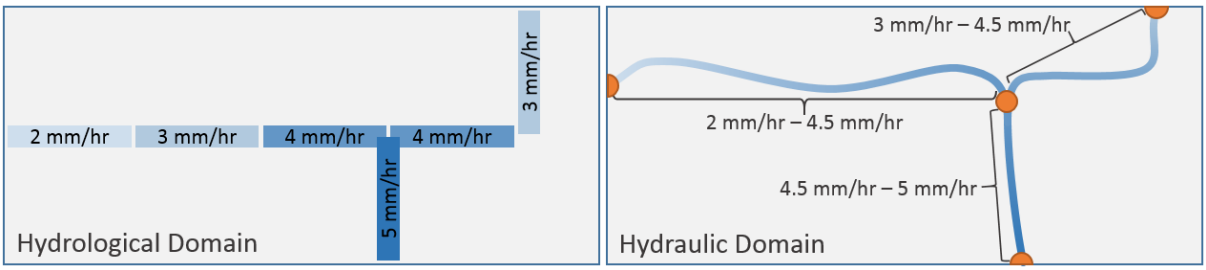

Figure 19.1: If desired, future work could remap hydrological channels into the hydrological domain to allow for the coupling of river bed groundwater emergence. This could be done by mapping the hydrological vertical flows between nodes within the hydraulic domain.

In Section 16.1 it was found that double counting of inputs did not influence the results of the hydraulic modelling. As the groundwater emergence into the channel occurs over a relatively small area relative to the rest of the domain this is also unlikely to cause issue. However, if this is a concern then the solution proposed in Section 16.1 could be applied here also: the iterative removal of rainfall through repeated model runs using the *hotstart* ability.

19.4 Conclusion

The modelling system developed in this chapter takes groundwater and stream flow inputs from a hydrological model (SHETRAN) and successfully inputs them into a hydraulic model (HiPIMS). This enables the capturing of rapid processes (such as rainfall events and variable stream flows) along with slower processes (such as fluctuations in groundwater level within a catchment). In order to link the models, the differences in spatial resolution had to be addressed.

The sensitivity of the modelling system to the redistribution of emergent groundwater into the hydraulic model was tested using three model suites. These can be seen in Table 17.1. The system was not found to be sensitive to the redistribution method when conducted on a cell-by-cell basis (rather than at the domain scale). As such, it is concluded that emergences should be used in their original form so as to avoid unjustified complexity.

The alignment of the hydrological model's grid relative to local topography was found to

be an important factor when linking the models. Horizontal offsets between topographic lows in the hydrological model and reality meant that emergence occurred 100 m south of where it was expected and was therefore only present on one side of the village valley. This limited the realism of the emergence patterns. Various approaches may be suited to improve this, such as using nested hydrodynamic models, using a sufficiently high-resolution hydrological model, using a hydrological model with variable grid structure or the interpolation of hydrological outputs. The latter of these would not fully eliminate the offset, but would reduce the consequence and is the most computationally and practically justifiable.

The modelling approach developed here does appear capable of simulating multisourced events as it can capture both surface and subsurface processes. Further work should include experimenting with larger and more topographically complex hydraulic domains, the interpolation of hydrological outputs and the coupling of overland flows between the models. The modelling system is demonstrated in Chapter VI to assess the multisource flood risk in Kilham.

VI

Assessing Multisource Flood Risk

20. Background

This PhD sought to develop a methodology for assessing multisource flood risk. The tools for doing this have been developed in previous chapters and are combined here to create the proposed methodology, which is implemented for Kilham, the case study site used in Chapter IV. The aim of this chapter is to demonstrate the developed methodology and to discuss its usefulness and implications by comparing the single source flood risk (posed by either groundwater or surface water flooding) to the multisource flood risk.

To assess flood risk, a similar approach was taken to that of the Environment Agency in their Flood Maps For Planning (Environment Agency, 2013a) by simulating flooding for certain return period events. In line with the Environment Agency (EA), these events have return periods of 1/30, 1/100 and 1/1000 years. This gave the *risk* of a range of events that can be easily compared to the existing flood maps. Existing flood maps include the *Flood Map for Planning* (Environment Agency, 2013a) and the *Long Term Flood Risk Map* (Environment Agency, 2019a), which includes estimated surface water flood extents.

The term *risk* is highlighted above as this approach by the EA does not consider vulnerability and so should technically be defined as a hazard (Sec. 1.2). To truly assess risk, further work is needed looking at the effects of the hazard (e.g. damage to property and health). Although steps for assessing flood risk are developed here, the final step on assessing vulnerability directly is not included as this is done in other works (e.g Balica and Wright, 2010; Merz et al., 2010b; Zhou et al., 2012; Aldridge et al., 2017) and so is thought beyond the scope of this project.

Cobby et al. (2009) state that one of the major difficulties in assessing groundwater flood risk is establishing likelihoods for events. Jacobs (2007) propose that this can be achieved by assessing the frequency of observed flooding, proxies (e.g. observed groundwater levels) and drivers (e.g. rainfall) as well as mathematical modelling. The latter two of these were used here via the generation of driving synthetic meteorological data and hydrological modelling through SHETRAN.

To assess 1/1000, 1/100 and 1/30 year flood events, the modelling system requires meteorological data from which it can hydrologically model catchment conditions, which are then fed into the hydraulic model. In order to hydraulically model these events, the 1/1000 year catchment conditions are required. The meteorological data needed to facilitate this approach does not exist and so 1000 years of weather data was generated synthetically. Simulating catchment hydrology over this extended period provided a picture of potential catchment conditions and flood events, including extremes.

Simulated river flows immediately downstream of Kilham village were used to identify periods of peak flow and thus potential flooding. These flows were used to determine the 1/30, 1/100 and 1/1000 year events. Using the modelling system developed in Chapter V, hydrological outputs from SHETRAN were extracted during these events and entered into the hydraulic model

(HiPIMS). The proposed *methodology for assessing flood risk from multiple sources* can be seen in Figure 20.1. A more detailed methodology of the processes involved in this methodology can be found in Section 21.

A similar but separate line of enquiry will demonstrate the potential to use this modelling system for estimating potential single source groundwater flooding. This parallels the work of Morris et al. (2018) who extrapolated groundwater emergence surfaces and used them, along with estimated emergence rates, as inputs to a hydraulic model.

A realistic, calibrated and validated hydrological model is needed to provide antecedent hydrological conditions for the hydraulic model. The SHETRAN model of the Kilham catchment was used again in this chapter as it already fulfilled these requirements. Details on the Kilham catchment and its historical flooding can be found in Chapter V. The model was adapted for use in this chapter only by changing the runtime and meteorological inputs so as to use the synthetic weather data as well as altering the model version to one that includes a *hotstart*.

The *hotstart* version of SHETRAN used here means that the model can be restarted at any month during the simulation using the pre-simulated catchment conditions at that timestep without the need for a spin up period. The ability to restart the model also reduced the risk of lost data via potential model crashes. This enables an optional additional phase of modelling that solves the potential *double counting* of rainfall discussed in Chapter V. The additional modelling step enables the user to alter the model inputs for the re-run. As such, the rainfall over the domain of the hydraulic model can be removed during the period of interest. This means that when outputs are taken from the hydrological model they do not include rainfall and so this is not double counted. Testing in Chapter V showed that, at least in the case study site, removing the rainfall for this period had minimal effect on the outputs extracted for hydraulic modelling and so this step was not undertaken here.

The model ran at a 200 m spatial resolution with an extended catchment that takes into account the surrounding groundwater conditions beyond the surface water watershed. The model is well calibrated and has good agreement with measured river flows and groundwater levels (Tab. 28.3 & 28.4).

20.1 The Multisource Modelling System (MMS)

The modelling system consists of two models (SHETRAN and HiPIMS), although these can in practice be any models that enable the user to generate realistic spatially distributed catchment processes and any model that enables high-resolution flow routing. It is important that the catchment scale model can output groundwater emergence, river flows and, ideally, overland flows in a relatively simple structure and that these can be input relatively easily into the high-resolution model. Here, a suite of R scripts automate the process of extracting flow data from the hydrological model, identifying flow events with 1/30, 1/100 and 1/1000 year return periods, extracting additional outputs for these periods, reformatting them into the form desired by the hydraulic model and then setting up the hydraulic model around these inputs. The hydraulic model is then run by hand, however this to could be automated if a higher number of runs were desired.

The proposed modelling system employs the following procedure:

1. A hydrological model is set up for the area of interest using observed meteorological conditions and calibrated and validated using observed river flows and groundwater levels.
2. A synthetic weather generator is used to produce 1000 years of meteorological data. This study uses the Newcastle University UKCP09 Weather Generator (Kilsby et al., 2007) (Sec. 21.1).
3. 1000 years of catchment hydrology are simulated using the hydrological model.

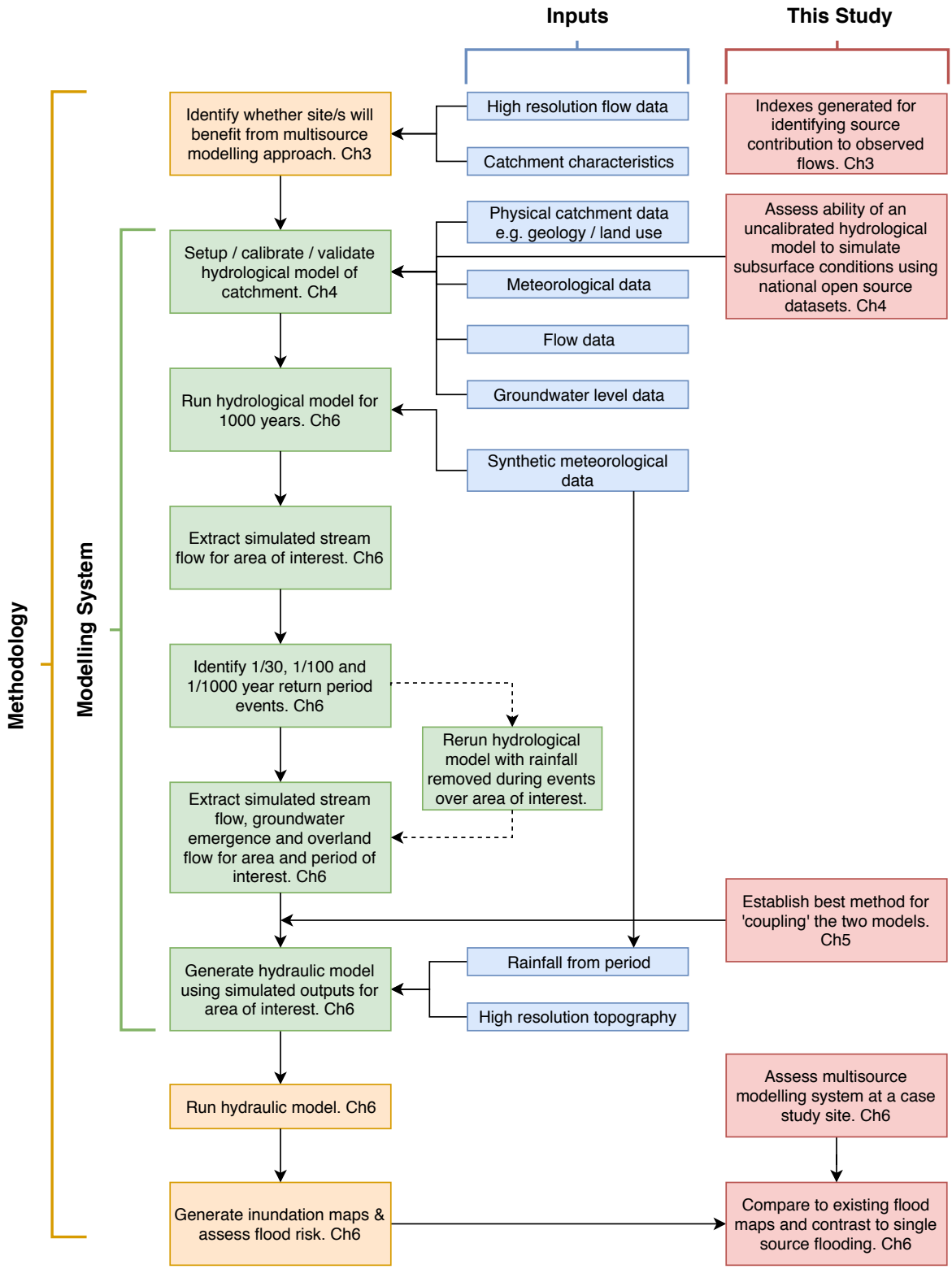

Figure 20.1: This methodology will be used for establishing multisource flood risk in Kilham, a village with known multisource flooding. Boxes annotated with an R indicate automated processes coded in R. Additional work undertaken in this study that does not form part of the proposed methodology is noted in the red boxes.

4. Flow data is extracted from below the area of interest (in this case from the stream leaving Kilham village) and is analysed to identify periods of peak flow. This is then used as a proxy for flooding and used to identify the 1/30, 1/100 and 1/1000 year flow events that will be fed into the hydraulic model.
5. OPTIONAL: Simulations covering each of the events of interest are re-simulated in the hydrological model. This allows the removal of rainfall over the area and time period of interest and thus avoids double counting of inputs. (Sec. 16.1)
6. Groundwater emergence and river flows are extracted as inputs for the hydraulic model.
7. For each of the events of interest, groundwater emergence and rainfall are input within the domain of the hydraulic model along with river flows at the domain boundaries. The multisourced groundwater, fluvial and pluvial inputs are then routed across the domain at a high resolution appropriate for urban scenarios. In order to capture the antecedent conditions, groundwater emergence rates are extracted for five days prior to the peak flow. The simulation continues for three days following the peak flow. The duration of the hydraulic model may be constrained by computational power, however modelling for an extended period will better capture effect of the groundwater contribution.

21. Methodology

This section describes how the methodology described in Section 20.1 was undertaken. This covers model setups and the practicalities of implementing such an approach.

21.1 Meteorological Data

The proposed methodology for assessing multisource risk developed in this study requires long term hydrological modelling to create inputs for the shorter term hydraulic modelling of events. In this instance, 1000 years of hydrological simulation time were desired. Synthetic data was produced using the UKCP09 Weather Generator (Kilsby et al., 2007).

Weather Generators produce synthetic meteorological data using statistical functions, as opposed to climate models, which use physical processes. The resultant data sets have similar statistical characteristics to observed datasets and focus on producing realistic, meteorologically plausible data (Culley et al., 2019; Zhou et al., 2019). The meteorological dataset created for this study is statistically accurate, spatially distributed, 5 km resolution data that is capable of capturing extreme conditions. The Weather Generator was used to create hourly precipitation as well as the necessary data to calculate evapotranspiration (daily temperature range, relative humidity & wind speed at 10 m). Daily evapotranspiration was calculated using the Penman-Monteith method (Eq. 21.1.1) and then downscaled to hourly according to the number of sunshine hours per day. Details and guidelines of this can be found in Allen et al. (1998).

Equation 21.1.1 — Penman-Monteith Equation. Evapotranspiration was calculated using the the Penman-Monteith equation (Allen et al., 1998). All necessary variables could be found in the literature or were provided by the weather generator.

$$ET_o = \frac{0.408\Delta(R_n - G) + \gamma\frac{900}{T+273}u_2(e_s - e_a)}{\Delta + \gamma(1 + 0.34u_2)}$$

ET_o is the reference evapotranspiration (mm day^{-1})
Δ is the slope vapour pressure curve (kPa$^oC^{-1}$)
r_n is the net radiation at the vegetation surface (MJm^{-2}day^{-1})
G is the soil heat flux density (MJm^{-2}day^{-1})
γ is the psychrometric constant (kPa$^oC^{-1}$)
T is air temperature at 2 m (^{o}C)
u_2 wind speed at 2 m (ms^{-1})
e_s is saturation vapour pressure (kPa)
e_a is actual vapour pressure (kPa)

The generated data was checked to make sure it was in line with the expected conditions. For the first century of generated rainfall, there was an annual total of 689 mm of precipitation/year with 174 wet days/year. This corresponds well with the estimated mean rainfall of 719 mm/year for the area (Climate-Data.Org) and mean observed rainfall for the Foston Beck catchment of 709 mm/year with 222 wet days/year (NRFA, 2019b). A histogram of the observed and synthetic daily rainfall for Foston Beck and the hydrological domain are plotted in Figure 21.2 and show good general agreement in terms of the distribution of intensities.

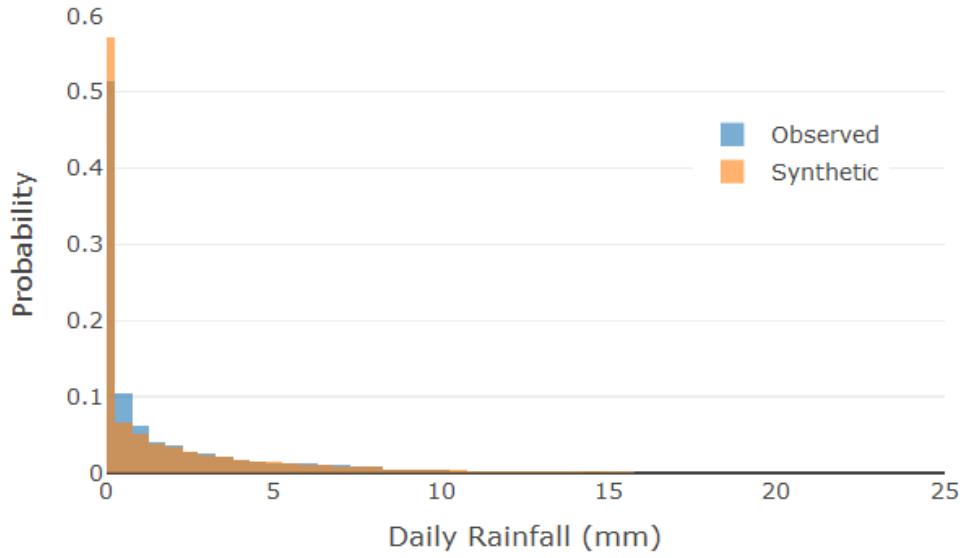

Figure 21.1: Two normalised histograms are plotted showing the distribution of daily rainfall values. Blue shows observed values from 1959-2015 NRFA (calculated from 2019b)) and orange shows the values from the first century of synthetic data (aggregated from hourly to daily).

The hydrological model contains 17 5×5 km weather cells, two of which cover the domain of the hydraulic model. Weather cells have a meteorologically consistent spatial distribution and so share similar weather patterns. This can be seen in Figure 21.1, which shows three cells - one from the north westerly corner of the catchment and the two that cover the hydraulic model. Consistent cell-to-cell weather patterns are crucial in order to maintain realism within the hydrological simulation. It is also required to enable realistic antecedent conditions within the simulations. If there is a storm over the hydraulic model domain, there needs to be an appropriate groundwater and streamflow response from the upstream region of the hydrological model. This would be unlikely if the meteorological cells were not related.

21.1.1 Multisource Flooding and Climate Change

The UK's climate is recorded to be warming at a rate 20% larger than the global average and there is an increasing view that extreme daily rainfall rates may increase over the coming years, with heavy rainfall occurring more frequently (Met Office Hadley Centre, 2014). Furthermore, it is likely that UK winters will become milder and wetter, whilst summers become hotter and drier. A change in climate would almost certainly alter the antecedent groundwater conditions prior to a rainfall event (Woods, 2015). Such a change in climate may increase the seasonality of multisource flooding by confining groundwater contributions to the winter months. Despite this, there are relatively few studies that investigate the effect of climate change on groundwater levels, especially at a national scale. Those which do exist have predicted extremely varied groundwater recharge rates (Watts et al., 2015). Predictions of future groundwater levels that use historical data are also limited and so little is known regarding long term fluctuations in groundwater levels

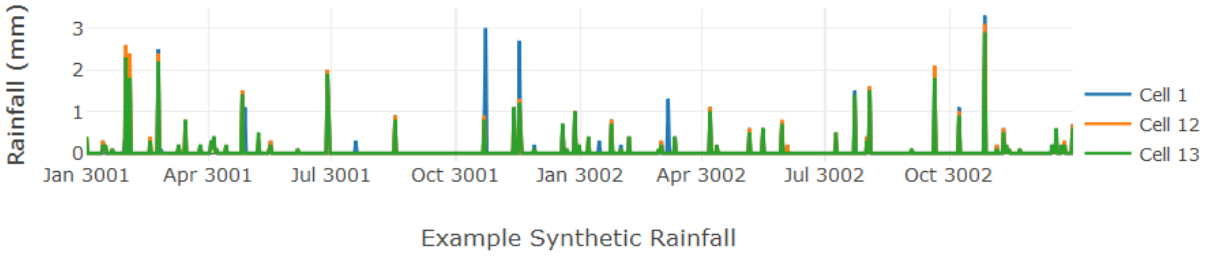

Figure 21.2: Three years of hourly synthetic rainfall created using The Weather Generator. 3 of the 17 cells used in the hydrological model are shown, cells 12 and 13 are also used in the hydraulic model as they cover Kilham village. This shows the spatial and temporal consistency of the data.

(Jackson et al., 2015). Jackson et al. (2015) state that more research is required into the effects of climate change on groundwater in order to better assess the future risk posed by groundwater flooding. There is evidence both that groundwater flooding may become much more likely in the coming years (Jimenez-Martinez et al., 2015) but also that recharge rates may fall and lead to a decrease in groundwater levels around the UK (Garner et al., 2017).

While the consequences of climate change on antecedent groundwater conditions are uncertain, there is an argument that both the frequency and magnitude of flooding in the UK is set to increase in coming years in line with predictions made for the rest of Europe (Watts et al., 2015; Garner et al., 2017).

Typically, studies of climate change and floods focus on pluvial and fluvial risks, rather than groundwater. A review by Miller and Hutchins (2017) indicates that pluvial flood risk in urban areas is likely to increase with the changing climate due to the increase in high intensity, short duration rainfall. In Europe one study estimates that the number of people affected by fluvial flooding may increase from approximately 250,000 to 400,000 with associated costs doubling or even tripling by 2100 (Feyen et al., 2012). Future fluvial flood risk in the UK is also likely to change, with future flow regimes differing on a catchment specific basis, rather than on a UK wide scale (Miller and Hutchins, 2017).

As such, while flood risk is predicted to change, the direction of change is uncertain. With the increase in intense rainfall there may be more surface water dominated summer and an increase in multisource events in the winter due to increased winter recharge. The methodology for assessing multisourced flood risk described in this chapter could easily be used to increase understanding of changing flood risk levels by modelling with synthetic climate forecasts data. Automated summaries of flood sources (such as Figure 23.7) could be generated to indicate how the roles of each source may change, as well as any change in the seasonality of different source contributions.

21.2 Simulations

Two suites of models were run. The first set simulated single and multisource events so that comparisons could be made between them. These simulated events were selected according to the simulated streamflow immediately downstream of the village (Sec. 21.3).

The second suite of events simulated only groundwater to demonstrate a separate functionality of the developed methodology - the ability to simulate groundwater induced floods (following comments in Morris et al. (2018) - Sec. 4.3.6). These simulated events selected according to the sum of groundwater emergence within the village. It is important that these two sets of model runs used different proxies (flow vs. total emergence) to determine events as the 1/x groundwater event is unlikely to be the same as the 1/x multisource event and so simulating a groundwater event determined using streamflow would be likely to underestimate the emergence. The simulations are listed below. Each contains three runs: the 1/30, 1/100 and 1/1000 year

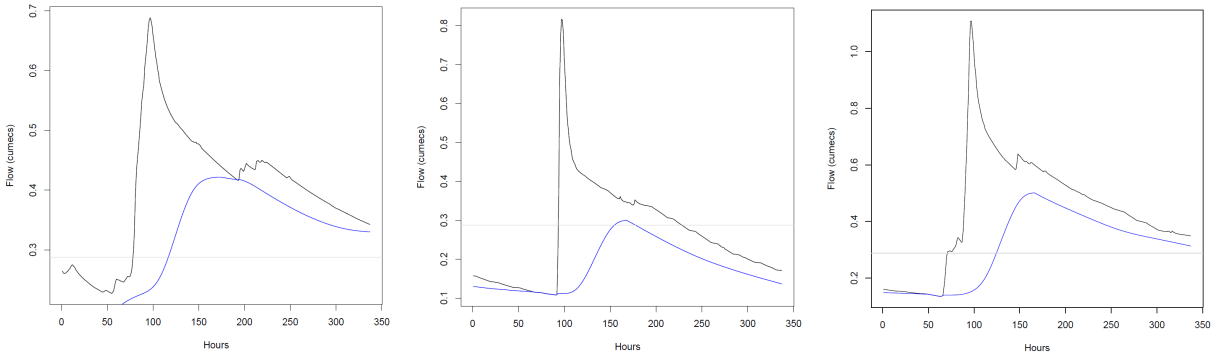

(a) 1/30 year event. (b) 1/100 year event. (c) 1/1000 year event.

Figure 21.3: The events selected for simulations 1a, 1b & 1c in the modelling system were based on the peak flows simulated directly downstream of Kilham village in the hydrological model. Hydrographs of these flows are show above. The black line shows streamflow, the blue line represents base flow.

events, making 12 simulations in total.

1a **Surface water** - River flows and rainfall within the village.
1b **Groundwater** - Groundwater emergence within the village.
1c **Multisource** - River flows, rainfall and groundwater emergence.
2 **Groundwater specific** - Groundwater emergence specific to groundwater flooding events. This simulates different events to those of 1b.

In Section 19.4 it was suggested that the groundwater emergence should be interpolated to a higher resolution to create more realistic emergence patterns. In this chapter the groundwater emergence was interpolated so that each 200×200 meter groundwater cell covered eight 50×50 meter cells, which were then input into to HiPIMS. When interpolating, care must be taken to ensure that the total groundwater emergence following the calculations are in approximate mass balance to the original hydrological simulation.

In the hydraulic model, streamflows are initiated from the domain boundaries as this facilitates a simple linkage between the two models. Future work may choose to integrate overland flow from the hydrological model into the hydraulic model. Its absence here is not thought to affect the demonstration of the methodology, its inclusion but may increase performance in future studies, where it would increase the volume of surface water in the domain.

21.3 Event Selection

For simulations in suite 1, the 1/x year streamflow peaks were used to identify events. In suite 2, which used only groundwater emergence as an input, events were selected by identifying the peak simulated groundwater emergences summed across the hydraulic domain. Peaks were identified and ranked using the same method as was used in Chapter III. Hydrographs of the flows that were used to classify events 1a-c can be seen in Figure 21.3.

The ranks of the peaks were then divided by the length of the simulation in years to infer a return period (Eq. 21.3.1). While more complex methods exist for classifying return periods and annual exceedance probabilities (e.g. Yue et al., 1999), this method offers a simple approach that is appropriate for demonstrating the methodology and is in line with an approach taken by the Environment Agency for establishing approximate annual likelihoods (Aldridge et al., 2017). The first, tenth and thirty-third highest peaks are taken to represent the 1/1000, 1/100 and 1/30 year events.

Equation 21.3.1 — Calculating Return Intervals. Events to be used in the multisource modelling system were chosen by first identifying peak flow events in the hydrological model, ranking them and then dividing their rank by the number of years of simulated data. Taken from (Aldridge et al., 2017).

$$Return\ \ Interval = \frac{Event\ \ Rank}{Length\ \ of\ \ Simulation\ \ in\ \ Years}$$

One caveat of this method for peak identification is the assumption that river flows are an appropriate proxy for groundwater levels (and, by extrapolation, groundwater flooding). In Kilham the groundwater system is in good hydraulic connection to the streams and so it is thought that this is an appropriate mechanism for defining peak hydrological conditions, however this may not be the case in other catchments or in areas where flooding is not local to the river system. Furthermore, high groundwater levels can occur without high stream flows, especially if groundwater from a recharge zone arrives at the area of interest much later than river flows or if the area of recharge is outside of the surface water catchment or if a high proportion of rainfall infiltrates and does not enter the river system. In such cases it may be more appropriate to assess multiple processes, such groundwater levels or emergence volumes. It should also be noted, as it was in Chapter III, that peak hydrological conditions may occur without causing flooding, however this was not found to be the case in this instance.

21.4 Computing

Much of the methodology described in this work revolves around the use of the developed modelling system. This requires a significant computational resources, especially when running large hydrological and hydraulic models for extended periods. With the developments in computing over recent years, and in years to come, these are unlikely to be limitations on the method (Jaros et al., 2019).

With a standard PC the hydrological model can be calibrated and validated, although the user may have to wait several hours or even a day per run for larger domains. In this instance the PC used had 16 GB RAM and a 3.5 GHz processor. Multiple simulations were run simultaneously, which greatly reduced the waiting time. The hydraulic modelling is also manageable using a desktop PC, however a GPU is required if using HiPIMS. In this instance a NVIDIA GeForce GTX 1060 3 GB graphics card was installed into the PC along with a 1 TB hard drive for storing the high volume of outputs. The GPU is relatively accessible, priced in the region of a few hundred pounds. In Chapter V, setting up the hydraulic model required multiple runs, each taking a few hours. The hydraulic model had a domain of 1411×566 cells and ran at approximately 1/4 real-time speed (e.g. a 24 hours simulation would take ≈6 hours to run). Multiple simulations could be run simultaneously, however this did increase the run times. The modelling in this chapter required considerably greater computational resources due to the extended model durations of both the hydrological and hydraulic models.

The 1000 years of hydrological modelling were split into 10×120 year simulations so that the simulations could be run in parallel across multiple different machines. The initial 20 years of each run consisted of reflected data from the first 20 years of each 100 year period. This 20 year spin up period ensured that the 100 year period was initiated with realistic catchment conditions. This spin up time will vary between models but is likely to be longer in larger or more complex models. The hydrological models were run on the Newcastle University Blades, with each 5130 cell, 120 year simulation taking ≈1 week. The Blades make up a high performance server with an Intel(R) Zeon(R) Gold 6134 CPU with two 3.2 GHz processors and 512 GB of RAM.

In addition to the increased model durations, the domain of the hydraulic model was extended

downstream to 1411×800 cells in order to combat instances of water backing up at the downstream domain boundary during the testing in Chapter V. All cells over 5 meters higher than the original stream sink were masked out in the extended domain but the additional ≈83,000 active cells noticeably increased the computational time to 1/2 real-time. Although many of the models could be trimmed where there were no inputs for the first few days or hours, this was still impractical and so models were run on a higher performance Linux server with 4 NVIDIA Tesla K80 GPUs. This decreased the run time for each model to 1-2 days meaning a combined run time for the twelve hydraulic models in this chapter of 18 days. Split across the 4 GPUs, the simulations were completed within 1 week.

22. Results

Four sets of hydraulic simulations were run. The first three sets (from suite 1) contrasted multisource and single source events for 1/30, 1/100 and 1/1000 year meteorological conditions. The fourth set (from suite 2) simulated single source groundwater induced flooding using the 1/30, 1/100 and 1/1000 year groundwater conditions. The results of these can be seen in hydrographs of flood depth at Church Street in Kilham (Fig. 22.1) and in maps of flood extent (Fig. 22.2). Maps of flood extent show all cells that were inundated by more than 10 cm of water during the simulation. Depths less than 10 cm are not shown as this aids clarity and helps to distinguish and compare flood extents without a loss of important information. This is also in line with recommendations from the Environment Agency (Environment Agency, 2010). The inputs for the simulations can be seen plotted with the hydrographs.

Figure 22.1 shows the differences in the depth and duration of the flooding between the different simulations. The hydrograph shapes are specific to the synthetic weather patterns that generated them and so it is not appropriate to compare hydrographs between different events, as was done in Chapter V. The hydrographs show that there is flooding of up to 70 cm in the village. This is enough to cause both inconvenience and damage to the local community, flooding properties and roads.

Figure 22.2 shows the comparisons, within the events, between single source and multiple source flood extents. The smallest and most frequent of the modelled events, the 1/30 year scenario, has almost no groundwater component (Fig. 22.1a) - it is essentially single sourced and has the highest intensity rainfall of the three events at 30 mm/hr. The lack of groundwater input meant that the simulation only lasted around 90 hrs. As a single sourced event the multisourced flood extent is near identical to that of the surface water extent (Fig. 22.2a). The minimal groundwater input can be seen in the bottom right of the figure, with emergence occurring in the lowest cells of the domain. This demonstrates that although these simulations are being used to estimate multisource flood risk, they do not necessarily require the presence of all sources.

In the 1/100 year event, the groundwater contribution is much greater, with an approximately equal volume of rainfall and groundwater emergence through the simulation. The vast majority of this rainfall input, and resultant streamflow input, occur through a single intense pulse (Fig. 22.1b). Although there is a steady 0.3 mm/hr of groundwater input for the first 120 hrs of the simulation, the majority of the groundwater emergence initiates a few hours following this pulse and continues until the end of the simulation. In both the multisource and surface water simulations this pulse leads to flood depths of around 60 cm at Church Street. The groundwater simulation sees resultant flood depths of only around 10 cm, however these persist until the end of the simulation. The inclusion of groundwater into the multisource simulation means that the flood waters do not subside below 10 cm.

As with the 1/100 year event, the 1/1000 year event is clearly multisource. It has the largest

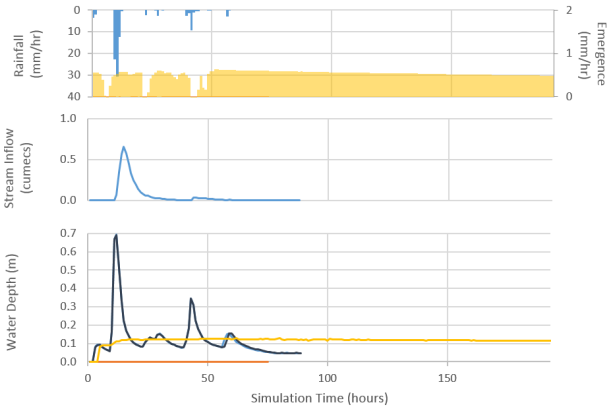

(a) 1/30 year simulation.

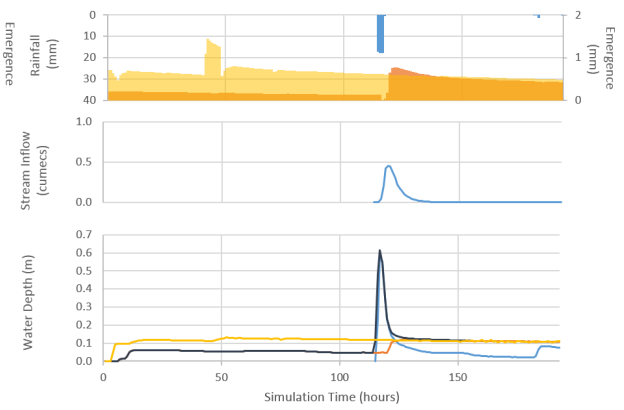

(b) 1/100 year simulation.

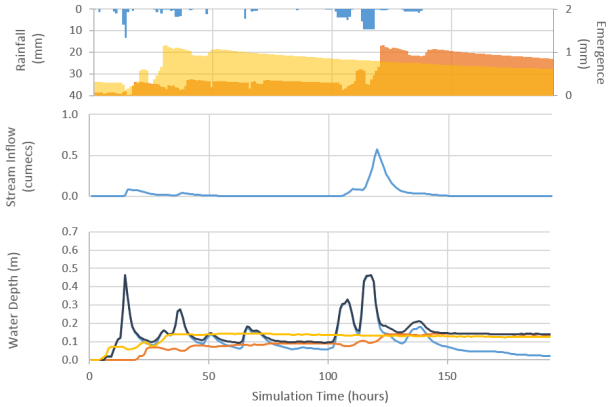

(c) 1/1000 simulation.

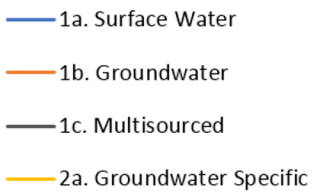

Figure 22.1: Hydrographs from the four sets of hydraulic simulations show the flood depths at Church Street as this is representative of flooding in the village (Fig. 17.7). Groundwater emergence is averaged across the whole domain.

rainfall, streamflow and groundwater inputs of the three suites of simulations however does not have the largest flood extent. In fact, the 1/1000 year multisource simulation has the smallest flood extent of the three multisource events while the 1/30 year event has both the largest extent and greatest extent volume (Tab. 22.1).

The fourth set of simulations, which took single source groundwater inputs only, can be seen in Figure 22.3b. As expected, these have a smaller extent than the multisource floods but are larger than the equivalent likelihood groundwater flood extents in Figure 22.2. This is because they are modelled on the greatest periods of groundwater emergence, whereas the multisource simulations use a range of groundwater and surface water conditions. The 1/30, 1/100 and 1/1000 groundwater floods have maximum extents of 68,500 m^2, 77,600 m^2 and 117,100 m^2 respectively (Tab. 22.1). The flood hydrographs at Church street (Fig. 22.1) show that these events can lead to persistent surface water depths of 0-10 cm, lasting the duration of the 8 day simulations. Differences between these single source groundwater floods are relatively minor but they show that groundwater flooding alone is capable of causing damage within the village, even on the 1/30 year likelihood.

The 1/1000 year groundwater flood samples the same event as the 1/1000 year multisourced

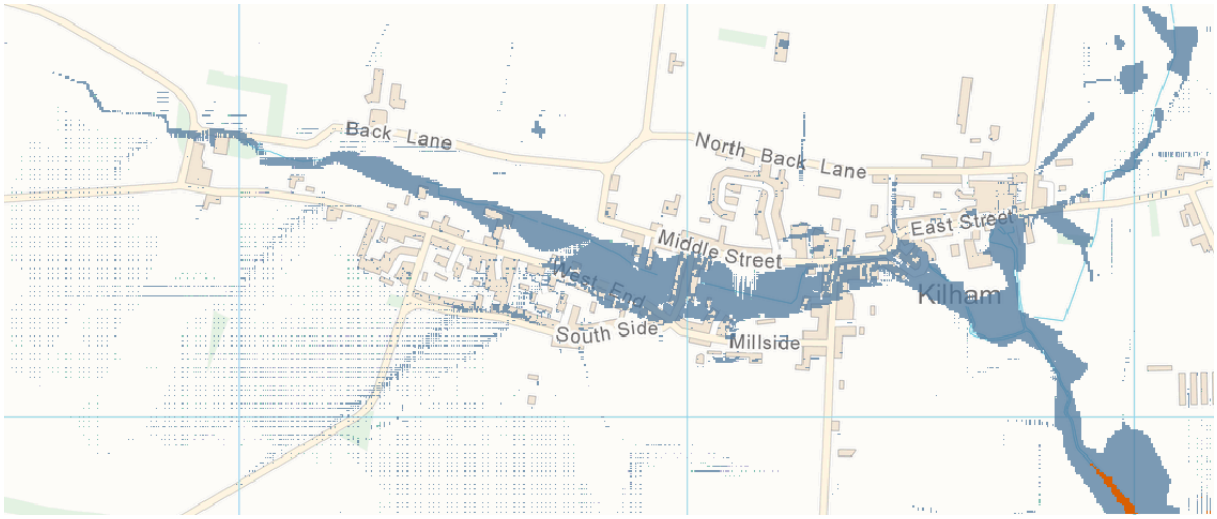

(a) The 1/30 year return period event.

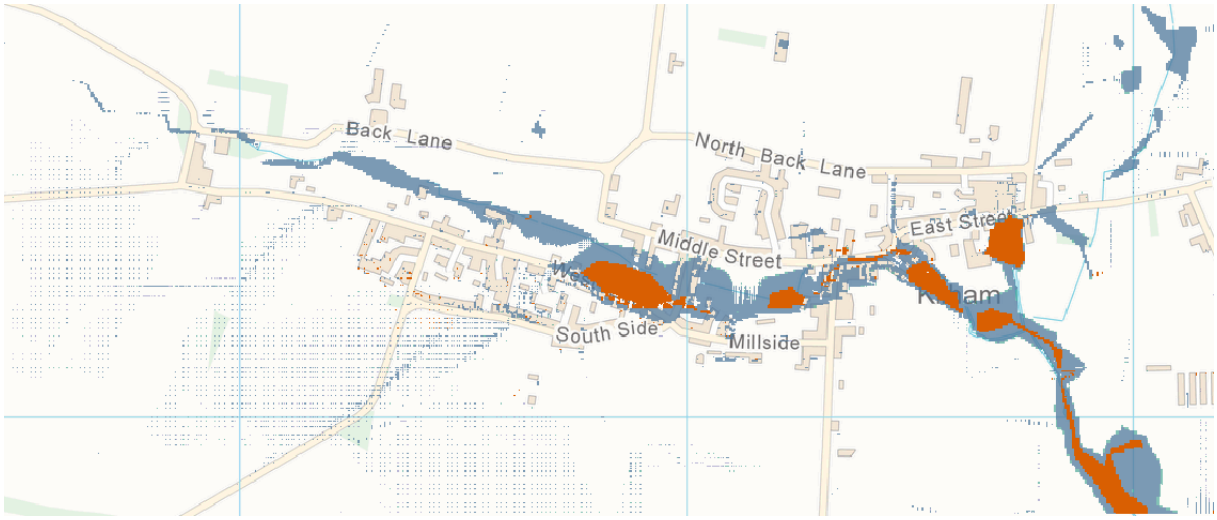

(b) The 1/100 year return period event.

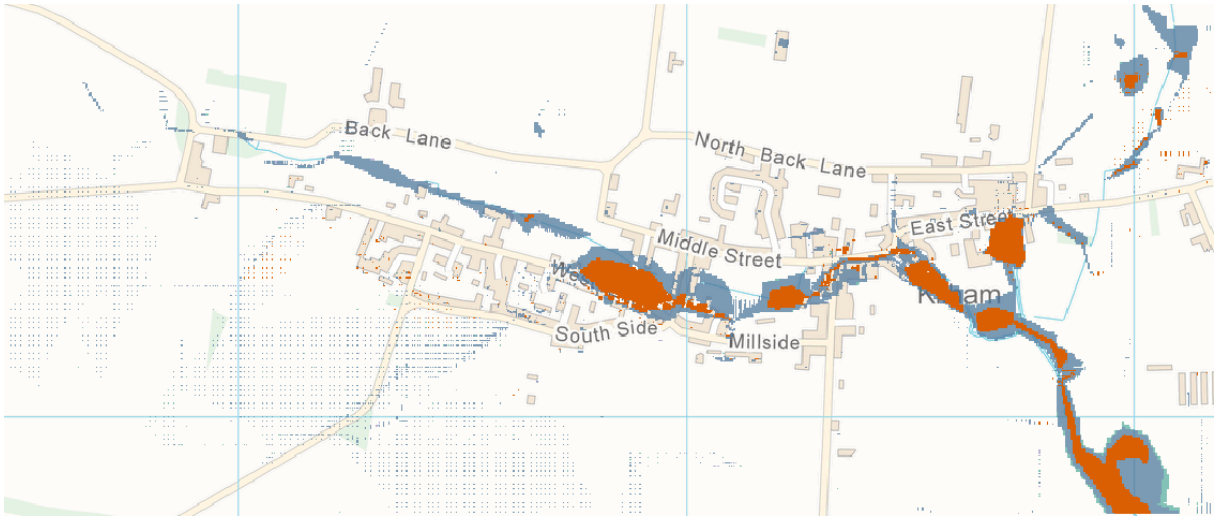

(c) The 1/1000 year return period event.

Figure 22.2: The first three sets of simulations can be seen here contrasting the flood extents caused by the different sources. Multisourced flood extents are always the largest, although how much larger varies between events. Orange - groundwater simulation; purple - surface water simulation, green - multisource simulation. Individual extents for the simulations can be seen in the Appendix. The chequerboard pattern seen in the hills surrounding the village is a result of the method used for processing the DTM. OS VectorMap^{TM} (Ordnance Survey (GB), 2019).

Table 22.1: The inputs and quantified outputs of the multisource (1c) and groundwater specific (2) simulations. In the multisource simulations the total rainfall and groundwater emergence per cell is shown along with the total stream inputs. The second table shows the total emergence for each cell in the domain, the number of active input cells and their mean emergence. Both tables show the number of cells covered by >10 cm of water during the simulation and the maximum flood volume during the simulation.

Simulation	**Rainfall**	**Inflow**	**Emergence**	**Flooded Extent**	**Max. Extent Volume**
MS 1/1000	143 mm	101 cumecs	105 mm	≈329540 m^2	90129 m^3
MS 1/100	55 mm	37 cumecs	59 mm	≈394550 m^2	108486 m^3
MS 1/30	92 mm	12 cumecs	0 mm	≈484900 m^2	122457 m^3

Simulation	**Emergence**	**Input Cells**	**Emerg. / Active Cell**	**Flooded extent**	**Max. Extent Volume**
GW 1/1000	147 mm	329238	1.84 mm/hr	117104 m^2	27180 m^3
GW 1/100	124 mm	798626	0.64 mm/hr	77600 m^2	20992 m^3
GW 1/30	97 mm	798626	0.51 mm/hr	68508 m^2	15987 m^3

flood, which initiates around 90 hrs earlier. This is because the greatest flow (used to define the multisource event) coincides with the period of greatest emergence (used to define the groundwater specific event). The considerable difference in extent between the 1/1000 multisource and 1/1000 groundwater specific flood extents demonstrates the importance of considering multiple sources.

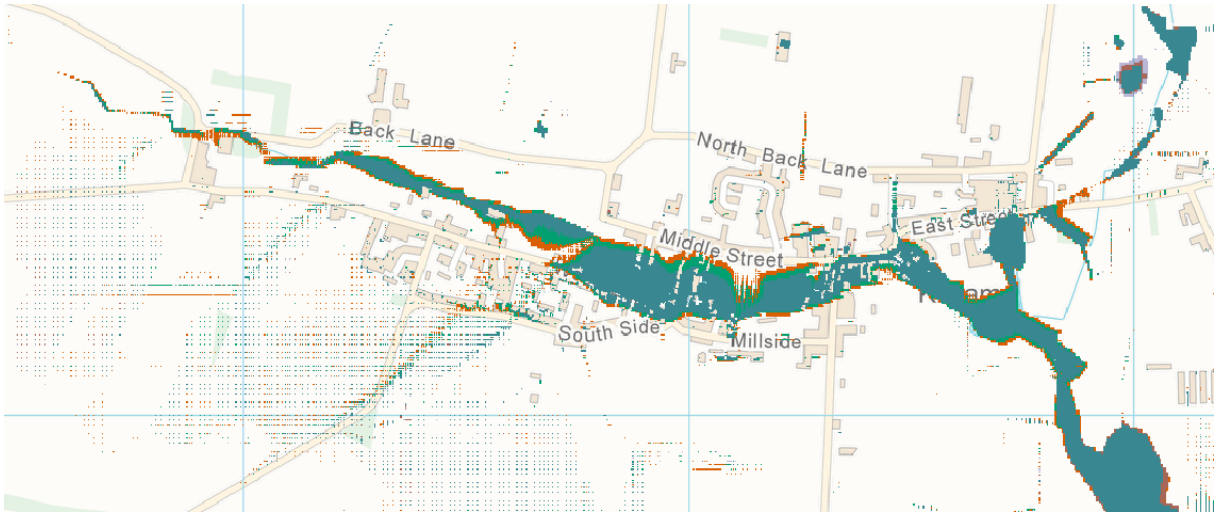

(a) Multisource simulations used groundwater, rainfall and streamflows as inputs in the hydraulic model.

(b) Groundwater simulations were modelled using groundwater as a sole input. These events, unlike the other simulations in this chapter, were selected according to the volume of emergent groundwater simulated by the hydrological model.

Figure 22.3: The flood extents of the multisource and groundwater simulations can be seen. Return periods of 1/30 years (orange), 1/100 years (green) and 1/1000 years (purple) are shown. Individual extents for the simulations can be seen in the Appendix. OS VectorMap^{TM} (Ordnance Survey (GB), 2019).

23. Discussion

23.1 Single Source vs. Multisource Flood Risk

The simulation results described in the previous section show that flooding from multiple sources does differ to flooding from a single source and that considering multiple sources will affect the estimated flood risk. This is clearly visible from the hydrographs in Figure 22.1. Considering multiple sources does not necessarily require modelling both sources, though when multiple sources were considered the flood risk was shown to be greater.

Results showed that modelling multisource flood events (such as the 1/100 and 1/1000 year events) cannot be reproduced by simply adding together two single source groundwater and surface water flood events, as is proposed in Horritt et al. (2010). These do not stack linearly in either extent, depth or duration - the relationship is more complex. This is evident from Figure 22.1, where adding the surface water trace to the groundwater trace does not produce the multisource trace. This non-linearity is also discussed in Kappes et al. (2012).

Simply adding single sources together may also lose important aspects with regard to the flood timings. The events used here show that groundwater flux into the model only increases following the surface water peak (see hours 120-140 in Fig. 22.1c), and so did not increase the maximum flood depth. If the sources are treated separately then this relationship may not be captured and combined depths could be overestimated.

While there are increases in the depth of the floods the clearest effect of modelling multiple sources is the increased duration of flooding when groundwater is considered. This matches expectations as groundwater flooding typically lasts longer than surface water floods and, as such, acts as a buffer when surface flood waters recede, not allowing levels to drop below that of the single source groundwater flood. Sommer et al. (2009), who created a coupled groundwater-sewerage system-surface water model for Dresden (Germany), also found that the multisource flood extents were not notably larger than those of the single source event. This does conflict with a more recent study by Saksena et al. (2019), who find that including surface-groundwater interactions increased flood extents in saturated conditions. They also note the importance of simulating both groundwater and surface water processes and find flood extents can decrease for events during dry periods when both processes are considered.

23.2 Comparisons with Other Flood Maps

While there are very few multisource flood hazard maps available (Sec. 4.4), and none found that include groundwater, there are some that look at single sources alone. Two examples of these are included below to benchmark the results from this study. These are the Environment Agency's River and Sea and surface water flood risk map and the BGS groundwater susceptibility map.

As discussed in Section 20, although the former of these are termed *risk* maps by the EA, they actually refer to hazard.

23.2.1 Environment Agency Flood Maps

As discussed in Section 4.2, the Environment Agency produce two freely accessible online maps: the Flood Map for Planning and the Long Term Flood Risk Map. The latter of these includes both the risk of flooding from rivers and sea and the risk of flooding from surface water. As such it is the Long Term Flood Risk map that will be used here. In Kilham, the extents from these two maps are approximately identical. There is no *low risk* rivers and sea flood category for this area on the EA map.

Figures 23.1 & 23.2 show the estimated flood risk from rivers and the sea and from surface water respectively. A guidance document provided by the EA upon request suggests cropping all flood depths less than 10 cm from flood outline (Environment Agency, 2010). The Risk of Flooding from Surface Water map crops flood extents based on a hazard score (Equation 23.2.1). Whichever is used here, the level of depth or hazard should be similar between the EA maps and the maps produced here.

Equation 23.2.1 — EA Hazard Score. The Environment Agency use a hazard score to crop the flood extents in their Flood Risk from Surface Water map (Environment Agency, 2013c).

$$Hazard\ \ Score = depth \times (velocity + 0.5) + debris factor$$

As stated above regarding the maps produced here, the multisource maps are largely similar in extent to the surface water maps. As such, any comparisons made between the extents produced by the EA and those produced here do not reflect groundwater processes.

Both of the EA maps show flooding following the river network flowing through the village, a pattern well matched in the maps produced here. The multisourced extents are typically larger than those produced by the EA for Kilham but are less continuous and do not precede as uniformly up the valley. This may be due to the different inputs between the two methods, with the inputs in this study being more persistent. The EA surface water map is therefore perhaps more comparable to the maps in Figure 18.4, to which it is again similar.

The EA maps show a significant difference between the extents of the different events. This is not seen to the same extent in the multisource map. The 1/30 year multisource event is considerably larger in extent than the equivalent high risk EA extent. This is due to limitations with the model coupling - see Section 23.3.3.

If a greater variety of multisource events were modelled it may be possible to see the extents vary between the two endmember EA maps as the ratio of fluvial:pluvial input varied. However, it can be seen from Figure 23.7 that river flows are present in all of the peak 100 events.

Table 23.1: The flood risk categories for the Flood Map for Planning (Environment Agency, 2013a) and the Long Term Flood Risk Map for England (Environment Agency, 2019a).

Flood Map for Planning	Long Term Flood Risk Map	Annual Flood Probability
Flood Zone 1	Very Low Risk	<1/1000
Flood Zone 2	Low Risk	>1/1000
Flood Zone 3	Medium Risk	>1/100
-	High Risk	>1/30

Figure 23.1: The Environment Agency's long term flood risk map (Environment Agency, 2019a) showing the estimated flood risk from rivers and the sea in Kilham.

Figure 23.2: Environment Agency Long Term Flood Risk Map for England (Environment Agency, 2019a) showing the estimated pluvial risk in Kilham.

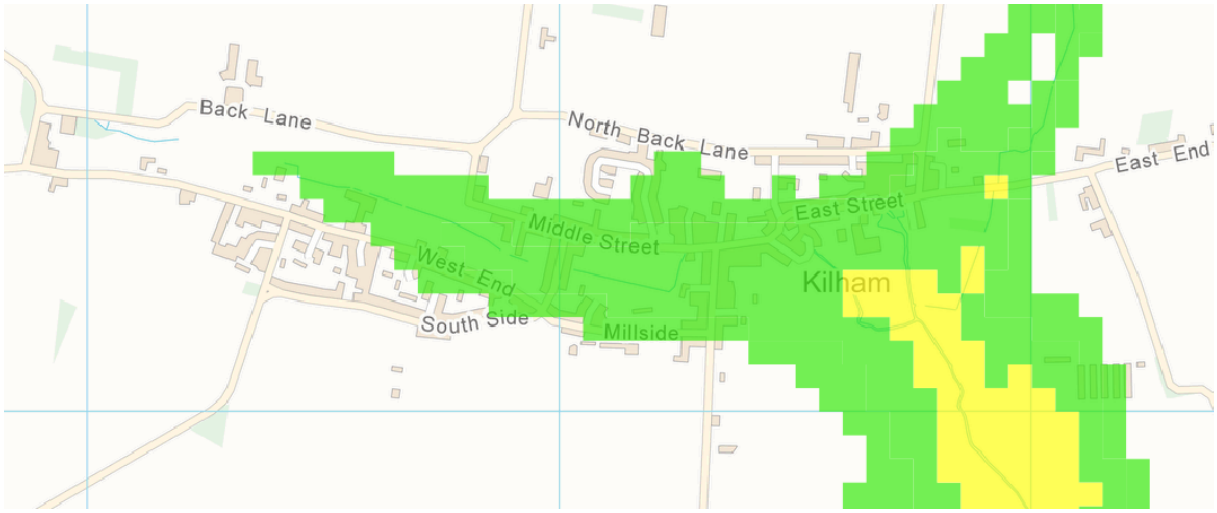

Figure 23.3: This map shows the BGS groundwater susceptibility for Kilham. Green represents areas with potential for subsurface flooding (e.g. basements and cellars) and yellow represents areas with potential for groundwater flooding at the surface. Derived from 1:50 000 scale BGS digital Data under Licence No. 2019/055 British Geological Survey. ©UKRI. OS VectorMap™ (Ordnance Survey (GB), 2019).

23.2.2 BGS Groundwater Susceptibility Maps

The British Geological Survey have produced groundwater susceptibility maps for the UK. These show areas where it is thought that groundwater flooding has the potential to occur (for more information, see Section 4.3.2). An extract from the BGS map can be seen in Figure 23.3 showing suspected potential groundwater emergence patterns in Kilham (British Geological Survey, 2019b). The BGS map has two colour categories: green indicates areas that may flood in the subsurface (e.g. cellars, sewerage systems etc.) and yellow indicates areas where groundwater may emerge at the surface. Although the hydrological model used in this work has not been used to indicate any flooding of subsurface structures, it does have the potential to be used for this.

Comparing the BGS map to the groundwater inundation map produced in this study (Fig. 22.3b) and the emergence pattern from the hydrological modelling (Fig. 23.6a), we see that there are similarities in the emergence patterns. Both the BGS map and the work of this study indicate that the main emergence is concentrated in the village's valley, and, more specifically, towards the lower, east end of the village. The hydrological model does indicate that there is much larger potential for emergence higher up the valley, occurring from the central field down to the field south of Church Street. This is reasonable as groundwater emergence has historically been found at higher elevations than those estimated on the BGS map, such as the springs, found within the village (East Riding of Yorkshire Council, 2013).

One benefit of the modelling approach undertaken in simulation suite 2b of this study is that it allows for the production of groundwater induced flood maps (following the work of Morris et al. (2018). Maps of groundwater induced flooding are highly relevant for those areas down slope of the emergence - they give more of an indication of the severity of the flood (i.e. whether it will be compounded by emergence from other areas) and can be used to generate depths if desired. One of the benefits of the BGS approach is its relative simplicity as it does not require detailed hydrological modelling or the associated data and poses less risk of introducing uncertainty. This allows the approach to be more easily applied nationally where the geological data exists.

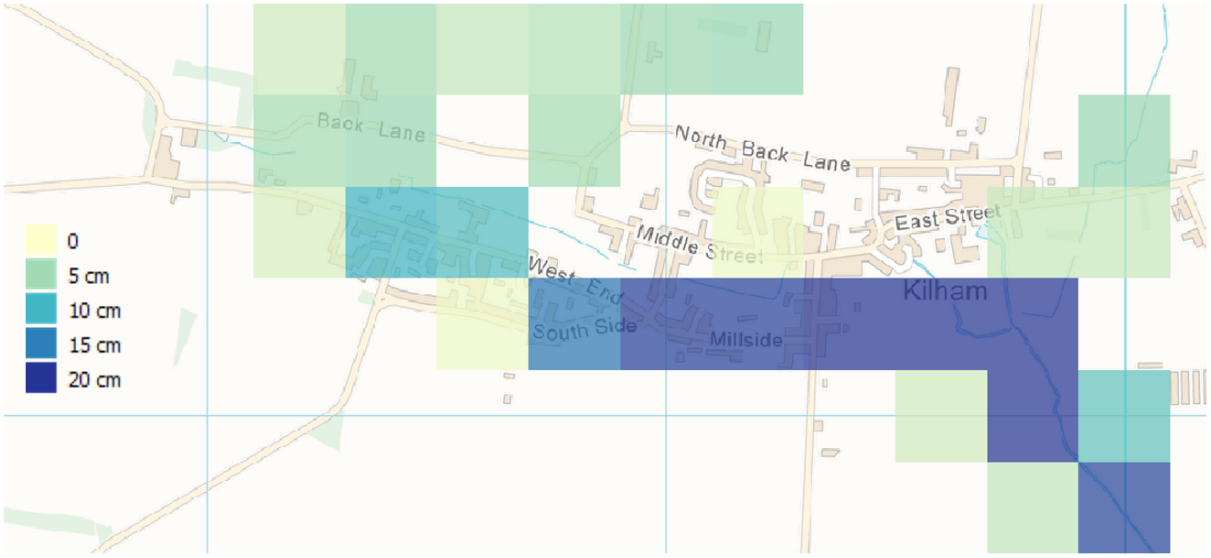

Figure 23.4: This figure shows the depth of surface water in Kilham as simulated by SHETRAN at the point of peak flow in the 1/1000 year event. OS VectorMap^{TM} (Ordnance Survey (GB), 2019).

23.3 Critique of the Methodology

The methodology used here demonstrates one process for modelling and quantifying multisourced floods. This is, to some extent, possible via the use of integrated hydrological models (Sec. 3.3.1). As discussed, SHETRAN itself is able to simulate flooding from multiple sources, but at a much lower spatial resolution than in the methodology used here.

Figure 23.4 shows the flood extent for the 1/1000 year event as simulated by SHETRAN at the time of peak flow, prior to hydraulic modelling. Much of the lower valley has around 15-20 cm of flooding and there are shallower depths of around 5 cm higher up the village around Back Lane. This volume of water totals around 108 500 m^3, with an additional 1800 m^3 of water in the channel system. This is not far from the 90 129 m^3 present in the hydraulic model at the point of maximum extent a few hours later (Tab. 22.1). This smaller volume may be due to the lack of overland flows passed to the hydraulic model, as these were found present in the hydrological 1/1000 year event.

The main difference between the hydrological and hydraulic models is in the extent pattern, where the use of the hydraulic model drastically alters the consequence of the flooding. In the hydrological extent, there are deep floods over much of the south side of the village, whereas in the hydraulic model these have been routed slightly further north, following the stream and greatly reducing the number of properties and roads exposed to flooding.

To those familiar with the field of hydrology it would be clear that floods would not follow the blocky pattern in Figure 23.4 and that they would most likely follow the valley profile. However, the use of the MMS removes the necessity of this interpretative step and creates extents that are simple to interpret and communicate.

The increased resolution provided by the hydraulic modelling is therefore shown to be a valuable tool. It generates a more realistic estimate of potential flooding that should aid the estimation, conveyance and mitigation of flood risk.

23.3.1 Reducing Computational Requirements

The hydraulic simulations conducted here all used spin up periods of five days. This was to ensure that the simulations had long enough to generate the appropriate antecedent conditions

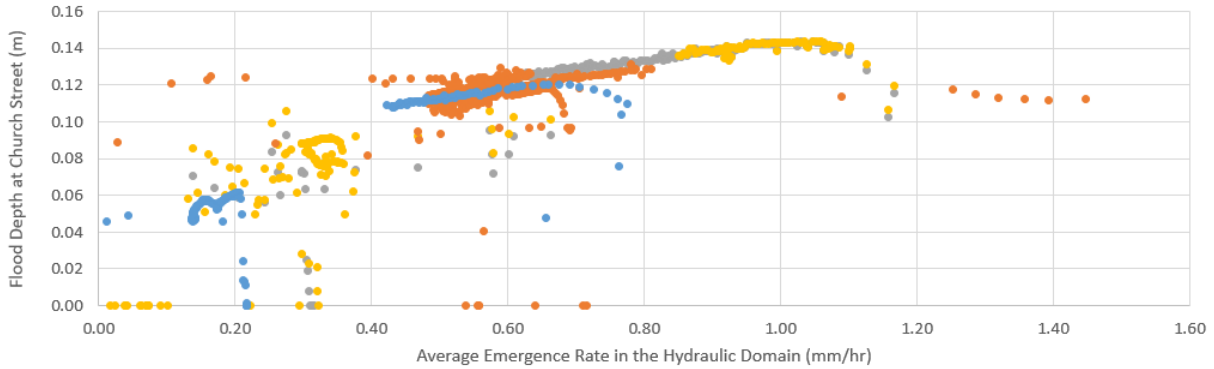

Figure 23.5: Average groundwater emergence from the events are plotted against their paired simulated flood depths (at Church Street). A broad correlation between emergence rate and flood depth can be seen. It is proposed that emergence rates could be used in a simplified method to estimate depths for points in the domain. Data taken from Figure 22.1.

and to allow for any stream flows to permeate through the domain, as these were only input at the domain boundaries. From Figure 22.1 it can be seen that these long run-in periods are not necessary. In all of the events the groundwater induced flooding rises and become relatively steady over a period of hours. This period alters depending on the location of the measuring site within the domain, but at all times stabilised within 24 hrs. This period is likely to change depending on the nature of the case study site, but a five day period proves to be unnecessary.

One benefit of this is the reduction in the computational resources required for the hydraulic modelling. This enables shorter simulations and therefore the potential to run a wider range of events but also opens up the opportunity to simulate a longer period following the flood peak. This may indicate further hazards following storms, where water on the surface causes smaller subsequent pulses of rainfall, emergence or streamflow to cause further issue. It should be noted that if future work introduces infiltration then the length of the spin up period may need to be increased.

In some instances, groundwater flooding can last for many weeks - even with the initial 5 day spin up period removed, modelling such durations with the modelling system designed here would be computationally expensive. Such modelling may not be necessary however as the duration of continuing emergence can be determined from the hydraulic model inputs or the hydrological outputs and used to estimate the duration of any flooding.

Figure 23.5 shows emergence rates and paired flood depths (taken from the Church Street location) for the different simulations. It shows that, at least to some extent, the depth of flooding can be estimated from the emergence rate. This plot does not take into account any lag between the emergence and the flood response and so the relationship is likely to be able to be improved with further analysis. The duration and rate of any persistent groundwater emergence following a flood peak it could be determined, along with an estimation of the resultant depths at sites across the village without the need for further detailed modelling.

This process of estimating groundwater flood depth from emergence rates does first require hydraulic modelling to generate depths, however there is potential to do this synthetically without the need for the complex coupling process. Figure 23.6a shows the groundwater emergence pattern for the village, counting all cells that exhibit emergence at some point during the 100 year simulation containing the 1/1000 year groundwater induced flood event. The hydrological Kilham model produces spatially consistent patterns of groundwater emergence across different events. These use only 10 of the 15×7 cells covering the village domain. As there are a relatively limited number of cells within the model that produce emergence it would be relatively simple to

generate a range of possible emergence rates from these cells. Figures 23.6b & 23.6c go on to show that many of these cells have strong correlations to one another (in this example correlations are calculated in relation to cell [11,2]) and as such it is plausible that the range of emergence values can be realistically distributed between these cells. From here a hydraulic model could be used with stepped inputs within this range of emergence rates, with each step lasting long enough to reach a steady flood depth. The hydrological data could then be analysed to determine the likelihood of each of the emergence rates to give the probability of groundwater flooding in the village.

This simplistic approach would reduce the computational resources required to estimate the groundwater flood in comparison to using the MMS and could be used as a rough benchmarking tool. However, uncertainty would be introduced with each of the above steps and could only be used to estimate single source groundwater risk, not that from all sources.

23.3.2 Event Classification

The method used for classifying events seems appropriate for the task, showing, in the hydrological model at least, that the events build in size as they become more extreme. However, this method of event selection was chosen for its simplicity and so does bring limitations. The most striking limitation is the variation in the active sources in terms of their input volumes, intensities and durations. This is shown by Figure 23.7, which plots the relative proportion of sources making up each of the top ranked 100 flow events (event 1 is the largest, i.e the simulated 1/1000 year event). The relative contribution of the different sources to each event varies greatly - event number 33 (the 1/30 year event) is shown to be entirely surface water driven, while event number 32 (1/31 year event) is dominated by groundwater. Had the events ranked differently, they may have been differently proportioned and thus delivered different results. This confirms that flood drivers (e.g. rainfall, upstream streamflow or groundwater emergence) should not be used to identify multisource flood events.

This then demonstrates an issue of using single events to assess multisource risk. One method for addressing this would be to simulate a range of events for each return period. I.e. the 32^{rd}, 33^{rd} and 34^{th} ranked events could be used to represent the 1/30 year flood. While this may be appropriate for the more likely events, it would be difficult for the more extreme conditions as a much larger volume of hydrological modelling would be required as the current difference in average return interval between the 1^{st} and 2^{nd} events is 500 years, which is not appropriate. As such, this method is not considered applicable for the larger magnitude events. It should also be noted that simulating a range of events does not guarantee the capture the full range of possible sources for those events.

A second approach was also considered, but discredited: creating events synthetically by using separate inputs, with the combined probability of the component sources equal to that of the desired event. E.g. :

$$\frac{1}{100}yr\ Flood = \frac{1}{25}yr\ Groundwater\ Emergence \times \frac{1}{2}yr\ River\ Flow \times \frac{1}{2}yr\ Rainfall$$

There are multiple combinations of source likelihoods that could create a 1/x flood. A range of these combinations could be modelled and the worst case scenario flood could be used to represent the desired event by using the common metrics of extent, depth duration etc. This method of using different sources is similar to other work that uses different rainfall intensities to represent the range of plausible storms that may generate 1/x year flooding (e.g. Environment Agency, 2013c). Such a simplistic method should not be applied to flooding from multiple sources as it would not take into account the relationships between the sources. Furthermore, with regard to the methodology developed in this thesis, it would detract from the purpose of using the

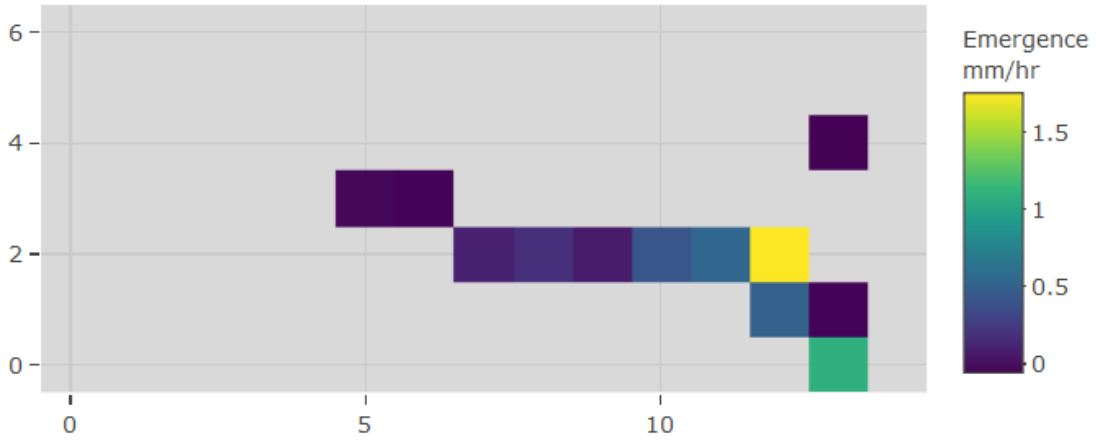

(a) Only six cells have average emergences of over 0.2 mm/hr.

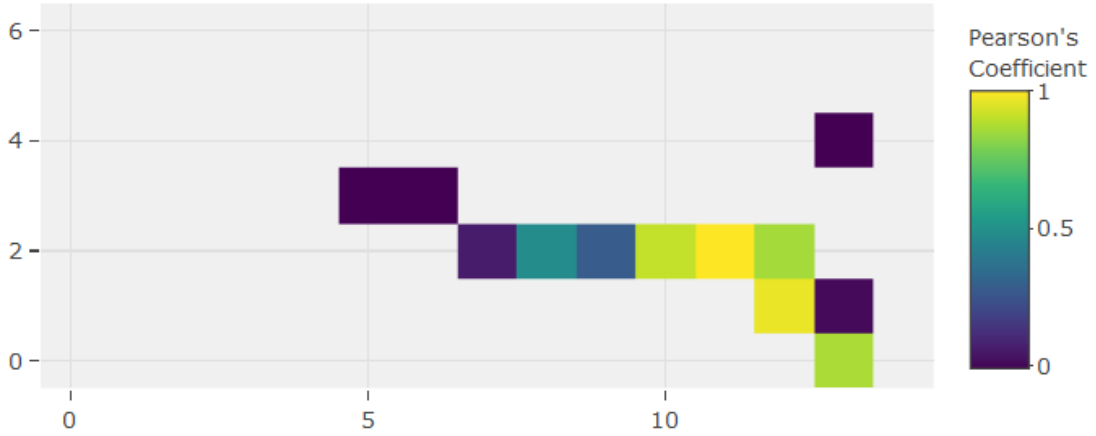

(b) The cell with the greatest emergence shows good correlations (upwards of 0.77) to the emergence time series of four of the other five cells with emergences over 0.2 mm/hr.

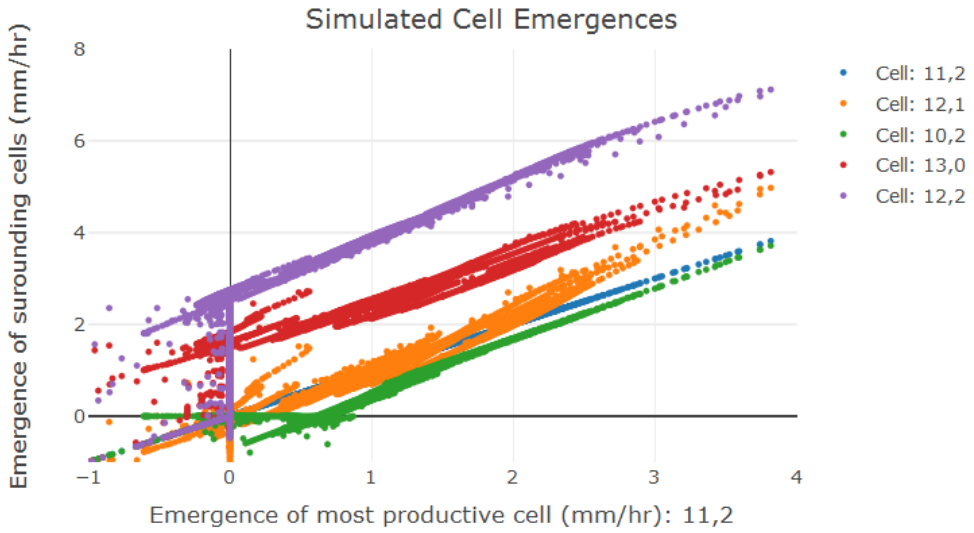

(c) 200 days of simulated hourly emergence is plotted for five cells against the cell with the greatest emergence: cell 11,2.

Figure 23.6: These plots show groundwater emergence in the 15×7 SHETRAN cells that cover Kilham village. Of these, only 12 show groundwater emergence. Emergence data is taken from 100 years of the hydrological simulation and uses only periods of positive emergence.

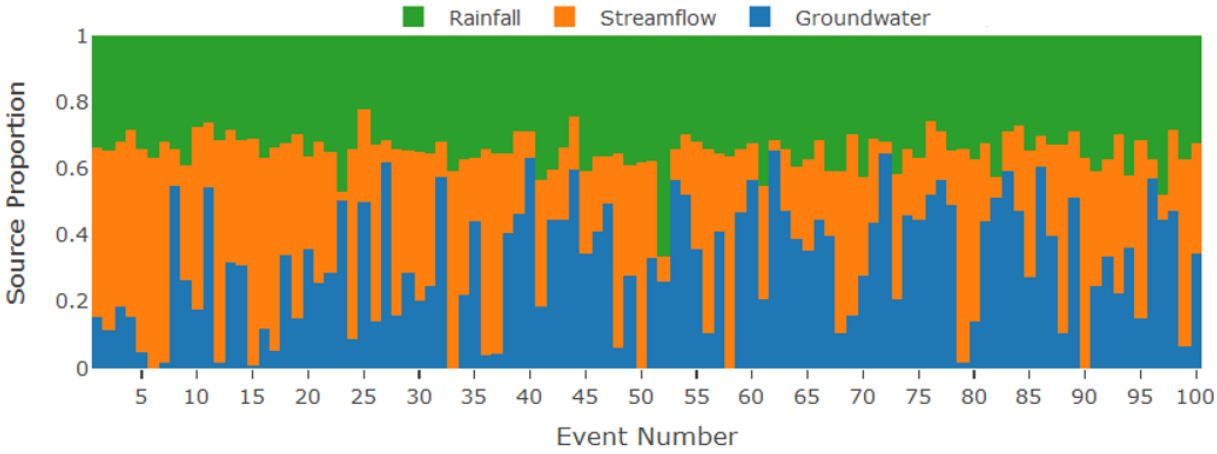

Figure 23.7: The relative source inputs are shown for the top 100 flow events in the hydrological model. Streamflow and combined rainfall and groundwater inputs have been normalised by their means to enable comparisons. By normalising the rainfall and groundwater together their initial comparable state is preserved. Interestingly, no source becomes more or less dominant with event magnitude.

physically based modelling system, much of which is to generate a plausible range of hydrological scenarios. It would not be known whether such source combinations are plausible and would assume that all sources are equally responsible for generating flooding, which is not true.

Both of these proposals involve using multiple scenarios to describe a single risk. The Environment Agency (2013c) combine different scenarios to create a worse case scenario - this is a legal requirement in the design of some potentially hazardous infrastructure and has been of interest to some insurance companies governments over past decades (Felder et al., 2017). While others (e.g JBA Consulting, 2014a) have chosen to display the range of potential outcomes.

One further complication of event selection is that this variation in the proportion of the component sources varies spatially within catchments. Using the Kilham catchment as an example, events for areas north and west of Kilham (e.g. Langtoft and Burton Fleming) are likely to contain groundwater as these lie directly on the Flamborough Chalk Formation whereas those locations to the south and east (e.g. Driffield) sit on the less permeable Devensian till and are thus expected to suffer more from surface water events. Furthermore, the topography or land use of different areas may make some sources more prevalent. As such, simulating multisourced events may be applicable for one location but not another. Assuming that events apply equally to all locations in the catchment may falsely infer a reduced flood risk. Flood assessments should therefore use events specific to different areas, rather than the much more spatially homogeneous methods that are suitable for use in single sourced risk assessments.

23.3.3 Model Coupling

While there is good agreement between the extent volumes in the hydraulic and hydrological modelling of 1/1000 event, this is not so for the 1/100 and 1/30 year events. There are differences in the streamflows downstream of the village. In the hydrological model, these streamflows peak at approximately 1.1 m^3/s, 0.8 m^3/s and 0.7 m^3/s for the 1/1000, 1/100 and 1/30 year events (Fig. 21.3). In the hydraulic model, surface water depths peaked at 1.25 m, 1.15 m and 1.27 m for the relative events, a different order to what was expected. Although the latter set of values are depths rather than flows, these are proportional to one another and so are still an appropriate metric for ranking processes.

This inconsistency between the hydraulic and hydrodynamic model is thought to be due to the lack of infiltration in the model coupling. When the modelling system was developed,

infiltration was not thought to be consequential to the modelling process as, during storm periods, the ground surface was assumed to already be, or to rapidly become, saturated and unable to transmit notable volumes of water out of the system. It was also thought that this would be of decreasing importance as event magnitude increased (Glenis et al., 2018). This may not be what is implied by the simulation results here however. Figure 23.8 shows the minimum, mean and maximum vertical flows at the surface in the hydrological model over the village area during the three storm events. In the 1/100 and 1/1000 year events there are periods of emergence between 0-14 mm/hr, as would be expected considering their sizeable groundwater components. However during these events, and especially in the pluvially dominated 1/30 year event, there are periods of significant infiltration. During the rainfall pulse in the 1/30 year event the mean downwards vertical flow (i.e. infiltration) is approximately equal to the rainfall. This explains the greatly reduced flood extent in the hydrological model for this event. Following each of the infiltration spikes, there are increases in emergence, this, presumably, is from the infiltrated water flowing through the subsurface and emerging downslope. Furthermore, there is support for the presence of infiltration during storm events in the literature (e.g. Wilson et al., 1990; Xue and Gavin, 2008). It is unclear whether emergence is a result of piston flow, or from the inputted rainfall flowing just below the surface, or whether this is caused by rising groundwater levels.

Future work on the modelling system should build in the capacity to account for infiltration. This could be achieved at the input level during coupling by removing the hydrologically estimated infiltration from the inputs. This could also be achieved using a model capable of calculating infiltration (e.g. Glenis et al., 2018).

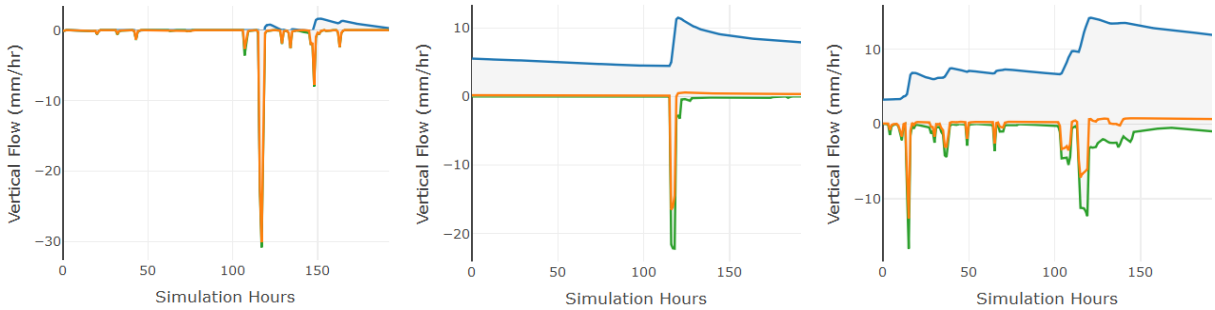

(a) 1/30 year event. (b) 1/100 year event. (c) 1/1000 year event.

Figure 23.8: the above plots show the maximum, mean and minimum vertical flows across Kilham village in the hydrological model. In all three events, some cells show large infiltration rates of up to 30 mm/hr.

One initial concern with the MMS was that the lack of coupling of groundwater emergence from river cells in the hydrological model to the stream areas of the hydraulic model would impact the results of the modelling system. These were not coupled due to the complexity of re-mapping the 200 m long orthogonal cells into a realistic pattern on the 2 m resolution hydraulic grid. At the peak of the 1/1000 year event the average emergence for the 21 river cells in the domain is less than 0.1 mm/hr. Spread across the entire domain, this makes an average input of only around 0.002 mm/hr of emergence per cell. This is very minor when compared to the other model inputs (Tab. 22.1). As such, this is not thought to have a noticeable affect on the simulations.

23.4 Conveying Multisource Flood Risk

Combining groundwater and surface water sources makes comparing and displaying flood events much more challenging, one of the issues with multi-hazard risk discussed by Kappes et al. (2012). One aspect of this is the variability of the flood extents; with different active sources, water

enters the domain via different points, which opens up different storages and floods different areas. For example, a rainfall dominated event will distribute water relatively evenly across the whole hydraulic domain and accesses extensive storage opportunities whereas a groundwater dominated event will distribute the majority of the input in the lower regions of the domain with less access to storage. This can be seen to some extent in Figure 22.3a where the 1/1000 event (which contains the greatest volume of groundwater) has the widest extent of the three simulations in east of the domain, but the narrowest extent in the west of the domain.

A further complication is the necessity to convey information on event duration, as this is found to vary greatly when multiple sources are considered. This challenge was identified by Horritt et al. (2010) during the scoping phases of the MAST project (Sec. 4.4) but is not something that the current flood maps take into account. Such issues are also prone when considering joint coastal and fluvial flood risk, where information is rarely provided concerning the likelihood and intensity of fluvial floods that are conditional on coastal water levels (Ganguli and Merz, 2019).

The traditional method of using average return periods to quantify single source events can be effective and is a useful standardised measure of likelihood, providing their correct interpretation (see Pielke, 1999; Serinaldi, 2014). Return periods also facilitate the mapping of flood extents, which are an effective tool for conveying flood risk. However, for multisourced assessments this approach is less useful and a more novel solution may be required in order to communicate multisourced risk effectively.

Before moving on to more complex methods however, it may be possible to develop the current approach into something capable of conveying multisource risk by adapting the figures used here. Taking the multisourced extents from Figure 22.3a and combining them with the groundwater extents of Figure 22.2 would be a simplistic way of indicating those areas that may flood from a 1/x event, while also indicating those (groundwater) areas in which the flood may be especially persistent. While this would begin to address the issue of the lack of temporal information in extent mapping, it would not combat the issues associated with using specific events to describe risk (Sec. 21.3).

One approach for reducing the volume of data to convey may be to give each flood a hazard score based on factors such as duration, depth, intensity, extent etc., such as in Odeh (2002). One caveat is that the nature of the flood would be lost: a shallow, long duration groundwater flood may be indistinguishable from a deep, short lived surface water flood.

Alternatively, these factors could be displayed in a hazard matrix, with events described according to their maximum extents, depths and durations. This would retain information on each of the events while giving the reader an understanding of the possible range of hazards and, therefore, the information to make mitigating decisions appropriately. A 4th dimension, likelihood, could be shown using a second descriptor such as colour or size. An example of this can be seen in Figure 23.9b.

There may be the potential to develop this further by associating the axes with event drivers. This, as previously discussed, is difficult, however in the case of groundwater at least, this is thought plausible. This may then have the potential to be linked to existing tools such as the Hydrological Outlook UK system (Centre for Ecology and Hydrology, 2019), which provides monthly forecasts on streamflows and groundwater levels for the following 3 month period (Prudhomme et al., 2017). Forecasts could be benchmarked against the hazard matrix to estimate the potential for flooding.

A review by Kappes et al. (2012) outlines a method for going one step further and developing risk scores. Kappes et al. (2012) propose quantifying risk numerically in terms of resultant risk metrics such as damages, loss of life, etc. rather than displaying maps of hazard extent and duration. This is the next step in the methodology proposed here, to develop hazard into risk.

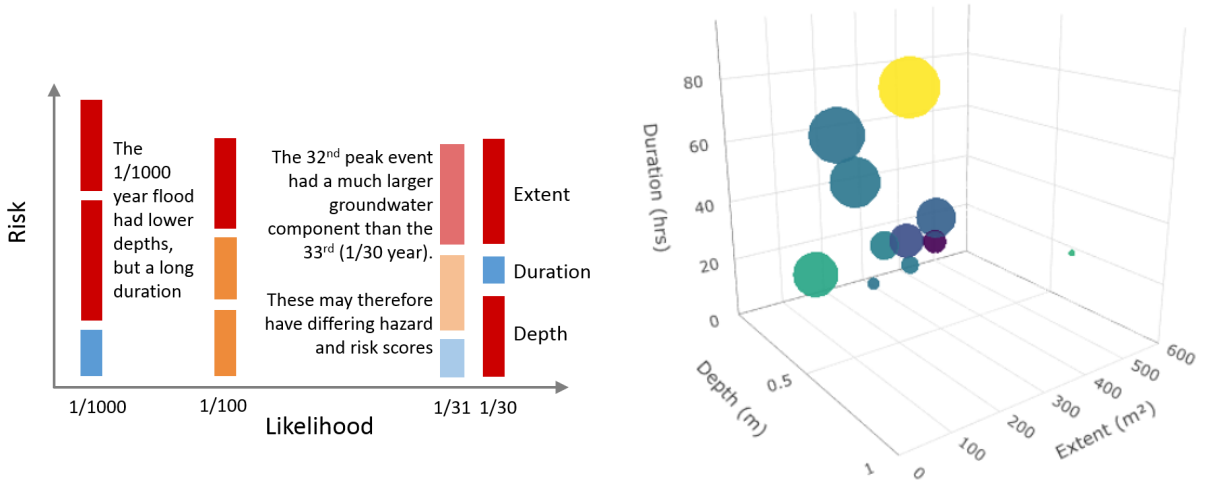

(a) A simpler plot showing the risk and its likelihood. Coloured bars represent the hazard components.

(b) The proposed method for conveying risk takes into account multiple factors and shows a likelihood (colour) and risk or hazard (size).

Figure 23.9: Different proposed visualisations for conveying the more complex multisource risk.

This involves calculating the vulnerability of the area being affected by the hazard. This will be dependent on both the vulnerability of the area and the nature of the flood (flow speed, depth duration etc.). As there are mechanisms for doing this already, this is not discussed further.

It is proposed that to best convey the multisourced flood risk of an area all peak events should be modelled and then plotted according to the physical descriptors deemed most valuable. These should then be combined with vulnerability to generate risk scores which can be added to the plot (Fig. 23.9b) to generate a risk matrix. An overall score for the risk matrix could be used to describe different areas and identify hot spots that warrant a more in-depth investigation. It can be argued that describing the risk in multiple variables, such as with the proposed 3D plot, is not simple to visualise. Such plots are not necessary, the important step is to transition into showing risk, rather than flood extents with likelihoods (e.g. Figure 23.9a), as this step reduces the number of descriptors and variability of events to convey.

Although this would require more processing than a simpler hazard score, it would be simpler to convey and would achieve the ultimate aim of transitioning from *hazard* to *risk*. Mapping the risk scores could identify hotspots where damages are likely to be greatest or that may benefit most from investment in mitigation or adaptation. In comparison to current tools like the Flood Maps for Planning, describing and displaying risk in this manner would be more directed at decision makers, such as the Environment Agency and local councils, rather than property owners or prospective buyers. If risk is calculated and used for describing potential flooding then it is important that the methodology for doing this is uniform across all areas that the maps may be used in. If not, then the ability to compare multisource maps in different locations or countries could be lost (De Moel et al., 2009).

24. Conclusion

The methodology for assessing flood risk from multiple sources developed in previous chapters was implemented at a case study site in East Yorkshire. 1000 years of synthetic meteorological data were generated and used to run a 1000 year hydrological simulation. From this, peak flood events are identified and used to represent 1/x year return period multisource events. Inputs to these events were then fed into a hydraulic model for high resolution surface routing. Flood extents, depths and durations were compared between multisource simulations and simulations of their separated component sources.

Combining surface water and groundwater processes in the hydraulic model increased flood depths following flood peaks. In the 1/1000 year simulation including groundwater increased flood depths at one location within the village by over 4 cm, a third of the total depth at that point. High rates of groundwater emergence were only found to occur following flood peaks and so did not increase the peak depths. As the time to peak for different sources are different it was not possible confirm that combined sources also have the potential to increase peak depth. One useful outcome from this is the ability to estimate the severity of smaller rainfall pulses following events in the presence of persistent groundwater emergence. Summing depths of the single sourced groundwater and single sourced surface water simulations does not return the depth of the multisource simulations.

Flood durations are increased when groundwater is included in the modelling process. Groundwater emergence was found to be persistent during both the 1/1000 and 1/100 year events and caused flooding to persist beyond the end of the simulation (72 hrs after the estimated flood peak). During this period, and throughout the simulation, flood waters were unable to decrease below the depth of water caused by groundwater alone.

One unexpected result was that combining sources did not appear to greatly increase maximum flood extent. This is likely to be because the delayed groundwater inputs were typically low during the time of peak.

For single source groundwater simulations the approach used here is capable of producing maps indicating the likely extents of groundwater induced flooding for different emergence events. This offers more functionality than current groundwater flood susceptibility maps as these indicate only the areas likely to witness emergence and are unable to indicate the likelihood of such events. The methodology used here does however require increased computational resources and the development and validation of an accurate hydrological model. This approach addresses the potential for using hydrological models to simulate groundwater induced flooding identified by Morris et al. (2018).

Significant variability was found between the flood volumes from the hydraulic simulation and those from the hydrological simulations for the intense 1/100 and 1/30 year events. This was attributed to the lack of infiltration coupling in the modelling system. Infiltration was not

included in the coupling process as it was not thought to be prevalent during storm periods as the surface was though to rapidly become saturated and to thus transform rainfall directly into overland flow. Furthermore, it was assumed that during periods of groundwater emergence the ground surface would already be at saturation point and thus not allow further infiltration. Further investigation indicated that the hydrological domain has significant spatial variability in vertical flow rates with some hydrological cells infiltrating water at rates of up to 30 mm/hr during intense rainfall of the equivalent rate. In the 1/1000 year event there were mean infiltration rates of around 7 mm/hr in the upper domain while groundwater was emerging at rates up to 10 mm/hr in the lower domain. As such, it is essential to build in the capacity to account for infiltration in future work. This could be done at the input level, by removing the hydrologically estimated infiltration from the inputs, either using infiltration rates from the hydrological model itself or via simple functions (e.g. Environment Agency, 2013c), or it could be achieved using a model capable of calculating infiltration.

Further modelling work should therefore focus on the inclusion of infiltration into the modelling system as well as overland flows, as these were present in the 1/1000 year simulation. The methodology should also be implemented at a second case study site to establish what effects are locally specific to Kilham village.

It is clear from the range of events simulated that there is variability in terms of event sources, with the 1/30 year event simulated here proving to be entirely surface water driven. While modelling single sourced events is part of the assessment process the variability between event sources leaves work for assessing the potential for a more comprehensive method of event modelling, whether using a Monte Carlo type investigation that simulates a greater range of peak events or by classifying hydrological conditions to create more generalised hydraulic input patterns.

The methodology implemented here proved useful for both increasing understanding of multisource systems and for assessing the risk from multisourced floods. Using a hydrological model to simulate long hydrological period informs the user of the range of potential flood events while the hydraulic modelling aids their interpretation by generating understandable and mitigatable flood extents and depths.

The increased understanding of source interaction and the quantification of flood likelihoods offered by this methodology creates potential for improving flood management strategies. Such strategies, as well as flood tolerances for new infrastructure, have the potential to be developed based on multisource events, rather than single source events of the same likelihood. As shown, these multisource events are likely to be of greater consequence than their separated component sources and may require increased levels of mitigation. However, the increased understanding of flood sources may enable more effective, unified management solutions than are possible when mitigating flood sources separately. With further research into the interaction of different sources and their conditional probabilities it will become increasingly possible to refine and tailor mitigation strategies according to a flood's component sources.

VII

Conclusion

25. Conclusion

25.1 Project Summary and Findings

Despite there being a considerable risk of flooding from multiple sources in the UK, with 980 000 properties identified as being at risk flooding in which groundwater plays a role (McKenzie and Ward, 2015), sources are rarely assessed together. This is especially true of groundwater, which is typically ignored in coupled flood risk assessments (e.g. Horritt et al., 2010) and which is often either described as a susceptibility with no indication of event likelihood (e.g. British Geological Survey, 2019b) or is attributed a likelihood based on historical flooding (e.g. GeoSmart Information, 2015), of which data is known to be sparse. This may stem from a lack of study into groundwater flooding compared to fluvial and pluvial flooding, a shortage of data and understanding of processes, and the difficulties associated with groundwater modelling (Cobby et al., 2009).

While physically based, spatially distributed hydrological models (e.g. SHETRAN & MODFLOW) are able to consider processes from multiple sources, they typically have relatively low resolutions, that are much lower than those used in surface water based assessments of flood risk (e.g. Environment Agency, 2019a). This project developed a methodology capable of assessing and quantifying flood risk from multiple sources that can also be used for increasing the understanding of flooding and the interaction between the different sources. This methodology focussed on the interaction between groundwater and surface water processes and did not include coastal processes.

Each of the paragraphs below briefly outlines the work carried out and bullets the major findings from each chapter.

Identifying Catchments at Risk of Multisourced Flooding

The primary step in the methodology was to create an automated process for identifying locations likely to benefit from the multisource approach. Two novel indexes were developed that assessed the groundwater and surface water contribution to peak streamflows for 435 catchments around England and Wales.

- An initial 29 multisourced catchments were identified around the UK.
- Multisource catchments were widely distributed but typically required the presence of highly permeable bedrock and catchments with split characteristics. Multisource catchments are generally located around the major aquifers of the south of England and are especially prevalent around London due to the presence of highly permeable bedrocks and low permeability superficial clay deposits or expansive urban areas.

The Automated Setup of Hydrological Models

The methodology used hydrological models to simulate surface and subsurface catchment processes that provide inputs for a higher resolution hydraulic model. However, as the development of hydrological models is known to be both time and data intensive, automated setup methods were first investigated.

This investigation used the hydrological model SHETRAN-GB: a physically based model that has recently been developed to include an automated national set up for Great Britain (Lewis et al., 2018). The base model (SHETRAN) is known to be capable of accurately representing catchment processes (e.g. Koo and O'Connell, 2006) however the automated setup system is still being developed. The automated setup has been shown to be a useful tool in streamflow modelling (Lewis, 2015) and development is now focussed on improving its groundwater modelling capabilities, which were untested. National geology and aquifer property datasets used in previous work were retested here and the simulated groundwater depths were compared to observed water levels for boreholes in five catchments in England. Use of parameters from the aquifer properties manual were promising but the BGS detailed 3D geology dataset was found to frequently misclassify the subsurface. In general, automated performance was poor and very few of the models were able to capture groundwater processes. Further development work was therefore conducted using the River Allen catchment in Dorset, which proved more successful.

- Modelling an extended groundwater catchment, rather than a topographically constrained surface water catchment, dramatically improved performance and increased the model sensitivity to improved hydrological parameters taken from the literature. This decreased the average root mean squared error to 9 m and increased the average Pearson's correlation coefficient to 0.86.
- The addition of simple subsurface flow boundary conditions allowed the model to drain and therefore greatly reduced significant problems with overly saturated subsurface cells.
- Further, necessary development opportunities for the automated online setup system were identified: (1) the development of a database of groundwater catchments; (2) potential for adding multiple fluvial outflows; (3) the automated generation of simple subsurface flow boundary conditions; and (4) further investigations in the use of BGS 3D geology data (ideally including superficial cover).
- SHETRAN-GB was found to be a useful tool in the overall methodology as it provides a strong platform from which hydrological models can be built and subsequently developed.

Creating a Multisource Modelling System

An existing SHETRAN model of the village of Kilham in East Yorkshire was used to create a multisource modelling system that converted hydrological outputs into inputs for a hydraulic model (HiPIMS) capable of high resolution surface water routing. Rainfall, streamflow and groundwater emergence were passed from the hydrological model to the hydraulic model in order to create realistic and detailed outputs. Different methods for redistributing the groundwater emergence from the 200 m resolution hydrological model to the 2 m resolution hydraulic model were tested.

- The severity of flooding was sensitive to the spatial distribution of the inputs over the domain but not the redistribution of inputs within the hydrological cells. Emergences can therefore be exchanged between the models without the need for spatial redistribution.
- The emergence of groundwater directly into the stream network and the removal of water from the simulation via evapotranspiration were not found to be dominant processes and were not included in the coupling.

Assessing Multisourced Flood Risk

The methodology for assessing multisource risk was implemented at the Kilham case study. The methodology used 1000 years of synthetic meteorological data to run a 1000 year hydrological simulation for the catchment. Simulated streamflow peaks from below the village were used to identify 1/30, 1/100 and 1/1000 year hydrological conditions and rainfall, river flow and groundwater emergence from these was hydraulically routed at a high resolution through the village.

- The risk of flooding from multiple sources (fluvial, pluvial and groundwater) was greater when all sources were considered.
- Modelling the combined groundwater and surface water sources increased the duration of the flooding dramatically with extents persisting beyond the duration of the 3 day simulation period following the flood peaks.
- The flood depths in the multisourced simulations increased following the peak depths as the groundwater emergence rates increased.
- As such, maximum flood depths were consistent between the single sourced and multisourced simulations. Additional rainfall following the flood peak was found to increase the risk of further flooding when groundwater emergence is persistent.

The Developed Methodology

A schematic describing the developed methodology can be found in Figure 20.1. The methodology is a useful tool and provides a platform for future developments. These are particularly promising considering the continuing development of high performance computing, the expansion of available datasets and more accessible hydrological modelling. The indexes created in Chapter III can be used to identify locations where this approach will be especially beneficial and on which future work can be focussed. This methodology is targeted for use by flood authorities and those making decisions on flood management and planning. This is thought to be more likely with increasing interest in complex modelling and network systems that can account for multiple interacting processes. One current project that demonstrates the relevance of this work is Hydro-Jules, which aims to create a modelling system capable of simulating complex and interacting land-surface science and hydrology. This involves the use of national multisource modelling of flood risk, including groundwater (Trevis, 2018).

It is envisaged that the methodology developed here would progress to allow its application at broader spatial scales. It is hoped that developments in computing and data collation and availability reduce the need for localised calibration of the hydrological models and that multisourced modelling systems could therefore be used to estimate risk at a catchment scale, rather than for a specific case study sites, as was done here. This would require increased automation in the hydraulic modelling to allow for a greater number of events to be simulated and for results to be compiled and summarised into reports and statistics detailing risk levels across larger areas and the sources involved.

25.2 Limitations

The following sections detail the main limitations associated with this work.

25.2.1 Hydrological Grid Alignment

The importance of appropriate alignment between the hydrological grid and area of interest was discussed while developing the modelling system in Chapter V. A hydrological resolution of 200 m allows for a potential horizontal error of ±100 m in the emergence pattern. In the case study model the emergence pattern was found to be offset from the expected emergence pattern in the topographic low of the valley, which resulted in groundwater emergence in areas thought

unlikely to experience emergence (see Fig. 17.7). It may be possible to align the hydrological domain prior to modelling, however this is difficult to do without hindsight and may cause issues elsewhere. Instead it may be more appropriate to treat this as a caveat of the modelling system. Emergence patterns offset upslope are likely to be of little consequence due to the subsequent hydraulic routing.

25.2.2 Accuracy of Hydrological Models

It is vital that the hydrological model is accurate, else the added precision of the hydraulic model is not justified. As almost all hydrological systems have significant spatial variation, the modelling system developed here should be applied locally and should undergo location specific calibration, as was done for Kilham. If, instead, the modelling system was applied at a catchment scale, then it is likely that representation of the groundwater levels will be poor. Modelled groundwater level inaccuracies of a few meters, or less, could significantly misinform estimated flood risk.

When calibrating hydrological models it is therefore key important to use local groundwater data and to match emergence events or spring activation with reported or surveyed information. With the development of high performance computing, machine learning and data availability, it is hoped that improved calibration and validation of the hydrological systems may allow the modelling system to be applied at a catchment scale.

25.2.3 Lack of Parametrisation and Validation Data

One additional limitation of this is the lack of available parametrisation and validation data. Without detailed and localised hydrogeological parameters (such as saturated conductivities and permeabilities) hydrological models have to be developed using standardised or regional data. This builds uncertainty into the model and increases the need for calibration and subsequent validation. Validating the methods and models used in this thesis was difficult, due to a lack of precise flood documentation. As such the methods used in Chapter III were forced to rely on data based metrics rather than flood data and the automated SHETRAN-GB models had to use regionally generalised parameters (Chapter IV). The case study model implemented at Kilham was fortunate to be able to make use of multiple nearby groundwater level observations and detailed geological surveys to ensure that it was fit for use, however emergence patterns could only be validated against generalised reports and a single historical flood extent. The lack of data of groundwater flooding is being addressed in the Environment Agency's 2019 project: *Rapid evidence assessment and overview of groundwater flood risk management in England*, which aims to synthesise groundwater flood risk management knowledge and practice.

25.2.4 Processes not Included in the Model Linkage

Infiltration

The lack of infiltration in the hydraulic component of the multisource modelling system was found to be a significant limitation (demonstrated in Chapter VI). Infiltration rates varied significantly across the 3 km^2 hydrological domain. In some events, infiltration rates of 10 mm/hr occurred in the upper domain while there was emergence at a similar rate in the lower domain (Fig. 23.8). Furthermore, infiltration rates of up to 30 mm/hr were able to almost nullify intense storms in the hydrological model whereas the lack of infiltration in the hydraulic model led to extensive flooding. Further work should focus on including an infiltration component into the coupling mechanism. This could be achieved either by removing infiltration directly from hydraulic inputs, or by updating HiPIMS to a more recent version (Xing et al., 2019) or using an alternative hydraulic model, such as CityCAT (Glenis et al., 2018). If choosing to remove infiltration from the hydraulic inputs, then this could be done cell by cell during the same process that combines rainfall inputs with groundwater emergence. Infiltration rates, using HiPIMS at least, would

be limited by the rate of input, as water cannot easily be removed from the domain on a time depended, cell by cell basis.

A further limitation was considered and dismissed - the lack of hydraulic connection between the groundwater system and the SHETRAN channel cells, which are considered separately to standard grid cells, and so have their own vertical groundwater flow rates. Vertical flow to and from the river cells was not taken into account as the mechanics of coupling these to the hydraulic model was deemed too complex for the task. However, this was not found to be a limitation on the modelling system as flows to and from the channels were very minor relative to the volume of groundwater emergence in the surrounding model domain. More information on this, as well as a proposed mechanism for coupling can be found in Section 19.3.

Overland Flows

Overland flows from the hydrological model were not coupled to the hydraulic model due to time constraints. Coupling overland flows between the models would not be difficult and should be added in future work. Overland flows were present in the 1 in 1000 year hydrological event in Chapter VI and are likely to be important in many flood scenarios. This is especially important for areas in which surface runoff is not heavily confined to channel systems.

Subsurface Infrastructure

In many flood events, subsurface infrastructure such as drains and sewers can play a key role. Drains and sewers can offer the storage and rapid transit of water away from areas of potential flooding, but can also pose additional flood risks when overwhelmed or blocked. With the premise of coupled modelling of multisource systems demonstrated in previous chapters, it is recommended that such capabilities be included in future work. Although SHETRAN has long had the capability to simulate flow through pipe networks (Adams and Parkin, 2002) it is proposed that pipe networks would more reasonably be represented at a finer scale within the hydraulic model. HiPIMS does not yet allow for integrating pipe networks however this is possible in other hydraulic models (e.g. TUFLOW or CityCAT) that could be used in its place.

Both of the models used in this work have the capability to model subsurface features such as subways and basements. Furthermore, SHETRAN's ability to calculate horizontal and vertical subsurface flows and groundwater levels allow it to be used in assessing the impact of flooding or high groundwater levels on such features.

25.3 Recommendations for Further Work

Multisource Catchment Identification

Further multisourced catchments are likely to be identified by applying the indexes created in Chapter III to over 800 additional stream flow records around the UK (Fig. 26.6). This would identify additional multisource catchments and may aid the understanding of factors leading to multisourced flooding.

Additional Case Studies

The methodology should be implemented at fresh case study sites to determine whether the findings here are generally applicable or hydrologically specific to the case study site. This would also further assess the practicalities of using SHETRAN-GB for groundwater modelling.

National Flow Validation

Points for future development of the SHETRAN-GB modelling system were outlined above. Following these steps the system should be reassessed against flow data as in the initial study by Lewis (2015). This would show whether the improved representation of groundwater processes also improves the model's ability to capture surface water processes nationally.

National Emergence Validation

Following further development of the SHETRAN-GB modelling system it would be interesting to compare hydrological emergence patterns to those of the BGS Groundwater Susceptibility Maps. It may be possible to use these maps, which are generated using non-hydrological methods, to assess the key national scale issues with the modelling system. If such an approach proves effective then this would also help to overcome issues with availability and accessibility of groundwater level data.

Adding Value to Susceptibility Mapping

If SHETRAN-GB is found to correlate well with the BGS susceptibility maps, or can be calibrated to do so, then there may be future scope for combining such resources to estimate emergence rates for susceptible areas or likelihoods for the susceptibility extents (a key data gap identified by Horritt et al., 2010).

A Call for Better Datasets

Implementing either this methodology or similar hydrological modelling at a national scale requires improvements in the existence and availability of national scale datasets.

- With regard to the hydrological modelling, a georeferenced database of groundwater catchments is required. This would allow for the automated setup of hydrological models capable of capturing groundwater processes.
- A database of regionally specific rock types and their hydraulic properties should be collated to enable the improved parametrisation of hydrological models – where possible, this should include information on transmissivity as well as bedrock thickness and hydraulic conductivities. Information on the required properties is largely available, but is contained within reports rather than in a centralised database.
- Manual calibration of hydrological models would benefit from increased availability of groundwater level data and linked borehole metadata describing borehole depths and screens. Ideally, this would be through an online repository system similar to those used for river flow and climate data by the National River Flow Archive.
- The validation of hydrological models and the subsequent hydraulic models is made significantly more plausible by the availability of historical flooding data. At current, the validation of flood models is limited by the choice of study site and whether any flooding has been well documented. Georeferenced flood extent datasets are available but, while these are a fantastic resource, they are very patchy and thus not fitting for use at the desired scale. Reports containing information on historical flooding (e.g. Strategic Flood Risk Assessments and Section 19 reports) are available for much of the UK but are typically vague (DEFRA, 2015). Reports tend not to include specifics on the nature of the flood (e.g. date, time, source, extent, depth etc.) and often instead indicate only the general area of the flood at a town or village scale and the month or season of flooding. In order to successfully validate the discussed models there needs to be an improvement in the method by which flood data is collected and collated. This should be nationally standardised to include the desired metrics, such as those proposed by Jacobs (2007). With the improvements in the acquisition rate, image processing and resolution of remote sensing data(Teng et al., 2017) as well as increasing use of social media data (e.g. Rosser et al., 2017) and digital flood reporting tools (e.g. Floodline Scotland, 2019), there is great potential for the development of a time referenced geospatial database of observed floods. Such information would also decrease the reliance on automated methods for identifying catchments at risk of multisource flooding.

References

Abbott, M., J. Bathurst, J. Cunge, P. O'Connell, and J. Rasmussen. An introduction to the European Hydrological System — Systeme Hydrologique Europeen, "SHE", 1: History and philosophy of a physically-based, distributed modelling system. *Journal of Hydrology*, 87(1-2): 45–59, oct 1986. ISSN 0022-1694. doi: 10.1016/0022-1694(86)90114-9. https://www.sciencedirect.com/science/article/pii/0022169486901149?via%3Dihub. 28

Abboud, J., M. Ryan, and G. Osborn. Groundwater flooding in a river-connected alluvial aquifer. *Journal of Flood Risk Management*, 11(4), 2018. ISSN 1753318X. doi: 10.1111/jfr3.12334. http://doi.wiley.com/10.1111/jfr3.12334. 16

Adams, B., J. P. Bloomfield, A. J. A Gallagher, C. R. A Jackson, H. K. A Rutter, and A. T. A Williams. An early warning system for groundwater flooding in the Chalk. *Quarterly Journal of Engineering Geology and Hydrogeology*, 43(Geological Society of London):185–193, 2010. http://nora.nerc.ac.uk/9834/. 25

Adams, R. and G. Parkin. Development of a coupled surface-groundwater-pipe network model for the sustainable management of karstic groundwater. *Environmental Geology*, 42(5):513–517, aug 2002. ISSN 0943-0105. doi: 10.1007/s00254-001-0513-8. http://link.springer.com/10.1007/s00254-001-0513-8. 28, 80, 117, 176

Aldridge, T., R. Allan, B. Gouldby, O. Gunawan, N. Hunter, R. Lamb, J. Tawn, and E. Wood. Spatial joint probability for FCRM and strategic assessments - method report. SC140002/R1. Technical report, Environment Agency, Bristol, 2017. http://evidence.environment-agency.gov.uk/FCERM/Libraries/FCERM_Project_Documents/Spatial_joint_probability_for_flood_and_coastal_risk_management_and_strategic_assessments_method_report.sflb.ashx. 142, 149, 150

Alfieri, L., P. Salamon, A. Bianchi, J. Neal, P. Bates, and L. Feyen. Advances in pan-European flood hazard mapping. *Hydrological Processes*, 28(13):4067–4077, 2014. ISSN 08856087. doi: 10.1002/hyp.9947. http://doi.wiley.com/10.1002/hyp.9947. 30

Allen, D. J. and E. J. Crane. The Chalk aquifer of the Wessex Basin - Research Report No. RR/11/02. Technical report, British Geological Survey, Nottingham, UK, 2019. http://nora.nerc.ac.uk/id/eprint/522484/1/RR11002.pdf. 11, 86

Allen, D. J., L. J. Brewerton, L. M. Coleby, B. R. Gibbs, M. A. Lewis, A. M. MacDonald, S. J. Wagstaff, and A. T. Williams. The physical properties of major aquifers in England and Wales. Report WD/97/34. Technical report, British Geological Survey, 1997. http://nora.nerc.ac.uk/id/eprint/13137/1/WD97034.pdf. 12, 13, 15, 16, 84, 86, 89, 90, 91, 112

Allen, R. G., L. S. Pereira, D. Raes, and M. Smith. Crop evapotranspiration - Guidelines for computing crop water requirements, 1998. http://www.fao.org/3/X0490E/x0490e00.htm{#}Contents. 146

Ambiental Risk Analytics. Groundwater Flood Risk, 2019a. https://www.ambientalrisk.com/groundwater-flood-risk/. 38

Ambiental Risk Analytics. UK FloodMap4^{TM}, 2019b. https://www.ambientalrisk.com/uk-floodmap4/. 35

An, H. and S. Yu. Finite volume integrated surface-subsurface flow modeling on nonorthogonal grids. *Water Resources Research*, 50(3):2312–2328, 2014. doi: 10.1002/2013WR013828. http://dx.doi.org/10.1002/2013WR013828. 2, 16, 29

Andoh, R. Y. G. and K. O. Iwugo. Sustainable Urban Drainage Systems: A UK Perspective. In *Global Solutions for Urban Drainage*, pages 1–16, Portland, 2002. American Society of Civil Engineers. ISBN 9780784406441. doi: 10.1061/40644(2002)19. http://ascelibrary.org/doi/10.1061/40644%282002%2919. 8

Arnold, J. G., P. M. Allen, and G. Bernhardt. A comprehensive surface-groundwater flow model. *Journal of Hydrology*, 142:47–69, 1993. https://www.sciencedirect.com/science/article/pii/002216949390004S. 27

Ascott, M. J., B. P. Marchant, D. Macdonald, A. A. McKenzie, and J. P. Bloomfield. Improved understanding of spatio-temporal controls on regional scale groundwater flooding using hydrograph analysis and impulse response functions. *Hydrological Processes*, 31(25):4586–4599, 2017. ISSN 08856087. doi: 10.1002/hyp.11380. http://doi.wiley.com/10.1002/hyp.11380. 11, 12

Ashley, R. M., D. J. Balmfort, A. J. Saul, and J. D. Blanskby. Flooding in the future - Predicting climate change, risks and responses in urban areas. *Water Science and Technology*, 52(5): 265–273, 2005. ISSN 02731223. doi: 10.2166/wst.2005.0142. https://iwaponline.com/wst/article/52/5/265/12262/Flooding-in-the-future-predicting-climate-change. 7

Balica, S. and N. G. Wright. Reducing the complexity of the flood vulnerability index. *Environmental Hazards*, 9(4):321–339, 2010. doi: 10.3763/ehaz.2010.0043. http://www.tandfonline.com/doi/abs/10.3763/ehaz.2010.0043. 3, 142

Barthel, R. and S. Banzhaf. Groundwater and Surface Water Interaction at the Regional-scale – A Review with Focus on Regional Integrated Models. *Water Resources Management*, 30(1): 1–32, 2016. ISSN 0920-4741. doi: 10.1007/s11269-015-1163-z. http://link.springer.com/10.1007/s11269-015-1163-z. 27, 29, 31

Bates, P. LISFLOOD-FP, 2017. http://www.bristol.ac.uk/geography/research/hydrology/models/lisflood/. 24

BBC News. Yorkshire Dales flash flooding: Devastation clean-up under way, 2019a. https://www.bbc.co.uk/news/uk-england-york-north-yorkshire-49189605. 8

BBC News. Chinook races to save damaged reservoir, 2019b. https://www.bbc.co.uk/news/av/uk-england-derbyshire-49197455/whaley-bridge-dam-chinook-races-to-save-damaged-reservoir. 8

Bence, R. *Rapid Hydrology: Improved Integrated Catchment Modelling Through the Integration of 3D Geology*. Masters thesis, School of Engineering, Newcastle University, 2019. 104, 109, 112

Bennett, B., M. Leonard, Y. Deng, and S. Westra. An empirical investigation into the effect of antecedent precipitation on flood volume. *Journal of Hydrology*, 567:435–445, 2018. ISSN 0022-1694. doi: 10.1016/J.JHYDROL.2018.10.025. https://www.sciencedirect.com/science/article/pii/S0022169418307868. 2, 16

Bennis, S., F. Berrado, and N. Kang. Improving single-variable and multivariable techniques for estimating missing hydrological data. *Journal of Hydrology*, 191:87–105, 1997. https://www.sciencedirect.com/science/article/pii/S0022169496030764. 42

Beven, K. J. *Rainfall-Runoff Modelling: The Primer*. Wiley-Blackwell, Chichester, 2nd edition, 2012. ISBN 1119951011. 22, 80

Binley, A. M., K. J. Beven, A. Calver, and L. G. Watts. Changing responses in hydrology: Assessing the uncertainty in physically based model predictions. *Water Resources Research*, 27 (6):1253–1261, 1991. ISSN 00431397. doi: 10.1029/91WR00130. http://doi.wiley.com/10.1029/91WR00130. 21

Birkinshaw, S. J. Physically-based modelling of double-peak discharge responses at Slapton Wood catchment. *Hydrological Processes*, 22(10):1419–1430, 2008. doi: 10.1002/hyp.6694. http://dx.doi.org/10.1002/hyp.6694. 47, 224

Blenkinsop, S., E. Lewis, S. Chan, and H. Fowler. Quality control of an hourly rainfall dataset and climatology of extremes for the UK. *International Journal of Climatology*, 37(2), 2016. https://rmets.onlinelibrary.wiley.com/doi/full/10.1002/joc.4735. 108

Bloomfield, J. P., B. P. Marchant, S. H. Bricker, and R. B. Morgan. Regional analysis of groundwater droughts using hydrograph classification. *Hydrology and Earth System Sciences*, 19:4327–4344, 2015. doi: 10.5194/hess-19-4327-2015. www.hydrol-earth-syst-sci.net/19/4327/2015/. 46

Boardman, J., R. Evans, and J. Ford. Muddy floods on the South Downs, southern England: Problem and responses. *Environmental Science and Policy*, 6(1):69–83, 2003. ISSN 14629011. doi: 10.1016/S1462-9011(02)00125-9. https://www.sciencedirect.com/science/article/pii/S1462901102001259{#}FIG1. 8

Bonnifait, L., G. Delrieu, M. L. Lay, B. Boudevillain, A. Masson, P. Belleudy, E. Gaume, and G.-M. Saulnier. Distributed hydrologic and hydraulic modelling with radar rainfall input: Reconstruction of the 8–9 September 2002 catastrophic flood event in the Gard region, France. *Advances in Water Resources*, 32(7):1077–1089, 2009. doi: 10.1016/j.advwatres.2009.03.007. https://www.sciencedirect.com/science/article/pii/S0309170809000554?via%3Dihub. 31

Brassington, R. *Field Hydrogeology*. John Wiley & Sons, Ltd, forth edit edition, 2017. ISBN 9781118397367. 25, 27

Breinl, K., U. Strasser, P. Bates, and S. Kienberger. A joint modelling framework for daily extremes of river discharge and precipitation in urban areas. *Journal of Flood Risk Management*, 10(1):97–114, 2017. ISSN 1753318X. doi: 10.1111/jfr3.12150. http://doi.wiley.com/10.1111/jfr3.12150. 16, 17

British Geological Survey. BGS 1:10 000 Bedrock and Superficial Geology. https://www.bgs.ac.uk/products/digitalmaps/digmapgb_10.html. 91

British Geological Survey. BGS 1:625 000 Bedrock and Superficial Geology. 2007. https://www.bgs.ac.uk/products/digitalmaps/digmapgb_625.html. 89

British Geological Survey. BGS Lexicon of Named Rock Units, 2008. https://www.bgs.ac.uk/lexicon/lexicon.cfm?pub=FE. 89

British Geological Survey. Groundwater Flooding Susceptibility, 2013a. http://www.bgs.ac.uk/discoverymetadata/13603085.html. 2

British Geological Survey. Groundwater Flooding Susceptibility, 2013b. https://www.bgs.ac.uk/discoverymetadata/13603085.html. 38

British Geological Survey. Groundwater flooding in the UK: Feb 2014, 2014a. https://www.bgs.ac.uk/research/highlights/2014/groundwaterFloodingFeb.html. 16

British Geological Survey. 1:625 000 scale digital hydrogeological data, 2014b. 81

British Geological Survey. Onshore GeoIndex, 2015. http://mapapps2.bgs.ac.uk/geoindex/home.html. 42

British Geological Survey. UK3D - 3D geology for the United Kingdom. *www.BGS.ac.uk*, 2016a. https://www.bgs.ac.uk/research/ukgeology/nationalGeologicalModel/GB3D.html. 91

British Geological Survey. BGS hydrogeology 625k, 2016b. https://www.bgs.ac.uk/products/hydrogeology/maps.html. 4, 75, 76, 81, 216

British Geological Survey. British Geological Survey | Groundwater Flooding Susceptibility, 2018. https://data.gov.uk/dataset/f0329412-b46a-49b0-9f30-abef8c4b807e/groundwater-flooding-susceptibility. 37

British Geological Survey. BGS 1:50 000 Bedrock and Superficial Geology. 2019a. https://www.bgs.ac.uk/products/digitalmaps/DiGMapGB_50.html. 89, 91, 120

British Geological Survey. BGS Groundwater Flooding | 1:50,000 Groundwater Susceptibility Map, 2019b. http://www.bgs.ac.uk/products/hydrogeology/groundwaterFlooding.html. 37, 160, 172

Brodie, R. S. and S. Hostetler. A review of techniques for analysing baseflow from stream hydrographs. In *Proceedings of the NZHS-IAH-NZSSS conference.*, volume 28, 2005. 56, 57, 74

Brunner, P. and C. T. Simmons. HydroGeoSphere: A Fully Integrated, Physically Based Hydrological Model. *Ground Water*, 50(2):170–176, 2012. doi: 10.1111/j.1745-6584.2011.00882.x. http://doi.wiley.com/10.1111/j.1745-6584.2011.00882.x. 28

Brunner, P., C. T. Simmons, P. G. Cook, and R. Therrien. Modeling Surface Water-Groundwater Interaction with MODFLOW: Some Considerations. *Ground Water*, 48(2):174–180, 2010. doi: 10.1111/j.1745-6584.2009.00644.x. http://doi.wiley.com/10.1111/j.1745-6584.2009.00644.x. 28

BTM Group Ltd. TUFLOW - Overview, 2018. https://www.tuflow.com/TuflowFV.aspx. 24

Buckinghamshire County Council. Flood Investigation Report | Old Amersham, Amersham. Technical report, 2014. http://old.buckscc.gov.uk/media/2616182/141017-Old-Amersham-S19-report_FINAL2.pdf. 19, 218

Buckinghamshire County Council. Strategic Flood Management | Flood Investigations, 2017. https://www.buckscc.gov.uk/services/environment/flooding/strategic-flood-management/flood-investigations/. 19, 218

Butler, A. P., A. G. Hughes, C. R. Jackson, A. M. Ireson, S. J. Parker, H. S. Wheater, and D. W. Peach. Advances in modelling groundwater behaviour in Chalk catchments. *Geological Society, London, Special Publications*, 364:113–127, 2012. http://sp.lyellcollection.org/content/specpubgsl/364/1/113.full.pdf. 12, 13, 25, 220

Camporese, M., C. Paniconi, M. Putti, and S. Orlandini. Surface-subsurface flow modeling with path-based runoff routing, boundary condition-based coupling, and assimilation of multisource observation data. *Water Resources Research*, 46(2), 2010. ISSN 00431397. doi: 10.1029/2008WR007536.
http://doi.wiley.com/10.1029/2008WR007536. 29

CAPITA SYMONDS. King's Lynn and West Norfolk Settlements Surface Water Management Plan: Stage 2. Technical report, Borough Council of King's Lynn and West Norfolk, 2012.
https://www.norfolk.gov.uk/what-we-do-and-how-we-work/policy-performance-and-partnerships/policies-and-strategies/flood-and-water-management-policies/surface-water-management-plans/kings-lynn-and-west-norfolk-settlements-swmp. 70

Centre for Ecology & Hydrology. Flood Risk Modelling, 2016.
https://www.ceh.ac.uk/services/flood-modelling. 30

Centre for Ecology and Hydrology. Hydrological Outlook UK, 2019.
https://hydoutuk.net/. 167

Centre for Ecology and Hydrology (NERC). Rainfall: CEH-GEAR, 2015.
https://eip.ceh.ac.uk/rainfall. 85

Chapman, T. G. Comment on "Evaluation of automated techniques for base flow and recession analyses" by R. J. Nathan and T. A. McMahon. *Water Resources Research*, 27(7):1783–1784, 1991. ISSN 00431397. doi: 10.1029/91WR01007.
http://doi.wiley.com/10.1029/91WR01007. 219

Chen, A. S., S. Djordjević, J. Leandro, and D. A. Savić. An analysis of the combined consequences of pluvial and fluvial flooding. *Water Science and Technology*, 62(7):1491–1498, 2010. ISSN 02731223. doi: 10.2166/wst.2010.486.
https://iwaponline.com/wst/article/62/7/1491/16606/An-analysis-of-the-combined-consequences-of. 16, 23

Climate-Data.Org. Driffield Climate.
https://en.climate-data.org/europe/united-kingdom/england/driffield-8624/. 147

Cobby, D., S. Morris, A. Parkes, and V. Robinson. Groundwater flood risk management: advances towards meeting the requirements of the EU floods directive. *Journal of Flood Risk Management*, 2(2):111–119, 2009. ISSN 1753318X. doi: 10.1111/j.1753-318X.2009.01025.x.
http://doi.wiley.com/10.1111/j.1753-318X.2009.01025.x. 1, 9, 10, 11, 17, 27, 35, 36, 38, 142, 172

Collier, C. G. Flash flood forecasting: What are the limits of predictability? *Quarterly Journal of the Royal Meteorological Society*, 133(622):3–23, 2007. ISSN 00359009. doi: 10.1002/qj.29.
http://doi.wiley.com/10.1002/qj.29. 222

Coulthard, T. J., J. C. Neal, P. D. Bates, J. Ramirez, G. A. M. de Almeida, and G. R. Hancock. Integrating the LISFLOOD-FP 2D hydrodynamic model with the CAESAR model: implications for modelling landscape evolution. *Earth Surface Processes and Landforms*, 38(15):1897–1906, 2013. doi: 10.1002/esp.3478.
http://doi.wiley.com/10.1002/esp.3478. 24

Crossley, A., R. Lamb, and S. Waller. Fast solution of the Shallow Water Equations using GPU technology. Technical report, JBA Consulting, 2010.
http://www.jflow.co.uk/sites/default/files/CrossleyLambWaller-BHS2010.pdf. 24

Culley, S., B. Bennett, S. Westra, and H. Maier. Generating realistic perturbed hydrometeorological time series to inform scenario-neutral climate impact assessments. *Journal of Hydrology*, 2019. ISSN 0022-1694. doi: 10.1016/J.JHYDROL.2019.06.005.
https://www.sciencedirect.com/science/article/pii/S0022169419305529. 146

Dance, S. and H. Cloke. Flooding From Intense Rainfall | Project FRANC & Project SINATRA, 2013.
http://www.met.reading.ac.uk/flooding/. 41

de Almeida, G., P. Bates, and H. Ozdemir. Modelling urban floods at submetre resolution: challenges or opportunities for flood risk management? *Journal of Flood Risk Management*, 11: 855–865, 2018. ISSN 1753318X. doi: 10.1111/jfr3.12276.
http://doi.wiley.com/10.1111/jfr3.12276. 116

De Moel, H., J. Van Alphen, and J. C. J. H. Aerts. Flood maps in Europe - methods, availability and use. *Natural Hazards and Earth System Sciences*, 9:289–301, 2009.
www.nat-hazards-earth-syst-sci.net/9/289/2009/. 33, 168

Deb, P., A. S. Kiem, and G. Willgoose. A linked surface water-groundwater modelling approach to more realistically simulate rainfall-runoff non-stationarity in semi-arid regions. *Journal of Hydrology*, 575:273–291, 2019. doi: 10.1016/J.JHYDROL.2019.05.039.
https://www.sciencedirect.com/science/article/pii/S0022169419304846?dgcid=raven_sd_aip_email. 26

Dechant, C. M. and M. Hamid. Hydrologic Prediction and Uncertainty Quantification. In Eslamian, S., editor, *Handbook of Engineering Hydrology*, chapter 20, pages 388–414. Taylor & FrancisGroup, 1 edition, 2014. 21

DEFRA. Evidence review of factors contributing to surface water flooding from Section 19 LLFA reports. Final report FD2692. Technical report, DEFRA, 2015.
www.gov.uk/defra. 18, 177

Desbarats, A. J., C. E. Logan, M. J. Hinton, and D. R. Sharpe. On the kriging of water table elevations using collateral information from a digital elevation model. *Journal of Hydrology*, 255:25–38, 2002.
www.elsevier.com/locate/jhydrol. 126, 138

Devia, G. K., B. Ganasri, and G. Dwarakish. A Review on Hydrological Models. *Aquatic Procedia*, 4:1001–1007, 2015. ISSN 2214-241X. doi: 10.1016/J.AQPRO.2015.02.126.
https://www.sciencedirect.com/science/article/pii/S2214241X15001273. 21

Doble, R. C., R. S. Crosbie, B. D. Smerdon, L. Peeters, and F. J. Cook. Groundwater recharge from overbank floods. *Water Resources Research*, 48(9), 2012. ISSN 00431397. doi: 10.1029/2011WR011441.
http://doi.wiley.com/10.1029/2011WR011441. 16

Dorset County Council. Dorset County Council July 2012 - Flood Investigation Report. Technical report, Dorset County Council, 2012.
https://www.dorsetforyou.gov.uk/media/181167/Flood-Risk-Investigation-report/pdf/Flood_Risk1001_01.Rev_0.pdf. 34

Dorset County Council and Environment Agency. July 2012 Flood Investigation Report. Technical report, Dorset County Council, 2012.
https://www.dorsetforyou.gov.uk/emergencies-severe-weather/severe-weather/flooding/pdfs/july-2012-flood-investigation-report.pdf. 73

Dudley, R., G. Hodgkins, M. Nielsen, and S. Qi. Estimating historical groundwater levels based on relations with hydrologic and meteorological variables in the U.S. glacial aquifer system. *Journal of Hydrology*, 562:530–543, 2018. ISSN 0022-1694. doi: 10.1016/J.JHYDROL.2018.05.019.
https://www.sciencedirect.com/science/article/pii/S0022169418303469?_rdoc=1&_fmt=high&_origin=gateway&_docanchor=&md5=b8429449ccfc9c30159a5f9aeaa92ffb&dgcid=raven_sd_aip_email. 56, 93

Dumedah, G. and P. Coulibaly. Evaluation of statistical methods for infilling missing values in high-resolution soil moisture data. *Journal of Hydrology*, 400(1):95–102, 2011. ISSN 00221694. doi: 10.1016/j.jhydrol.2011.01.028.
https://www.sciencedirect.com/science/article/pii/S0022169411000539. 42

East Riding of Yorkshire Council. Flood Investigation Report - Kilham Village During Winter 2012-2013. Technical report, 2013. 88, 120, 121, 132, 138, 160

East Riding of Yorkshire Council. Local Flood Risk Management Strategy - Consultation Draft. Technical report, East Riding of Yorkshire Council, 2015a.
https://geosmartinfo.co.uk/wp-content/uploads/sfra/East-Riding-Flood.pdf. 88

East Riding of Yorkshire Council. Local Flood Risk Management Stratergy - Strategic Environmental Assessment - Scoping Report. Technical report, East Riding of Yorkshire Council, 2015b. 88

Ebel, B. A., B. B. Mirus, C. S. Heppner, J. E. VanderKwaak, and K. Loague. Surface-subsurface flow modeling with path-based runoff routing,boundary condition-based coupling, and assimilation of multisource observation data. *Hydrological Processes*, 23(13):1949–1959, 2009. ISSN 08856087. doi: 10.1002/hyp.7279.
http://doi.wiley.com/10.1002/hyp.7279. 29

Elliott, A. H., F. Oehler, J. Schmidt, and J. C. Ekanayake. Sediment modelling with fine temporal and spatial resolution for a hilly catchment. *Hydrological Processes*, 26:3645–3660, 2012.
https://onlinelibrary.wiley.com/doi/pdf/10.1002/hyp.8445. 138

Elshorbagy, A. A., U. S. Panu, and S. P. Simonovic. Group-based estimation of missing hydrological data: I. Approach and general methodology. *Hydrological Sciences Journal*, 45(6):849–866, 2000.
https://www.tandfonline.com/doi/abs/10.1080/02626660009492388. 41

Entec. Flood Risk and Sustainable Drainage. Technical report, Borough of King's Lynn and West Norfolk, 2009.
file://campus/home/home2015/b5066167/Downloads/7._Flood_Risk_and_Sustainable_Drainage.pdf. 70, 72

Environment Agency. Computational modelling to assess flood and coastal risk - Operational Instruction 379_05. Technical report, 2010. 152, 158

Environment Agency. Prototype tool for mapping flooding from all sources. Project Summary SC080050/S2. Technical report, 2011a. 2

Environment Agency. Prototype tool for mapping flooding from all sources. Technical Report Project Summary SC080050/S2, 2011b. 40

Environment Agency. Flood map for planning, 2013a. https://flood-map-for-planning.service.gov.uk/. 34, 35, 142, 158

Environment Agency. What is the updated Flood Map for Surface Water? Report version 1.0. Technical report, Environment Agency, 2013b. 24

Environment Agency. What is the Risk of Flooding from Surface Water map? (UPDATED VERSION). Technical report, The Environment Agency, Bristol, 2013c. https://www.gov.uk/government/publications/flood-maps-for-surface-water-how-they-were-produced. 34, 35, 158, 163, 165, 170

Environment Agency. Flood Risk Maps Risk of Flooding from Rivers and Sea | Thames River Basin District | Publication Catalogue Code: LIT 8978. Technical report, 2013d. https://assets.publishing.service.gov.uk/government/uploads/system/uploads/attachment_data/file/456955/LIT8978_FloodRiskMaps_Thames_RiversSea_v2.pdf. 34

Environment Agency. Environment Agency area structure map, 2014. https://www.gov.uk/government/publications/environment-agency-area-and-region-operational-locations. 36

Environment Agency. Risk of Flooding from Multiple Sources | Dataset Document. Technical report, 2017. https://environment.data.gov.uk/DefraDataDownload/?mapService=SURVEY/RoFMSRiskContribution&Mode=spatial. 40

Environment Agency. Long term flood information (Long Term Flood Risk Map for England), 2019a. https://flood-warning-information.service.gov.uk/long-term-flood-risk/. 1, 34, 35, 142, 158, 159, 172

Environment Agency. Risk of Flooding from Multiple Sources: Risk Band, 2019b. https://data.gov.uk/dataset/0afc0a17-cb2c-4221-bcb8-947e61ac30f0/risk-of-flooding-from-multiple-sources-risk-band. 40

ESI. ESI Launches Ground-Breaking 5 Metre Groundwater Flood Risk Map, 2015. http://esi-consulting.co.uk/esi-launches-ground-breaking-5-metre-groundwater-flood-risk-map/. 2, 38

Ewen, J., G. Parkin, and P. E. O'Connell. SHETRAN: distributed river basin flow and transport modeling system. *Journal of hydrologic engineering*, 5(3):250–258, 2000. https://research.ncl.ac.uk/shetran/SHETRAN_ASCE_paper.pdf. 3, 28

Falconer, R. H., D. Cobby, P. Smyth, G. Astle, J. Dent, and B. Golding. Pluvial flooding: new approaches in flood warning, mapping and risk management. *Journal of Flood Risk Management*, 2(3):198–208, 2009. ISSN 1753-318X. doi: 10.1111/j.1753-318X.2009.01034.x. https://onlinelibrary.wiley.com/doi/full/10.1111/j.1753-318X.2009.01034.x. 1, 7, 33

Farrell, R. Report on Groundwater Flooding - Burton Flemming and Kilham. Technical report, Environment Agency, 2001. 88

Farrell, R., M. Ververs, P. Davison, P. Howlett, and M. Whiteman. Splicing recharge and groundwater flow models in the Environment Agency National Groundwater Modelling System. *Geological Society, London, Special Publications*, 408:55–69, 2017. doi: 10.1144/SP408.14. http://sp.lyellcollection.org/lookup/doi/10.1144/SP408.14. 26

Felder, G., A. Zischg, and R. Weingartner. The effect of coupling hydrologic and hydrodynamic models on probable maximum flood estimation. *Journal of Hydrology*, 550:157–165, 2017. ISSN 00221694. doi: 10.1016/j.jhydrol.2017.04.052. http://www.sciencedirect.com/science/article/pii/S002216941730272X. 29, 165

Fewtrell, T. J., P. D. Bates, M. Horritt, and N. M. Hunter. Evaluating the effect of scale in flood inundation modelling in urban environments. *Hydrological Processes*, 22(26):5107–5118, 2008. ISSN 08856087. doi: 10.1002/hyp.7148. http://doi.wiley.com/10.1002/hyp.7148. 116

Feyen, L., R. Dankers, K. Bódis, P. Salamon, and J. I. Barredo. Fluvial flood risk in Europe in present and future climates. *Climatic Change*, 112(1):47–62, 2012. ISSN 01650009. doi: 10.1007/s10584-011-0339-7. https://link.springer.com/article/10.1007/s10584-011-0339-7. 148

Finch, J., T. Marsh, and A. Mckenzie. A preliminary risk assessment of the potential for groundwater flooding during the winter of 2007/8 - an update. Technical report, Centre for Ecology & Hydrology and the British Geological Survey., 2007. http://nora.nerc.ac.uk/id/eprint/1387/. 11, 16

Fleckenstein, J. H., R. G. Niswonger, and G. E. Fogg. River-Aquifer Interactions, Geologic Heterogeneity, and Low-Flow Management. *Groundwater*, 44(6):837–852, 2006. ISSN 0017-467X. doi: 10.1111/j.1745-6584.2006.00190.x. http://doi.wiley.com/10.1111/j.1745-6584.2006.00190.x. 16

Flood and Water Management Act. Part 1 - Flood and Coastal Erosion Risk Management. chapter 29, pages 18–81. Queen's Printer of Acts of Parliament, 2010. http://www.legislation.gov.uk/ukpga/2010/29/part/1. 33

Floodline Scotland. Report a Flood, 2019. http://floodlinescotland.org.uk/report-a-flood/. 177

Franco-Villoria, M., M. Scott, T. Hoey, and D. Fischbacher-Smith. Temporal Investigation of Flow Variability in Scottish Rivers Using Wavelet Analysis. *Journal of Environmental Statistics*, 3(6), 2012. http://eprints.gla.ac.uk/62946/. 226

Furman, A. Modeling Coupled Surface-Subsurface Flow Processes: A Review A: PDE, partial diff erential equation. *www.vadosezonejournal.org ·*, 7(2):741–756, 2008. doi: 10.2136/vzj2007.0065. www.vadosezonejournal.org. 22, 27, 29

Gaitan, S., N. C. van de Giesen, and J. A. ten Veldhuis. Can urban pluvial flooding be predicted by open spatial data and weather data? *Environmental Modelling and Software*, 85:156–171, 2016. ISSN 13648152. doi: 10.1016/j.envsoft.2016.08.007. https://www.sciencedirect.com/science/article/pii/S136481521630473X. 7

Gale, I. N. and H. K. Rutter. The Chalk aquifer of Yorkshire - Research Report RR/06/04. Technical report, British Geological Survey, 2006. http://nora.nerc.ac.uk/id/eprint/3700/1/RR06004.pdf. 88, 89

Ganguli, P. and B. Merz. Extreme Coastal Water Levels Exacerbate Fluvial Flood Hazards in Northwestern Europe. *Scientific Reports - Nature Research*, 9(1), dec 2019. ISSN 20452322. doi: 10.1038/s41598-019-49822-6.
https://ui.adsabs.harvard.edu/abs/2019NatSR...913165G/abstract. 167

Gannett, M. W., K. E. Lite, J. C. Risley, E. M. Pischel, and J. L. La Marche. Simulation of Groundwater and Surface-Water Flow in the Upper Deschutes Basin, Oregon. Technical report, U.S. Geological Survey Scientific Investigations Report, 2017.
https://pubs.er.usgs.gov/publication/sir20175097. 28

Garner, G., D. M. Hannah, and G. Watts. Climate change and water in the UK: Recent scientific evidence for past and future change. *progress in Physical Geography*, 41(2):151–174, 2017. doi: 10.1177/0309133316679082.
https://journals.sagepub.com/doi/pdf/10.1177/0309133316679082. 148

Georgakakos, K. P. On the Design of National, Real-Time Warning Systems with Capability for Site-Specific, Flash-Flood Forecasts. *Bulletin of the American Meteorological Society*, 67(10): 1233–1239, 1986. doi: 10.1175/1520-0477(1986)067<1233:OTDONR>2.0.CO;2.
http://journals.ametsoc.org/doi/abs/10.1175/1520-0477%281986%29067%3C1233%3AOTDONR%3E2.0.CO%3B2. 222

GeoSmart Information. Groundwater Flood Risk Map, 2015.
https://geosmartinfo.co.uk/data/groundwater-flood-risk-map/. 38, 172

GeoSmart Information. Groundwater flood forecasting services, 2019a.
https://geosmartinfo.co.uk/services/gwflood/. 39

GeoSmart Information. Groundwater flooding season begins early, 2019b.
https://geosmartinfo.co.uk/2019/12/groundwater-flooding-season/. 16

Glenis, V., V. Kutija, and C. Kilsby. A fully hydrodynamic urban flood modelling system representing buildings, green space and interventions. *Environmental Modelling & Software*, 109:272–292, 2018. doi: 10.1016/j.envsoft.2018.07.018.
https://linkinghub.elsevier.com/retrieve/pii/S1364815217310009. 23, 166, 175

Grahn, T. and L. Nyberg. Assessment of pluvial flood exposure and vulnerability of residential areas. *International Journal of Disaster Risk Reduction*, 21:367–375, 2017. ISSN 22124209. doi: 10.1016/j.ijdrr.2017.01.016.
https://www.sciencedirect.com/science/article/pii/S2212420916307919. 7

Green, C., T. Wilson, T. Masterson, and N. Boothby. An assessment of the additional flood losses associated with groundwater flooding: a report to Hampshire County Council and Winchester City Council. Technical report, Flood Hazard Research Centre, Middlesex University, 2006.
http://docplayer.net/16189480-An-assessment-of-the-additional-flood-losses-associated-with-groundwater-flooding-a-report-to-hampshire-county-council-and-winchester-city-council.html. 2

Guérin, A., O. Devauchelle, V. Robert, T. Kitou, C. Dessert, A. Quiquerez, P. Allemand, and E. Lajeunesse. Stream-Discharge Surges Generated by Groundwater Flow. *Geophysical Research Letters*, 46(13):7447–7455, 2019. ISSN 0094-8276. doi: 10.1029/2019GL082291.
https://onlinelibrary.wiley.com/doi/abs/10.1029/2019GL082291. 16

Guerreiro, S., V. Glenis, R. Dawson, and C. Kilsby. Pluvial Flooding in European Cities - A Continental Approach to Urban Flood Modelling. *Water*, 9(4), 2017a. ISSN 2073-4441. doi: 10.3390/w9040296.
http://www.mdpi.com/2073-4441/9/4/296. 117

Guerreiro, S. B., S. Birkinshaw, C. Kilsby, H. J. Fowler, and E. Lewis. Dry getting drier - the future of transnational river basins in Iberia. *Journal of Hydrology: Regional Studies*, 12: 238–252, 2017b. ISSN 22145818. doi: 10.1016/j.ejrh.2017.05.009.
https://www.sciencedirect.com/science/article/pii/S221458181630129X. 28

Gustard, A., A. Bullock, and J. M. Dixon. *Low flow estimation in the United Kingdom*. Institute of Hydrology, 1992. ISBN 0948540451.
http://nora.nerc.ac.uk/id/eprint/6050/1/IH_108.pdf. 56, 57

Halcrow. Regional Flood Risk Appraisal for South East England - Summary. Technical report, South East England Regional Assembly, 2008. 17

Halcrow Group Limited. Strategic Flood Risk Assessment: Bournemouth, Dorset & Poole. Level 1 SFRA for minerals & waste Volume I - SFRA Report. Technical report, Dorset County Council, 2010.
https://www.dorsetforyou.gov.uk/planning-buildings-land/planning-policy/dorset-county-council-planning-policy/pdfs/planning/sfra/dorset-strategic-flood-risk-assessment-december-2010.pdf. 73

Hannaford, J., L. Barker, M. Lewis, and S. Clemas. Hydrological Summary for the United Kingdom: August 2019. Technical report, Centre for Ecology & Hydrology, Wallingford, 2018.
www.hydoutuk.net/latest-outlook/. 8

Hannah, D. M., B. P. G. Smith, A. M. Gurnell, and G. R. Mcgregor. An approach to hydrograph classification. *Hydrological Processes*, 14:317–338, 2000.
https://onlinelibrary.wiley.com/doi/pdf/10.1002/%28SICI%291099-1085%2820000215%2914%3A2%3C317%3A%3AAID-HYP929%3E3.0.CO%3B2-T. 46, 58

Harbaugh, A. W. MODFLOW-2005, The U.S. Geological Survey Modular Ground-Water Model-the Ground-Water Flow Process. In *Techniques and Methods*, chapter 6-A16. U.S. Geological Survey, 2005.
http://water.usgs.gov/software/ground_water.html/. 25

Harish Kumar, S. and M. K. Nagaraj. Assessment of Interactions between River and Aquifer in the Gowri-hole Sub-catchment. *Journal of the Geological Society of India*, 92(4):435–440, 2018. ISSN 09746889. doi: 10.1007/s12594-018-1038-2.
https://link.springer.com/article/10.1007/s12594-018-1038-2. 16

Hdeib, R., C. Abdallah, F. Colin, L. Brocca, and R. Moussa. Constraining coupled hydrological-hydraulic flood model by past storm events and post-event measurements in data-sparse regions. *Journal of Hydrology*, 565:160–176, 2018. ISSN 00221694. doi: 10.1016/j.jhydrol.2018.08.008.
https://www.sciencedirect.com/science/article/pii/S0022169418306048. 27

He, S., S. Li, R. Xie, and J. Lu. Baseflow separation based on a meteorology-corrected nonlinear reservoir algorithm in a typical rainy agricultural watershed. *Journal of Hydrology*, 535:418–428, 2016. doi: 10.1016/j.jhydrol.2016.02.010.
https://www.sciencedirect.com/science/article/pii/S002216941630035X. 57

Hoehn, E. and A. Scholtis. Exchange between a river and groundwater, assessed with hydrochemical data. *Hydrology and Earth System Sciences*, 15(3):983–988, 2011. ISSN 1607-7938. doi: 10.5194/hess-15-983-2011.
https://www.hydrol-earth-syst-sci.net/15/983/2011/. 16

Horritt, M., L. Lovell, J. Wicks, and S. Buss. Developing a prototype tool for mapping flooding from all sources. Phase 1: Scoping and conceptual method development. Technical Report Project: SC080050/R1, Environment Agency, Bristol, 2010.
https://assets.publishing.service.gov.uk/government/uploads/system/uploads/attachment_data/file/291202/scho0310bsgq-e-e.pdf. 2, 40, 157, 167, 172, 177

Houston, D., A. Werritty, D. Bassett, A. Geddes, A. Hoolachan, and M. Mcmillan. Pluvial (rain-related) flooding in urban areas: the invisible hazard. Technical report, Joseph Rowntree Foundation, 2011.
http://eprints.gla.ac.uk/162145/7/162145.pdf. 7

Hughes, A. G., T. Vounaki, D. W. Peach, A. M. Ireson, C. R. Jackson, A. P. Butler, J. P. Bloomfield, J. Finch, and H. S. Wheater. Flood risk from groundwater: examples from a Chalk catchment in southern England. *Journal of Flood Risk Management*, 4(3):143–155, 2011.
http://nora.nerc.ac.uk/id/eprint/16078/. 1, 9, 10

Hughes, D. A. and V. Smakhtin. Daily flow time series patching or extension: a spatial interpolation approach based on flow duration curves. *Hydrological Sciences Journal*, 41(6), 1996.
https://www.tandfonline.com/doi/abs/10.1080/02626669609491555. 42

Hunter, N., R. Moore, S. Warren, B. Revilla-Romero, S. J. Cole, R. J. Moore, and S. C. Wells. Surface Water Flooding Component for NHP HIM: Phase 2 Report. D2.5 i Linking G2G to JFlow Inundation Model: SWF Hazard Footprint. Final Project Report. Technical report, Flood Forecasting Centre, 2016.
http://www.naturalhazardspartnership.org.uk/wp-content/uploads/2016/03/NHP-SWF-HIM-D2.5-Linking-G2G-and-JFlow-Models-Full-Report.pdf. 30

Hunter, N. M., P. D. Bates, M. S. Horritt, and M. D. Wilson. Simple spatially-distributed models for predicting flood inundation: A review. *Geomorphology*, 90(3-4):208–225, 2007. ISSN 0169555X. doi: 10.1016/j.geomorph.2006.10.021.
https://www.sciencedirect.com/science/article/pii/S0169555X07001304. 23

Hunter, N. M., P. D. Bates, S. Neelz, G. Pender, I. Villanueva, N. G. Wright, D. Liang, R. A. Falconer, B. Lin, S. Waller, A. J. Crossley, and D. C. Mason. Benchmarking 2D hydraulic models for urban flood simulations. *Proceedings of the Institution of Civil Engineers: Water Management*, 161(1):13–30, 2008. doi: 10.1680/wama.2008.161.1.13.
http://eprints.whiterose.ac.uk/77249/. 131

Innovyze. Infoworks ICM, 2020.
https://www.innovyze.com/en-us/products/infoworks-icm. 23

Institute of Geological Sciences. *Hydrogeology Map of the Permo-Triassic and Other Minor Aquifers of South West England*. British Geological Survey, 1982.
http://mapapps2.bgs.ac.uk/geoindex/home.html. 87

Institute of Geological Sciences & Wessex Water Authority. Hydrogeological Map of the Chalk and Associated Minor Aquifers of Wessex. British Geological Survey, 1979.
http://mapapps2.bgs.ac.uk/geoindex/home.html. 84, 86, 91, 103, 108, 109

Ireson, A., A. Butler, A. Butler, and A. Gallagher. Groundwater flooding in fractured permeable aquifers. In Blöschl, G., N. Giesen, D. Muralidharan, L. Ren, F. Seyler, U. Sharma, and J. Vrba, editors, *Improving Integrated Surface and Groundwater Resources Management in a Vulnerable and Changing World*, pages 165–172, 2009.
http://hydrologie.org/redbooks/a330/iahs_330_0165.pdf. 12

ITV News. Two years on from the devastation of Storm Desmond, 2017.
https://www.itv.com/news/border/2017-12-05/two-years-on-from-the-devastation-caused-by-storm-desmond/. 9

Iwagami, S., M. Tsujimura, Y. Onda, J. Shimada, and T. Tanaka. Role of bedrock groundwater in the rainfall-runoff process in a small headwater catchment underlain by volcanic rock. *Hydrological Processes*, 24(19):2771–2783, 2010. ISSN 08856087. doi: 10.1002/hyp.7690.
http://doi.wiley.com/10.1002/hyp.7690. 223

Jackson, C. R., J. P. Bloomfield, and J. D. Mackay. Evidence for changes in historic and future groundwater levels in the UK. *Progress in Physical Geography*, 39(1):49–67, 2015. ISSN 0309-1333. doi: 10.1177/0309133314550668.
http://ppg.sagepub.com/cgi/doi/10.1177/0309133314550668. 148

Jacobs. Groundwater Flooding Scoping Study (LDS 23) - Final Report. Technical report, 2004. 1, 13, 16, 35, 36, 37, 64, 74

Jacobs. Groundwater flooding records collation, monitoring and risk assessment (reference HA5). Consolidated Report. Technical report, Environment Agency, 2007.
https://webarchive.nationalarchives.gov.uk/20130403071227/http://archive.defra.gov.uk/environment/flooding/documents/risk/groundwaterreport.pdf. 1, 9, 10, 12, 142, 177

Jacobs. Strategic Flood Risk Assessment (SFRA) - Level 1. Technical report, Chiltern District Council, 2008.
http://www.chiltern.gov.uk/CHttpHandler.ashx?id=1595&p=0. 15, 19, 218

Jacobs. Strategic Flood Risk Assessment - Level 1 - Royal Borough of Windsor & Maidenhead. Technical report, Royal Borough of Windsor & Maidenhead, 2009.
http://www.rbwm.gov.uk/public/pp_sfra_level1_apr09_report.pdf. 19

Jacobs. Strategic Flood Risk Assessment - Level 1 Update - Wycombe District Council. Technical report, Wycombe District Council, 2014.
https://www.wycombe.gov.uk/uploads/public/documents/Wycombe-DC-Level-1-SFRA-Update-v03-FINAL.pdf. 19

Jacobs. Flood Modeller, 2020.
https://www.floodmodeller.com/. 23

Jaros, A., P. M. Rossi, A.-K. Ronkanen, and B. Kløve. Parameterisation of an integrated groundwater-surface water model for hydrological analysis of boreal aapa mire wetlands. *Journal of Hydrology*, 575:175–191, 2019. doi: 10.1016/J.JHYDROL.2019.04.094.
https://www.sciencedirect.com/science/article/pii/S0022169419304342?dgcid=raven_sd_aip_email. 150

JBA Consulting. Sevenoaks Stage 1 Surface Water Management Plan. Technical report, Kent County Council, 2013.

https://www.kent.gov.uk/__data/assets/pdf_file/0013/50008/Sevenoaks-Stage-1-SWMP-Report.pdf. 217

JBA Consulting. The Comprehensive Flood Map UK, 2014a.
http://www.jflow.co.uk/Great-Britain-flood-map/flood-modelling. 35, 165

JBA Consulting. JFlow | Award-winning 2D hydraulic model, 2014b.
http://www.jflow.co.uk/. 24

JBA Consulting. JBA launches national groundwater flood map, 2014c.
http://www.jbaconsulting.com/news/jba-launches-national-groundwater-flood-map. 38

JBA Consulting. JBA launches 5m resolution groundwater flood map, 2016.
https://www.jbaconsulting.com/knowledge-hub/jba-launches-5m-resolution-groundwater-flood-map/. 2, 38

JBA Consulting. Strategic Flood Risk Assessment - Appendix F - Areas Susceptible to Groundwater Flooding, 2017a.
https://www.sevenoaks.gov.uk/downloads/file/864/strategic_flood_risk_assessment_-_appendix_f_-_areas_susceptible_to_groundwater_flooding. 217

JBA Consulting. Strategic Flood Risk Assessment - Appendix E - Surface Water Flood Risk, 2017b.
https://www.sevenoaks.gov.uk/downloads/file/863/strategic_flood_risk_assessment_-_appendix_e_-_surface_water_flood_risk. 217

Jimenez-Martinez, J., M. Smith, and D. Pope. Prediction of groundwater-induced flooding in a chalk aquifer for future climate change scenarios. *Hydrological Processes*, 30(4):573–587, 2015. doi: 10.1002/hyp.10619.
http://doi.wiley.com/10.1002/hyp.10619. 148

Kappes, M. S., M. Keiler, K. von Elverfeldt, and T. Glade. Challenges of analyzing multi-hazard risk: a review. *Natural Hazards*, 64(2):1925–1958, nov 2012. ISSN 0921-030X. doi: 10.1007/s11069-012-0294-2.
http://link.springer.com/10.1007/s11069-012-0294-2. 157, 166, 167

Karam, H. A comparison between the ESI National Groundwater Flood Risk Map and the Environment Agency Areas Susceptible to Groundwater Flooding (AStGwF), 2016.
https://esi-consulting.co.uk/comparison-esi-national-groundwater-flood-risk-map-environment-agency-areas-susceptible-groundwater-flooding-astgwf/. 2, 39

Käser, D., T. Graf, F. Cochand, R. McLaren, R. Therrien, and P. Brunner. Channel Representation in Physically Based Models Coupling Groundwater and Surface Water: Pitfalls and How to Avoid Them. *Groundwater*, 52(6):827–836, 2014. doi: 10.1111/gwat.12143.
http://doi.wiley.com/10.1111/gwat.12143. 123

Keef, C., R. Lamb, J. Tawn, P. Dunning, C. Batstone, and M. Lawless. The risk of widespread flooding - Capturing spatial patterns in flood risk from rivers and coasts. SC060088/R3 Spatial Coherence of Flood Risk - Results from a national case study. Technical report, Environment Agency, Bristol, 2011.
https://assets.publishing.service.gov.uk/government/uploads/system/uploads/attachment_data/file/290835/scho1011bubq-e-e.pdf. 40

Kent County Council. Preliminary Flood Risk Assessment. Technical report, Kent County Council, 2011.
https://www.kent.gov.uk/__data/assets/pdf_file/0013/12091/Preliminary-flood-risk-assessment.pdf. 217

Kent County Council. Introduction to Flood Risk to Communities [DRAFT]. Technical report, Kent County Council, 2017.
https://www.kent.gov.uk/__data/assets/pdf_file/0008/71666/Flood-risk-to-communities-in-Sevenoaks.pdf. 217

Kilsby, C., P. Jones, A. Burton, A. Ford, H. Fowler, C. Harpham, P. James, A. Smith, and R. Wilby. A daily weather generator for use in climate change studies. *Environmental Modelling & Software*, 22(12):1705–1719, 2007. doi: 10.1016/J.ENVSOFT.2007.02.005.
https://www.sciencedirect.com/science/article/pii/S136481520700031X?via%3Dihub. 4, 42, 143, 146

Kim, J., A. Warnock, V. Y. Ivanov, and N. D. Katopodes. Coupled modeling of hydrologic and hydrodynamic processes including overland and channel flow. *Advances in Water Resources*, 37:104–126, 2012. doi: http://dx.doi.org/10.1016/j.advwatres.2011.11.009.
http://www.sciencedirect.com/science/article/pii/S0309170811002211. 31

Kollet, S., M. Sulis, R. M. Maxwell, C. Paniconi, M. Putti, G. Bertoldi, E. T. Coon, E. Cordano, S. Endrizzi, E. Kikinzon, E. Mouche, C. Mügler, Y.-J. Park, J. C. Refsgaard, S. Stisen, and E. Sudicky. The integrated hydrologic model intercomparison project, IH-MIP2: A second set of benchmark results to diagnose integrated hydrology and feedbacks. *Water Resources Research*, 53(1):867–890, 2017. doi: 10.1002/2016WR019191.
http://doi.wiley.com/10.1002/2016WR019191. 27

Komi, K., J. Neal, M. A. Trigg, and B. Diekkrüger. Modelling of flood hazard extent in data sparse areas: a case study of the Oti River basin, West Africa. *Journal of Hydrology: Regional Studies*, 10:122–132, 2017. doi: 10.1016/j.ejrh.2017.03.001.
https://linkinghub.elsevier.com/retrieve/pii/S2214581817300757. 125

Koo, B. and P. O'Connell. An integrated modelling and multicriteria analysis approach to managing nitrate diffuse pollution: 1. Framework and methodology. *Science of The Total Environment*, 359(1-3):1–16, 2006. ISSN 0048-9697. doi: 10.1016/J.SCITOTENV.2005.05.042.
https://www.sciencedirect.com/science/article/pii/S004896970500416X. 173

Krause, S., A. Bronstert, and E. Zehe. Groundwater-surface water interactions in a North German lowland floodplain - Implications for the river discharge dynamics and riparian water balance. *Journal of Hydrology*, 347(3-4):404–417, 2007. ISSN 00221694. doi: 10.1016/j.jhydrol.2007.09.028.
https://www.sciencedirect.com/science/article/pii/S002216940700529X. 16

Kreibich, H. and A. H. Thieken. Assessment of damage caused by high groundwater inundation. *Water Resources Research*, 44(9), 2008. ISSN 00431397. doi: 10.1029/2007WR006621.
http://doi.wiley.com/10.1029/2007WR006621. 9

Kreibich, H., A. H. Thieken, H. Grunenberg, K. Ullrich, and T. Sommer. Extent, perception and mitigation of damage due to high groundwater levels in the city of Dresden, Germany. *Natural Hazards and Earth System Sciences*, 9:1247–1258, 2009.
www.nat-hazards-earth-syst-sci.net/9/1247/2009/. 36

Kundzewicz, Z. W., I. Pińskwar, and G. R. Brakenridge. Changes in river flood hazard in Europe: a review. *Hydrology Research*, 49(2):294–302, apr 2018. ISSN 22247955. doi: 10.2166/nh.2017.016.
https://iwaponline.com/hr/article/49/2/294/37824/Changes-in-river-flood-hazard-in-Europe-a-review. 8

Ladson, A., R. Brown, B. Neal, and R. Nathan. A standard approach to baseflow separation using the Lyne and Hollick filter. *Australian Journal of Water Resources*, 17(1), 2013. ISSN 13241583. doi: 10.7158/W12-028.2013.17.1.
http://www.engineersmedia.com.au/journals/ajwr/2013/17_1/W12_028.html. 219

Landmark Information Group. New reports incorporate the first groundwater flood risk map available for England and Wales, 2015.
https://www.landmark.co.uk/news-archive/new-reports-incorporate-first-groundwater-flood-risk-map-available-england-and-wales. 38

Lane, S. N. Natural flood management. *Wiley Interdisciplinary Reviews: Water*, 4(3), 2017. ISSN 20491948. doi: 10.1002/wat2.1211.
http://doi.wiley.com/10.1002/wat2.1211. 8

Lerat, J., C. Perrin, V. Andréassian, C. Loumagne, and P. Ribstein. Towards robust methods to couple lumped rainfall-runoff models and hydraulic models: A sensitivity analysis on the Illinois River. *Journal of Hydrology*, 418-419:123–135, 2012. ISSN 00221694. doi: 10.1016/j.jhydrol.2009.09.019.
https://www.sciencedirect.com/science/article/pii/S0022169409005824. 27

Lewis, E. *A robust multi-purpose hydrological model for Great Britain*. PhD thesis, Newcastle University, 2015. 81, 83, 84, 86, 106, 173, 176

Lewis, E., S. Birkinshaw, C. Kilsby, and H. J. Fowler. Development of a system for automated setup of a physically-based, spatially-distributed hydrological model for catchments in Great Britain. *Environmental Modelling & Software*, 108:102–110, 2018. ISSN 1364-8152. doi: 10.1016/J.ENVSOFT.2018.07.006.
https://www.sciencedirect.com/science/article/pii/S1364815216311331?via%3Dihub. 4, 22, 28, 29, 33, 39, 70, 80, 81, 84, 107, 173

Li, L., H. Maier, M. Lambert, C. Simmons, and D. Partington. Framework for assessing and improving the performance of recursive digital filters for baseflow estimation with application to the Lyne and Hollick filter. *Environmental Modelling & Software*, 41:163–175, 2013. ISSN 13648152. doi: 10.1016/j.envsoft.2012.11.009.
http://linkinghub.elsevier.com/retrieve/pii/S1364815212002800. 56, 57

Li, Y., Q. Zhang, J. Lu, J. Yao, and Z. Tan. Assessing surface water-groundwater interactions in a complex river-floodplain wetland-isolated lake system. *River Research and Applications*, 35 (1):25–36, 2019. ISSN 1535-1459. doi: 10.1002/rra.3389.
https://onlinelibrary.wiley.com/doi/abs/10.1002/rra.3389. 16

Lian, J. J., K. Xu, and C. Ma. Joint impact of rainfall and tidal level on flood risk in a coastal city with a complex river network: a case study of Fuzhou City, China. *Hydrology and Earth System Sciences*, 17(2):679–689, 2013. ISSN 1607-7938. doi: 10.5194/hess-17-679-2013.
https://www.hydrol-earth-syst-sci.net/17/679/2013/. 17

Liang, Q. and L. S. Smith. A high-performance integrated hydrodynamic modelling system for urban flood simulations. *Journal of Hydroinformatics*, 17(4):518–533, 2015. ISSN 1464-7141. doi: 10.2166/hydro.2015.029.
https://iwaponline.com/jh/article/17/4/518-533/3563. 3, 23, 24, 117

Liedekerke, M., A. Jones, and P. Panagos. ESDBv2 Raster Library - a Set of Rasters Derived from the European Soil Database Distribution v2.0. Technical Report. Technical report, European Commission and the European Soil Bureau Network, 2006. 81

Lim, Y.-H. and L. M. Lye. Wavelet Analysis of Tide-affected Low Streamflows Series. *Journal of Data Science*, 2:149–163, 2004. 226

Liu, Q., Y. Qin, Y. Zhang, and Z. Li. A coupled 1D-2D hydrodynamic model for flood simulation in flood detention basin. *Natural Hazards*, 75(2):1303–1325, dec 2015. ISSN 15730840. doi: 10.1007/s11069-014-1373-3.
https://link.springer.com/article/10.1007/s11069-014-1373-3. 27

Local Government Association. Managing flood risk: roles and responsibilities, 2017.
https://www.local.gov.uk/topics/severe-weather/flooding/local-flood-risk-management/managing-flood-risk-roles-and. 33

Löwe, R., C. Urich, N. Sto. Domingo, O. Mark, A. Deletic, and K. Arnbjerg-Nielsen. Assessment of urban pluvial flood risk and efficiency of adaptation options through simulations – A new generation of urban planning tools. *Journal of Hydrology*, 550:355–367, 2017. ISSN 00221694. doi: 10.1016/j.jhydrol.2017.05.009.
https://www.sciencedirect.com/science/article/pii/S0022169417302962. 7

Lyne, V. and M. Hollick. Stochastic time-variable rainfall-runoff modelling. *Institute of Engineers Australia National Conference*, 1979.
https://www.researchgate.net/profile/Vincent_Lyne2/publication/272491803_Stochastic_Time-Variable_Rainfall-Runoff_Modeling/links/54f45fb40cf299c8d9e6e6c1.pdf. 219, 221

MacDonald, A. M. and D. J. Allen. Aquifer properties of the Chalk of England. *Quarterly Journal of Engineering Geology and Hydrogeology*, 34(4):371–384, 2001. doi: 10.1144/qjegh.34.4.371.
http://qjegh.lyellcollection.org/lookup/doi/10.1144/qjegh.34.4.371. 4, 12, 13, 81, 82, 94

MacDonald, A. M., D. J. Lapworth, A. G. Hughes, C. A. Auton, L. Maurice, A. Finlayson, and D. C. Gooddy. Groundwater, flooding and hydrological functioning in the Findhorn floodplain, Scotland. *Hydrology Research*, 45(6):755–773, dec 2014. ISSN 22247955. doi: 10.2166/nh.2014.185.
https://iwaponline.com/hr/article/45/6/755/1201/Groundwater-flooding-and-hydrological-functioning. 16

Macdonald, D. Groundwater Flooding - Science Briefing 2010. Technical report, British Geological Survey, 2010. 2, 38

Macdonald, D., R. Hall, D. Carden, A. Dixon, M. Cheetham, S. Cornick, and M. Clegg. Investigating the interdependencies between surface and groundwater in the Oxford area to help predict the timing and location of groundwater flooding and to optimise flood mitigation measures. 2007.
http://nora.nerc.ac.uk/id/eprint/9884/. 10

Macdonald, D., J. Bloomfield, A. Hughes, A. MacDonald, B. Adams, and A. McKenzie. Improving the understanding of the risk from groundwater flooding in the UK. 2008. http://nora.nerc.ac.uk/id/eprint/7760/. 1, 9, 10

Macdonald, D., A. Dixon, A. Newell, and A. Hallaways. Groundwater flooding within an urbanised flood plain. *Journal of Flood Risk Management*, 5(1):68–80, 2012. doi: 10.1111/j.1753-318X.2011.01127.x. http://dx.doi.org/10.1111/j.1753-318X.2011.01127.x. 10, 11, 47

Macdonald, D. M., A. J. Dixon, and D. C. Gooddy. Water and nitrate exchange between a managed river and peri-urban floodplain aquifer: Quantification and management implications. *Ecological Engineering*, 123:226–237, 2018. ISSN 09258574. doi: 10.1016/j.ecoleng.2018.09.005. https://www.sciencedirect.com/science/article/pii/S0925857418303276. 16

Marker, P. A., N. Foged, X. He, A. V. Christiansen, J. C. Refsgaard, E. Auken, and P. Bauer-Gottwein. An automated method to build groundwater model hydrostratigraphy from airborne electromagnetic data and lithological borehole logs. *Hydrology & Earth System Sciences Discussions*, 19:3875–3890, 2015. doi: 10.5194/hessd-12-1555-2015. www.hydrol-earth-syst-sci.net/19/3875/2015/. 39

Marsh, T. A hydrological overview of the summer 2007 floods in England and Wales. Technical report, Centre for Ecology & Hydrology, Wallingford, 2007. https://rmets.onlinelibrary.wiley.com/doi/pdf/10.1002/wea.305. 11

Martínez-Carreras, N., C. Hissler, J. François Iffly, J. Klaus, L. Gourdol, J. Juilleret, J. J. McDonnell, and L. Pfister. The Hunt for the explanation of the Double Peak hydrograph. In *EGU General Assembly Conference Abstracts*, volume 17, page 7280, 2015. 47, 223

Martínez-Carreras, N., C. Hissler, L. Gourdol, J. Klaus, J. Juilleret, J. F. Iffly, and L. Pfister. Storage controls on the generation of double peak hydrographs in a forested headwater catchment. *Journal of Hydrology*, 543:255–269, 2016. doi: 10.1016/J.JHYDROL.2016.10.004. https://www.sciencedirect.com/science/article/pii/S0022169416306370?via%3Dihub. 47

Mathers, S. J., R. L. Terrington, C. N. Waters, and A. G. Leslie. GB3D - a framework for the bedrock geology of Great Britain. *Geoscience Data Journal*, 1(1):30–42, jun 2014. ISSN 20496060. doi: 10.1002/gdj3.9. http://doi.wiley.com/10.1002/gdj3.9. 4, 82

Maxwell, R. M., M. Putti, S. Meyerhoff, J.-O. Delfs, I. M. Ferguson, V. Ivanov, J. Kim, O. Kolditz, S. J. Kollet, M. Kumar, S. Lopez, J. Niu, C. Paniconi, Y.-J. Park, M. S. Phanikumar, C. Shen, E. A. Sudicky, and M. Sulis. Surface-subsurface model intercomparison: A first set of benchmark results to diagnose integrated hydrology and feedbacks. *Water Resources Research*, 50(2):1531–1549, 2014. doi: 10.1002/2013WR013725. http://doi.wiley.com/10.1002/2013WR013725. 27

McKenzie, A. A. and R. S. Ward. Estimating numbers of properties susceptible to groundwater flooding in England. Technical report, British Geological Survey, 2015. http://nora.nerc.ac.uk/id/eprint/510064/1/OR15016.pdf. 2, 16, 26, 172

McKenzie, A. A., H. K. Rutter, and A. G. Hulbert. The use of elevation models to predict areas at risk of groundwater flooding. *Geological Society, London, Special Publications*, 345:75–79, 2010. doi: 10.1144/SP345.9. http://sp.lyellcollection.org/lookup/doi/10.1144/SP345.9. 2, 38

Merz, B., J. Hall, M. Disse, and A. Schumann. Fluvial flood risk management in a changing world. *Natural Hazards and Earth System Science*, 10(3):509–527, 2010a. ISSN 1684-9981. doi: 10.5194/nhess-10-509-2010.
http://www.nat-hazards-earth-syst-sci.net/10/509/2010/. 8

Merz, B., H. Kreibich, R. Schwarze, and A. Thieken. Assessment of economic flood damage. *Natural Hazards and Earth System Sciences*, 10:1697–1724, 2010b. doi: 10.5194/nhess-10-1697-2010.
www.nat-hazards-earth-syst-sci.net/10/1697/2010/. 142

Met Office. How much does it rain in the UK?, 2017.
https://www.metoffice.gov.uk/learning/rain/how-much-does-it-rain-in-the-uk. 75

Met Office Hadley Centre. Too hot cold dry wet: Drivers and impacts of seasonal weater in the UK. Technical Report CS01, 2014.
https://naturalresources.wales/media/2757/drivers-and-impacts-of-seasonal-weather-in-the-uk-met-office-report.pdf. 147

Meyer, V., C. Kuhlicke, J. Luther, S. Fuchs, S. Priest, W. Dorner, K. Serrhini, J. Pardoe, S. Mccarthy, J. Seidel, G. Palka, H. Unnerstall, C. Viavattene, and S. Scheuer. Natural Hazards and Earth System Sciences Recommendations for the user-specific enhancement of flood maps. *Hazards Earth System Sciences*, 12:1701–1716, 2012. doi: 10.5194/nhess-12-1701-2012.
www.nat-hazards-earth-syst-sci.net/12/1701/2012/. 35

Mid Sussex District Council. Strategic Flood Risk Assessment - Level 1. Technical report, 2015.
https://www.midsussex.gov.uk/media/2609/strategic-flood-risk-assessment.pdf. 18

Mignot, E., X. Li, and B. Dewals. Experimental modelling of urban flooding: A review. *Journal of Hydrology*, 568:334–342, 2019. doi: 10.1016/j.jhydrol.2018.11.001.
https://linkinghub.elsevier.com/retrieve/pii/S0022169418308485. 116

Miller, J. D. and M. Hutchins. The impacts of urbanisation and climate change on urban flooding and urban water quality: A review of the evidence concerning the United Kingdom. *Journal of Hydrology: Regional Studies*, 12:345–362, 2017. ISSN 22145818. doi: 10.1016/j.ejrh.2017.06.006.
https://www.sciencedirect.com/science/article/pii/S2214581817300435. 148

Mills, C. *The value and integrity of Fire Service call out records for identifying groundwater flooding locations*. Msc thesis, Birmingham University, 2004. 36

Morris, D., R. Flavin, and R. Moore. A digital terrain model for hydrology. In *4th International Symposium on Spatial Data Handling*, Zurich, 1990. 81

Morris, S., D. Cobby, and A. Parkes. Towards groundwater flood risk mapping. *Quarterly Journal of Engineering Geology and Hydrogeology*, 40(3), 2007.
http://qjegh.lyellcollection.org/content/40/3/203. 2, 35, 36, 37, 128

Morris, S., D. Cobby, M. Zaidman, and K. Fisher. Modelling and mapping groundwater flooding at the ground surface in Chalk catchments. *Journal of Flood Risk Management*, 11:251–268, 2018. doi: 10.1111/jfr3.12201.
https://onlinelibrary.wiley.com/doi/pdf/10.1111/jfr3.12201. 30, 35, 39, 143, 148, 160, 169

Morton, D., C. Rowland, C. Wood, L. Meek, C. Marston, G. Smith, R. Wadsworth, and I. Simpson. Countryside Survey: Final Report for LCM2007 the New UK Land Cover Map, Technical Report. Technical report, Centre for Ecology Hydrology, 2011.
https://www.ceh.ac.uk/sites/default/files/LCM2007FinalReport.pdf. 81

Munar, A. M., J. R. Cavalcanti, J. M. Bravo, F. M. Fan, D. da Motta-Marques, and C. R. Fragoso. Coupling large-scale hydrological and hydrodynamic modeling: Toward a better comprehension of watershed-shallow lake processes. *Journal of Hydrology*, 564:424–441, 2018. ISSN 00221694. doi: 10.1016/j.jhydrol.2018.07.045.
https://www.sciencedirect.com/science/article/pii/S0022169418305547. 27

Nathan, R. J. and T. A. McMahon. Evaluation of automated techniques for base flow and recession analyses. *Water Resources Research*, 26(7):1465–1473, 1990. ISSN 00431397. doi: 10.1029/WR026i007p01465.
http://doi.wiley.com/10.1029/WR026i007p01465. 219

National River Flow Archive. Hydrometric areas for Great Britain and Northern Ireland, 2004.
https://nrfa.ceh.ac.uk/hydrometric-areas. 64, 210

Naughton, O., P. M. Johnston, T. McCormack, and L. W. Gill. Groundwater flood risk mapping and management: examples from a lowland karst catchment in Ireland. *Journal of Flood Risk Management*, 2015.
https://onlinelibrary.wiley.com/doi/full/10.1111/jfr3.12145. 1

Naughton, O., T. Mccormack, R. Bradford, and J. Mcacteer. Developing historic and predictive groundwater flood maps for Ireland. In *Irish National Hydrology Conference*, pages 90–99. Hydrology Ireland, 2018a.
http://hydrologyireland.ie/wp-content/uploads/2018/11/08-Naughton-O.-Developing-historic-and-predictive-groundwater-flood-maps-for-Ireland.pdf.
11, 26

Naughton, O., T. Mccormack, L. Gill, and P. Johnston. Groundwater flood hazards and mechanisms in lowland karst terrains. In Parise, M., F. Gabrovsek, G. Kaufmann, and N. Ravbar, editors, *Advances in Karst Research: Theory, Fieldwork and Applications*, pages 397–410. Geological Society Special Publications, London, 2018b. doi: 10.1144/SP466.9.
https://doi.org/10.1144/SP466.9. 9, 12

Neal, J., G. Schumann, T. Fewtrell, M. Budimir, P. Bates, and D. Mason. Evaluating a new LISFLOOD-FP formulation with data from the summer 2007 floods in Tewkesbury, UK. *Journal of Flood Risk Management*, 4(2):88–95, 2011. ISSN 1753318X. doi: 10.1111/j.1753-318X.2011.01093.x.
http://doi.wiley.com/10.1111/j.1753-318X.2011.01093.x. 25

Néelz, S. and G. Pender. Benchmarking of 2D Hydraulic Modelling Packages. Technical report, Environment Agency, Bristol, 2010.
https://assets.publishing.service.gov.uk/government/uploads/system/uploads/attachment_data/file/290884/scho0510bsno-e-e.pdf. 117

Néelz, S. and G. Pender. Benchmarking the Latest Generation of 2D Hydraulic Modelling Packages. Technical report, Environment Agency, Bristol, 2013.
BenchmarkingtheLatestGeneration%0Aof2DHydraulicModellingPackages. 23, 25, 117

Nejadhashemi, A. P., A. Shirmohammadi, J. M. Sheridan, H. J. Montas, and K. R. Mankin. Case Study: Evaluation of Streamflow Partitioning Methods. *Journal of Irrigation and Drainage Engineering*, 135(6):791–801, 2009. ISSN 0733-9437. doi: 10.1061/(ASCE)IR.1943-4774.0000093.
http://ascelibrary.org/doi/10.1061/%28ASCE%29IR.1943-4774.0000093. 56, 57

Nelson, A., H. Reuter, and P. Gessler. DEM Production Methods and Sources. chapter 3, pages 65–85. 2009. doi: 10.1016/S0166-2481(08)00003-2.
http://linkinghub.elsevier.com/retrieve/pii/S0166248108000032. 43

Nguyen, P., A. Thorstensen, S. Sorooshian, K. Hsu, A. AghaKouchak, B. Sanders, V. Koren, Z. Cui, and M. Smith. A high resolution coupled hydrologic-hydraulic model (HiResFlood-UCI) for flash flood modeling. *Journal of Hydrology*, 541:401–420, 2016. ISSN 00221694. doi: 10.1016/j.jhydrol.2015.10.047.
https://www.sciencedirect.com/science/article/pii/S0022169415008185. 27

NRFA. National River Flow Archive | FEH Catchment Descriptors, 2019a.
https://nrfa.ceh.ac.uk/feh-catchment-descriptors. 74

NRFA. National River Flow Archive | Search Data, 2019b.
https://nrfa.ceh.ac.uk/data/search. 19, 20, 70, 72, 75, 87, 88, 90, 91, 147

Ó Dochartaigh, B., D. Diaz Doce, H. Rutter, and A. MacDonald. User guide : Aquifer Productivity (Scotland) GIS Datasets. Version 2, revised report (OR/15/003). Technical report, Nottingham, UK, 2015a.
http://nora.nerc.ac.uk/id/eprint/509619/. 13

Ó Dochartaigh, B. É., A. M. Macdonald, V. Fitzsimons, and R. Ward. Scotland's aquifers and groundwater bodies - British Geological Survey Open Report OR/15/028. Technical report, 2015b.
www.bgs.ac.uk/gsni/. 12, 13

Odeh, D. J. Natural Hazards Vulnerability Assessment for Statewide Mitigation Planning in Rhode Island. *Natural Hazards Review*, 3:177–187, 2002. doi: 10.1061/ASCE1527-698820023:4177.
https://ascelibrary.org/doi/pdf/10.1061/%28ASCE%291527-6988%282002%293%3A4%28177%29. 167

Onda, Y., Y. Komatsu, M. Tsujimura, and J.-i. Fujihara. The role of subsurface runoff through bedrock on storm flow generation. *Hydrological Processes*, 15(10):1693–1706, 2001. ISSN 0885-6087. doi: 10.1002/hyp.234.
http://doi.wiley.com/10.1002/hyp.234. 223

Onda, Y., M. Tsujimura, J.-i. Fujihara, and J. Ito. Runoff generation mechanisms in high-relief mountainous watersheds with different underlying geology. *Journal of Hydrology*, 331(3): 659–673, 2006. ISSN 00221694. doi: 10.1016/j.jhydrol.2006.06.009.
https://www.sciencedirect.com/science/article/pii/S0022169406003246. 223

Op de Hipt, F., B. Diekkruger, G. Steup, Y. Yira, T. Hoffmann, and M. Rode. Applying SHETRAN in a tropical West African Catchment (Dano, Burkina faso) - Calibration, Validation, Uncertainty Assessment. *Water*, 9(2):101, 2017. ISSN 2073-4441. doi: 10.3390/w9020101.
http://www.mdpi.com/2073-4441/9/2/101. 28, 117

Ordnance Survey. Land-form PANORAMA User Guide and Technical Specification v5.2. Technical Report. Technical report, Ordnance Survey, 2013a.
https://digimap.edina.ac.uk/webhelp/os/data_files/os_manuals/land-form-panorama-user-guide_5_2.pdf. 81

Ordnance Survey. Ordnance Survey Meridian 2 User Guide and Technical Specification v6.0. Tech. Rep. Technical report, Ordnance Survey, 2013b.

https://digimap.edina.ac.uk/webhelp/os/data_files/os_manuals/meridian-2-user-guide_6_0.pdf. 81

Ordnance Survey (GB). OS VectorMap^{TM} District [TIFF geospatial data], Scale 1:25000. Using: EDINA Digimap Ordnance Survey Service, 2019.
https://digimap.edina.ac.uk. 129, 154, 156, 160, 161

Ozdemir, H., C. C. Sampson, G. A. M. De Almeida, and P. D. Bates. Evaluating scale and roughness effects in urban flood modelling using terrestrial LIDAR data. *Hydrology and Earth System Sciences*, 17:4015–4030, 2013. doi: 10.5194/hess-17-4015-2013.
www.hydrol-earth-syst-sci.net/17/4015/2013/. 116

Park, Y.-J., E. A. Sudicky, A. E. Brookfield, and J. P. Jones. Hydrologic response of catchments to precipitation: Quantification of mechanical carriers and origins of water. *Water Resources Research*, 47(12), 2011. doi: 10.1029/2010WR010075.
http://doi.wiley.com/10.1029/2010WR010075. 56

Parkin, G., S. Birkinshaw, P. Younger, Z. Rao, and S. Kirk. A numerical modelling and neural network approach to estimate the impact of groundwater abstractions on river flows. *Journal of Hydrology*, 339(1-2):15–28, jun 2007. ISSN 0022-1694. doi: 10.1016/J.JHYDROL.2007.01.041.
https://www.sciencedirect.com/science/article/pii/S0022169407000285. 16, 28, 80, 117

Parrott, A., W. Brooks, O. Harmar, and K. Pygott. Role of rural land use management in flood and coastal risk management. *Journal of Flood Risk Management*, 2(4):272–284, 2009. ISSN 1753318X. doi: 10.1111/j.1753-318X.2009.01044.x.
http://doi.wiley.com/10.1111/j.1753-318X.2009.01044.x. 8

Parry, S., T. Marsh, and M. Kendon. 2012: from drought to floods in England and Wales. *Weather*, 68:268–274, 2012.
https://rmets.onlinelibrary.wiley.com/doi/pdf/10.1002/wea.2152. 9

Parry, S., L. Barker, I. Prosdocimi, M. Lewis, J. Hannaford, and S. Clemas. Hydrological summary for the United Kingdom: December 2015. Technical report, Centre for Ecology and Hydrology, Wallingford, 2015.
http://www.metoffice.gov.uk/publicsector/contingency-planners. 9

Patra, J. P., R. Kumar, and P. Mani. Combined Fluvial and Pluvial Flood Inundation Modelling for a Project Site. *Procedia Technology*, 24:93–100, 2016. ISSN 22120173. doi: 10.1016/j.protcy.2016.05.014.
https://www.sciencedirect.com/science/article/pii/S2212017316300974. 16

Perry, M. and D. Hollis. The generation of monthly gridded datasets for a range of climatic variables over the UK. *International Journal of Climatology*, 25(8):1041–1054, 2005. ISSN 0899-8418. doi: 10.1002/joc.1161.
http://doi.wiley.com/10.1002/joc.1161. 81

Perry, M., D. Hollis, and M. Elms. The Generation of Daily Gridded Datasets of Temperature and Rainfall for the UK. Technical Report. Technical report, Met Office National Climate Information Centre, 2009. 81

Peters, E. and H. A. J. van Lanen. Separation of base flow from streamflow using groundwater levels illustrated for the Pang catchment (UK). *Hydrological Processes*, 19(4):921–936, 2005.

ISSN 0885-6087. doi: 10.1002/hyp.5548.
http://doi.wiley.com/10.1002/hyp.5548. 19

Pielke, R. A. NINE FALLACIES OF FLOODS. *Climatic Change*, 42:413–438, 1999.
https://link.springer.com/content/pdf/10.1023%2FA%3A1005457318876.pdf. 3, 167

Pinault, J.-L., N. Amraoui, and C. Golaz. Groundwater-induced flooding in macropore-dominated hydrological system in the context of climate changes. *Water Resources Research*, 41(5), 2005. ISSN 00431397. doi: 10.1029/2004WR003169.
http://doi.wiley.com/10.1029/2004WR003169. 1, 9

Practical Law. Environment Agency publishes improved flood maps, 2013.
https://uk.practicallaw.thomsonreuters.com/8-552-1425?transitionType=Default&contextData=(sc.Default)&firstPage=true. 34

Prudhomme, C., J. Hannaford, S. Harrigan, D. Boorman, J. Knight, V. Bell, C. Jackson, C. Svensson, S. Parry, N. Bachiller-Jareno, H. Davies, R. Davis, J. Mackay, A. McKenzie, A. Rudd, K. Smith, J. Bloomfield, R. Ward, and A. Jenkins. Hydrological Outlook UK: an operational streamflow and groundwater level forecasting system at monthly to seasonal time scales. *Hydrological Sciences Journal*, 62(16):2753–2768, 2017. doi: 10.1080/02626667.2017.1395032.
https://www.tandfonline.com/doi/full/10.1080/02626667.2017.1395032. 167

Raj, P. Classification and interpretation of piezometer well hydrographs in parts of southeastern peninsular India. *Environmental Geology*, 46:808–819, 2004. doi: 10.1007/s00254-004-1031-2.
https://link.springer.com/content/pdf/10.1007%2Fs00254-004-1031-2.pdf. 46

Refsgaard, J. C., B. Storm, and T. Clausen. Système Hydrologique Européen (SHE): review and perspectives after 30 years development in distributed physically-based hydrological modelling. *Hydrology Research*, 41(5):355–377, 2010. doi: 10.2166/nh.2010.009.
https://iwaponline.com/hr/article-pdf/41/5/355/371012/355.pdf. 28, 33

Reynolds, L. Flash floods cause chaos in British town of Amersham in Buckinghamshire, 2016.
http://www.express.co.uk/news/uk/680264/Flash-floods-cause-chaos-British-town. 218

Rinderer, M., H. J. van Meerveld, and J. Seibert. Topographic controls on shallow groundwater levels in a steep, prealpine catchment: When are the TWI assumptions valid? *Water Resources Research*, 50(7):6067–6080, 2014. doi: 10.1002/2013WR015009.
http://doi.wiley.com/10.1002/2013WR015009. 126

Rivett, M., J. Smith, S. Buss, and P. Morgan. Nitrate occurrence and attenuation in the major aquifers of England and Wales. *Quarterly Journal of Engineering Geology and Hydrogeology*, 40(4):335–352, 2007. doi: 10.1144/1470-9236/07-032.
http://qjegh.lyellcollection.org/lookup/doi/10.1144/1470-9236/07-032. 12, 14

Rizeei, H. M., B. Pradhan, and M. A. Saharkhiz. An integrated fluvial and flash pluvial model using 2D high-resolution sub-grid and particle swarm optimization-based random forest approaches in GIS. *Complex & Intelligent Systems*, 5(3):283–302, 2019. ISSN 2199-4536. doi: 10.1007/s40747-018-0078-8.
https://link.springer.com/article/10.1007/s40747-018-0078-8. 16, 17

Robins, N. S. and J. W. Finch. Groundwater flood or groundwater-induced flood? *Quarterly Journal of Engineering Geology and Hydrogeology*, 45(1):119–122, 2012. ISSN 1470-9236. doi: 10.1144/1470-9236/10-040.
http://qjegh.lyellcollection.org/cgi/doi/10.1144/1470-9236/10-040. 9, 11, 16

Rosser, J. F., D. G. Leibovici, and M. J. Jackson. Rapid flood inundation mapping using social media, remote sensing and topographic data. *Natural hazards*, 87(1):103–120, 2017. doi: 10.1007/s11069-017-2755-0.
https://link.springer.com/article/10.1007/s11069-017-2755-0. 177

Rust, W., R. Corstanje, I. Holman, and A. Milne. Detecting land use and land management influences on catchment hydrology by modelling and wavelets. *Journal of Hydrology*, 517: 378–389, 2014. ISSN 00221694. doi: 10.1016/j.jhydrol.2014.05.052.
https://www.sciencedirect.com/science/article/pii/S0022169414004168. 227

Saksena, S., V. Merwade, and P. J. Singhofen. Flood inundation modeling and mapping by integrating surface and subsurface hydrology with river hydrodynamics. *Journal of Hydrology*, 575:1155–1177, 2019. doi: 10.1016/J.JHYDROL.2019.06.024.
https://www.sciencedirect.com/science/article/pii/S0022169419305657. 2, 26, 83, 125, 157

Salem, A., J. Dezső, M. El-Rawy, and D. Lóczy. Hydrological Modeling to Assess the Efficiency of Groundwater Replenishment through Natural Reservoirs in the Hungarian Drava River Floodplain. *Water*, 12(1):250, 2020. ISSN 2073-4441. doi: 10.3390/w12010250.
https://www.mdpi.com/2073-4441/12/1/250. 16

Schaefli, B., D. Maraun, and M. Holschneider. What drives high flow events in the Swiss Alps? Recent developments in wavelet spectral analysis and their application to hydrology. *Advances in Water Resources*, 30(12):2511–2525, 2007. ISSN 03091708. doi: 10.1016/j.advwatres.2007.06.004.
https://www.sciencedirect.com/science/article/pii/S0309170807001066. 228

Schanze, J. Flood Risk Management - A Basic Framework. In Schanze, J., E. Zeman, and J. Marsalek, editors, *Flood Risk Management - Hazards, Vulnerabilities and Mitigation Measures*, chapter 1, pages 1–20. NATO Science Series, vol 67. Springer, Dordrecht, 2006.
http://www.nato.int/science. 3

Scott Wilson. Strategic Flood Risk Assessment - Level 1 - Kennet District Council. Technical report, Kennet District Council, 2008a.
http://www.wiltshire.gov.uk/kennet_strategic_flood_risk_assessment_level_1_2008_-_main_report.pdf. 19, 20

Scott Wilson. Strategic Flood Risk Assessment - Level 1 - Wiltshire County Council and Swindon Borough Council. Technical report, Wiltshire County Council and Swindon Borough Council, 2008b.
http://www.wiltshire.gov.uk/minerals-and-waste-level-1-sfra-final-report.pdf. 20

Seaburn, G. E. Effects of urban development on direct runoff to East Meadow Brook, Nassau County, Long Island, New York. In United States Geological Survey Professional Paper, editor, *Hydrology and Some Effects of Urbanisation on Long Island, New York*, chapter B, pages B1–B14. US Government Printing Office, Washington, 1969.
https://pubs.usgs.gov/pp/0627b/report.pdf. 47

Seibert, J., K. Bishop, A. Rodhe, and J. J. McDonnell. Groundwater dynamics along a hillslope: A test of the steady state hypothesis. *Water Resources Research*, 39(1):n/a–n/a, 2003. ISSN 00431397. doi: 10.1029/2002WR001404.
http://doi.wiley.com/10.1029/2002WR001404. 26

Serinaldi, F. Dismissing return periods! *Stochastic Environmental Research and Risk Assessment*, 29:1179–1189, 2014. doi: 10.1007/s00477-014-0916-1.
https://link.springer.com/content/pdf/10.1007%2Fs00477-014-0916-1.pdf. 167

Shepley, M. G., M. I. Whiteman, P. J. Hulme, and M. W. Grout. Introduction: groundwater resources modelling: a case study from the UK. *Geological Society, London, Special Publications*, 364(1):1 LP – 6, 2012.
http://sp.lyellcollection.org/content/364/1/1.abstract. 25, 26, 83

Shumway, R. and D. Stoffer. *Time series analysis and its applications: with R examples*. Springer Science & Business Media, second edi edition, 2006.
https://www.stat.pitt.edu/stoffer/tsa4/tsa4.pdf. 226, 227

Smith, L. C., D. L. Turcotte, and B. L. Isacks. Stream flow characterization and feature detection using a discrete wavelet transform. *Hydrological Processes*, 12(2):233–249, 1998. ISSN 08856087. doi: 10.1002/(SICI)1099-1085(199802)12:2<233::AID-HYP573>3.0.CO;2-3.
https://www.geog.ucla.edu/sites/default/files/users/lsmith/178.pdf. 226

Smith, L. S. and Q. Liang. Towards a generalised GPU/CPU shallow-flow modelling tool. *Computers & Fluids*, 88:334–343, 2013. ISSN 0045-7930. doi: 10.1016/J.COMPFLUID.2013.09.018.
https://www.sciencedirect.com/science/article/pii/S0045793013003630. 23, 24

Smith, L. S., Q. Liang, and P. F. Quinn. Towards a hydrodynamic modelling framework appropriate for applications in urban flood assessment and mitigation using heterogeneous computing. *Urban Water Journal*, 12(1):67–78, 2015. ISSN 1573-062X. doi: 10.1080/1573062X.2014.938763.
http://www.tandfonline.com/doi/abs/10.1080/1573062X.2014.938763. 24

Soley, R. W. N., T. Power, R. N. Mortimore, P. Shaw, J. Dottridge, G. Bryan, and I. Colley. Modelling the hydrogeology and managed aquifer system of the Chalk across southern England. *Geological Society, London, Special Publications*, 364(1):129–154, 2012. doi: 10.1144/SP364.10.
http://sp.lyellcollection.org/lookup/doi/10.1144/SP364.10. 12

Sommer, T., C. Karpf, N. Ettrich, D. Haase, T. Weichel, J.-V. Peetz, B. Steckel, K. Eulitz, and K. Ullrich. Coupled modelling of subsurface water flux for an integrated flood risk management. *Natural Hazards and Earth System Science*, 9:1277–1290, 2009. doi: 10.5194/nhess-9-1277-2009.
http://www.nat-hazards-earth-syst-sci.net/9/1277/2009/. 157

Sophocleous, M. Interactions between groundwater and surface water: the state of the science. *Hydrogeology Journal*, 10(1):52–67, 2002. ISSN 1431-2174. doi: 10.1007/s10040-001-0170-8.
http://link.springer.com/10.1007/s10040-001-0170-8. 56

Sörensen, J. and S. Mobini. Pluvial, urban flood mechanisms and characteristics – Assessment based on insurance claims. *Journal of Hydrology*, 555:51–67, 2017. ISSN 00221694. doi: 10.1016/j.jhydrol.2017.09.039.
https://www.sciencedirect.com/science/article/pii/S0022169417306431?via%3Dihub. 7

Sreekanth, P., P. Sreedevi, S. Ahmed, and N. Geethanjali. Comparison of FFNN and ANFIS models for estimating groundwater level. *Environmental Earth Sciences*, 62(6):1301–1310, 2011. doi: 10.1007/s12665-010-0617-0.
http://link.springer.com/10.1007/s12665-010-0617-0. 92

Stewart, M., J. Cimino, and M. Ross. Calibration of Base Flow Separation Methods with Streamflow Conductivity. *Ground Water*, 45(1):17–27, 2007. ISSN 0017-467X. doi: 10.1111/j.1745-6584.2006.00263.x.
http://doi.wiley.com/10.1111/j.1745-6584.2006.00263.x. 56

Stratford, C., J. Miller, A. House, G. Old, M. Acreman, M. Duenas-Lopez, T. Nisbet, L. Burgess-Gamble, N. Chappell, S. Clarke, L. Leeson, G. Monbiot, J. Paterson, M. Robinson, M. Rogers, and D. Tickner. Do trees in UK-relevant river catchments influence fluvial flood peaks? A systematic review. Technical report, Centre for Ecology and Hydrology, Wallingford, UK, 2017.
http://nora.nerc.ac.uk/id/eprint/517804/. 8

Tallaksen, L. A review of baseflow recession analysis. *Journal of Hydrology*, 165(1):349–370, 1995. ISSN 00221694. doi: 10.1016/0022-1694(94)02540-R. 56, 57

ten Veldhuis, J. A., F. H. Clemens, and P. H. van Gelder. Quantitative fault tree analysis for urban water infrastructure flooding. *Structure and Infrastructure Engineering*, 7(11):809–821, 2011. ISSN 1573-2479. doi: 10.1080/15732470902985876.
http://www.tandfonline.com/doi/abs/10.1080/15732470902985876. 7

Teng, J., A. Jakeman, J. Vaze, B. Croke, D. Dutta, and S. Kim. Flood inundation modelling: A review of methods, recent advances and uncertainty analysis. *Environmental Modelling & Software*, 90:201–216, 2017. doi: 10.1016/j.envsoft.2017.01.006.
https://linkinghub.elsevier.com/retrieve/pii/S1364815216310040. 22, 23, 177

Ternynck, C., M. Ali, B. Alaya, F. Chebana, and T. B. M. J. Ouarda. Streamflow Hydrograph Classification Using Functional Data Analysis. *Journal of hydrometeorology*, 17(1):327–344, 2016. doi: 10.1175/JHM-D-14-0200.1.
https://journals.ametsoc.org/doi/pdf/10.1175/JHM-D-14-0200.1. 46

The Geological Society. Greensand, Bedfordshire, 2008.
https://www.geolsoc.org.uk/ks3/gsl/education/resources/rockcycle/page3812.html. 15

Theanalysisfactor. Assessing the Fit of Regression Models, 2008.
https://www.theanalysisfactor.com/assessing-the-fit-of-regression-models/. 92

Thomas, B. F., R. M. Vogel, and J. S. Famiglietti. Objective hydrograph baseflow recession analysis. *Journal of Hydrology*, 525:102–112, 2015. ISSN 0022-1694. doi: 10.1016/J.JHYDROL.2015.03.028.
https://www.sciencedirect.com/science/article/pii/S0022169415001997. 47, 56

Tian, J., C. Li, J. Liu, F. Yu, S. Cheng, N. Zhao, and W. Z. W. Jaafar. Groundwater Depth Prediction Using Data-Driven Models with the Assistance of Gamma Test. *Sustainability*, 8 (1076):1–17, 2016.
https://www.mdpi.com/2071-1050/8/11/1076. 92, 93

Trémolières, M., I. Eglin, U. Roeck, and R. Carbiener. The exchange process between river and groundwater on the Central Alsace floodplain (Eastern France) - I. The case of the canalised

river Rhine. *Hydrobiologia*, 254:133–148, 1993. ISSN 15735117. doi: 10.1007/BF00014108. https://link.springer.com/article/10.1007/BF00014108. 9, 16

Trevis, H. Hydro-JULES | Project Overview, 2018. https://www.ceh.ac.uk/hydrojules. 174

UK Groundwater Forum. Groundwater in Depth - Aquifers of the UK, 2009. http://www.groundwateruk.org/downloads/the_aquifers_of_the_uk.pdf. 12

Upton, K. A. and C. R. Jackson. Simulation of the spatio-temporal extent of groundwater flooding using statistical methods of hydrograph classification and lumped parameter models. *Hydrological Processes*, 25(12):1949–1963, 2011. ISSN 08856087. doi: 10.1002/hyp.7951. http://doi.wiley.com/10.1002/hyp.7951. 25, 46, 224

U.S. Geological Survey. MODFLOW 6: USGS Modular Hydrologic Model, 2019a. https://www.usgs.gov/software/modflow-6-usgs-modular-hydrologic-model. 138

U.S. Geological Survey. SUMMARY OF PRMS Version 5.0.0. Technical report, U.S. Geological Survey, 2019b. http://dx.doi.org/10.3133/tm6B7. 27

U.S. Geological Survey. GSFLOW: Coupled Groundwater and Surface-Water Flow Model, 2019c. https://www.usgs.gov/software/coupled-ground-water-and-surface-water-flow-model-gsflow. 27

USGS. Guidance for determining applicability of the USGS GSFLOW and OWHM models for hydrologic simulation and analysis. Technical report, 2017. https://water.usgs.gov/ogw/modflow-owhm/GSFLOW-OWHM-guidance-20170518.pdf. 27

USGS. USGS MODFLOW and Related Programs, 2019. https://water.usgs.gov/ogw/modflow/. 25, 27

Vivoni, E. R., D. Entekhabi, R. L. Bras, and V. Y. Ivanov. Controls on runoff generation and scale-dependence in a distributed hydrologic model. *Hydrology and Earth System Sciences*, 11 (5):1683–1701, 2007. ISSN 1607-7938. doi: 10.5194/hess-11-1683-2007. http://www.hydrol-earth-syst-sci.net/11/1683/2007/. 16

Wang, K., Z. M. Xu, L. Tian, Z. Ren, K. Yang, Y. J. Tang, H. Y. Gao, and J. Y. Luo. Estimating the dynamics of the groundwater in vegetated slopes based on the monitoring of streams. *Engineering Geology*, 259, 2019. ISSN 00137952. doi: 10.1016/j.enggeo.2019.105160. https://www.sciencedirect.com/science/article/pii/S0013795218317186. 16

Wang, Y. and X. Yang. Sensitivity Analysis of the Surface Runoff Coefficient of HiPIMS in Simulating Flood Processes in a Large Basin. *Water*, 10(3):253, 2018. ISSN 2073-4441. doi: 10.3390/w10030253. http://www.mdpi.com/2073-4441/10/3/253. 24

Ward, R. Principal aquifers of England and Wales - The Lower Greensand, 2014. https://www.bgs.ac.uk/research/groundwater/shaleGas/aquifersAndShales/maps/aquifers/LowerGreensand.html. 15

Watson, C., J. Richardson, B. Wood, C. Jackson, and A. Hughes. Improving geological and process model integration through TIN to 3D grid conversion. *Computers & Geosciences*, 82: 45–54, 2015. ISSN 0098-3004. doi: 10.1016/J.CAGEO.2015.05.010. https://www.sciencedirect.com/science/article/pii/S0098300415001144. 4, 82

Watts, G., R. W. Battarbee, J. P. Bloomfield, J. Crossman, A. Daccache, I. Durance, J. A. Elliott, G. Garner, J. Hannaford, and D. M. Hannah. Climate change and water in the UK–past changes and future prospects. *Progress in Physical Geography*, 39(1):6–28, 2015. https://journals.sagepub.com/doi/full/10.1177/0309133314542957. 147, 148

West Berkshire Council. Pang Valley Flood Risk Management Plan 2013-2016. Technical report, West Berkshire Council, 2013. https://info.westberks.gov.uk/CHttpHandler.ashx?id=38234&p=0. 19

Wheater, H. and E. Evans. Land use, water management and future flood risk. *Land Use Policy*, 26(SUPPL. 1):S251–S264, 2009. ISSN 02648377. doi: 10.1016/j.landusepol.2009.08.019. https://www.sciencedirect.com/science/article/pii/S0264837709001082. 8

Wheater, H. S. Progress in and prospects for fluvial flood modelling. *Philosophical Transactions of the Royal Society of London. Series A: Mathematical, Physical and Engineering Sciences*, 360(1796):1409–1431, 2002. ISSN 1364-503X. doi: 10.1098/rsta.2002.1007. https://royalsocietypublishing.org/doi/10.1098/rsta.2002.1007. 21

Whiteman, M., C. Maginness, R. Farrell, P. Gijsbers, and M. Ververs. The National Groundwater Modelling System: providing wider access to groundwater models. In Shepley, M. G., M. I. Whiteman, and P. Hulme, editors, *Groundwater Resources Modelling: A Case Study from the UK*, pages 49–63. The Geological Society of London, London, 364 edition, 2012. doi: 10.1144/SP364.5. https://sp.lyellcollection.org/content/364/1/49. 26

Wicks, J. and L. Lovell. Developing a prototype tool for mapping flooding from all sources. Phase 2: final report. Technical report, Environment Agency, 2011. https://www.gov.uk/government/publications/developing-a-prototype-tool-for-mapping-flooding-from-all-sources. 40

Widaman, K. F. III. Missing data: What to do with or without them. *Monographs of the Society for Research in Child Development*, 71(1):210–211, 2006. ISSN 0037976X. doi: 10.1111/j.1540-5834.2006.00404.x. http://doi.wiley.com/10.1111/j.1540-5834.2006.00404.x. 42

Wilby, R. L., N. J. Clifford, P. De Luca, S. Harrigan, J. K. Hillier, R. Hodgkins, M. F. Johnson, T. K. Matthews, C. Murphy, S. J. Noone, S. Parry, C. Prudhomme, S. P. Rice, L. J. Slater, K. A. Smith, and P. J. Wood. The 'dirty dozen' of freshwater science: detecting then reconciling hydrological data biases and errors. *Wiley Interdisciplinary Reviews: Water*, 4(3):e1209, 2017. ISSN 20491948. doi: 10.1002/wat2.1209. http://doi.wiley.com/10.1002/wat2.1209. 54

Wilson, G. V., P. M. Jardine, R. J. Luxmoore, and J. R. Jones. Hydrology of a Forested Hillslope during Storm Events. *Geoderma*, 46:119–138, 1990. https://www.sciencedirect.com/science/article/pii/001670619090011W. 166

Woods, A. Using climate change projections in UK flood risk assessment. *Proceedings of the Institution of Civil Engineers - Water Management*, 168(4):162–173, 2015. ISSN 17517729. doi: doi:10.1680/wama.13.00064. http://www.icevirtuallibrary.com/doi/abs/10.1680/wama.13.00064. 147

World Meteorological Organization. Manual on Low-flow Estimation and Prediction. Operational Hydrology Report No. 50. Technical report, WMO, 2008.

http://www.wmo.int/pages/prog/hwrp/publications/low-flow_estimation_prediction/WMO1029en.pdf. 56, 57, 219, 221

Xia, X., Q. Liang, X. Ming, and J. Hou. An efficient and stable hydrodynamic model with novel source term discretization schemes for overland flow and flood simulations. *Water Resources Research*, 53(5):3730–3759, 2017. ISSN 00431397. doi: 10.1002/2016WR020055. http://doi.wiley.com/10.1002/2016WR020055. 117

Xia, X., Q. Liang, and X. Ming. High-Performance Integrated hydrodynamic Modelling of Storm Induced Floods at a Catchment Scale. In La Loggia, G., G. Freni, V. Puleo, and M. De Marchis, editors, *HIC 2018. 13th International Conference on Hydroinformatics (EPiC Series in Engineering)*, volume 3, pages 2359–2367. EasyChair, 2018. https://easychair.org/publications/paper/h6LV. 116, 117

Xia, X., Q. Liang, and X. Ming. A full-scale fluvial flood modelling framework based on a high-performance integrated hydrodynamic modelling system (HiPIMS). *Advances in Water Resources*, 132, 2019. ISSN 03091708. doi: 10.1016/j.advwatres.2019.103392. 117

Xing, Y., Q. Liang, G. Wang, X. Ming, and X. Xia. City-scale hydrodynamic modelling of urban flash floods: the issues of scale and resolution. *Natural Hazards*, 96(1):473–496, 2019. ISSN 15730840. doi: 10.1007/s11069-018-3553-z. https://link.springer.com/article/10.1007/s11069-018-3553-z. 175

Xue, J. and K. Gavin. Effect of Rainfall Intensity on Infiltration into Partly Saturated Slopes. *Geotechnical and Geological Engineering*, 26:199–209, 2008. doi: 10.1007/s10706-007-9157-0. https://link.springer.com/content/pdf/10.1007%2Fs10706-007-9157-0.pdf. 166

Yan, S.-f., S.-e. Yu, Y.-b. Wu, D.-f. Pan, and J.-g. Dong. Understanding groundwater table using a statistical model. *Water Science and Engineering*, 11(1):1–7, 2018. doi: 10.1016/j.wse.2018.03.003. http://linkinghub.elsevier.com/retrieve/pii/S1674237018300218. 56

Yang, Y., T. A. Endreny, M. Asce, and D. J. Nowak. Simulating Double-Peak Hydrographs from Single Storms over Mixed-Use Watersheds. *Journal of Hydrological Engineering*, 20(11), 2015. doi: 10.1061/(ASCE)HE.1943-5584.0001225. https://www.fs.fed.us/nrs/pubs/jrnl/2015/nrs_2015_yang-y_002.pdf. 47

Yue, S., T. Ouarda, B. Bobée, P. Legendre, and P. Bruneau. The Gumbel mixed model for flood frequency analysis. *Journal of Hydrology*, 226(1-2):88–100, 1999. doi: 10.1016/S0022-1694(99)00168-7. https://www.sciencedirect.com/science/article/pii/S0022169499001687. 149

Zaidman, M. Developments in Groundwater Flood Mapping, 2014. http://www.jbaconsulting.com/blog/developments-groundwater-flood-mapping. 1

Zhang, R. Impacts of Spatial and Temporal Scales on a Distributed Hydrological Model (Unpublished). *Institute of Mediterranean Agricultural and Environmental Sciences, University of Évora*, 2012. 107

Zhou, L., Y. Meng, and K. C. Abbaspour. A new framework for multi-site stochastic rainfall generator based on empirical orthogonal function analysis and Hilbert-Huang transform. *Journal of Hydrology*, 575:730–742, 2019. doi: 10.1016/J.JHYDROL.2019.05.047. https://www.sciencedirect.com/science/article/pii/S0022169419304925. 146

Zhou, Q. A Review of Sustainable Urban Drainage Systems Considering the Climate Change and Urbanization Impacts. *Water*, 6(4):976–992, 2014. ISSN 2073-4441. doi: 10.3390/w6040976. http://www.mdpi.com/2073-4441/6/4/976. 8

Zhou, Q., P. Mikkelsen, K. Halsnæs, and K. Arnbjerg-Nielsen. Framework for economic pluvial flood risk assessment considering climate change effects and adaptation benefits. *Journal of Hydrology*, 414-415:539–549, 2012. doi: 10.1016/j.jhydrol.2011.11.031. https://linkinghub.elsevier.com/retrieve/pii/S002216941100816X. 142

Zhou, Y. and W. Li. A review of regional groundwater flow modeling. *Geoscience Frontiers*, 2(2): 205–214, apr 2011. doi: 10.1016/J.GSF.2011.03.003. http://www.sciencedirect.com/science/article/pii/S167498711100020X. 25, 92

Zillgens, B., B. Merz, R. Kirnbauer, and N. Tilch. Analysis of the runoff response of an alpine catchment at different scales. Technical report, 2007. www.hydrol-earth-syst-sci.net/11/1441/2007/. 47

VIII

Appendix - Chapter III

26. Maps

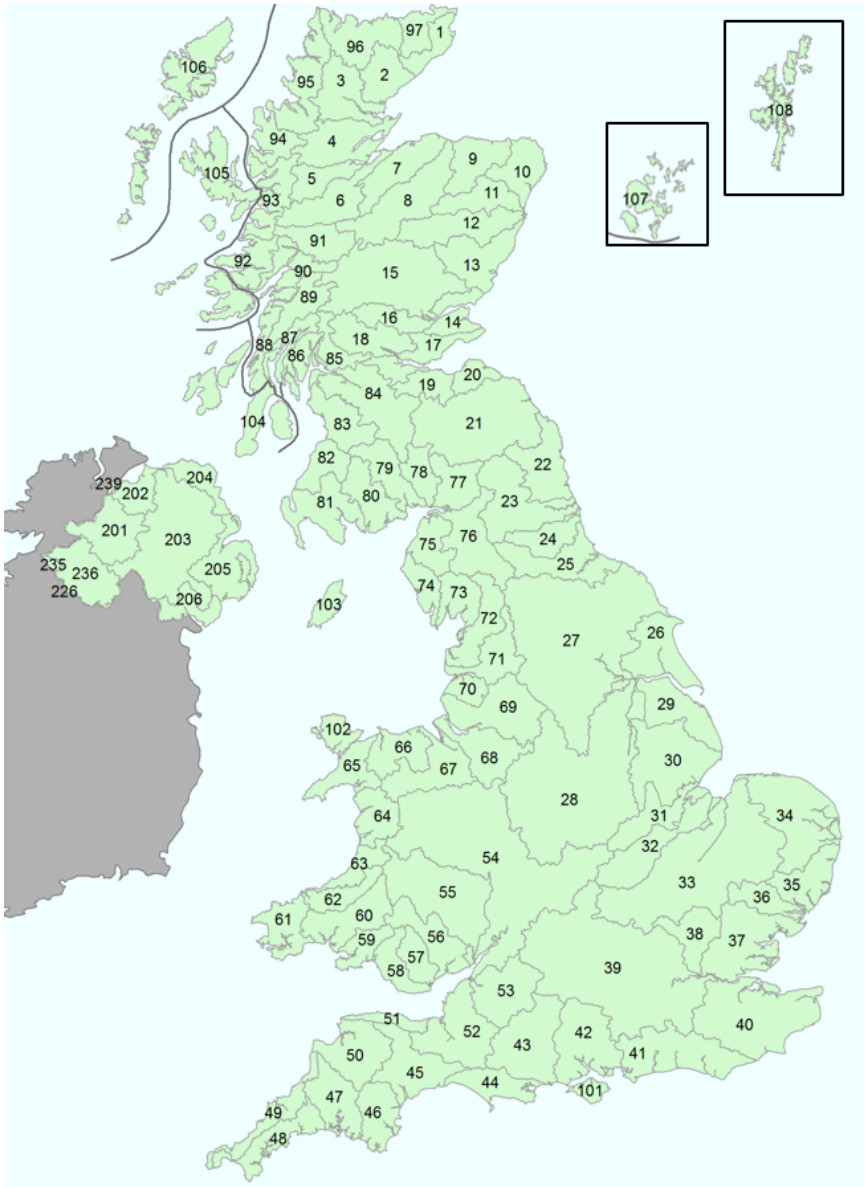

Figure 26.1: The UK's hydrometric areas are labelled clockwise. They make up the first two numbers of the gauging station IDs (National River Flow Archive, 2004).

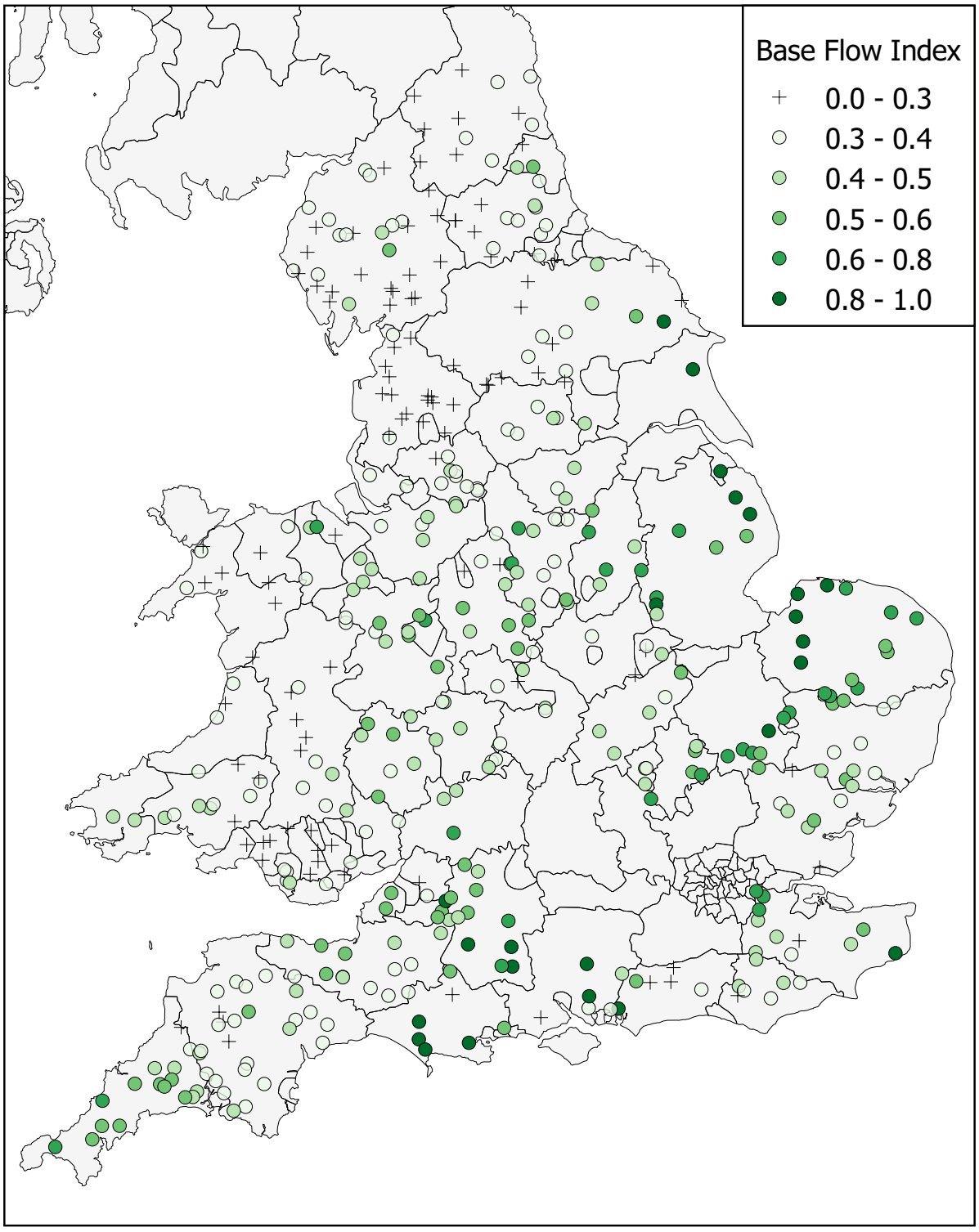

Figure 26.2: The base flow indexes during the highest 20% of flows are displayed.

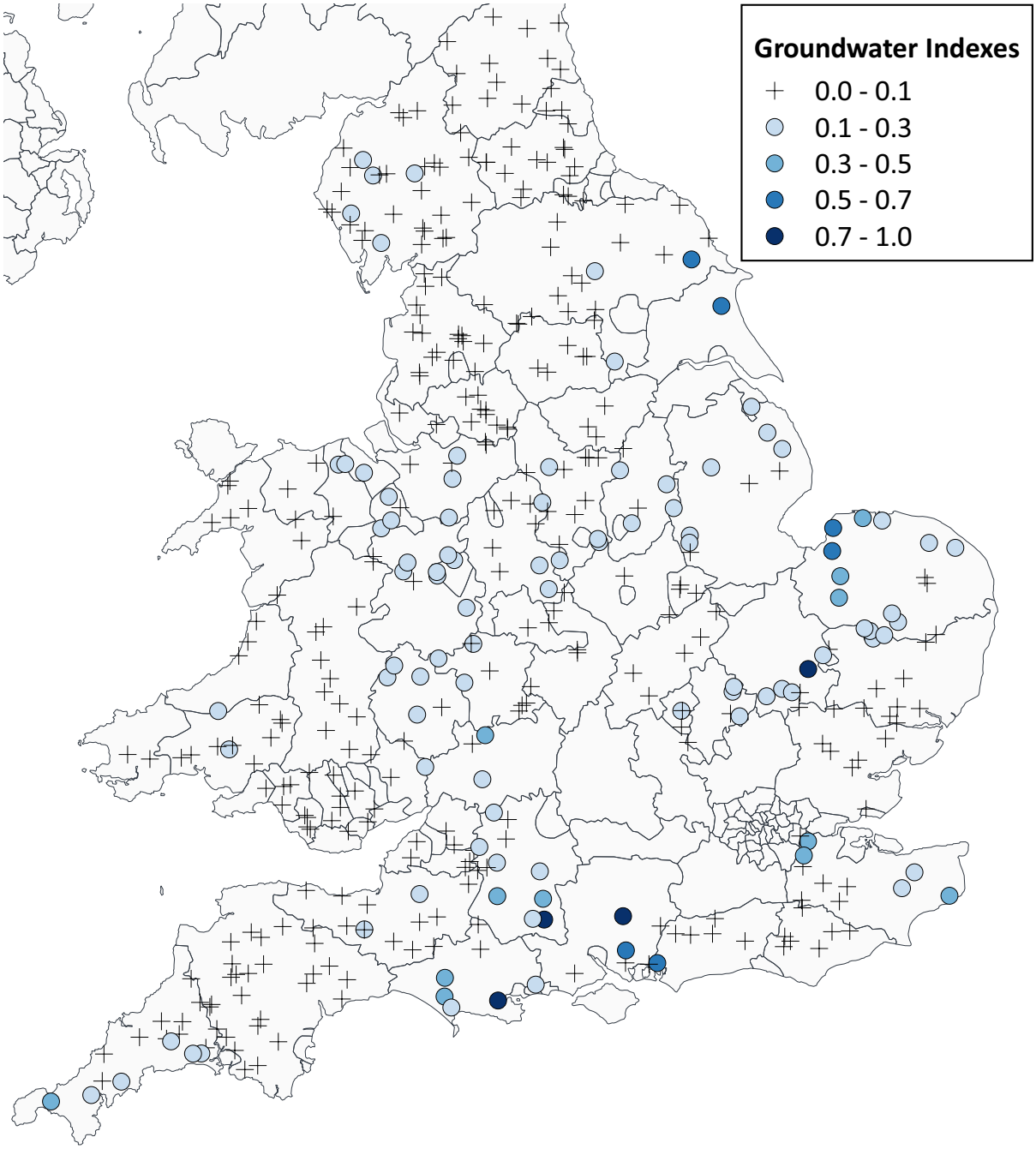

Figure 26.3: Groundwater Indexes.

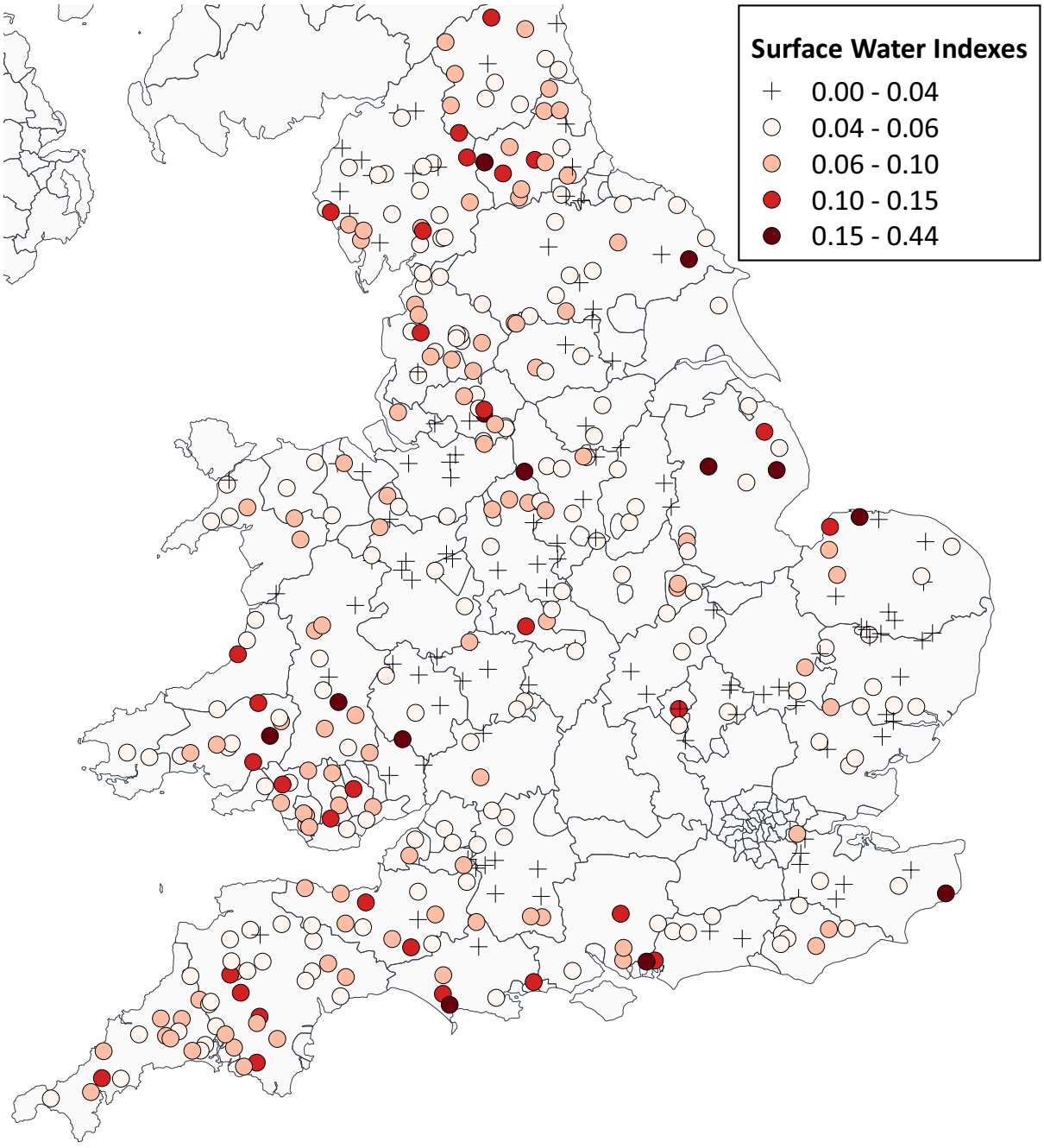

Figure 26.4: Surface water indexes.

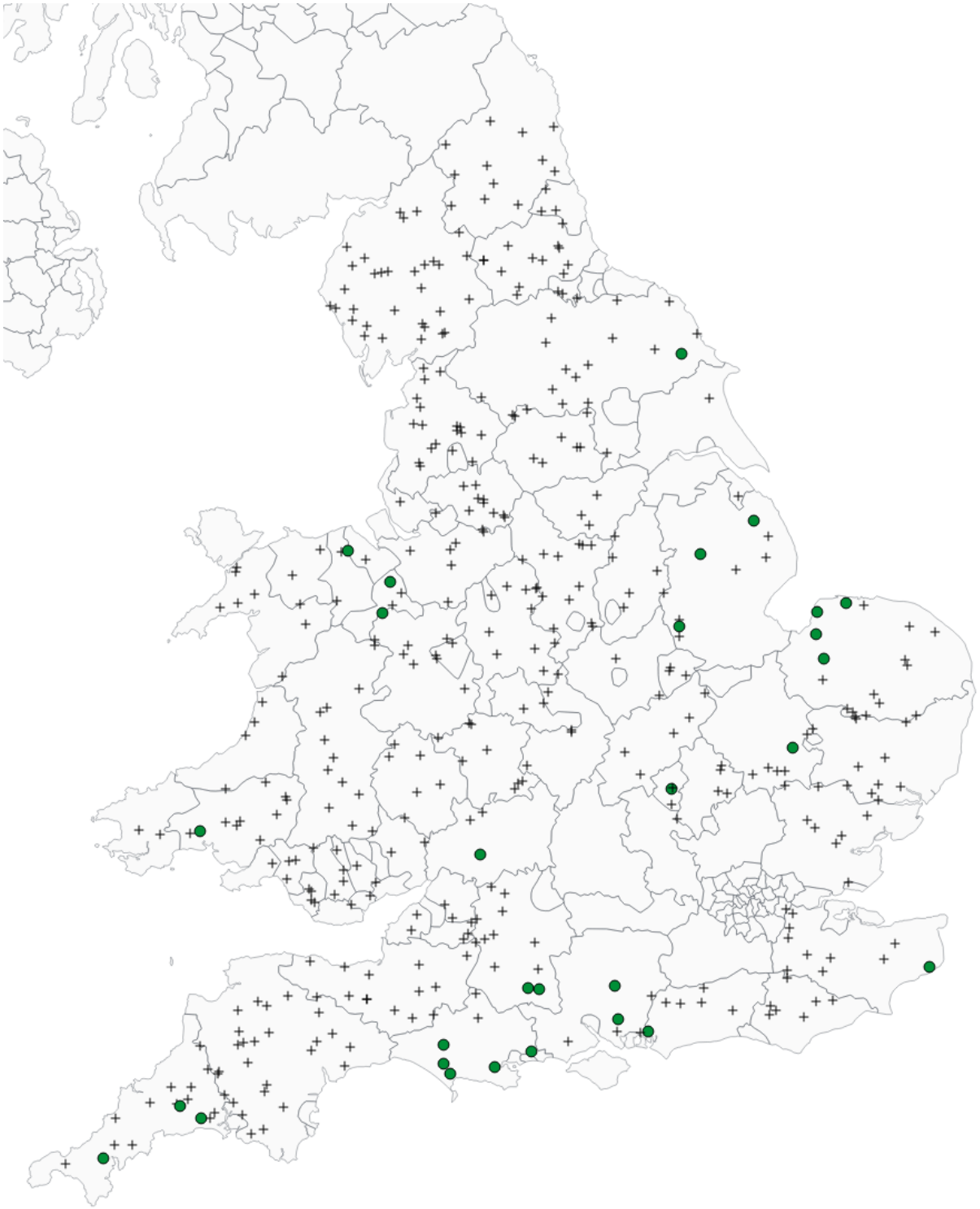

Figure 26.5: Identified multisource catchments.

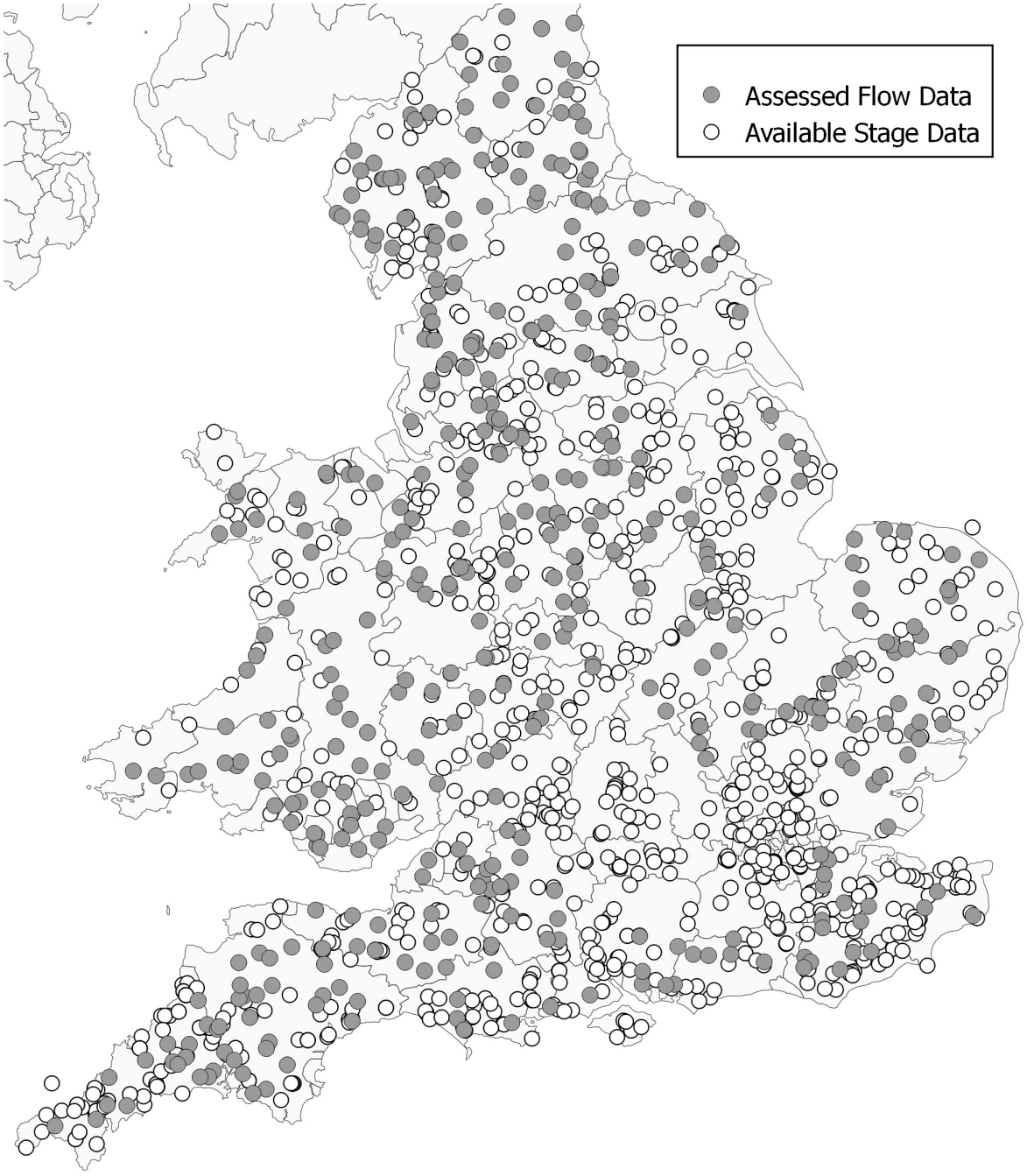

Figure 26.6: Points show the original stage data and those records converted into flow that were used in Chapter III. Data was also available for Scotland, but is not shown.

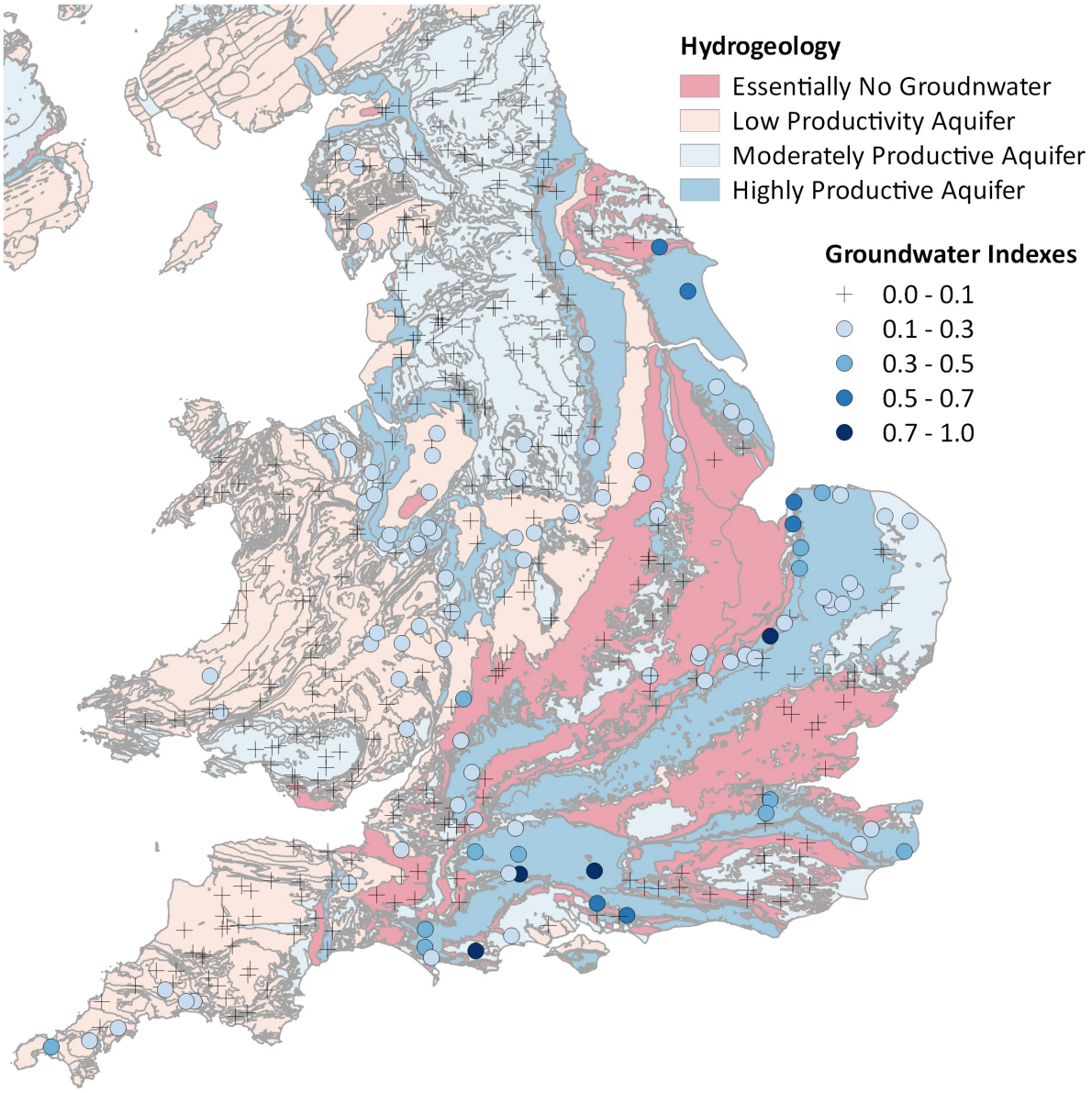

Figure 26.7: Groundwater indexes shown on the BGS 1:650 000 scale digital hydrogeology map (British Geological Survey, 2016b).

27. Additional Multisource Catchments

In addition to those catchments discussed in the literature review and in Chapter III there were some additional catchments that were thought to be multisourced. There are included here for reference.

27.1 River Darent

The River Darent sits to the south east of London, flowing into the Thames. It is a largely groundwater dominated catchment, spring-fed from chalk and Lower Greensand formations. The highest river portion of the catchment (gauged at Otford) shows the most potential for multisourced responses. The NRFA describe this catchment as *"Baseflow-dominated, but responsive to storms... Responsive regime (for a permeable catchment)"*. There is no mention of multisource potential below this, however the NRFA reports differ greatly in terms of content and so the lack of mention does not rule this out.

The Darent has recorded fluvial flooding in Eynsford, Shoreham, Chepstead, Farminham, Ottford, Sundridge, Brasted and Westerham JBA Consulting (2013). These events occurred in the years 1968, 1969, 1971, 1972, 1976, and 2003. More specifically, a draft report by Kent County Council (2017) states that South Darenth, Bradbourne Lakes and parts of Sevenoaks have experienced groundwater flooding. In the winter of 2002/2003, around 50 properties were flooded in Westerham, Brasted, Sundridge, Chipstead, Farningham and South Darenth. This series of floods is believed to have been caused by high river levels, surface runoff and blocked culverts. Modification and culverting of the river has led to the possibility of blockages that can lead to local surface water flooding (JBA Consulting, 2017b). Groundwater emergence from extreme rainfall is also known to have occurred at the A25 (Kent County Council, 2017) and is thought to be a notable hazard at many other sites (JBA Consulting, 2017a).

Interestingly, a report by Kent County Council (Kent County Council, 2011) demonstrates the difficulty of defining flood risks in catchments based on historical events. Despite stating that the risk from both surface water and groundwater being significant, the report states:

> *"It is technically challenging to quantify the risk from groundwater flooding. At present there is no data available on the probability or depth of groundwater flood events...Records of historical flooding are inconsistent... those organisations that record this data do not record all events...or certain types of events..."*

From the above information the Darent was anticipated to produce multisource indexes as there is evidence of groundwater and surface water floods in the literature. The surface water index from Chapter III does indicate a flashy component during peak events as expected however the groundwater index is lower than the threshold of 0.1 at 0.08. This is not so much that it

is implausible and thus may not rule out that the Darent is indeed multisourced as expected. The indexes above are for the top most gauge of the Darent, at Otford, as this is the most likely region of the catchment thought to exhibit multisource behaviour.

Further down the catchment, at Lullingstone the GWI increases to 0.38 while the SWI decreases to 0.04 - this may indicate that between the two gauges is an area of the catchment where the regime becomes more groundwater dominated and where the two sources may interact more strongly.

27.1.1 The River Misbourne Catchment

The Misbourne catchment is largely chalk and is thus dominated by groundwater. However, sharp peaks in river level have also been experienced and that these have been transmitted down the catchment with both upper and lower stage gauges recording peaks (R. Lamb, JBA, pers. com. 12th April 2016). High resolution, 15 minute flow data was not available for this catchment. The Misbourne drains from the Chiltern hills towards London. Although it rests on highly permeable chalk bedrock it has a 42% covering of low permeability superficial deposits. There are multiple Section 19 reports of a good standard for the area (Buckinghamshire County Council, 2017) including reports of flooding due to high groundwater levels and mentions of surface water (Buckinghamshire County Council, 2014). Figure 27.1 shows a flow hydrograph for the Misbourne at Little Missenden.

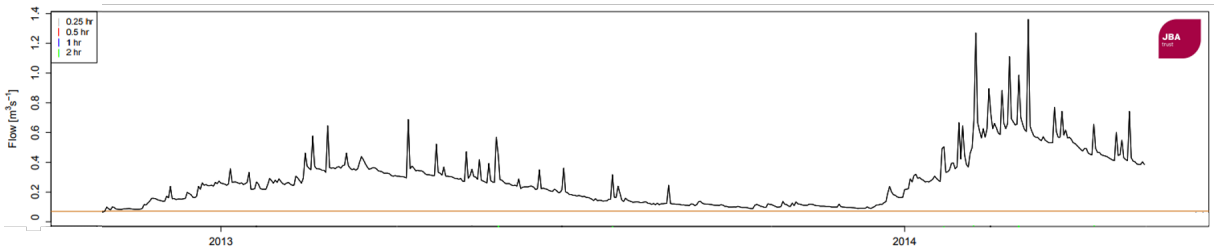

Figure 27.1: A flow hydrographs for the River Misbourne at Little Missenden, provided by the JBA Trust.

According to Jacobs (2008), both the Misbourne and the neighbouring River Chess have chalk catchments that cause both groundwater and surface water flooding. It is unclear however from the report whether "surface water flooding" is due to runoff in intense rainfall events or poorly maintained, blocked culverts during standard rainfall. This lack of distinction is a common problem when looking into surface water flooding. That said however, there is at least one report (Reynolds, 2016) of flash flooding in the town of Amersham, in the Misbourne catchment, from intense rainfall. The EA flooding from rivers map and their surface water map both show that there are vulnerable properties within the town of Amersham and there is prevalent groundwater within the chalk catchment. High resolution flow data is not available for this catchment and so it could not be included in analysis.

27.1.2 The River Itchen Catchment

The River Itchen in the south of England is suggested to be a dominantly groundwater catchment that has experienced sharp increases in level, along with flooding in Winchester (R. Lamb, JBA, pers. com. 12th April 2016). While investigations confirm flooding in Winchester and a very groundwater dominated catchment, no evidence could be found of any surface water incidents or rapid run off. High resolution flow data is not available for this catchment and so it could not be included in analysis.

28. Alternate Methodologies

28.1 Introduction

Initial attempts to define a methodology used stage data from 13 scoping catchments around the UK. These scoping catchments were selected according to the shape of their hydrographs so as to represent a range of surface water : groundwater ratios (essentially a range of smooth to flashy hydrographs). Their locations were also taken into account in order to get a national spread. The locations of the initial 13 gauges, along with some example hydrographs can be seen in Figure 28.1

A list of these gauges along with catchment information taken from the National River Flow Archive can be seen in Table 28.1. The hope was that by looking at this information the multisource potential of each river could be determined. This could then guide the following automated quantitative method. This used the relatively detailed information on the NFRA website and is not something that could be done for the national dataset. Proposed river sources, along with a summary of Table 28.1 can be seen in Figure 28.2. The rivers Lud and Ouzel were thought to indicate the greatest multisource potential. The River Piddle and River Hooke had hydrographs that appeared to have both slow groundwater and rapid surface water responses and were also considered to be potential multisource rivers, however these had reduced catchment information available.

In the final analysis the Lud had a GWI of 0.13 and a SWI of 0.12 (multisource). The Ouzel has a GWI of 0.11 and a SWI of 0.11 (multisource). The Piddle had a GWI of 0.91 and a SWI of 0.06 and so was just below the groundwater threshold and on the surface water threshold. Flow data was not available for the Hooke. This further supports the multisource classifications in Chapter III.

28.2 Identifying Groundwater Catchments

Before deciding on using the WMO base flow separation method, a second method, the Lyne and Hollick Filter, was also tested using aggregated daily data. The Lyne and Hollick Filter is a recursive digital filter based on signal analysis and processing techniques (Lyne and Hollick, 1979) that has gained popularity in Australia (Chapman, 1991) and been widely used as a result (Ladson et al., 2013). This was trialled due to its simplicity and reproducibility, helpfully demonstrated in a recent paper by Ladson et al. (2013) that offers R code and advice on a standardised approach. The Lyne and Hollick filter works by removing the high frequency signals (assumed to be the quick flow component of stream flow) from the time series (Nathan and McMahon, 1990).

Both methods produced similar BFIs however the BFI ranking of the scoping gauges differed between the two. Graphically, methods appeared to produce very similar separations. When compared against the NRFA BFI's the World Meteorological Organization (2008) method has a

Table 28.1: Details of the scoping catchments. Data is mostly collected from the NRFA website.

Scoping Catchments: Details	
JBA Gauge ID	Information
Ettrick Water (14987)	Ettrick Water is a small Scottish river with natural regime but a significant discharge (due to its high elevation). It has low permeability bedrock geology, which means that it is very unlikely to have any significant groundwater component although there is some permeability in superficial the deposits. Very high rainfall and 72% of land covered by grasses and mountainous terrain mean that this is likely to be a surface water dominated catchment with minimal MS potential. Geology: Mudstone + metamudstone. Superficial: Mostly till with some sand/gravels and peat.
River Nadder (432210)	The River Nadder is the second largest catchment in the study and has a high flow rate. In most other senses however, the River Nadder appears to be a middle of the range catchment. It has moderate elevation, slope and rainfall and is a mostly natural catchment although there is some minor GW abstraction. According to the NRFA there is minimal superficial drift cover but there is moderate–high permeability bedrock. It is thus likely that there is a reasonable GW component to river level, there is not likely to be a large amount of surface runoff although with around 50% of the land turned to arable uses this may depend on the local farming / drainage practices.
River Piddle (444310)	Relative to the previous two rivers, the River Piddle as arguably very aptly named, with a low discharge (although certainly not the lowest in the study). The Piddle at Briantspuddle is in the south west of England and has a reasonable catchment size of over 100 km^2 and a natural flow regime but limited other NRFA statistics. Its flow estimations are poor for levels above 0.6m – whether this affects the use of level data I am unsure. If so, how this could be combated at a large, automated scale I do not yet know. No geology information on this catchment.
River Hooke (445210)	As above, limited data is given by the NRFA for the River Hooke at this site, it is the second smallest catchment in this study with an area of only 12 km2 and a discharge of only 1 m^2/s. Geology is mostly chalk, then sandstone, then mudstone. Some superficial clay, silt sand and gravel
River Ems (255110010)	The gauging station for the River Ems is in Westbourne (near Portsmouth) a name that suggests chalk influences. It is unsurprising therefore that the bedrock geology is highly permeable. There are large GW abstractions in all but low flows but this is still a baseflow dominated catchment with minimal surface runoff. This is unlikely to have the capability for MS flooding, unless, due to the dual porosity of chalk (see Butler et al. (2012)), water permeates into the river at two distinct speeds.
River Lavant (255220018)	The Lavant is a small, baseflow dominated, ephemeral stream. It has a medium sized, largely permeable catchment and has significant groundwater extraction. Although flows mainly occur in winter, there are times following exceptional rainfall that spring outflows can increase significantly. In the winter of 1992-1993 Chichester, immediately downstream of the gauging site in Graylingwell, experienced groundwater flooding. This was one of the first instances of groundwater flooding that sparked interest and research in this field. It seems unlikely, with the minimal surface run off that the Lavant could have multisourced floods in any but the most extreme rainfall where springs significantly increase river level.
River Lud (29003)	The River Lud also has a highly permeable bedrock however also has some mixed permeability surface deposits. This could give it some surface runoff potential and Louth has flooded in the past. The most notable flood was in 1920 in which houses were destroyed and lives lost; more recent surface water flooding occurred in August 2014. The catchment has a large coverage of arable land, which may have the potential to decrease the response time of the river depending on farming practices and may make up for the low mean drainage path slope (mDPS). There is also an impact of river level from GW abstraction, although this is not to the same degree as in the Lavant. With the significant base flow component and recent surface water flooding, the River Lud is a prime suspect for multisource flooding.
River Nar (033007)	The River Nar has low slope and a high permeability, chalk bedrock and some high permeability surface deposits and so is likely to have some GW input. There is also some mixed permeability surface deposits that may mean that it has MS flooding potential. The stage record for the River Nar contains lots of missing data and there are several artificial surface water and groundwater abstractions and returns that may cause issues during analysis.
River Ouzel (33058)	The River Ouzel drains a large, mostly rural catchment and has reasonable flow. The presence of mixed permeability surface deposits and mostly low permeability bedrock indicate likely surface runoff. The low slope and presence of some high permeability bedrock and small groundwater abstractions may mean that there is a notable GW component to river flows. This leads me I suspect it may have MS potential.
River Ledr (066012)	The only Welsh River in the study, the Lledr drains the one of the steepest and smallest catchments in the study. It is a largely natural river that is unlikely to have multisource potential due to its low permeability bedrock. If fact, with the highest rainfall of any catchment in the study and large grassland coverage, surface flows are likely to me very dominant.
Snaiseholme Beck (F2290)	Snaizeholme Beck is in the smallest catchment in the study and, like the Lledr and Ettrick Water, is very steep, with high rainfall and a flashy, natural flow regime. The catchment does have some moderate permeability bedrock and mixed permeability surface deposits so there may be some GW discharge into the Beck but it is unlikely to be high due the high mDSP and grass cover. Geology: limestone. Superficial: till.
Gypsey Race (F3004)	Gypsy Race drains the largest catchment in the study and has a relatively shallow slope. Its permeable bedrock and dominant base flow mean that GW is a significant water source, however GW is abstracted/recharged and the river can stop flowing during drought periods. There is little to indicate any significant volume of surface runoff, although the possibility of this cannot be dismissed, and so a MS response in unlikely. Geology: Chalk. Superficial: clay, silt, sand and gravel.
Foston Beck (F3120)	Foston Beck is only a few miles from Gypsey Race, in a much smaller, neighbouring catchment. Foston Beck has similar slope, arable land use and high permeability bedrock. There are minimal responses to rainfall as the river has a sizeable, strongly seasonal GW influence. In the past, the river stage has been artificially maintained by local fishing club. Since 2012 there has been an eel pass however this rarely alters stage.

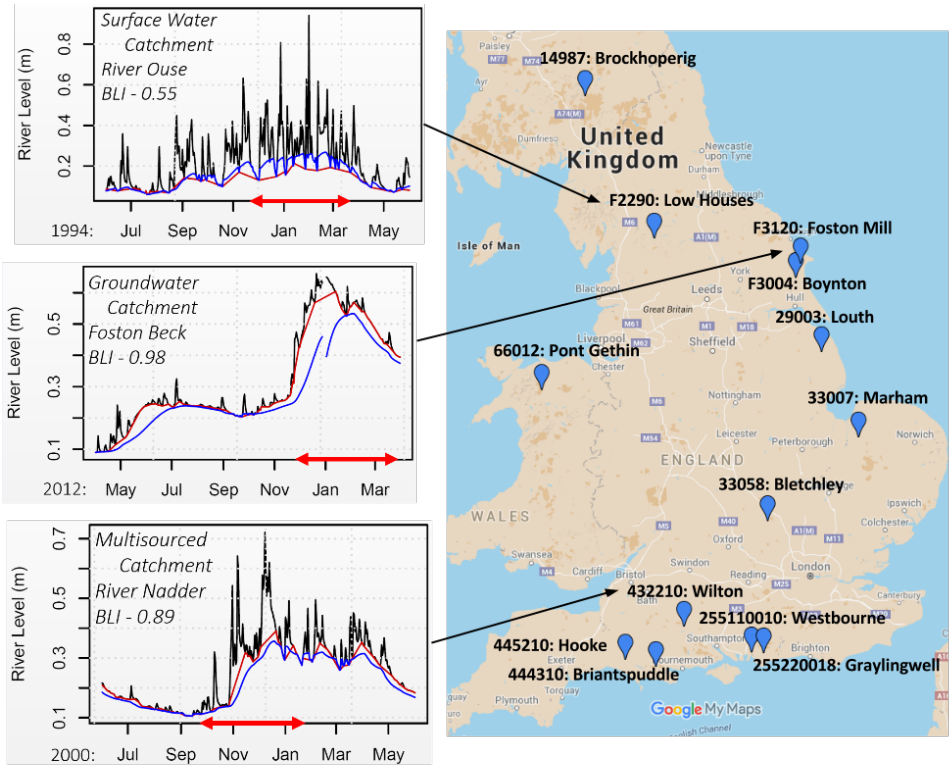

Figure 28.1: The sample catchments used to test potential methods were selected manually with an attempt to get a range of flashy-groundwater catchments, spread over the UK. LEFT - Three gauges thought to represent surface water, groundwater, and multisourced rivers. The black line shows river level, red and blue lines show base levels calculated using the World Meteorological Organization (2008) method and Lyne and Hollick (1979) filter respectively. RIGHT - The 13 scoping gauge locations, details of these catchments can be seen in Figure 28.2.

Spearman's rank of 0.99 whereas the Lyne and Hollick (1979) has a Spearman's rank of only 0.66. It is possible that this difference comes from the way in which each method treats errors; the Lyne and Hollick (1979) method has a detailed approach to any data gaps where are the WMO uses the data in its original form. The effects of this can be seen in the River Nadder hydrograph (Figure 28.1) where, due to missing data in January, the Lyne and Hollick filter trails off whilst the WMO method continues to rise. It is thought that the BFIs on the NRFA website also use the WMO method. For this reason the WMO method was chosen for further analysis.

28.3 Identifying Surface Water Catchments

Another approach for calculating a proxy for the defining flashy catchments was to look at the amount each river rose per hour and breaking this down into quantiles based on flow. As the Flashiness method of integrating peaks only used the top ten events (Sec. 8.2), a record wide approach was attractive. The river flows were broken into 20% quantiles and the average of the maximum rises were taken for each. This was done for each record. A full description of how the maximum rate of rise was calculated can be seen in Figure 28.3. This was not as simple as it first appeared and so is further detailed in the following R code:

```
    # ------------------------------------------------------------------------
    # CALCULATE THE MAXIMUM RISE PER HOUR FOR EVERY FOUR 15 MINUTE TIMESTEP.
    # ------------------------------------------------------------------------

    # Set up a function to do this when called:
    rise_fun <- function (data){

    # Create an empty vector to recieve maximium rises:
    rise <- rep(NA, length(data))

    # Caclulate the difference in flow between each time step:
    difference <- diff(data)

    # Cycle through every time step (in sets of 4, i.e. 1 hr):
    for (j in 4:(length(difference))){

    # Assign a-d the four flow values upto and including the one in question:
    a = difference[j-3]
    b = difference[j-2]
    c = difference[j-1]
    d = difference[j]

    # Find the largest rate of rise within this group. This must be a largest possitive
        rise, over the fewest timesteps:
    rise[j+1] <- suppressWarnings(
    max(a,b,c,d,
    a+b,
    a+b+c,
    a+b+c+d,
    b+c+d,
    c+d,
    b+c,
    na.rm = TRUE))
    # (Supressing warinings stops the code aborting if there are no flow readings)
    }

    # Remove any errant values:
    rise[is.infinite(rise)] = NA

    return(rise)
    }
```

Two approaches were considered for calculating a threshold above which rapid rise was considered to have occurred:

A fixed threshold: This worked poorly due to the very large range of river flows in the analysis. Some would not be large enough to trigger the threshold while others would break it almost every time step.

A variable threshold: A record specific threshold of 2% of Qmax was chosen. This was selected to be roughly in line with literature on flash flooding. Collier (2007) states that times to peak for small UK catchments is in the region of three to six hours and Georgakakos (1986) states that to classify an event as a flash flood it should peak within twelve hours. Although we are not trying to locate flash floods specifically, only those with rapid river rise events, it seemed that having a threshold that defined a rise rates as being high enough to occur in a twelve hour block was reasonable.

Although the second approach appeared to work better, it still had one significant issue. Rivers that were 'too flashy' got low ratings. This was because they would rise in very few time steps. For example, consider the River Snail (a river that responds slowly to rainfall) and the River Cheetah, which responds in a flashy manner to rainfall. If these have the same Qmax of 100 cumecs they will also have the same rise threshold of 2 cumecs. If the River Snail rose from 50 cumecs to 100 cumecs over 10 hrs (5 cumecs/hr) then it would count 10 instances of rapid rise.

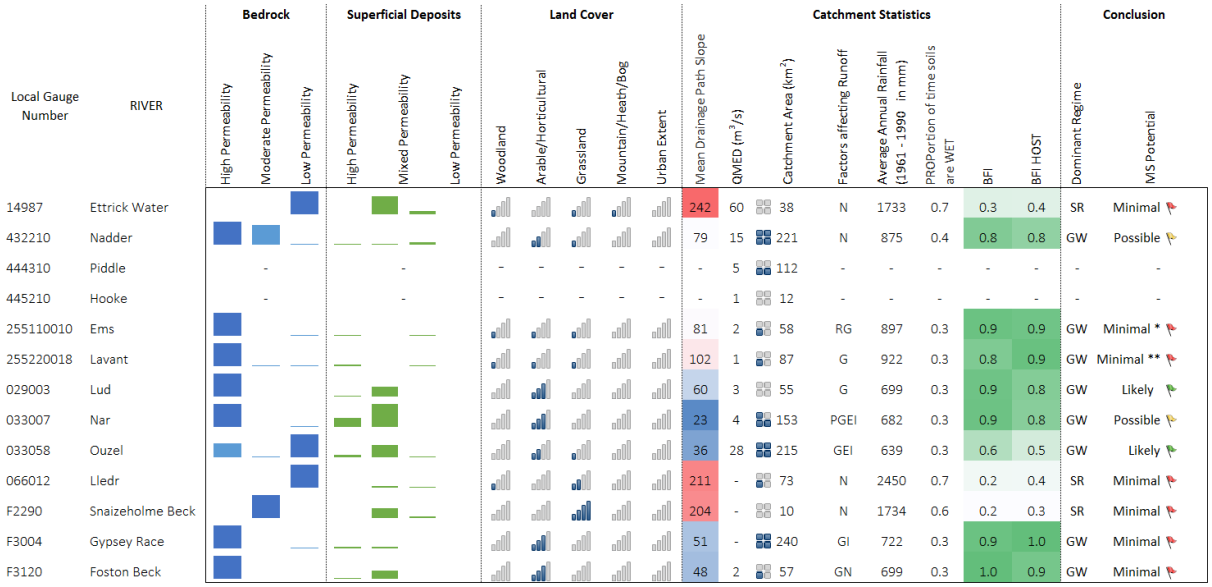

Figure 28.2: An initial screening of 13 scoping catchments was undertaken, attempting to assign their proposed multisource potentials so that they could be used for developing a method. The flags on the right are based upon an initial screening according to the literature.

If the River Chetah rose from 50 - 100 cumecs in 2 hrs and then started dropping off, then it would only have two counts, despite being a much flashier river. As this was not thought to be a good method, and the peak integration method was developed and used.

A second, separate method was tested, investigating whether it was possible to do a quantile based assessment such as in Section 8.1.2. This worked as follows: (1) The difference in each flow reading and its preceding neighbour was calculated within each gauge. (2) The flows were grouped into 20% quantiles as in previous approaches. (3) The mean positive differences (i.e. where river flow increased) were calculated for each flow quantile. (4) These mean values were divided by the peak flow in each record, normalising them to account for the vastly different flows in different rivers. The purpose of this was to see which rivers have high increases relative to their full potential during high flows; therefore which may, if antecedent groundwater conditions increased river flow, still have the potential for a flashy response, and therefore justifying multisource modelling.

Looking at the average rise through time did not yield useful results however. Although it intuitively seemed to work, in reality there was little difference between average rises at high quantiles and average rises at low quantiles. Differences could be seen between gauges however. Normalising results according to their 20% quantile did not prove useful, they were still heavily clumped and highly similar between quantiles. This can be seen in Figure 28.4. This indicates that the average rise rate perhaps averages too strongly, bringing results back to a central value within each gauge.

28.4 Searching for Double Peak Hydrographs

When discussing multisourced events, *double peaked hydrographs* were often mentioned. A double peaked hydrograph describes a sharp peak in river level caused by runoff from a storm event followed by a shallower peak from a delayed groundwater pulse. These peaks could be partially merged or distinct. These have been documented by several authors (e.g. Onda et al., 2001, 2006; Iwagami et al., 2010; Martínez-Carreras et al., 2015) and have been modelled at Kilham,

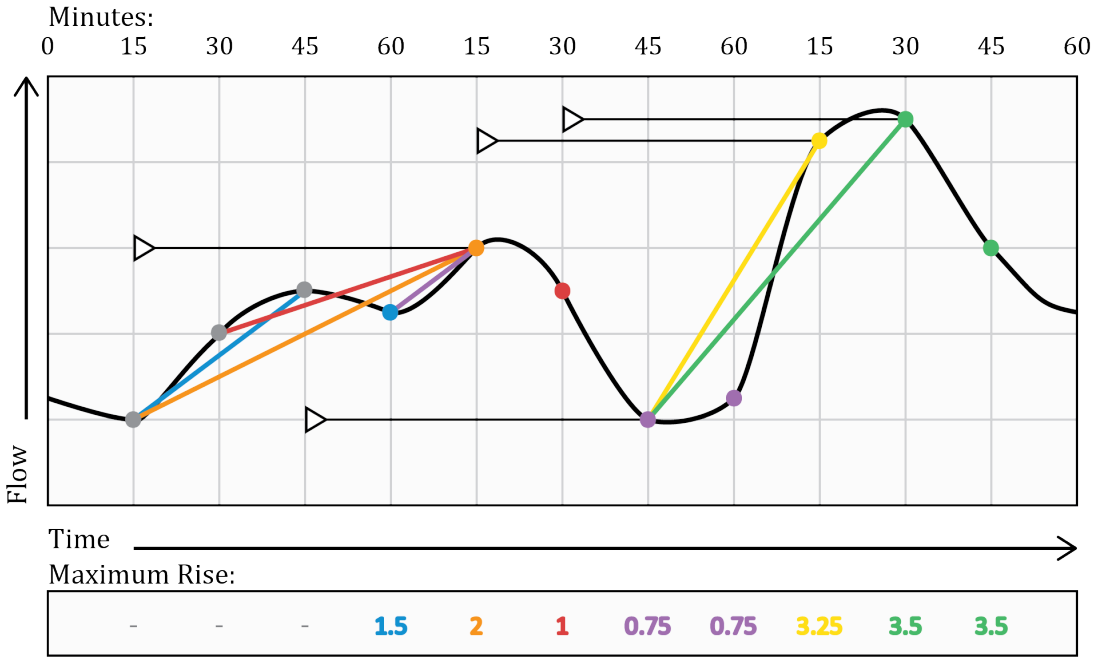

Figure 28.3: Here is shown an example of the method used to calculate the maximum amount of rise per hour throughout the flow records. The black arrows indicate the length of time (1 hour) that preceding data is looked at; the coloured lines, indicate the maximum rise for points of matching colour. This shows that the process was not as simple as taking the maximum and minimum aver a rolling hourly period. It may be worth noting that all records are point data and that the solid black line describing the hydrograph is purely a hypothetical representation of what the flow may have done between those points.

the case study site used throughout this thesis (Birkinshaw, 2008).

Hydrographs were plotted of peak over threshold events and inspected by eye. Several potential double peak hydrographs were identified. However, it was unclear whether these were genuine, as a double peaked rainfall event could produce a similar looking hydrographs. In order to constrain the cause of double peaks, the search was narrowed to those hydrographs that were caused by a discrete pulse of rainfall.

Again, this was a largely manual task due to the large amount of time that coding would have required. Gauged, hourly rainfall records from the nearest gauge were plotted alongside the hydrographs. In most instances rain gauges were within a few kilometres of the river gauge and all were sited in the same catchment. Where multiple rain gauges were present, preference was given according to distance, whether it was above or below the river gauge and according to topography.

Very few (most probably zero) hydrographs were found that exhibited a double peak from a single pulse of rainfall. Some may have been genuine double peaks however rainfall obscured these significantly enough to bring them into doubt. As such, this technique of multisourced identification was not deemed helpful.

28.5 Hydrograph Clustering

hydrograph clustering was also explored. The aim of this was to group peak event hydrographs according to shape characteristics using principal component analysis. Background information for this method can be found in Upton and Jackson (2011) and references within. Essentially, principal component analysis reduces the number of characteristics needed to describe something. This reduced number allows for more efficient clustering of hydrographs.

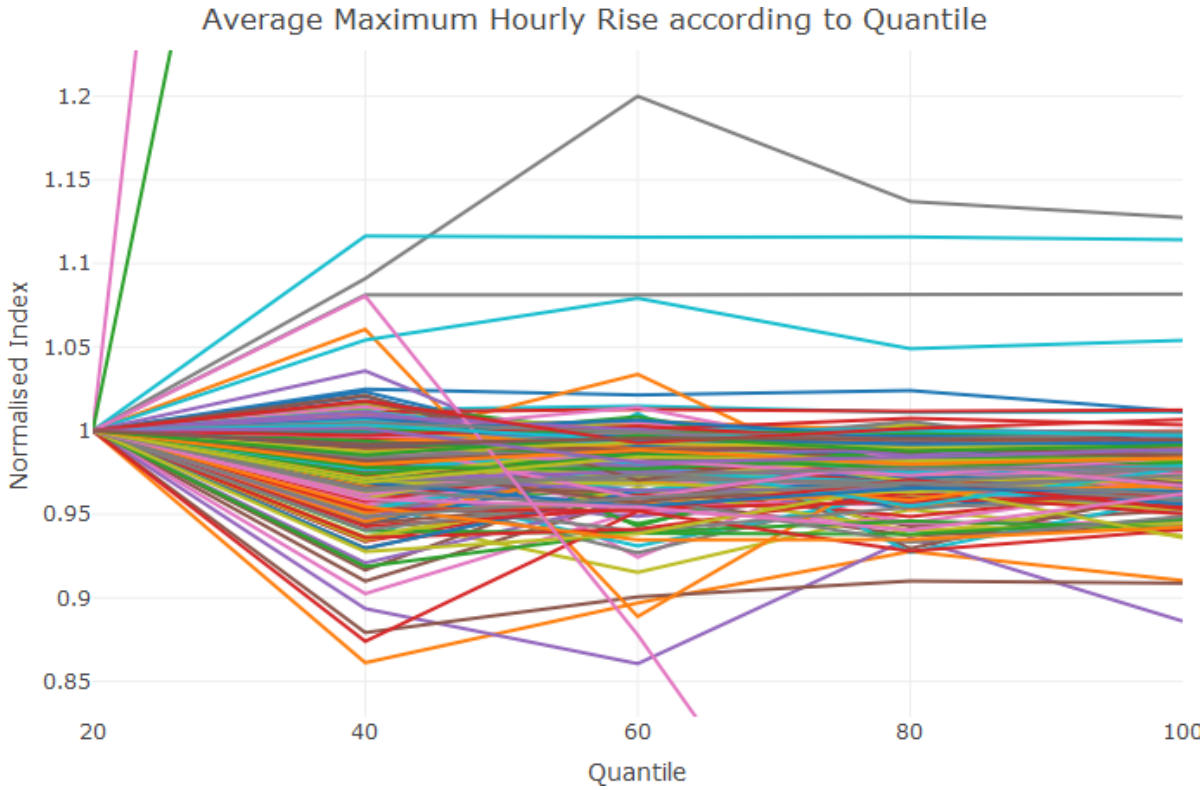

Figure 28.4: Average maximum hourly river level rise, split by quantile

The most recent three years of data were taken from each river stage record. Each three year period was broken into two week blocks and all (approx. 70 events $\times$ 13 scoping catchments) hydrographs were added to a single dataset. Each of these were then analysed and a set of index characteristics were calculated for each hydrograph. The indexes used to quantify shape were: mean, quartiles, BLI and the number of maximum hourly rises over a threshold. It would have been good to develop more of these however for the interest of time the above were deemed sufficient.

Principal component analysis was then used to create a set of principal components (PC) that consisted of each of the characteristic indexes weighted in such a way to make each component relatively unique (i.e. PCA 1 = 0.2 $\times$ BLI + 0.4 $\times$ fluctuation index + 0.4 $\times$ mean). Two principal components were calculated necessary to effectively cluster the hydrographs (according to their components). Each hydrograph was then attributed PC scores and cluster analysis was used to group hydrographs accordingly. The number of hydrographs in each group was then counted for each gauge and that data itself clustered. This grouped gauges according to the shape of two week blocks of river level data.

The clustered gauges can be seen in Figure 28.5. Some degree of clustering seems to reflect base level indexes however there are also some very unlikely pairings (e.g. group 3). As such, this was not considered reliable. Principal component analysis and hydrograph clustering seems like a very useful technique and one that with some further work on the characteristic indexes seems to have potential. Had time allowed, more refinement would be invested in the indexes for describing hydrograph shape and analysis reattempted with flow data.

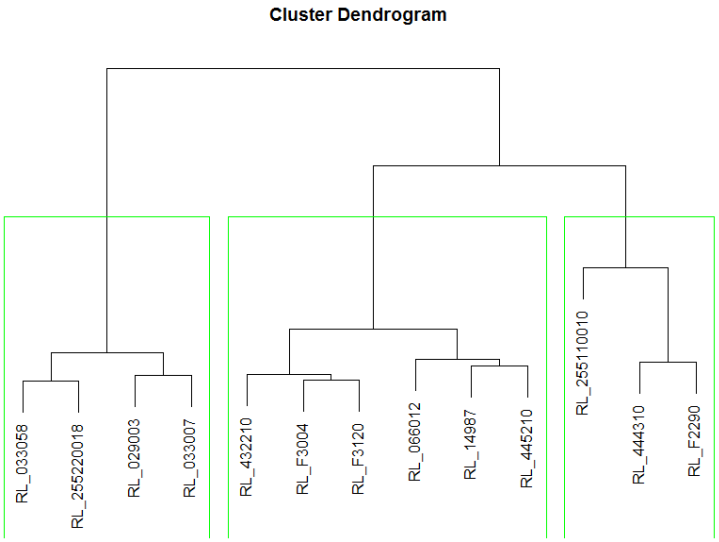

Figure 28.5: Clustered gauges, following principal component analysis and clustering on 3 years of stage data split into around 900 hydrographs.

28.6 Wavelet Analysis

Wavelet analysis is a method by which the rates, or frequencies, of river lever change can be extracted from records. This, unlike Fourier analysis, does not analyse the record as a whole, but rather assesses continuously - thus showing how changes in the rates of level river rise and fall have altered over time. This is useful as it should allow for the identification of rapid level rise due to surface run off and subsequent, slower level rise from groundwater. Wavelet analysis has been applied to many hydrological studies investigating climatic controls on river flow (Franco-Villoria et al., 2012), tidal controls on river flow (Lim and Lye, 2004), and the classification of hydroclimatic categories (Smith et al., 1998) to name just a few.

Wavelet analysis tests which frequencies are present in the data. In other words, whether river level fluctuations have any regularity to them and, if so, the frequency and strength of these fluctuations. An example of such a frequency or regularity is evident in many of the time series on a yearly scale where each year river levels increase over the winter months. Although the maths is non-trivial, the basis behind wavelet analysis is relatively simple to comprehend and so shall be described in brief below (along with the necessary background on *Fourier analysis*):

When investigating a *stationary time series* such as river level, it can be said that the series can be represented by superimposing sine and cosine waves in a range of frequencies and amplitudes (Shumway and Stoffer, 2006, p 232). *Fourier analysis* is able to take a time series and pull out those sine and cosine functions and display them graphically showing both their frequencies and amplitudes. However, one limitation with Fourier analysis is that it assumes that the sine and cosine waves are constant across the length of the time series. This becomes an issue in some instances however as this assumption may not hold true. An example of this may be when monitoring earthquakes at a tectonic fault - there may be occasional earth quakes recorded and these may be able to be described using the sine and cosine functions above, but this may be temporally constrained and so can't be broken into component waves when the time series is analysed as a whole. River level data is similar to this, where regular fluctuations in level may only occur following a rainfall event.

It is with this in mind that we move to *dynamic Fourier analysis*. This process is similar to that described above except that it is performed on multiple segments of the time series. These segments can overlap, although this is not a necessity (Shumway and Stoffer, 2006, p 233), and

so allow local, temporally confined fluctuations to be discerned. The size of these segments can be defined by the operator and so altered to capture both long and short term fluctuations.

Wavelet analysis is a further development on dynamic Fourier analysis, but, very basically, uses more ergonomic wave functions (in place of sine and cosine functions) that better describe localised frequencies and with improved performance on non-stationary time series (Shumway and Stoffer, 2006, p 234). This is appropriate as many of the frequencies we are interested in, such as those following a rainfall event, are temporally local events. Furthermore, such events may mean that, although the time series as a whole is stationary, the section under investigation may not be and is thus more suited to wavelet analysis rather than Fourier analysis.

It was presumed that variations in river level due to groundwater influences will occur over a number of days whereas those that are a direct result of runoff may only take a number of hours to pass into the river system. It was hoped that wavelet analysis would show which frequencies (i.e. hours or days, or even years) are present in each gauge record and help to expose those rivers that have multiple sourced influences.

Wavelet analysis was run on all two year periods of the scoping catchments. Two year periods of a theoretically surface water dominated record and a theoretically groundwater dominated record can be seen in Figure 28.6. A similar time period of the river level record they analyse can be seen in the top and bottom hydrographs of Figure 28.1.

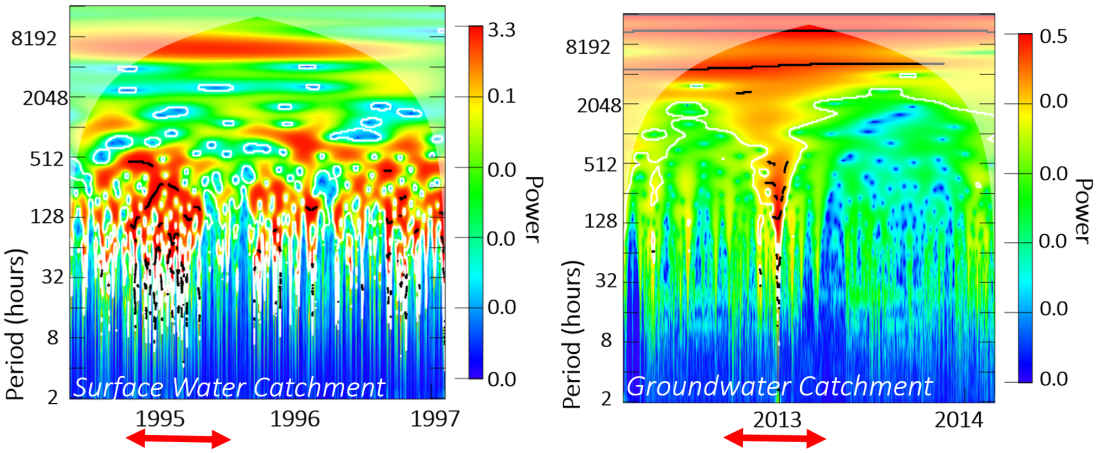

Figure 28.6: Wavelet analyses on the steep, grassy, semi-permeable catchment of the River Ouse (left) and the larger, less steep, highly permeable catchment of Foston Beck (right). These are hypothesised to indicate surface water and groundwater catchments respectively. Red arrows indicate peak river level events.

It is possible to tell from Figure 28.6 which is the groundwater record and which is the surface water record from just a glance. While this boded well, these figures do not lend themselves to the simple classification of groundwater, surface water and multisource records. Although it is apparently possible to display these diagrams in a simple quantitative way could not be managed. The use of average wavelets was also considered, in which the power of each period is averaged to display the average strengths of each. It was hoped that this would produce peaks at hourly frequencies for surface water catchments, at daily frequencies for groundwater catchments and at both for multisource catchments. This simplistic breakdown was not what was found in reality (see Figure 28.7). Furthermore, the average wavelets method is also difficult to display in a way that is ergonomic for automated comparisons between many records.

A second approach was considered: multi-resolution discrete wavelet analysis. This has been employed by (Rust et al., 2014) to investigate land use change within catchments. Rather than assessing all frequencies this looks at targeted frequencies. By looking at the strength of hourly,

daily or longer frequencies it may have been possible to display a rough spectrum of the frequencies present in the river level signal using only a few numbers (the strengths of a few frequencies of interest).

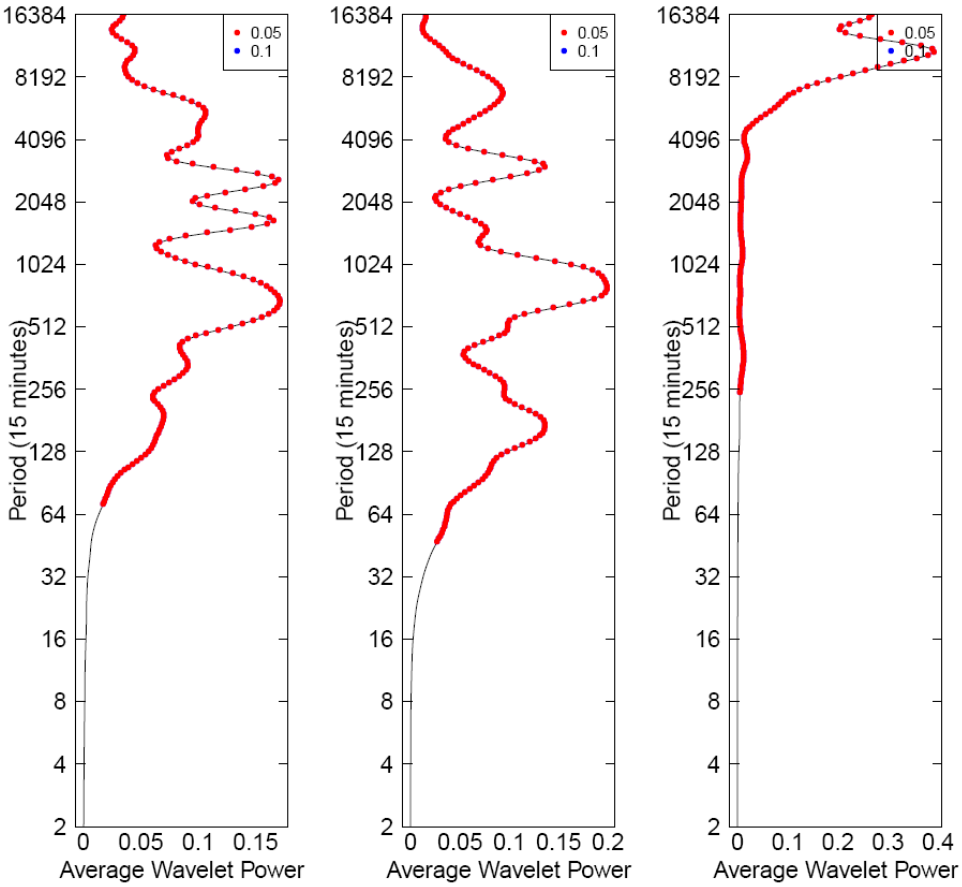

Figure 28.7: The average frequencies found a 2 year section of the river level records for the River Ouse, River Nadder and Foston Beck. Ideally, these records, which are thought to represent surface water, multisourced and groundwater catchments respectively, would display clear and unique dependencies on periods of different lengths. This is evidently not the case and so a different method for classifying frequency is required.

This line of analysis was not followed through however. While wavelet analysis allowed for some interesting reading, as well as some very eye catching graphs it was very computationally intensive and extremely complex. Everything from choosing the shape of the wave form to run through the data to pre-processing the time series to visualisation threw up problems with endless avenues of conflicting and complex 'solutions'. After significant time investment, this line of investigation was deemed more suited to a mathematician and so was dropped. It ended in agreement with Schaefli et al. (2007) who states that wavelet analysis has great potential in aiding our understanding of hydrology processes whilst warning against the misinterpretation of analyses.

28.7 Temporal Correlation with Rainfall

Some experiments took place assessing correlations between river level rainfall. To do this, the base flow, quick flow and total flow were analysed for correlation with rainfall averaged over hourly, 3 hourly, 6 hourly, 12 hourly, daily, and weekly periods of 1 to 12 weeks. Those rivers

found to have high correlation with hourly and 3 hourly rainfall data would have been taken to be flashier, whilst those that hold a correlation with the longer resolution data would be inferred to be dominated by groundwater processes. This was carried out for a number of the scoping catchments and also using groundwater data in Chapter IV. In the latter instance a matrix of correlation analysis was performed with both rainfall and groundwater data in both their raw form an averaged over the aforementioned durations. Correlations were also performed with a range of lags added to the groundwater data to counteract the delayed groundwater response. No significant correlations were observed.

IX

Appendix - Chapter IV

Figure 28.8: The Allen catchment - borehole locations used for groundwater level observations. ©OpenStreetMap

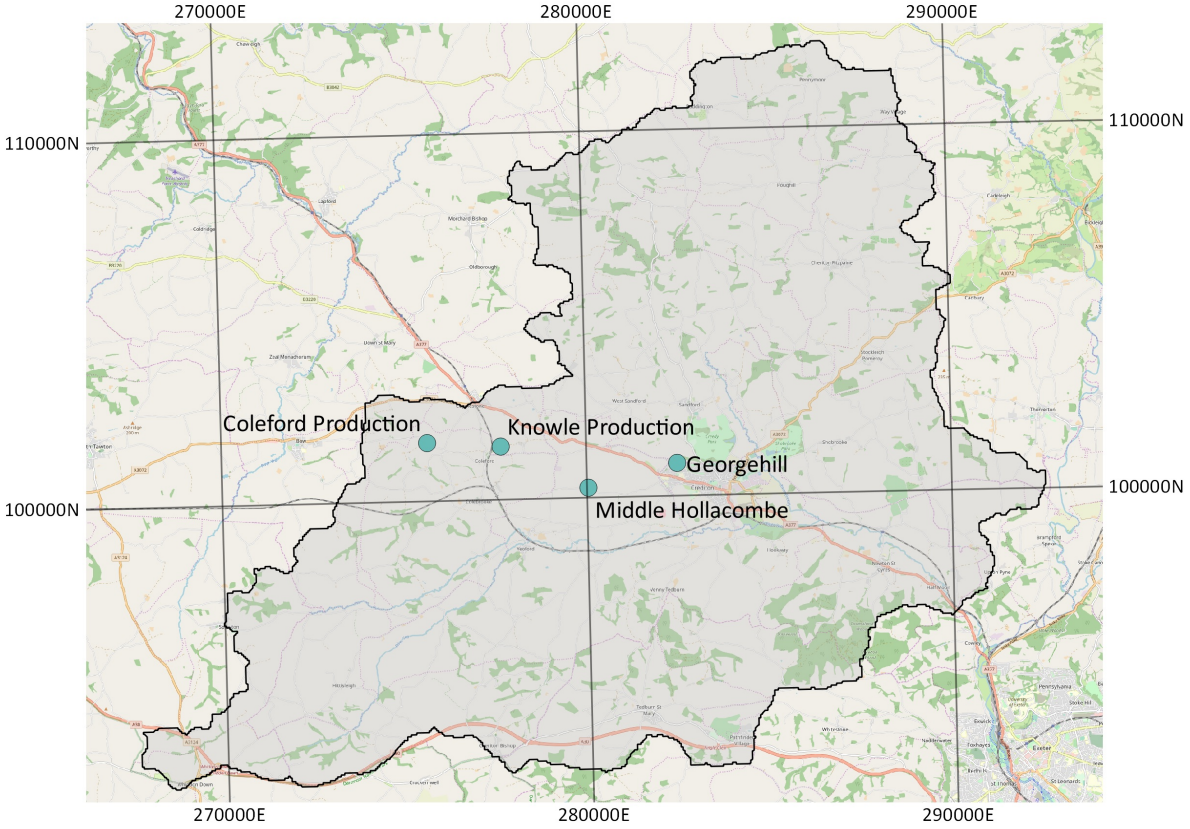

(a) The Creedy catchment

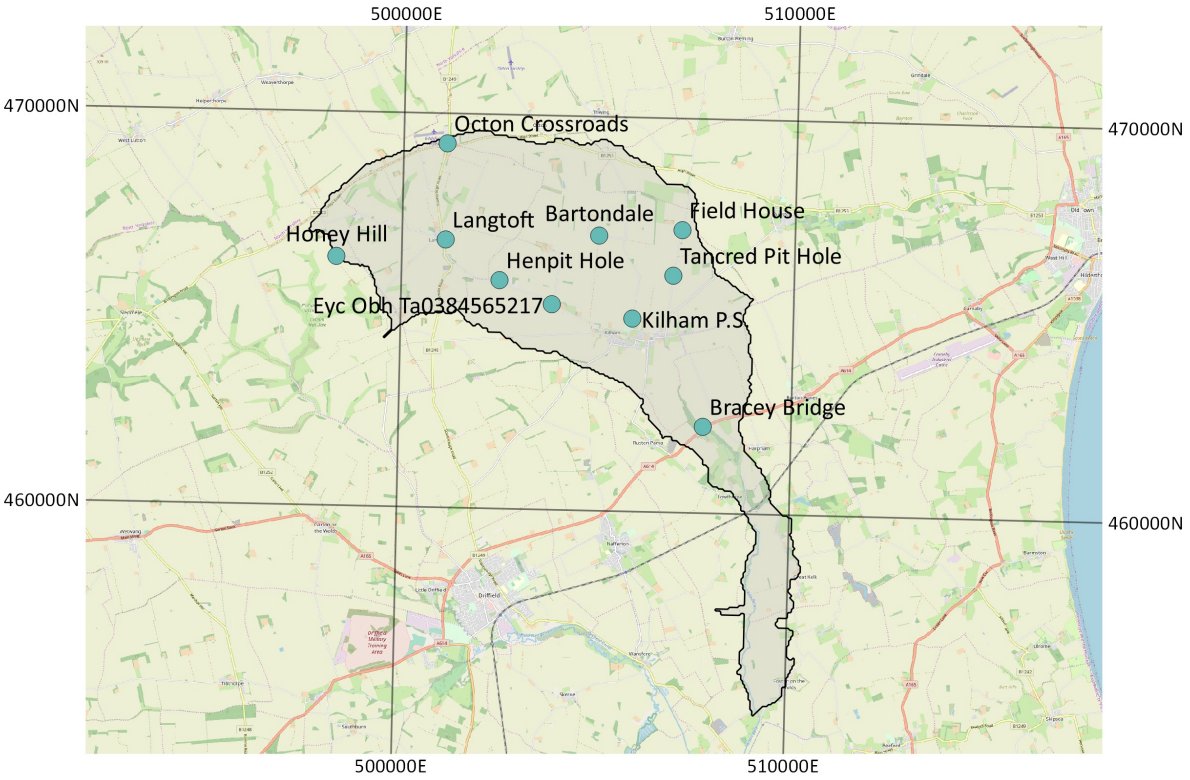

(b) The Foston Beck catchment

Figure 28.9: Borehole locations used for groundwater level observations. ©OpenStreetMap

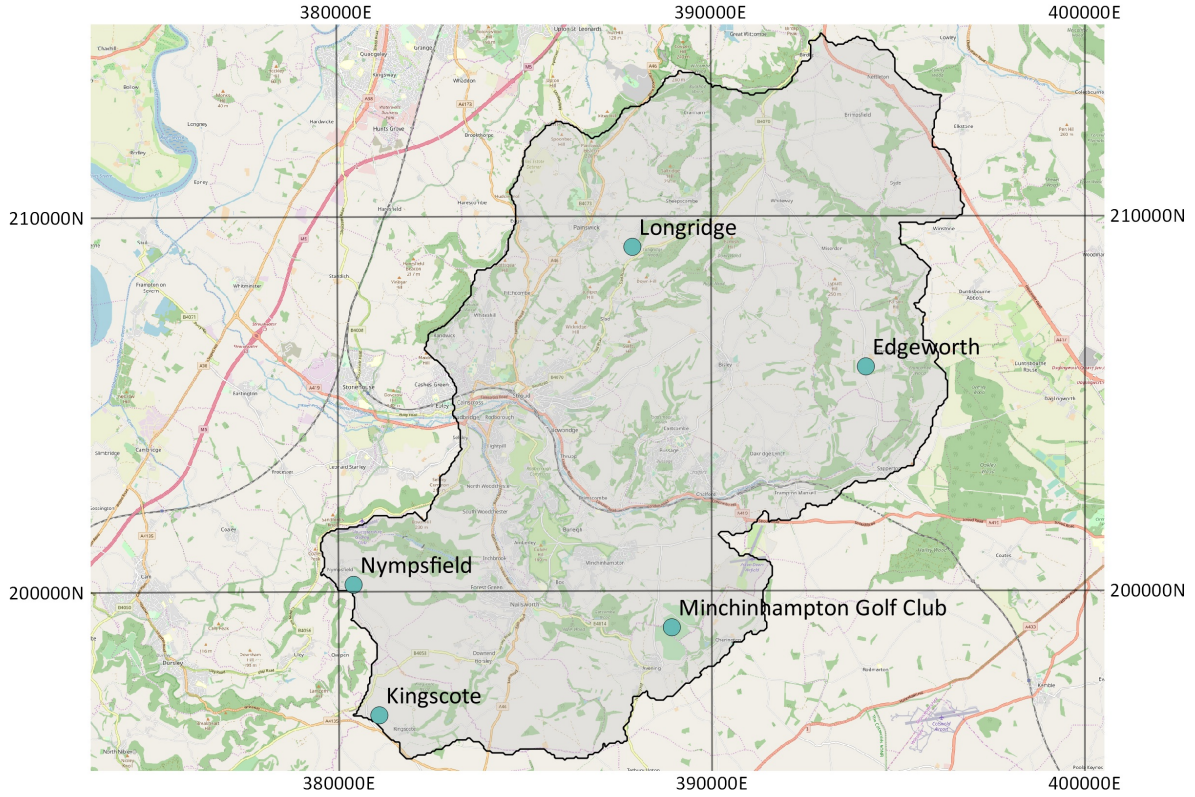

(a) The Frome catchment

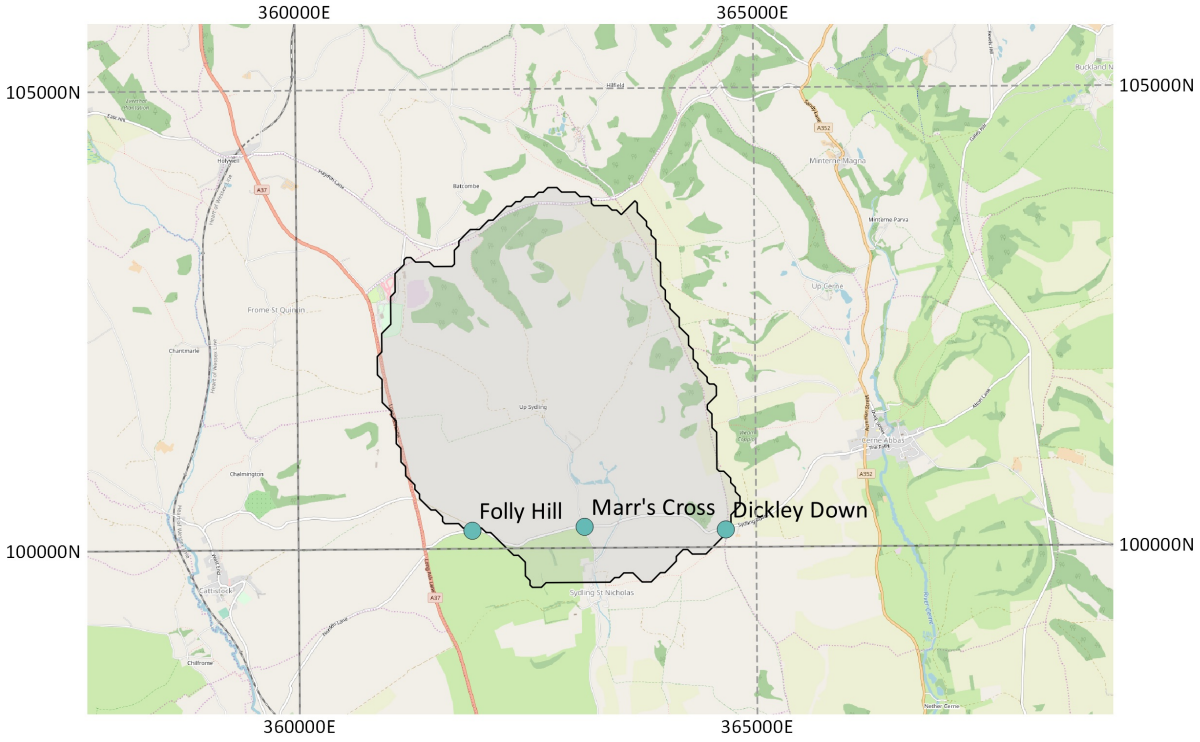

(b) The Sydling Water catchment

Figure 28.10: Borehole locations used for groundwater level observations. ©OpenStreetMap

Table 28.2: Groundwater Data used in this Chapter. Foston Beck data was provided in house. All other data was requested from the Environment Agency through freedom of information requests. *s indicate where their records contain periods of missing data. The Calibrated Allen statistics refers to run 2 in Section 13 that used an extended groundwater catchment and increased saturated conductivities.

Catchment	Borehole Name	Easting	Northing	Start Year	Finish Year	Resolution	Elevation (m)
Allen	High Hall	400110	102816	1991	2017	Monthly	35
	Nine Yews	403726	113623	1992	2017	Monthly	95
	Squirrels Corner	402455	115040	1976	2017	Monthly	95
	Hogstock Cottages	395076	106786	1992	2017	Monthly	85
	West Acre	397806	105396	1991	2017	Monthly	35
	Crichel Chitterwood	396069	108530	1992	2017	Monthly	98
	Barnsley Farm No.3	399594	103859	1992	2017	Monthly	28
	Tollard Royal	394770	117346	1905	2017	Monthly	100
	Dean Farm	397853	115169	1991	2017	Monthly	73
	Woodyates Telemetry	401600	119490	1992	2017	Daily	112
Creedy	Coleford Production	275648	101592	Pre 1992	Post 2002	Monthly	104
	Georgehill	282487	100894	Pre 1992	Post 2002	Monthly	141
	Knowle Production	277661	101450	Pre 1992	Post 2002	Monthly*	92
	Middle Hollacombe	280040	100270	Pre 1992	Post 2002	Monthly	87
Foston Beck	Bartondale	505012	466985	1996	Post 2002	Monthly	59
	Bracey Bridge	507758	462193	Pre 1992	Post 2002	Monthly	16
	EYC obh TA0384565217	503845	465217	Pre 1992	Post 2002	Monthly	44
	Field House	507127	467171	Pre 1992	Post 2002	Monthly	69
	Henpit Hole	502501	465799	Pre 1992	Post 2002	Monthly	59
	Honey Hill	498338	466324	Pre 1992	Post 2002	Monthly	163
	Kilham P.S.	505902	464899	Pre 1992	Post 2002	Monthly	38
	Langtoft	501110	466800	Pre 1992	Post 2002	Monthly*	64
	Octon Crossroads	501105	469238	Pre 1992	Post 2002	Monthly	160
	Tancred Pit Hole	506921	466010	Pre 1992	Post 2002	Monthly*	33
Frome	Edgeworth	394140	205980	1995	2017	Monthly	220
	Kingscote	381080	196690	1994	2017	Monthly	227
	Nympsfield	380402	200181	1994	2017	Monthly	215
	Minchinhampton Golf Club	388930	199020	1994	2017	Monthly	167
	Longridge	387896	209181	1995	2017	Monthly*	175
Sydling Water	Dickley Down	364668	100191	2006	2015	Daily	214
	Folly Hill	361900	100196	2008	2015	Monthly	222
	Marr's Cross	363126	100230	2008	2015	Monthly	122

Table 28.3: Pearson's correlation coefficients for all boreholes. *Stnd* refers to the Standard runs, *APM* refers to the Aquifer Properties Manual and *3DG* refers to the 3D geology simulations. *NA* means that it was not possible to calculate statistics. - means that the simulation was not conducted, or that the borehole was outside of the simulation. The Calibrated Allen statistics refers to run 2 in Section 13 that used an extended groundwater catchment and increased saturated conductivities.

Catchment	Borehole Name	Stnd 100m	Stnd 500m	Stnd 1000m	APM	3DG	3DG & APM	Calibrated
Allen	High Hall	-	0.75	0.81	0.80	0.66	0.63	0.69
	Nine Yews	-	NA	0.76	NA	0.85	0.79	0.91
	Squirrels Corner	-	0.54	0.71	NA	0.85	0.83	0.78
	Hogstock Cottages	-	0.65	0.55	NA	0.61	-0.03	0.93
	West Acre	-	0.93	0.73	0.88	0.80	0.20	0.91
	Crichel Chitterwood	-	0.55	0.62	NA	0.61	-0.01	0.93
	Barnsley Farm No.3	-	0.67	0.72	0.90	0.38	0.50	0.89
	Tollard Royal	-	0.57	0.59	NA	0.82	0.80	NA
	Dean Farm	-	0.63	0.50	0.80	0.60	0.76	0.83
	Woodyates Telemetry	-	0.70	0.51	0.89	0.67	0.70	0.90
Creedy	Coleford Production	-	0.65	0.57	0.40	0.37	0.37	-
	Georgehill	-	0.78	0.01	-0.01	0.45	0.38	-
	Knowle Production	-	0.31	0.53	0.33	0.30	0.30	-
	Middle Hollacombe	-	0.77	0.85	0.80	-0.09	-0.10	-
Foston Beck	Bartondale	0.76	0.40	0.88	NA	0.72	0.87	0.86
	Bracey Bridge	-0.29	0.36	0.25	0.37	0.50	0.35	0.61
	EYC obh TA0384565217	-0.37	0.46	0.52	0.72	0.69	0.50	0.82
	Field House	0.28	0.56	0.43	NA	0.66	0.01	0.8
	Henpit Hole	0.50	0.51	0.32	0.53	0.43	0.28	0.87
	Honey Hill	NA	-	0.69	NA	-0.34	-0.25	0.88
	Kilham P.S.	0.86	0.47	0.16	0.52	0.27	0.20	0.78
	Langtoft	0.43	0.84	0.61	NA	0.87	0.76	0.77
	Octon Crossroads	0.07	0.87	0.42	NA	0.63	-0.52	0.87
	Tancred Pit Hole	0.86	0.16	0.09	0.56	0.09	-0.05	0.79
Frome	Edgeworth	-	0.30	-0.03	NA	0.04	0.16	-
	Kingscote	-	0.00	0.42	NA	0.47	0.45	-
	Nympsfield	-	0.57	0.53	NA	0.55	0.55	-
	Minchinhampton Golf Club	-	0.58	0.71	NA	0.71	0.77	-
	Longridge	-	0.49	0.56	0.58	0.03	0.21	-
Sydling Water	Dickley Down	0.61	0.36	0.41	NA	0.45	-0.04	-
	Folly Hill	-0.03	0.68	0.60	NA	0.68	-0.30	-
	Marr's Cross	0.37	0.79	0.34	0.64	0.31	0.68	-

Table 28.4: Root mean squared error (RMSE) for all boreholes. *Stnd* refers to the Standard runs, *APM* refers to the Aquifer Properties Manual and *3DG* refers to the 3D geology simulations. *NA* means that it was not possible to calculate statistics. - means that the simulation was not conducted, or that the borehole was outside of the simulation.

Catchment	Borehole Name	Stnd 100m	Stnd 500m	Stnd 1000m	APM	3DG	3DG & APM	Calibrated
Allen	High Hall	-	4.95	10.24	11.62	10.41	20.19	10.17
	Nine Yews	-	0.00	23.69	4.75	23.43	23.30	11.35
	Squirrels Corner	-	18.37	28.74	8.70	28.49	28.45	6.16
	Hogstock Cottages	-	33.70	23.71	4.11	23.61	12.21	9.39
	West Acre	-	9.02	6.64	1.28	6.45	6.84	10.63
	Crichel Chitterwood	-	39.12	38.98	18.65	38.91	20.52	12.71
	Barnsley Farm No.3	-	1.85	4.55	6.38	3.75	6.97	3.15
	Tollard Royal	-	16.20	33.07	13.08	33.22	3.91	7.73
	Dean Farm	-	61.38	21.12	5.64	20.94	20.65	10.04
	Woodyates Telemetry	-	42.61	31.97	18.72	29.43	16.92	8.33
Creedy	Coleford Production	-	14.00	10.72	10.68	10.73	10.71	-
	Georgehill	-	39.39	11.59	11.56	10.84	10.70	-
	Knowle Production	-	8.78	4.33	4.38	4.35	4.35	-
	Middle Hollacombe	-	36.50	32.42	32.23	19.31	19.54	-
Foston Beck	Bartondale	26.86	33.69	42.41	22.83	41.52	41.11	2.93
	Bracey Bridge	15.36	1.36	1.49	4.90	1.40	6.07	1.15
	EYC obh TA0384565217	5.96	18.27	29.30	11.97	29.00	29.11	4.54
	Field House	36.00	44.95	55.46	34.85	55.23	44.62	1.95
	Henpit Hole	15.24	22.29	35.58	15.25	35.42	35.51	2.50
	Honey Hill	-	-	119.97	99.57	115.17	37.06	3.21
	Kilham P.S.	9.94	13.17	5.51	2.18	5.44	5.31	2.62
	Langtoft	26.73	36.66	58.25	38.88	58.04	58.67	4.02
	Octon Crossroads	118.08	123.54	124.25	103.56	124.08	77.09	2.99
	Tancred Pit Hole	7.65	11.92	11.70	5.09	11.65	11.74	1.98
Frome	Edgeworth	-	89.73	85.66	69.75	88.73	87.55	-
	Kingscote	-	17.41	1.50	21.96	1.63	1.66	-
	Nympsfield	-	19.97	7.20	13.54	7.09	7.08	-
	Minchinhampton Golf Club	-	88.37	85.20	66.83	86.37	85.56	-
	Longridge	-	0.95	22.00	22.18	22.60	23.13	-
Sydling Water	Dickley Down	53.52	58.09	49.77	29.39	50.01	6.46	-
	Folly Hill	81.92	104.50	111.65	91.61	111.58	47.98	-
	Marr's Cross	6.20	6.53	2.17	1.77	2.17	1.46	-

X

Appendix - Chapter V

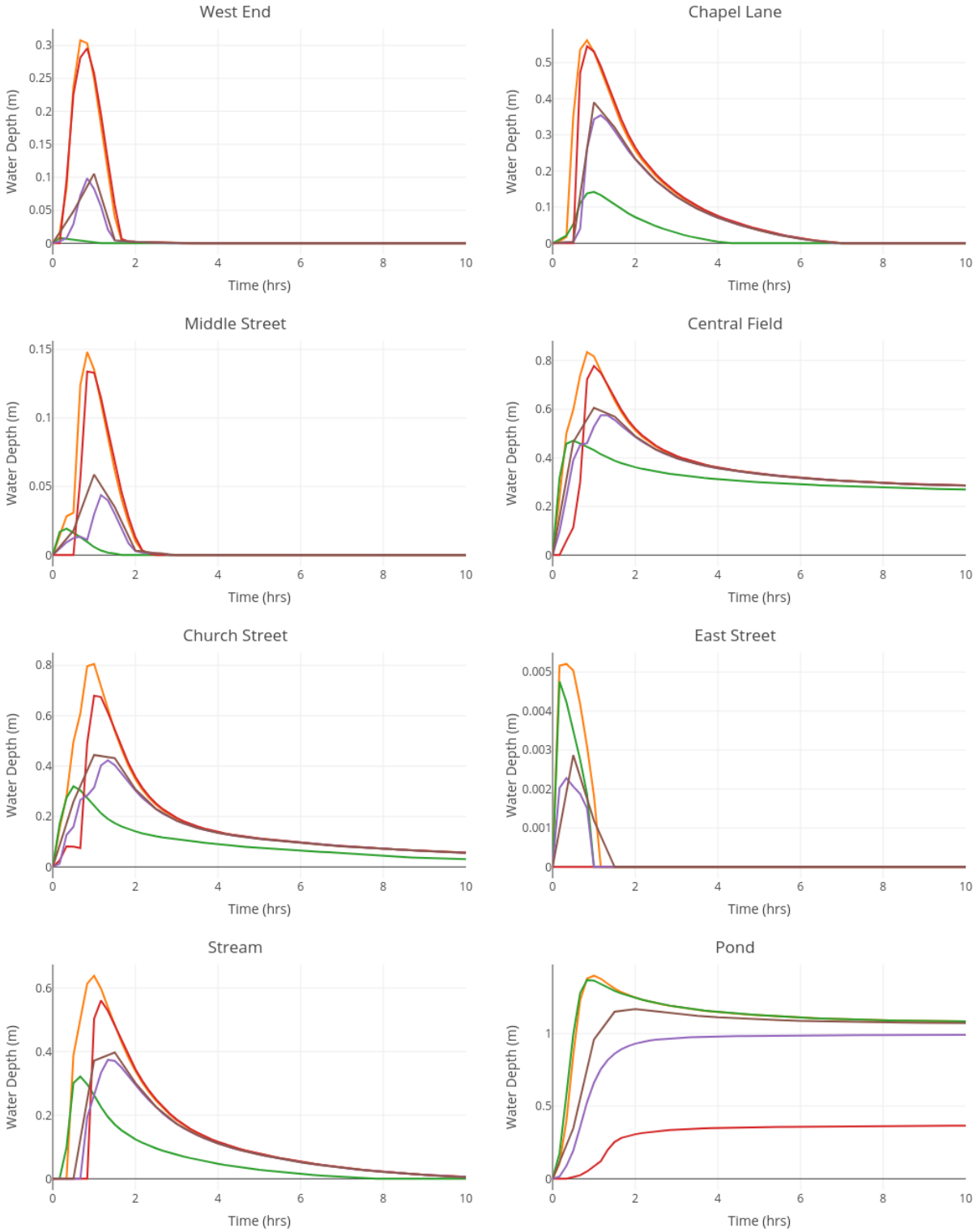

Figure 28.11: Hydrographs of domain scale distributions with inputs of 40 mm/hr for 1 hr. Orange - uniform, green - lowest, red - highest, purple - height weighted, brown - random.

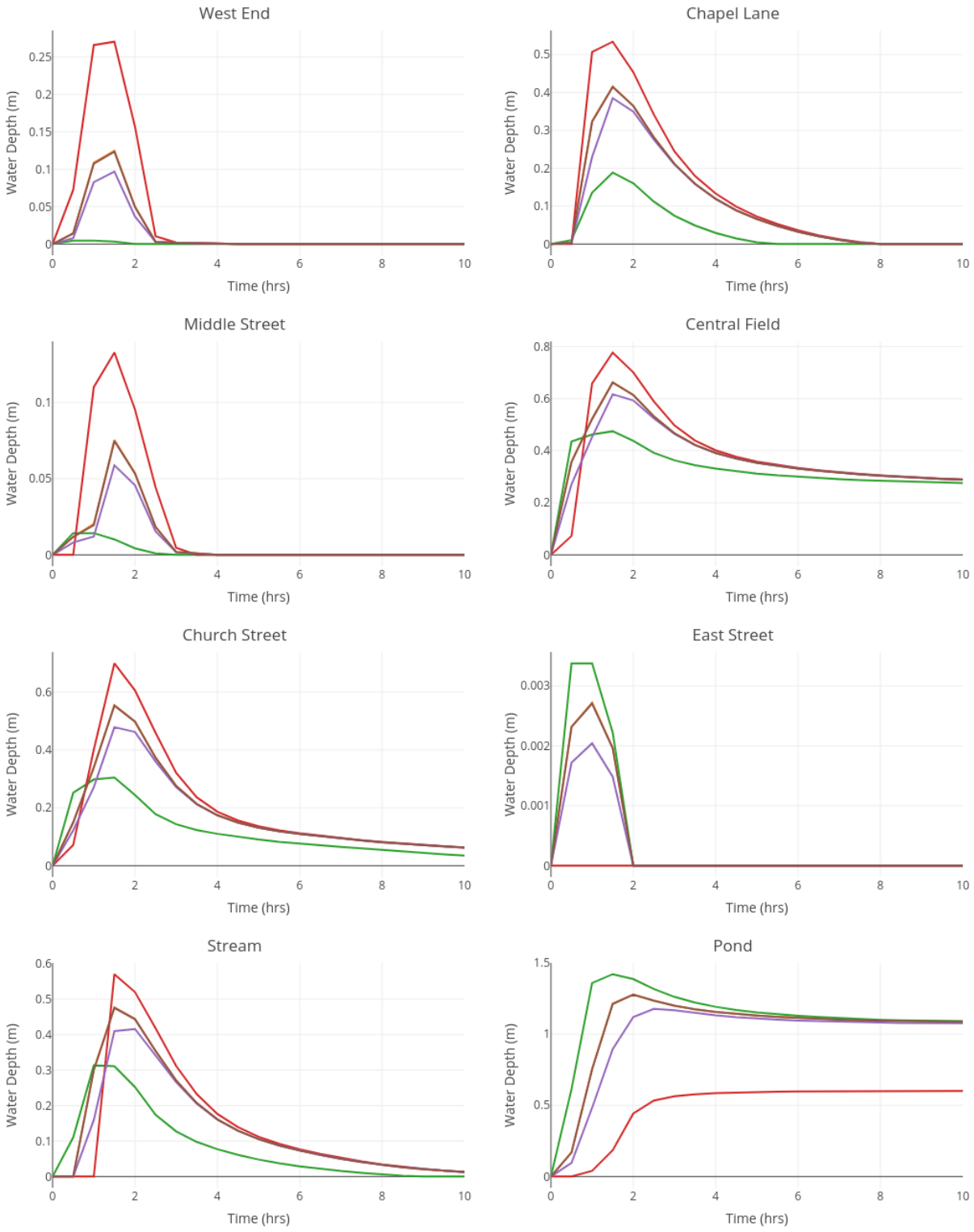

Figure 28.12: Hydrographs of domain scale distributions with inputs of 20 mm/hr for 2 hrs. Orange - uniform, green - lowest, red - highest, purple - height weighted, brown - random. The *uniform* simulation is plotted beneath the *random* simulation as they are approximately identical.

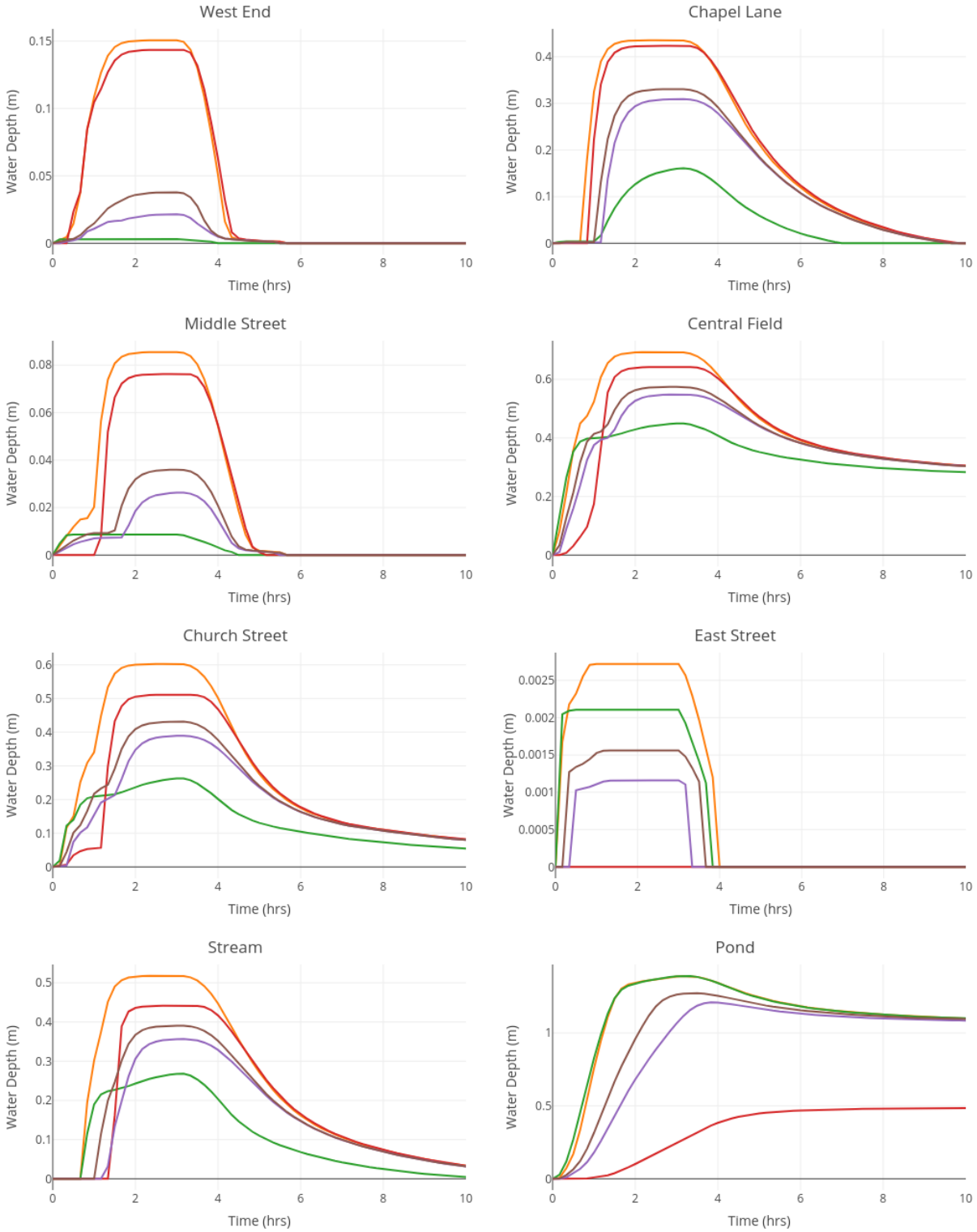

Figure 28.13: Hydrographs of domain scale distributions with inputs of 10 mm/hr for 4 hrs. Orange - uniform, green - lowest, red - highest, purple - height weighted, brown - random.

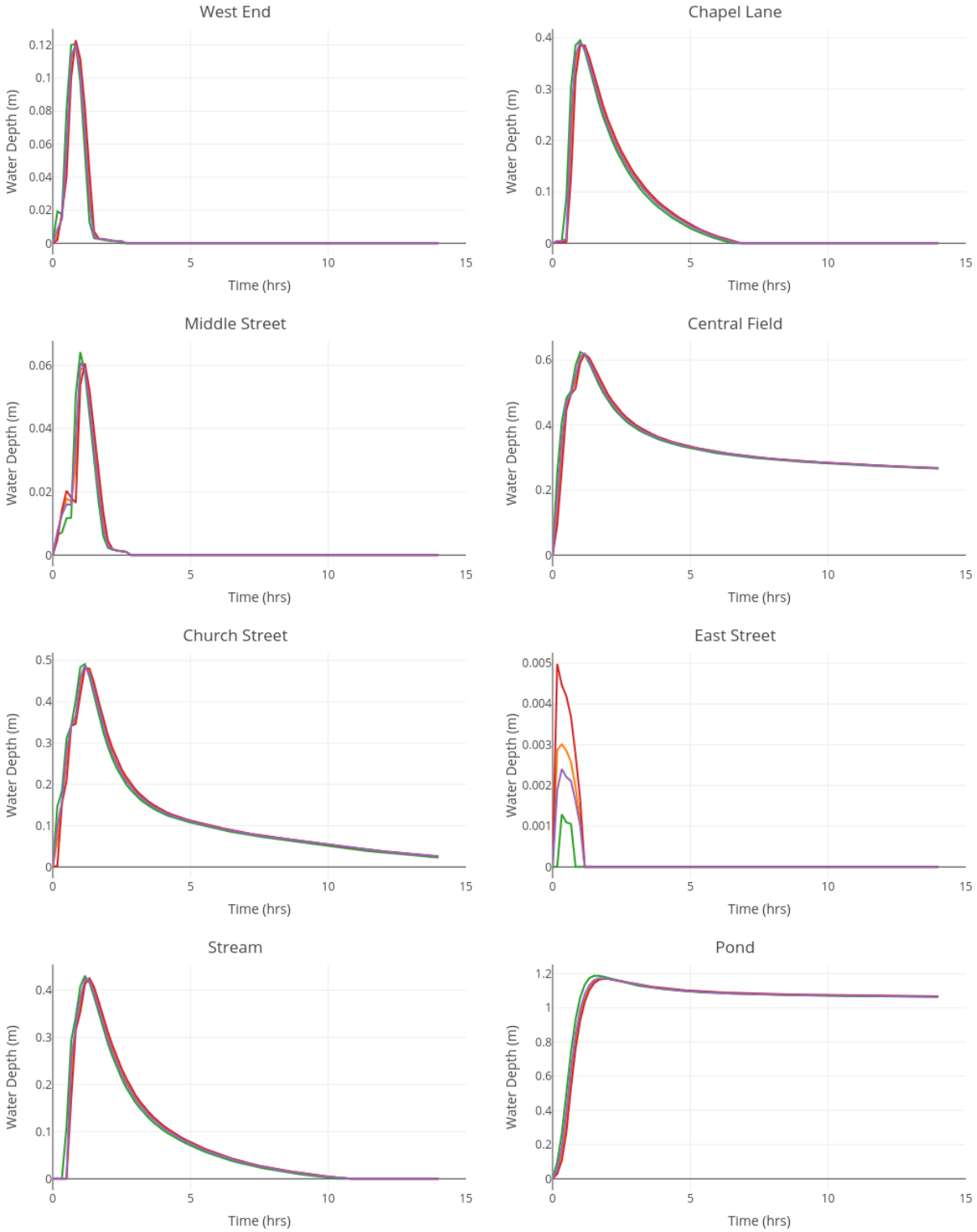

Figure 28.14: Hydrographs of cell scale distributions with inputs of 40 mm/hr for 1 hrs.
Orange - uniform, green - lowest, red - highest, purple - height weighted.

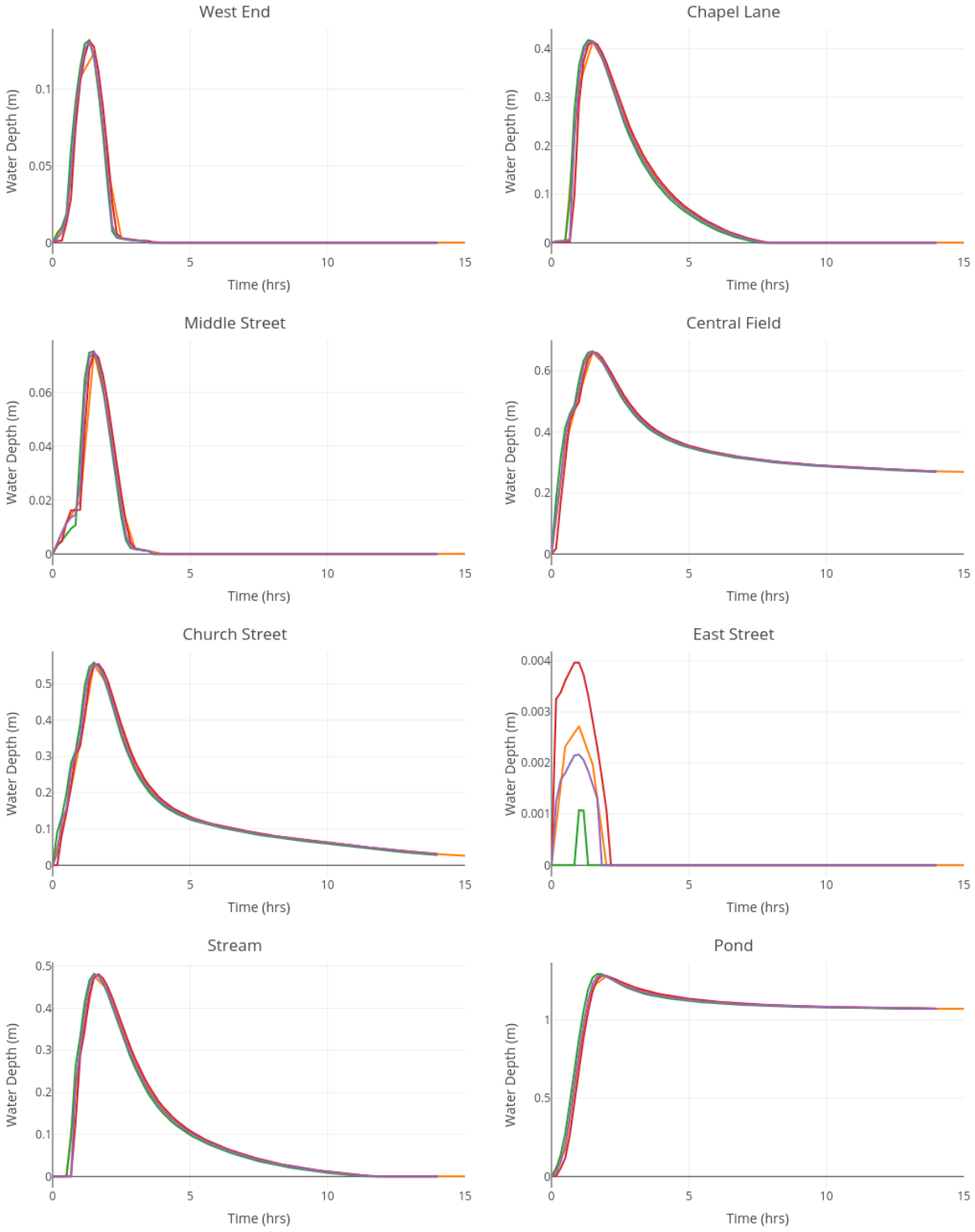

Figure 28.15: Hydrographs of cell scale distributions with inputs of 20 mm/hr for 2 hrs. Orange - uniform, green - lowest, red - highest, purple - height weighted.

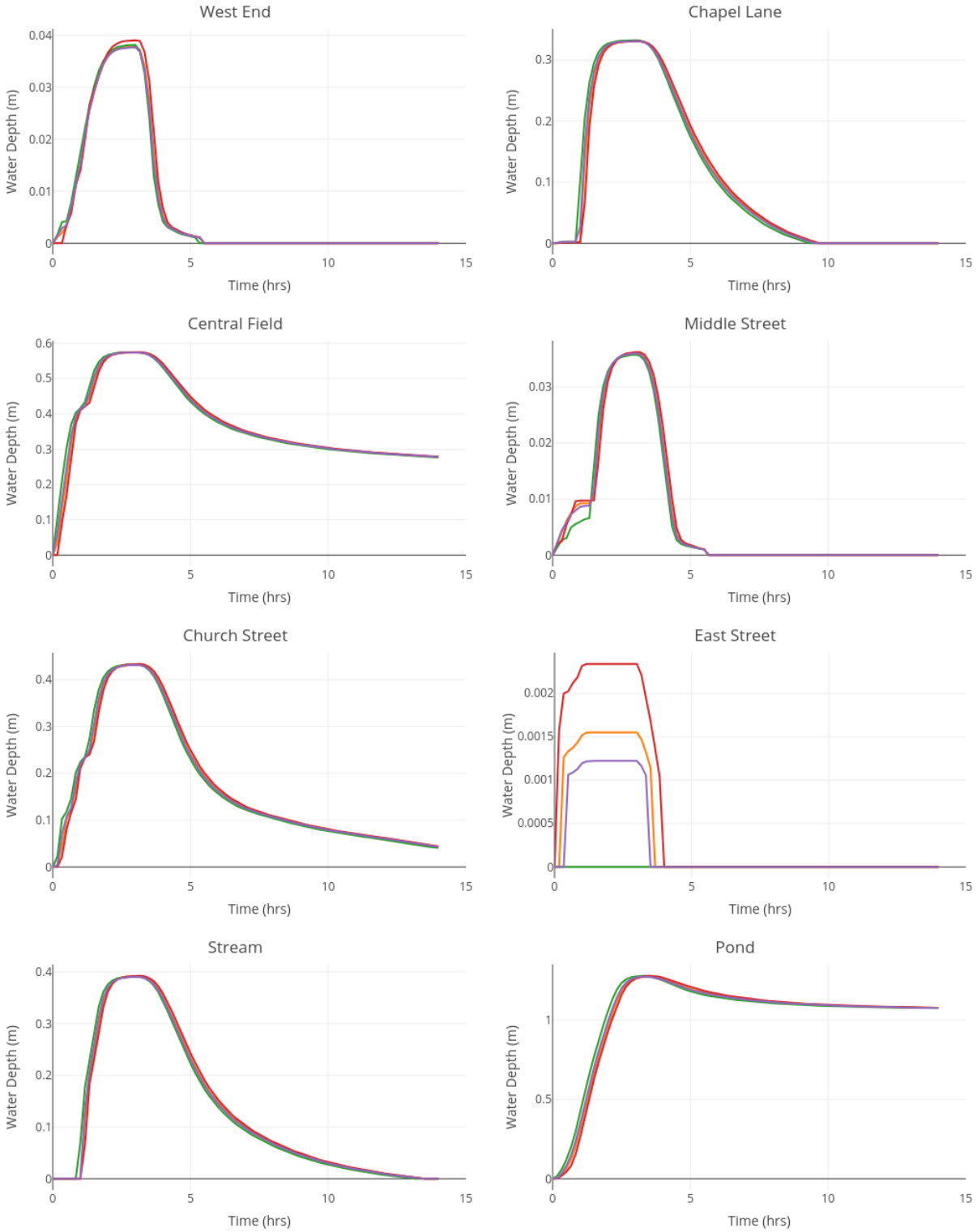

Figure 28.16: Hydrographs of cell scale distributions with inputs of 10 mm/hr for 4 hrs.
Orange - uniform, green - lowest, red - highest, purple - height weighted.

XI

Appendix - Chapter VI

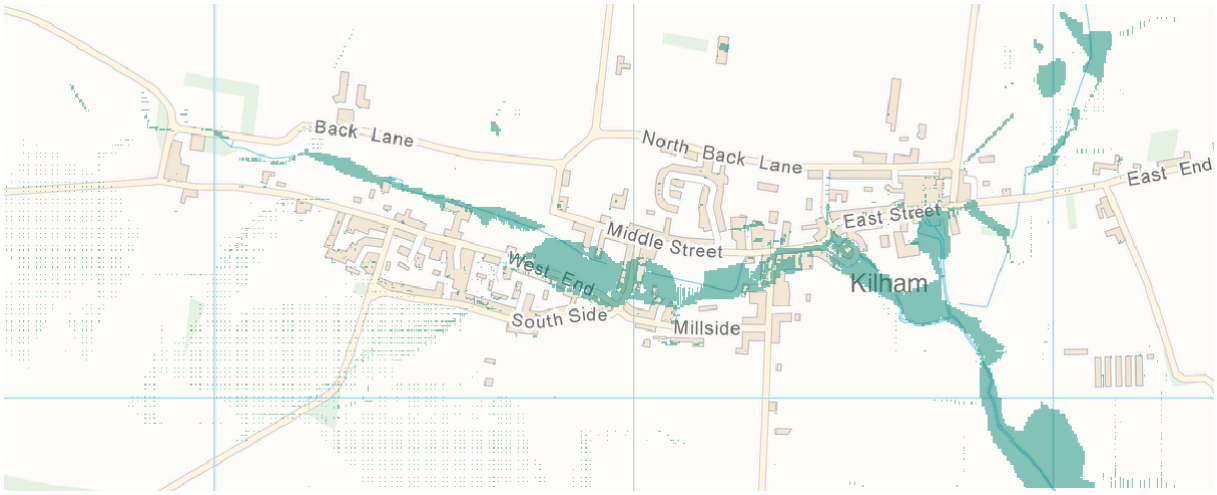

(a) Multisource

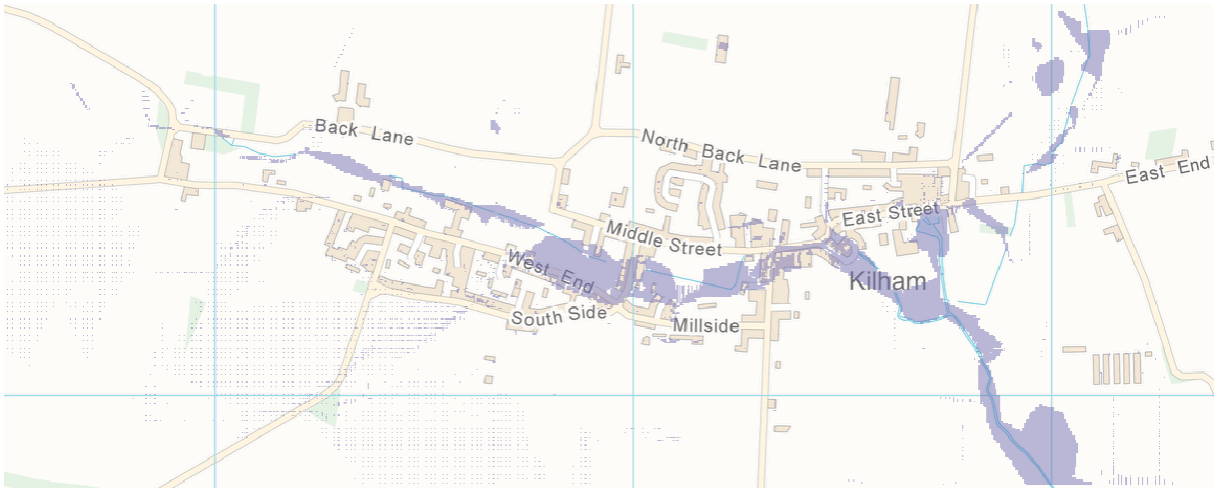

(b) Surface Water

(c) Groundwater

Figure 28.17: 1 in 1000 year flood extents from Chapter VI.

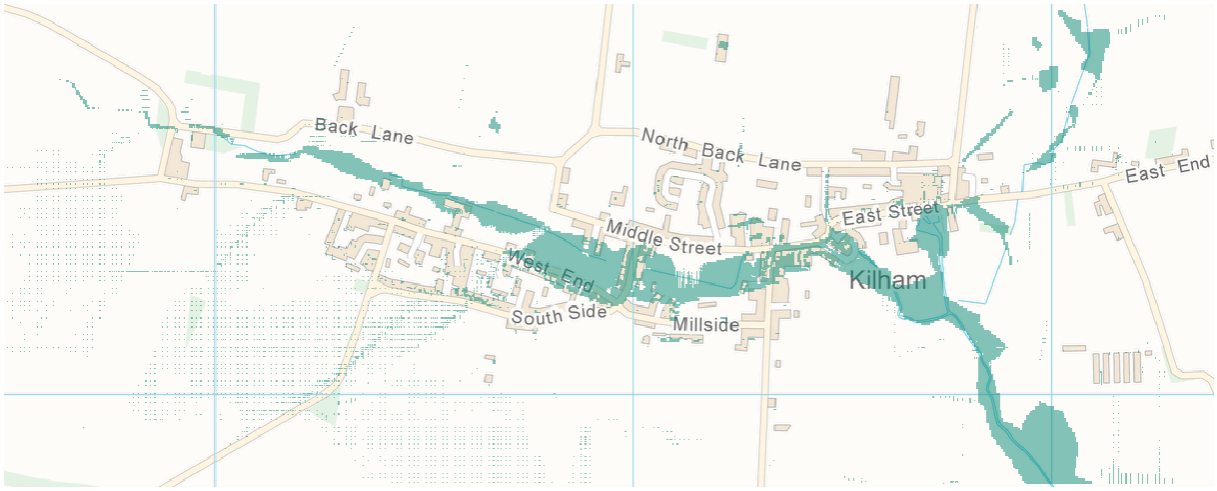

(a) Multisource

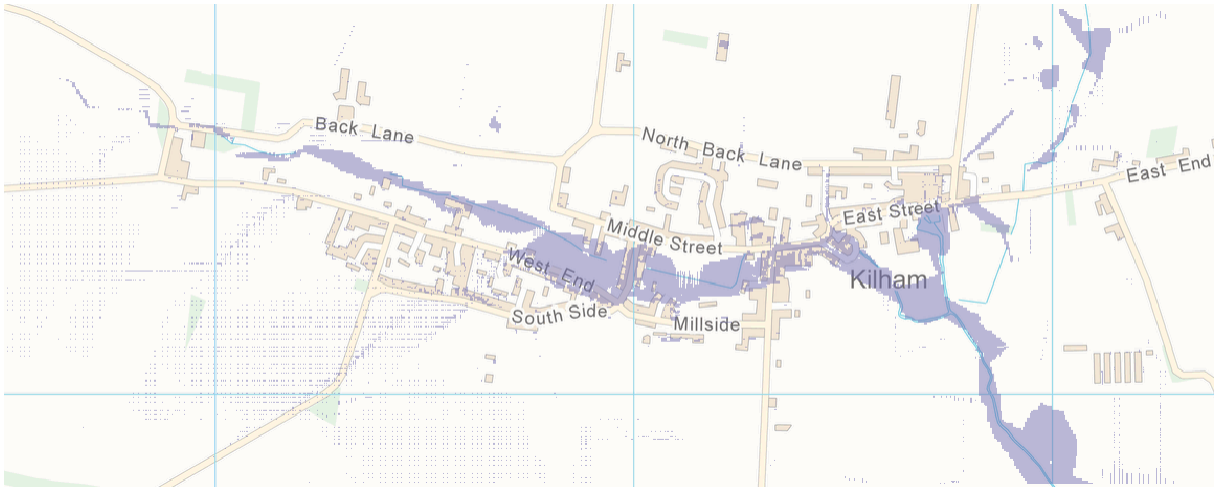

(b) Surface Water

(c) Groundwater

Figure 28.18: 1 in 100year flood extents from Chapter VI.

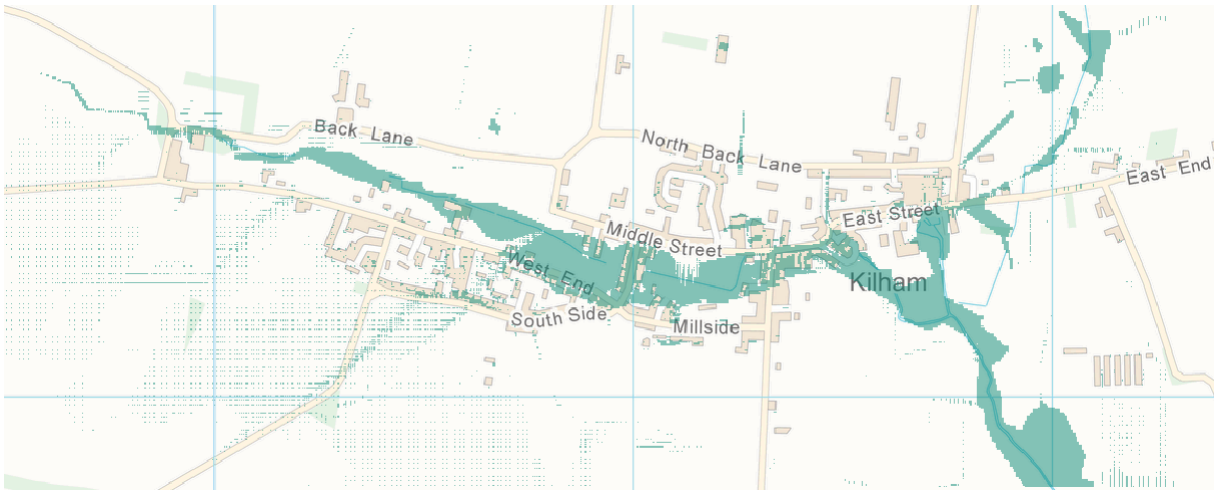

(a) Multisource

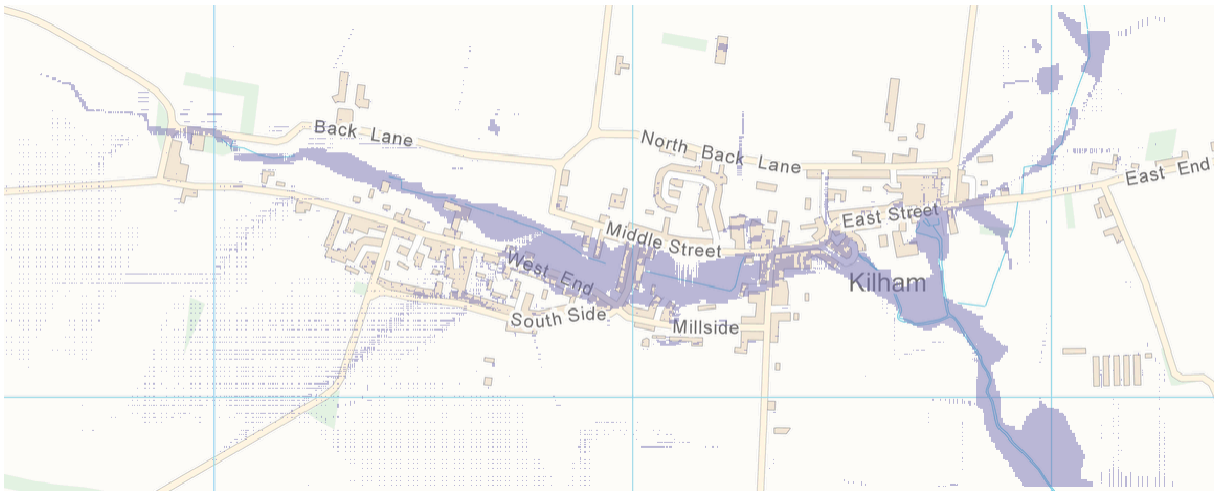

(b) Surface Water

(c) Groundwater

Figure 28.19: 1 in 30 year flood extents from Chapter VI.

(a) 1 in 1000 year Event.

(b) 1 in 100 year Event.

(c) 1 in 30 year Event.

Figure 28.20: Groundwater Induced Flood Extents from Chapter VI.